LEVEL II

SDAC-TR-77-10

SEISMIC DISCRIMINATION OF EARTHQUAKES AND EXPLOSIONS, WITH APPLICATION TO THE SOUTHWESTERN UNITED STATES

D.H. von Seggern and D.W. Rivers
Seismic Data Analysis Center
Teledyne Geotech, 314 Montgomery Street, Alexandria Virginia 22314

22 March 1979

Sponsored by
The Defense Advanced Research Projects Agency (DARPA)
DARPA Order No. 2151

Monitored By
AFTAC/VSC
312 Montgomery Street, Alexandria, Virginia 22314

Disclaimer: Neither the Defense Advanced Research Projects Agency nor the Air Force Technical Applications Center will be responsible for information contained herein which has been supplied by other organizations or contractors, and this document is subject to later revision as may be necessary. The views and conclusions presented are those of the authors and should not be interpreted as necessarily representing the official policies, either expressed or implied, of the Defense Advanced Research Projects Agency, the Air Force Technical Applications Center, or the US Government.

Unclassified

SECURITY CLASSIFICATION OF THIS PAGE (When Data Entered)

REPORT DOCUMENTATION PAGE

READ INSTRUCTIONS BEFORE COMPLETING FORM

1. REPORT NUMBER: SDAC-TR-77-10

2. GOVT ACCESSION NO.: AD-A084118

3. RECIPIENT'S CATALOG NUMBER:

4. TITLE (and Subtitle): SEISMIC DISCRIMINATION OF EARTHQUAKES AND EXPLOSIONS, WITH APPLICATION TO THE SOUTHWESTERN UNITED STATES

5. TYPE OF REPORT & PERIOD COVERED: Technical report

6. PERFORMING ORG. REPORT NUMBER:

7. AUTHOR(s): D. H. von Seggern, D. W. Rivers

8. CONTRACT OR GRANT NUMBER(s): F08606-78-C-0007, ARPA Order-2551

9. PERFORMING ORGANIZATION NAME AND ADDRESS: Teledyne Geotech, SDAC, 314 Montgomery Street, Alexandria, Virginia 22314

10. PROGRAM ELEMENT, PROJECT, TASK AREA & WORK UNIT NUMBERS: VT/8709 (Do Not Publish)

11. CONTROLLING OFFICE NAME AND ADDRESS: Defense Advanced Research Projects Agency, Nuclear Monitoring Research Office, 1400 Wilson Blvd. Arlington, Virginia 22209

12. REPORT DATE: 22 Mar 79

13. NUMBER OF PAGES: 244

14. MONITORING AGENCY NAME & ADDRESS (if different from Controlling Office): VELA Seismological Center, 312 Montgomery Street, Alexandria, Virginia 22314 (12 247)

15. SECURITY CLASS. (of this report): Unclassified

15a. DECLASSIFICATION/DOWNGRADING SCHEDULE:

16. DISTRIBUTION STATEMENT (of this Report)

APPROVED FOR PUBLIC RELEASE; DISTRIBUTION UNLIMITED

17. DISTRIBUTION STATEMENT (of the abstract entered in Block 20, if different from Report)

18. SUPPLEMENTARY NOTES

Author's Report Date 10/08/77

19. KEY WORDS (Continue on reverse side if necessary and identify by block number)

Southwestern United States
Seismic Discrimination
Underground Nuclear Explosions
M_s versus m_b
Seismic Source Spectrum
Multivariate Discriminant Function

20. ABSTRACT (Continue on reverse side if necessary and identify by block number)

This study examines seismic discrimination between underground nuclear explosions and earthquakes in the Southwestern United States. A thorough review of theoretical and applied research on this problem, especially as it relates to that region, is presented first, followed by a presentation of the seismic discrimination parameters computed for a suite of events in the Southwest and a series of experiments with multi-dimensional discrimination.

Review of past work finds some theoretical support for successful discrimination based upon several distinct measurements on seismic recordings.

next page

DD FORM 1 JAN 73 1473 EDITION OF 1 NOV 65 IS OBSOLETE

Unclassified

SECURITY CLASSIFICATION OF THIS PAGE (When Data Entered)

Although negative first motion and presence of pP both indicate a natural earthquake source, they cannot be found confidently in many cases. The relative level of shear-wave and Love-wave phases should be a good classification parameter. The long-period P spectrum of explosions should be diminished due to the surface interaction and consequent cancellation by pP. The surface-wave magnitude M_S should be only 0.2 higher for small, shallow earthquakes compared to equivalent m_b explosions, if the source time functions are identical. Observed M_S-m_b separation is routinely greater than 0.2 though, and this fact requires incoherent rupture for earthquakes and perhaps some overshoot in explosion source time functions. High frequency spectral decay of earthquakes should be ω^{-3} while that of explosions is ω^{-2}. However, other effects, such as attenuation, may overwhelm this difference. For earthquakes that have complex ruptures and appreciable focal depth, the complexity of the P-wave recording should be higher, but not greatly so. While Rayleigh-wave spectral shapes for earthquakes and explosions at shallow depths should not be much different, deeper earthquakes could be identified by higher modes and a relative decrease of shorter period amplitude.

The region under study extends from California to the southern Rocky Mountains and from roughly 40°N to the Gulf of California. A region of high seismicity, it is also a complex region encompassing several tectonic provinces, including the Basin-Range Province where the Nevada Test Site is located. Source mechanisms are diverse over the entire region and even within small subregions. Focal depths are almost all < 15 km and few depths can be determined reliably from teleseismic recordings. Twelve earthquakes, mostly selected because of low M_S estimates from other studies, and eleven explosions comprised the sources for this study. Seven teleseismic LRSM stations supplied the seismic data.

In general, seismic discriminant parameters obtained from the recordings reflected the theoretical expectations of earthquake-explosion differences. Path-station effects were large for every parameter, especially for short-period data. Love-wave magnitudes were a superior discriminant when plotted versus m_b. Shear waves, if measurable, were also excellent. The common M_S-m_b plot shows three earthquakes with anomalously low M_S: the Denver earthquake, a Benham aftershock, and a Baja California earthquake.

All the discrimination parameters (10) were applied in various combinations through a stepwise linear discriminant program, which treated the twenty-three events as a training set. Using all parameters, the lowest a posteriori probability of correct classification was .987. Multi-dimensional discrimination using network averages for parameters was superior to using single-station parameters or using linear combinations of individual stations' discriminant functions.

SEISMIC DISCRIMINATION OF EARTHQUAKES AND EXPLOSIONS, WITH APPLICATION TO THE SOUTHWESTERN UNITED STATES

SEISMIC DATA ANALYSIS CENTER REPORT NO.: SDAC-TR-77-10

AFTAC Project Authorization No.:	VELA T/8709/B/ETR
Project Title:	Seismic Data Analysis Center
ARPA Order No.:	2551
Name of Contractor:	TELEDYNE GEOTECH
Contract No.:	F08606-78-C-0007
Date of Contract:	01 October 1976
Amount of Contract:	$2,697,947
Contract Expiration Date:	30 September 1977
Project Manager:	Robert R. Blandford (703) 836-3882

P. O. Box 334, Alexandria, Virginia 22313

ABSTRACT

This study examines seismic discrimination between underground nuclear explosions and earthquakes in the Southwestern United States. A thorough review of theoretical and applied research on this problem, especially as it relates to that region, is presented first, followed by a presentation of the seismic discrimination parameters computed for a suite of events in the Southwest and a series of experiments with multi-dimensional discrimination.

Review of past work finds some theoretical support for successful discrimination based upon several distinct measurements on seismic recordings. Although negative first motion and presence of pP both indicate a natural earthquake source, they cannot be found confidently in many cases. The relative level of shear-wave and Love-wave phases should be a good classification parameter. The long-period P spectrum of explosions should be diminished due to the surface interaction and consequent cancellation by pP. The surface-wave magnitude M_s should be only 0.2 higher for small, shallow earthquakes compared to equivalent m_b explosions, if the source time functions are identical. Observed M_s-m_b separation is routinely greater than 0.2 though, and this fact requires incoherent rupture for earthquakes and perhaps some overshoot in explosion source time functions. High frequency spectral decay of earthquakes should be ω^{-3} while that of explosions is ω^{-2}. However, other effects, such as attenuation, may overwhelm this difference. For earthquakes that have complex ruptures and appreciable focal depth, the complexity of the P-wave recording should be higher, but not greatly so. While Rayleigh-wave spectral shapes for earthquakes and explosions at shallow depths should not be much different, deeper earthquakes could be identified by higher modes and a relative decrease of shorter period amplitude.

The region under study extends from California to the southern Rocky Mountains and from roughly 40°N to the Gulf of California. A region of high seismicity, it is also a complex region encompassing several tectonic provinces, including the Basin-Range Province where the Nevada Test Site is located. Source mechanisms are diverse over the entire region and even within small subregions. Focal depths are almost all < 15 km and few depths can be determined reliably from teleseismic recordings. Twelve earthquakes,

mostly selected because of low M_s estimates from other studies, and eleven explosions comprised the sources for this study. Seven teleseismic LRSM stations supplied the seismic data.

In general, seismic discriminant parameters obtained from the recordings reflected the theoretical expectations of earthquake-explosion differences. Path-station effects were large for every parameter, especially for short-period data. Love-wave magnitudes were a superior discriminant when plotted versus m_b. Shear waves, if measurable, were also excellent. The common M_s-m_b plot shows three earthquakes with anomalously low M_s: the Denver earthquake, a Benham aftershock, and a Baja California earthquake.

All the discrimination parameters (10) were applied in various combinations through a stepwise linear discriminant program, which treated the twenty-three events as a training set. Using all parameters, the lowest a posteriori probability of correct classification was .987. Multi-dimensional discrimination using network averages for parameters was superior to using single-station parameters or using linear combinations of individual stations' discriminant functions.

TABLE OF CONTENTS

TABLE OF CONTENTS (Continued)

LIST OF FIGURES

LIST OF FIGURES (Continued)

LIST OF TABLES

LIST OF TABLES (Continued)

INTRODUCTION

Past studies in seismic discrimination between earthquakes and underground nuclear explosions have generally been regional in scope, in which attempts at discrimination involved neighboring events on the globe. Although they should not be undervalued, these studies often failed to discern or to convey important regional properties of earthquake mechanisms and earth structure that may debilitate or enhance identification of events, either earthquakes or explosions, from other areas. Also, although most studies have been characterized as regional, in many cases the region chosen is so large that distinct subregions with peculiar properties exist which significantly affect discrimination parameters. Evernden and Filson (1971) and Marshall and Basham (1972), in the case of M_s, and Douglas et al. (1973), in the case of P-wave complexity, provide examples of attempts to overcome regional effects and to present discrimination parameters in a unified sense. Identification and estimation of path and receiver effects on discrimination parameters are essential if a sound physical basis for distinguishing natural and artificial seismic events is to be established not only in regions where they have been studied, but also in any unstudied region where seismic events may occur in isolated instances.

Magnitude determination shows the importance of removing or suppressing path-receiver effects. Here, investigators have distinguished between shallow earthquakes and explosions whose theoretical separation on the M_s scale (given equal m_b) amounts to only a half order of magnitude based on infinitesimal source theory (Gilbert, 1973). They accomplish this by using signal

---

Evernden, J. F., and J. Filson (1971). Regional dependence of surface-wave versus body-wave magnitudes. J. Geophys. Res., 27, 3303-3308.

Marshall, P. D., and P. W. Basham (1972). Discrimination between earthquakes and underground explosions employing an improved M_S scale. Geophys. J., 28, 431-458.

Douglas, A., P. D. Marshall, P. G. Gibbs, J. B. Young, and C. Blamey (1973). P signal complexity re-examined. Geophys. J., 33, 195-233.

Gilbert, F. (1973). The relative efficiency of earthquakes and explosions in exciting surface waves and body waves. Geophys. J., 33, 487-488.

amplitude estimates known typically to range over nearly two orders of magnitude for a well-recorded seismic event. A casual approach to magnitude determination results in explosion points ranging over almost two units of magnitude in M_s for a given m_b, and vice-versa, when data from several test sites are plotted together (Liebermann and Pomeroy, 1969). Although some of the observed variation is undoubtedly source-related, the Rayleigh-wave spectral ratios of von Seggern and Lambert (1970) and the short-period spectral ratios of Lacoss (1969) provide additional examples of severe regional effects on discrimination.

While most previous studies produced valuable detailed coverage of one aspect of discrimination, they failed to study several facets of the data in one region, an omission that impairs evaluation of various discrimination parameters and limits efforts to improve discrimination using parameters graphically and statistically, either alone or in combination. Only a few authors, together comprising only a small portion of the relevant literature, have used two or more distinct discriminants to separate natural and artificial seismic events. Among them are Booker and Mitronovas (1964), Lacoss (1969), Press et al., (1963), Evernden (1969), Rasmussen and Lande (1968),

---

Liebermann, R. C., and P. W. Pomeroy (1969). Relative excitation of surface waves by earthquakes and underground explosions. J. Geophys. Res., 74, 1575-1590.

von Seggern, D., and D. G. Lambert (1970). Theoretical and observed Rayleigh-wave spectra for explosions and earthquakes. J. Geophys. Res., 75, 7382-4702.

Lacoss, R. T. (1969). A large-population LASA discrimination experiment. Technical Note 1969-24, Lincoln Laboratory, Lexington, Massachusetts.

Booker, A., and W. Mitronovas (1964). An application of statistical discrimination to classify seismic events. Bull. Seism. Soc. Am., 54, 961-971.

Press, F., G. Dewart, and R. Gilman (1963). A study of diagnostic techniques for identifying earthquakes. J. Geophys Res., 68, 2909-2928.

Evernden, J. F. (1969). Identification of earthquakes and explosions by use of teleseismic data. J. Geophys. Res., 74, 3838-3856.

Rasmussen, D., and L. Lande (1968). Seismic analysis of the GASBUGGY explosion and an earthquake of similar magnitude and epicenter. Report No. 68-15, Teledyne Geotech, Garland, Texas.

Anglin (1971), and Dahlman et al. (1974). Even though high reliability of the M_s versus m_b discriminant has been established (Evernden et al., 1971; Ericsson, 1970; Pasechnik et al., 1970; Weichert and Basham, 1974; Evernden, 1975), the recognition of certain earthquakes generating anomalously low amplitude surface waves (Landers, 1972; Der, 1973) and the frequent inability to detect surface waves from explosions compels us to consider multiple-variable discrimination. The importance of this mode of surveillance is reinforced by the fact that anomalous earthquakes in those studies which were marginally identified or even unidentified by M_s versus m_b were quite clearly identified by means of other discriminants. (Whether anomalous M_s earthquakes in all regions of the globe can be so easily disposed of remains to be seen.) Another reason to consider several discriminants rather than one is the possibility of clandestine nuclear blasts under test-ban treaty controls. Evaders could either disguise the test to appear like an earthquake or hide the test in the coda signals of a large earthquake. However, such schemes may not be successful if a sophisticated,

---

Anglin, F. M. (1971). Discrimination of earthquakes and explosions using short-period seismic array data. Nature, 233, 51-52.

Dahlman, O., H. Israelson, A. Austegard, and G. Hornstrom (1974). Definition and identification of seismic events in the USSR in 1971. Bull. Seism. Soc. Am., 64, 607-636.

Ericsson, U. A. (1970). Event identification for test ban control. Bull. Seism. Soc. Am., 60, 1521-1546.

Pasechnik, I. P., G. G. Dashkov, L. A. Polikarpova, and N. G. Gamburtseva (1970). The magnitude method for identification of underground nuclear explosions. Izv. Phys. Solid Earth, No. 1, January 1970, (English translation).

Weichert, D. H., and P. W. Basham (1973). Deterrence and false alarms in seismic discrimination. Bull. Seism. Soc. Am., 63, 1119-1132.

Evernden, J. (1975). Further studies on seismic discrimination. Bull. Seism. Soc. Am., 65, 359-392.

Landers, T. (1972). Some interesting central Asian events on the M_s:m_b diagrams. Geophys. J., 31, 329-339.

Der, Z. A. (1973). M_s-m_b characteristics of earthquakes in the eastern Himalayan regions. SDL Report No. 296, Teledyne Geotech, Alexandria, Virginia.

multiple-discriminant effort is employed (Evernden, 1976).

The purpose of this study is to overcome these deficiencies through a comprehensive, coherent study of explosions and earthquakes in a selected region. This study attempts to identify and to quantify the numerous factors at the source, along the travel path, and at the receivers which affect discrimination for a particular region of the globe. Discrimination parameters are to be related to the nature of the sources and the structure of the region so that why they do or do not work can be understood. Although this is a regional study, the authors intend to emerge with enough knowledge that regional effects could be satisfactorily removed, if necessary, from discrimination parameters estimated here. The authors hope to refine discrimination techniques enough in the selected area to permit meaningful application to other regions.

The choice of an initial region--the Western United States (WUS)--for an integrated study was a natural one. Specifically, the region is composed largely of the Central Cordillera and the Pacific Ranges, plus a small northwestern section of the Southern Cordillera (in all, roughly 30°-40°N and 104°-124°W). This area is not, in any sense, a small or homogeneous region, but it was deliberately chosen to be large enough to include earthquakes and explosions of differing charactistics and to present some structural contrasts. At the same time it is small enough to allow analysis using a common seismic network and to avoid drastic path effects which might otherwise hinder development of conclusive or significant results.

Other reasons for selecting the Western United States are:

(1) Data, in the form of LRSM (Long Range Seismic Measurement) film and tape recordings and film chips for many WWSSN sites, are readily available and easily analyzed.

(2) This region contains several underground nuclear test sites and sites of peaceful nuclear explosions. The large explosions fired

---

Evernden, J. (1976). Study of seismological evasion, Part III. Evaluation of evasion possibilities using codas of large earthquakes. Bull. Seism. Soc. Am., 66, 549-592

in the Western United States are well documented, and many have been studied in detail. Parameters such as detonation depth, yield, and medium are known, and the seismic signals have been used for previous discrimination studies and for investigations into earth structure.

3) The Western United States is a region of pronounced seismicity, and many of the larger earthquakes in this region are well documented. Focal mechanism solutions, fault length, source spectral shape, as well as other characteristics, have been presented for literally hundreds of events.

4) Because some earthquakes apparently are only marginally discriminated by M_s-m_b diagrams (Basham, 1969; Peppin and McEvilly, 1974; Peppin, 1976; Savino et al., 1971) or by short-period spectral ratios (Bakun and Johnson, 1970), real discrimination problems exist for events in the Western United States. The one element that most confuses identification of explosions at the Nevada Test Site is the large amount of tectonic strain release accompanying many explosions, especially those of larger yield, (Toksöz and Kehrer, 1972a), which causes LQ/LR ratios for those explosions to equal or surpass those of earthquakes.

Basham, P. W. (1969). Canadian magnitudes of earthquakes and nuclear explosions in southwestern North America. Geophys. J., 17, 1-14.

Peppin, W. A., and T. V. McEvilly (1974). Discrimination among small magnitude events on Nevada Test Site. Geophys. J., 37, 227-243.

Peppin, W. A. (1976). P-wave spectra of Nevada Test Site events at near and very-near distances: Implications for a near-regional body wave - surface wave discriminant. Bull. Seism. Soc. Am., 66, 803-826.

Savino, J., L. R. Sykes, R. C. Liebermann, and P. Molnar (1971). Excitation of seismic surface waves with periods of 15 to 70 seconds for earthquakes and underground explosions. J. Geophys. Res., 76, 8003-8020.

Bakun, W. H. and L. R. Johnson (1970). Short period spectral discriminants for explosions. Geophys. J., 22, 139-152.

Toksoz, M. N., and H. H. Kehrer (1972a). Tectonic strain release by underground nuclear explosions and its effect on seismic discrimination. Geophys. J., 31, 141-161.

5) The geology and geophysics of the Western United States (from the surface down through the upper mantle) is known as well as, or better than, that of any other global region. Such knowledge will aid considerably in determining source and path effects on seismic waves because one should be able to relate peculiarities in seimic observations to known or hypothetical regional structural elements.

6) Because of the abundance of background and supporting material for the Western United States, the objectives of this study can be more easily accomplished than if an isolated and uncharted region were chosen.

7) Lastly, since so much discrimination literature on the Western United States has already been published, this study provides an appropriate forum from which to review it, to synthesize it, and to integrate it with any new results from this study.

This study is divided into three major sections. First, published theories and results pertinent to discrimination, especially those pertaining to events in the Western United States, are reviewed. Here, the physical bases of discrimination will be emphasized and illustrated. Then, by providing a description of the present structure of the Western United States, a specific framework for this study will be established. A review of the present tectonics will follow, including active crustal movements and recent seismicity. After this background information, the choice of data for the regional discrimination study will be listed and described. One part of the study will be signal analysis, leading to descriptions and estimations of source, path, and receiver effects and their impact on discrimination. A second part of the study will involve use of discrimination parameters in a stepwise multiple-discrimination scheme. Finally, the last section will present conclusions and recommendations for further study.

GENERAL REVIEW OF SEISMIC DISCRIMINATION

Some of the earliest discussions (e.g. VESIAC, 1962) of discrimination between earthquakes and underground nuclear explosions focused on the distinctness of the explosion source from the earthquake source in terms of symmetry, compactness, or absence of rotational components. Ironically, however, in these same volumes are reports of numerous observations that serve only to confound discrimination based upon this simple concept. Out of this confusion emerged a vigorous program of research that investigated the nature and effects of the two sources. Most of the earlier discrimination work involved explosions and earthquakes in the Western United States because of the numerous detonations at the Nevada Test Site, the high seismicity of this region, the proximity of existing seismograph stations, and the addition of many new recording sites in the form of LRSM (Long Range Seismic Measurement) stations and VELA Uniform observatories. The results of the empirical, as well as the theoretical, studies are reviewed below. For the purpose of this review, and the study in general, a discri inant is defined as any measurable information on seismograms that can be used, on a statistical or other basis, to determine the source of a seismic event.

Location, Including Depth

This discriminant is unique because it ignores the physical nature of the source. When an event has been located in an aseismic area, reference to number-versus-magnitude recurrence curves, which are presumably based on natural events, may suggest the events are artificial. Since a possibility exists for large events in even aseismic areas, this information does not provide conclusive evidence of an explosion, but it is sufficient to separate out the event for further study. The boundaries of aseismic areas are often sharply defined, a situation creating the need for high-quality seismic network locations for monitoring any test-ban agreement. Neglecting epicenter bias, such quality locations could be attained (95% confidence ellipses of <500 square

---

VESIAC (1962). Proceedings of the colloquium on detection of underground nuclear explosions, VESIAC Special Report No. 4410-36-X, Acoustics and Seismics Laboratory, University of Michigan, Ann Arbor, Michigan.

km) for events down to $m_b \sim 4$ over almost the entire globe (Evernden, 1971) with as few as twenty-five good stations. However, the epicenter bias from lateral inhomogeneity of the earth can severely undermine the utility of these confidence regions, unless relative location using master events is employed (Evernden, 1971), though serious bias is probably limited to descending plate areas (Davies and McKenzie, 1969). Note that because of the relatively high seismicity of the Western United States, especially in the areas surrounding the Nevada Test Site, discrimination based upon areal location would be impossible, even if confidence ellipses were precise and small.

In contrast, events in seismic areas can often be confirmed as earthquakes if the site itself would preclude an underground nuclear explosion (for example, beneath deep water at sea or within the boundaries of a nation known not to be capable of testing nuclear explosions). Again, high-quality location is the key to making these decisions.

The depth variable in location can also be considered a discriminant. An event located at a depth that would be too deep for a nuclear detonation, say >5 km, could be classified as a natural earthquake. However, limitations of a teleseismic network in this regard are severe; for with teleseismic location methods, depth cannot be shown by consideration of location error ellipses alone to be beyond very shallow, except for events located by travel-time inversion deeper than roughly 30 to 40 km (Evernden, 1969). Again, bias in depth equally serious to that of areal location can arise due to lateral inhomogeneities in the earth such as dipping plates, ocean ridges, and continental areas with anomalously thick crust; a well-known example is the location of LONG SHOT roughly 60 km deep (Lambert et al., 1969). Davies and McKenzie (1969) suggested that travel time will be badly biased relative to the

---

Evernden, J. F. (1971). Location capability of various seismic networks. Bull. Seism. Soc. Am., 61, 241-273.

Davies, D., and D. P. McKenzie (1969). Seismic travel-time residuals and plates. Geophys. J., 18, 51-63.

Lambert, D. G., D. H. von Seggern, S. S. Alexander, and G. A. Galat (1969). The LONG SHOT experiment. Volume II. Comprehensive analysis. SDL Report No. 234, Teledyne Geotech, Alexandria, Virginia.

standard curve in dipping plate areas. In the Western United States, almost all earthquakes are shallow (<15 km); therefore, a teleseismic network alone could not discriminate between earthquakes and explosions by routine location methods unless pP could be definitely identified.

Using the spectra of seismic events provides another approach to depth determination. However, results obtained from this method are questionable because no general statistical measure exists comparable to the error ellipses used with travel time. In fact, this method has produced little fruitful results in the field of discrimination because all events where spectral inversion was applied were already known to be either earthquakes or explosions. At this time, depth information derived from spectra can be considered only of diagnostic value; that is, only a very weak discriminant. Indeed, this method can admit gross errors in estimates of event depth because of the many other factors that influence the shape of seismic spectra, including source time function, lateral inhomogeneity, crustal and upper mantle layers, and attenuation. Also, the possibility exists that the inversion can converge on a completely wrong solution. Some workers resist these criticisms and contend that solution for source depth of earthquakes is feasible with spectra of either surface waves (Keilis-Borok and Yanovskaya, 1962; Tsai and Aki, 1970; Tsai and Aki, 1971; Weidner and Aki, 1973; Canitez and Toksöz, 1971) or body

---

Keilis-Borok, V. I., and T. B. Yanovskaya (1962). Dependence of the spectrum of surface waves on the depth of the focus within the earth's crust. Izv. Akad. Nauk. USSR, Geophys. Ser., 11, p. 1532-1539. (English Translation)

Tsai, Y. B., and K. Aki (1970). Precise focal depth determination from amplitude spectra of surface waves. J. Geophys, Res., 75, 5729-5743.

Tsai, Y. B., and K. Aki (1971). Amplitude spectra of surface waves from small earthquakes and underground nuclear explosions. J. Geophys. Res., 76, 3940-3952.

Weidner, D., and K. Aki (1973). Focal depth and mechanism of mid-ocean ridge earthquakes. J. Geophys. Res., 78, 1818-1831.

Canitez, N., and M. N. Toksöz (1971). Focal mechanism and source depth of earthquakes from body- and surface-wave data. Bull. Seism. Soc. Am., 61, 1369-1379.

waves (Guha and Stauder, 1970; Langston, 1976). In the case of surface waves, Canitez and Toksöz claim a depth precision of a few kilometers can be attained using ratios of LQ/LR spectra, which is a means of cancelling some of the propagation effects on spectra. However, in response Massé et al. (1973) pointed out that large errors in depth are still possible using the LQ/LR spectral ratios, especially if the earth structure is not accurately known.

Carrying this argument further, note that many investigators have estimated detonation depths of explosions from short-period P waves or their spectra (Cohen, 1970; Kulhanek, 1971; Douglas et al., 1972a; Frasier, 1972; Manchee and Hasegawa, 1973) and that the explosion depth estimates seem fairly accurate with this method because of the good agreement between different authors using differing stations for common events. However, these authors knew a priori that the events were explosions, and they are not able to suggest that the events can be classified as explosions on the basis of shallow-focus estimates. Discrimination is not really possible with this technique because earthquakes also

---

Guha, S. K., and W. Stauder, (1970). The effect of focal depth on the spectra of P waves. II. Observational studies. Bull. Seism. Soc. Am., 60, 1457-1477.

Langston, C. A. (1976). A body wave inversion of the Koyna, India, Earthquake of December 10, 1967, and some implications for body wave focal mechanisms. J. Geophys. Res., 81, 2517-2529.

Massé, R. P., D. G. Lambert, and D. G. Harkrider, (1973). Precision of the determination of focal depth from the spectral ratio of Love/Rayleigh surface waves. Bull. Seism. Soc. Am., 63, 59-100.

Cohen, T. (1970). Source-depth determinations using spectral, pseudo-autocorrelation, and cepstral analysis. Geophys. J., 20, 223-231.

Kulhanek, O. (1971). P-wave amplitude spectra of Nevada underground nuclear explosions. Pure Appl. Geophys., 88, 121-136.

Douglas, A. D., J. Corbishley, C. Blamey, and P. D. Marshall, (1972a). Estimating the firing depth of underground explosions. Nature, 237, 26-28.

Frasier, C. W. (1972). Observations of pP in the short-period phases of NTS explosions recorded at Norway. Geophys. J., 31, 99-109.

Manchee, E. B., and H. S. Hasegawa, (1973). Seismic spectra of Yucca Flat underground explosions observed at Yellowknife, Northwest Territories. Can. J. Earth Sci., 10, 421-427.

can be near the surface and because earthquakes at any depth may, through multiple-path effects or a complicated source function, show spectral shaping similar to that which was used to estimate explosion depth (Cohen et al., 1972).

First Motion

Because only natural earthquakes, not explosions, are ideally able to generate initial dilatational motions, the P-wave first motions on seismic recordings of an event should determine whether the event was an explosion or an earthquake. However, several difficulties exist with this simple approach. First, the spheroidal shape and layering of the earth may combine with teleseismic networks such that the two quadrants of a double-couple mechanism which generate the initial dilatational motions appear not to be well-sampled when raypaths are traced back to the source. Carpenter (1964) estimated that between 10% and 25% of all earthquakes have no teleseismic dilatations, depending upon assumptions made for network distribution, earth structure, and geometry of the focal mechanisms. Evernden (1969) pointed out some concrete examples of where first motion criteria would fail. Second, dilatational motion has been observed for explosions worldwide (Enescu et al., 1973) where obviously ideal source conditions are not satisfied and where some nonuniform forces are at work. This phenomenon is usually associated with the generation of S waves, another process that cannot occur with an ideal explosion. The explanation may be one or a combination of the following: Taylor instabilities in the inelastic region resulting from nonuniformities in the medium, simultaneous release of tectonic strain within the inelastic zone, or triggering actual earthquakes near the explosion. These hypotheses will be discussed in a later section dealing with shear-wave

---

Cohen, T. J., R. L. Sax, and H. L. Husted (1972). Spectral whitening with application to explosion pP. Seismic Data Laboratory Report No. 282, Teledyne Geotech, Alexandria, Virginia.

Carpenter, E. W. (1964). Teleseismic methods for the detection, identification, and location of underground explosions. VESIAC Report 4410-67-X, Acoustics and Seismics Laboratory, University of Michigan, Ann Arbor, Michigan.

Enescu, D., A. Georgesu, D. Jianu, and I. Zamarca (1973). Theoretical model for the process of underground explosions. Contributions to the problem of the separation of large explosions from earthquakes. Bull. Seism. Soc. Am., 73, 765-786.

discriminants. Finally, even if ideal conditions at the source are assumed, seismic background noise hampers the use of this discriminant by masking or confusing first motion direction creating a rather high effective threshold for its application, roughly m_b ~ 5 1/2 according to Evernden (1969). Still, in spite of drawbacks, this discriminant is often irrefutable in identifying earthquakes either when many clear dilatations are recorded or in identifying explosions when complete azimuthal coverage of an event at regional distances fails to show any dilatations.

Shear Waves

Assuming that an ideal explosion is purely a sphere of outward compression and that an earthquake is essentially a shear fracture, identification of explosions should be based upon the absence of shear waves on seismic recordings. However, numerous observations of explosion signals show that they almost always include S-wave motion (e.g., Kisslinger et al., 1961; Willis et al., 1963; Press et al., 1963; Booker and Mitronovas, 1964; Geyer and Martner, 1969; Hattori, 1972; von Seggern, 1972; von Seggern, 1973; and Blandford and Clark, 1974). Vertically-polarized S can be explained by conversion of P at

---

Kisslinger, C., E. J. Mateker, and T. V. McEvilly (1961). SH waves from explosions in soil. J. Geophys. Res., 66, 3487-3497.

Willis, D. E., J. DeNoyer, and J. T. Wilson (1963). Differentiation of earthquakes and underground nuclear explosions on the basis of amplitude characteristics. Bull. Seism. Soc. Am., 53, 979-987.

Geyer, R. C. and S. T. Martner (1969). SH waves from explosive sources. Geophysics, 34, 893-905.

Hattori, S. (1972). Investigation of seismic waves generated by small explosions. Bull. Int. Seismol. Earthquake Engineering, 9, 27-105.

von Seggern, D. (1972). Seismic shear waves as a discriminant between earthquakes and underground nuclear explosions. Seismic Data Laboratory Report No. 295, Teledyne Geotech, Alexandria, Virginia.

von Seggern, D. (1973). Seismic surface waves from Amchitka Island Test Site events and their relation to source mechanism. J. Geophys. Res., 78, 2467-2474.

Blandford, R. and D. Clark (1974). Detection of long-period S from earthquakes and explosions at LASA and LRSM stations with application to positive and negative discrimination of earthquakes and underground explosions. Report No. SDAC-TR-74-15, Teledyne Geotech, Alexandria, Virginia.

interfaces in the earth, but the studies under review here also usually report horizontally-polarized S waves which, because of their arrival time, are likely to be generated only at the source. Observations of LQ surface waves from explosions (e.g., Press et al., 1963; Lambert et al., 1972; Toksöz and Kehrer, 1972b) are also prevalent and, based upon travel time, further attest to a shear-wave generating mechanism at or near the explosion.

Any one of several hypotheses can explain horizontally-polarized shear waves from an explosion. Among these are mode conversion, radiation asymmetry, radial cracking, relaxation of non-uniform prestress, stable sliding on existing faults, and earthquake triggering. Of these, the first three could be operative in a stress-free or hydrostatically stressed environment, while the others require some degree of shear stress in the immediate area of the explosion. Evidence from various explosion sites indicates that no single explanation is usually correct and that explanations may vary with magnitude, depth, and exact location of the detonation. (In addition to our discussion of these effects, see Press and Archambeau (1962), Aki and Tsai (1972), or Toksöz et al. (1971) who may provide additional insight.) In regard to mode conversion of P or SV at irregular interfaces along the travel path, Oliver et al. (1960) early suggested that this mechanism may be responsible for observed LQ waves from underground explosions. Press et al. (1963) also presented

---

Lambert, D. G., E. A. Flinn, and C. B. Archambeau, (1972). A comparative study of the elastic wave radiation from earthquakes and underground explosions. Geophys. J., 29, 403-432.

Toksöz, M. N., and H. H. Kehrer, (1972b). Tectonic strain-release characteristics of CANNIKIN. Bull. Seism. Soc. Am., 62, 1425-1438.

Press, F., and C. Archambeau (1962). Release of tectonic strain by underground nuclear explosions. J. Geophys. Res., 67, 337-343.

Aki, K., and Y.-B. Tsai, (1972). Mechanism of Love-wave excitation by explosive sources. J. Geophys. Res., 77, 1452-1475.

Toksöz, M. N., K. C. Thomson, and T. J. Ahrens (1971) Generation of seismic waves by explosions in prestressed media. Bull. Seism. Soc. Am., 61, 1589-1623.

Oliver, J., P. Pomeroy, and M. Ewing (1960). Long-period surface waves from nuclear explosions in various environments. Science, 131, 1804-1805.

evidence for mode conversion in the case of nuclear detonations in the air. LQ waves observed in the collapse of the MILROW explosion on Amchitka Island (von Seggern, 1973) also indicated some degree of mode conversion since this type of event is presumed to be symmetrical (Smith, 1963). For the Nevada Test Site, however, Brune and Pomeroy (1963) noted minimal LQ waves from several collapses associated with underground detonations where LQ was seen. In all cases the collapse LQ/LR ratios were much less than those for explosions, indicating that mode conversion, if operative, accounts for only a small portion of the SH motion recorded for explosions.

Perhaps the most convincing argument against mode conversion as a cause of explosion SH and LQ waves is the success in inferring double-couple mechanisms for strain release or earthquake triggering by underground nuclear detonations (e.g., Toksöz and Kehrer, 1972a; Aki and Tsai 1972). Random generation of SH motion by mode conversion, well away from the source along the path to the detecting station, could not be expected to result in the type of patterned data that has been reliably inverted in numerous cases to get these mechanisms. Other evidence in the form of dilatational first motions and effects on Rayleigh-wave amplitudes (to be discussed later) integrate well with observed SH and LQ motion to prove that it is generated primarily at the source and not by mode conversion.

Commenting on effects within the source itself, Wright and Carpenter (1962) offered an explanation for the generation of SH by showing the asymmetric plaster casts of cavities formed by small detonations in soft clay. They tentatively explained that the asymmetry was the result of instabilities that arise when a light material (explosion gases) accelerated a heavy one (surround-

---

Smith, S. W. (1963). Generation of seismic waves by underground explosions and the collapse of cavities. J. Geophys. Res. 68, 1477-1483

Brune, J. N., and P. W. Pomeroy (1963). Surface-wave radiation patterns for underground nuclear explosions and small magnitude earthquakes. J. Geophys. Res., 68, 5005-5028.

Wright, J. K., and E. W. Carpenter (1962). The generation of horizontally polarized shear waves by underground explosions. J. Geophys. Res., 67, 1957-1962.

ing solid) as described by Taylor (1950). The theoretical work of Enescu et al. (1973) attempted to model this type of phenomenon by adding three unequal, mutually perpendicular forces to the three mutually perpendicular and equal dipoles ordinarily used for an explosion. Lacking, however, was evidence for the magnitude of this effect in large-scale explosions, and it is most likely small in comparison to other remaining explanations for SH generation.

One remaining explanation of SH generation not requiring non-uniform prestress around the explosion would be the effects of radial cracking that Kisslinger et al. (1961) suggested in reporting on a series of explosions in soil. Grover (1973), on the basis of model experiments, supported radial cracking as the cause of significant SH motion from explosions. Again, evidence of such a mechanism is missing for large-scale nuclear detonations where observable effects in support of some mechanism that requires shear or non-uniform prestress are dominant. Indeed, explanations for SH which invoke no prestress cannot account for a level of SH generation that will hinder discrimination. Only mechanisms associated with a release of non-uniform or shear prestress can generate the high SH and LQ amplitudes, equivalent to or greater than P and LR, which are observed on explosion recordings such as for PILE DRIVER, HARDHAT, BILBY, GREELEY, or BENHAM at the Nevada Test Site.

Press and Archambeau (1962) offered the first of these prestress explanations. It involved relaxation of ambient shear stress within a volume surrounding the explosion cavity where rigidity vanishes ("cavity" includes all of the inelastic zone). However, actual calculations showed that only liberal values of the elastic radius (300 m) and of the ambient stress level ($\sim$10 bars) could account for the observed SH motion from RAINIER. Later, Archambeau (1972) calculated that observed SH motion could be predicted by increasing

---

Taylor, G. I. (1950). The instabilities of liquid surfaces when accelerated in a direction perpendicular to their planes. Proc. Roy. Soc. London, Series A., 201, 192-196.

Grover, A. (1973). Radiation from an explosion in a non-uniformly pre-stressed medium. Geophys. J., 32. 351-371

Archambeau, C. B. (1972). The theory of stress wave radiation from explosions in prestressed media. Geophys. J., 29, 329-366.

the stress level by roughly an order of magnitude and including stress relaxation within a volume having a radius roughly four times the elastic radius of several explosions at the Nevada Test Site. Toksöz et al. (1965) found that HAYMAKER and SHOAL LQ could be accounted for by stress relaxation. Archambeau and Sammis (1970) calculated that the BILBY anomalous radiation field could be satisfied with the stress relaxation theory, if 420 m is assumed for the elastic radius and 75 bars is assumed for the ambient stress level. All these calculations assumed complete stress relaxation.

Archambeau did not specify the actual mechanism of stress relaxation; it could be either isotropic or along specific cracks as Toksöz et al. (1971) have suggested. A further confinement of the stress relaxation about a single plane is a possibility. Separation of this plane from the cavity brings us to the "triggered earthquake" model in which the shear stresses of an explosion trigger a distinct tectonic event. This situation appears to be the case for HARDHAT (Toksöz et al., 1965) and for BENHAM (Aki et al., 1969). In both cases the anomalous radiation field is so large that it dominates the explosion field. Such explosions are characterized by high "F" factors (ratio of tectonic-to-explosion source-function amplitudes --see Toksöz and Kehrer, 1972a). Archambeau (1972) demonstrated the equivalence of the stress relaxation theory to a shear dislocation commonly used in models of earthquake source mechanisms. Thus this theory, corrected by Snoke (1976), is probably compatible with most observations of SH waves from explosions, regardless of the actual release

---

Toksöz, M. N., D. G. Harkrider, and A. Ben-Menahem (1965). Determination of source parameters by amplitude equalization of seismic surface waves. 2. Release of tectonic strain by underground nuclear explosions and mechanisms of earthquakes. J. Geophys. Res., 70, 907-922.

Archambeau, D. B., and C. Sammis (1970). Seismic radiation from explosions in prestressed media and the measurement of tectonic stress in the earth. Rev. Geophys., 8, 473-499.

Aki, K., P. Reasenberg, T. DeFazio, and Y.-B. Tsai (1969). Near-field and far-field seismic evidences for triggering of an earthquake by the BENHAM explosion. Bull. Seism. Soc. Am., 59, 2197-2207.

Snoke, J. A. (1976). Archambeaus's elastodynamic source model solution and low-frequency peaks in the far-field displacement amplitude from earthquakes and explosions. Geophys. J., 44, 27-44.

mechanism. Consequently, the usual double-couple model of earthquake source mechanisms can be applied to SH and LQ observations from explosions.

A considerable number of studies support the accuracy of the tectonic strain release model, and among them are numerous successful interpretations of SH and Love waves from explosions (Toksöz et al., 1965; Brune and Pomeroy, 1963; Nuttli, 1969; Lambert et al., 1972; Hirasawa, 1971; Toksöz et al., 1971). Much evidence also exists to support the generation of patterns like those observed from underground nuclear explosions from model experiments with explosions in prestressed sheets of material (Kim and Kisslinger, 1967; Grover, 1973; and Toksöz et al., 1971). Observations of fault displacements (McKeown and Dickey, 1969) near the explosion site further support tectonic strain release as the cause of observed SH and LQ waves from explosions. In addition, the periodic and natural release of accumulated strain in the crust at the Nevada Test Site by shallow earthquakes (Molnar et al., 1969; Slemmons et al., 1965) also supports tectonic strain release by explosions in this area.

However, exceptions to the theory exist, notably the Amchitka Island test site which is aseismic (considering only shallow crustal seismicity at Amchitka). Toksöz and Kehrer (1972b) calculated F factors for the MILROW and CANNIKIN explosions equal to ones for typical large explosions at the Nevada

---

Nuttli, O. W. (1969). Travel times and amplitudes of S waves from nuclear explosions in Nevada. Bull. Seism. Soc. Am., 59, 385-398.

Hirasawa, T., (1971). Radiation patterns of S waves from underground nuclear explosions. J. Geophys. Res., 76, 6440-6454.

Kim, W. H., and C. Kisslinger (1967). Model investigations of explosions in prestressed media. Geophysics, 32, 633-651.

McKeown, F. A., and D. D. Dickey (1969). Fault displacements and motion related to nuclear explosions. Bull. Seism. Soc. Am., 59, 2253-2270.

Molnar, P., K. Jacob, and L. R. Sykes (1969). Microearthquake activity in eastern Nevada and Death Valley, California, before and after the nuclear explosion BENHAM. Bull. Seism. Soc. Am., 59, 2177-2184.

Slemmons, D. B., A. E. Jones, and J. I. Gimlett (1965). Catalog of Nevada earthquakes, 1852-1960. Bull. Seism. Soc. Am., 55, 537-583.

Test Site. The cause of the large LQ waves from Amchitka shots is not clear. Toksöz and Kehrer (1972a) also inferred strain release at the Kazakh and Novaya Zemlya test sites. Although the F factors for these regions are in the same range as NTS shots, strain release is unexpected; and other mechanisms which do not require shear prestress are probably responsible for SH generation.

One other model to be considered is that of Andrews (1973), who studied stable sliding on pre-existing faults. This sliding resulted from reduced normal stresses on faults caused by passage of compressional waves or the interaction of the surface reflection with the primary P wave, like for spalling occurrences (Eisler et al., 1966). This model is also a trigger model, but differs from Toksöz and Kehrer's because only compressional waves are required and because tension forces, not shear forces, are considered as critical on the fault. Andrews shows the feasibility of his model with numerical finite-difference calculations.

Despite the less than ideal behavior of explosions in terms of S waves, discrimination work has often successfully focused on these waves. Willis et al. (1963) reported that S/P amplitude ratios for explosions at the NTS were roughly one-third of that for earthquakes in the surrounding region. Press et al. (1963) and Booker and Mitronovas (1964) also showed that SH and LQ are lower for explosions than earthquakes in this region. Evernden (1969), in examining recordings from all known nuclear explosions through 1966, found only two long-period S waves and concluded that the difference in generation of long-period S for equivalent m_b earthquakes and explosions must be at least an order of magnitude. Nuttli (1969), in a comprehensive analysis of LRSM and WWSSN recordings of HALFBEAK and GREELEY, reported 131 long-period S waves, which gave magnitudes roughly one unit less than the short-period P-wave magnitudes for these two events. Blandford and Clark (1974) reported 40 long-period S measurements from several large shots at NTS and Amchitka Island and suggested that long-period S-wave magnitude versus M_s is a good discriminant. However, because m_b

---

Andrews, D. J. (1973). A numerical study of tectonic strain release by underground explosions. Bull. Seism. Soc. Am., 63, 1375-1391.

Eisler, J. D., F. Chilton, and F. M. Sauer (1966). Multiple subsurface spalling by underground nuclear explosions. J. Geophys. Res., 71, 3023-3027.

versus M_s is an excellent discriminant, m_b versus long-period S-wave magnitude should be as good or even better. By reviewing Seismic Data Laboratory reports on NTS shots and LRSM and VELA Observatory earthquake bulletins, histograms of S-wave amplitude over P-wave amplitude for earthquakes and explosions have been constructed as shown in Figure 1 (details of the data base can be found in von Seggern, 1972). Although the explosion sample is very small, because of the limitation of background noise, the sample is not biased. In fact, the true density may lie toward lower ratios. Distribution for a subset of large earthquakes is shown separately to prove that the earthquake histograms are unbiased by threshold problems. Roughly an order of magnitude separation appears for both cases between explosions and earthquakes. Although noise obviously hampers application of this discriminant, recent advances in the theory of negative discriminants (identification by absence of an observation) should extend its usefulness to lower magnitudes.

Because LQ waves are representative of the long-period SH spectrum, they will also serve as useful discriminants. Pertinent to this supposition, another histogram from von Seggern (1972) is shown in Figure 2. The explosions are again from NTS where known tectonic strain release repeatedly generates significant LQ waves, and evidently little separation exists between observed LQ/LR ratios for earthquakes and explosions from this area. However, since LR, in terms of M_s, is an excellent discriminant, LQ is inferred to be as good or better, especially for shots where tectonic strain release is not as great as at NTS. Savino et al. (1971) demonstrated this theory by estimating M_s for many events from both the LQ and the LR waves. Further discriminating information exists in the spectra of the LQ waves because apparently there is relatively more long-period energy in the LQ waves than the LR waves from NTS events (Lambert et al., 1972; Toksöz et al., 1971), indicating a tectonic origin for the LQ waves as opposed to the dominantly explosive origin for the LR waves. As for S waves, noise hampers application of LQ discriminants and suggests that negative discrimination should be employed.

---

von Seggern, D. H. (1972). Seismic shear waves as a discriminant between earthquakes and underground nuclear explosions. Seismic Data Laboratory Report No. 295, Teledyne Geotech, Alexandria, Virginia.

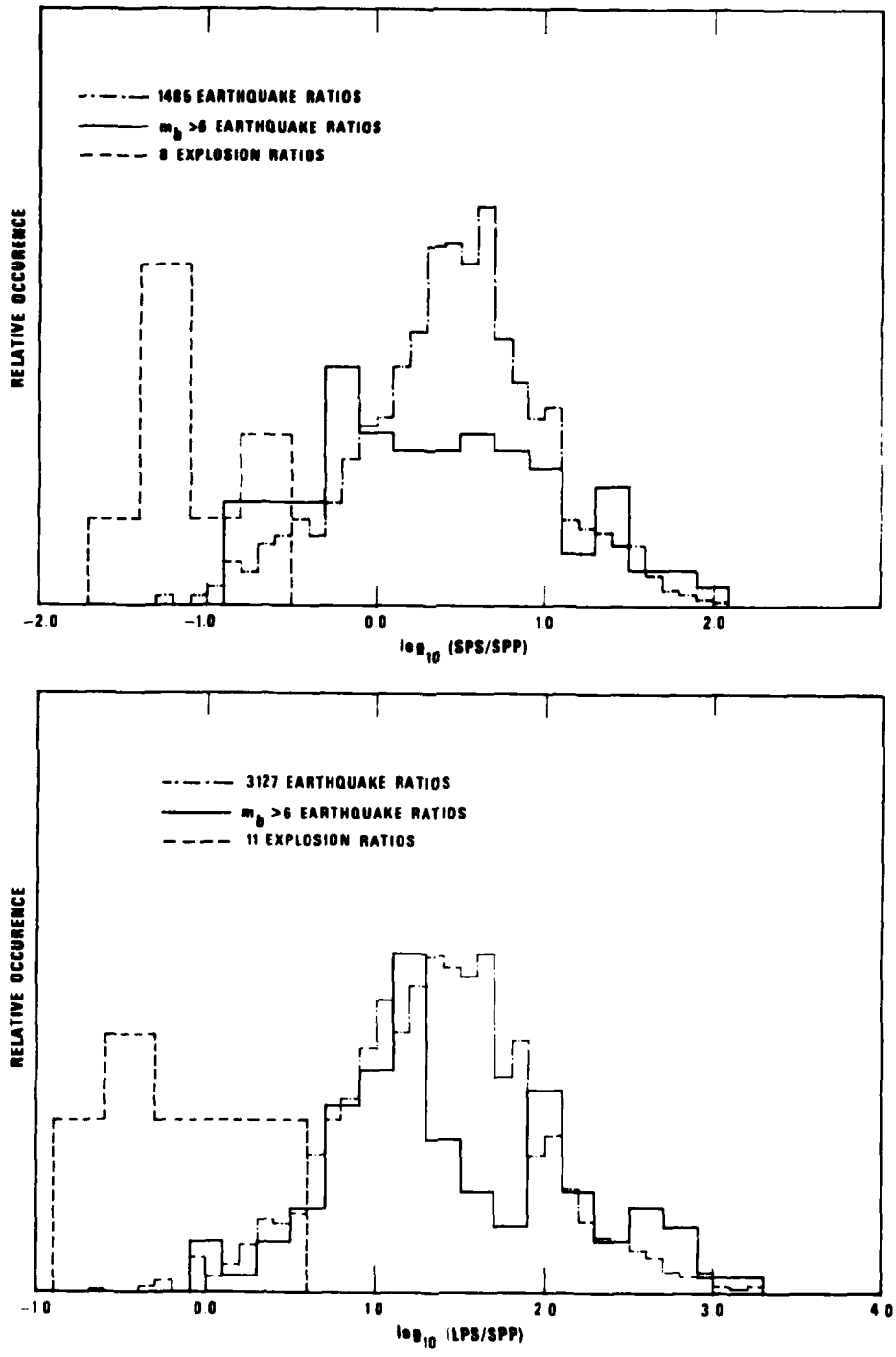

Figure 1 Ratios of shear-wave amplitude to compressional-wave amplitude for NTS explosions and global earthquakes.

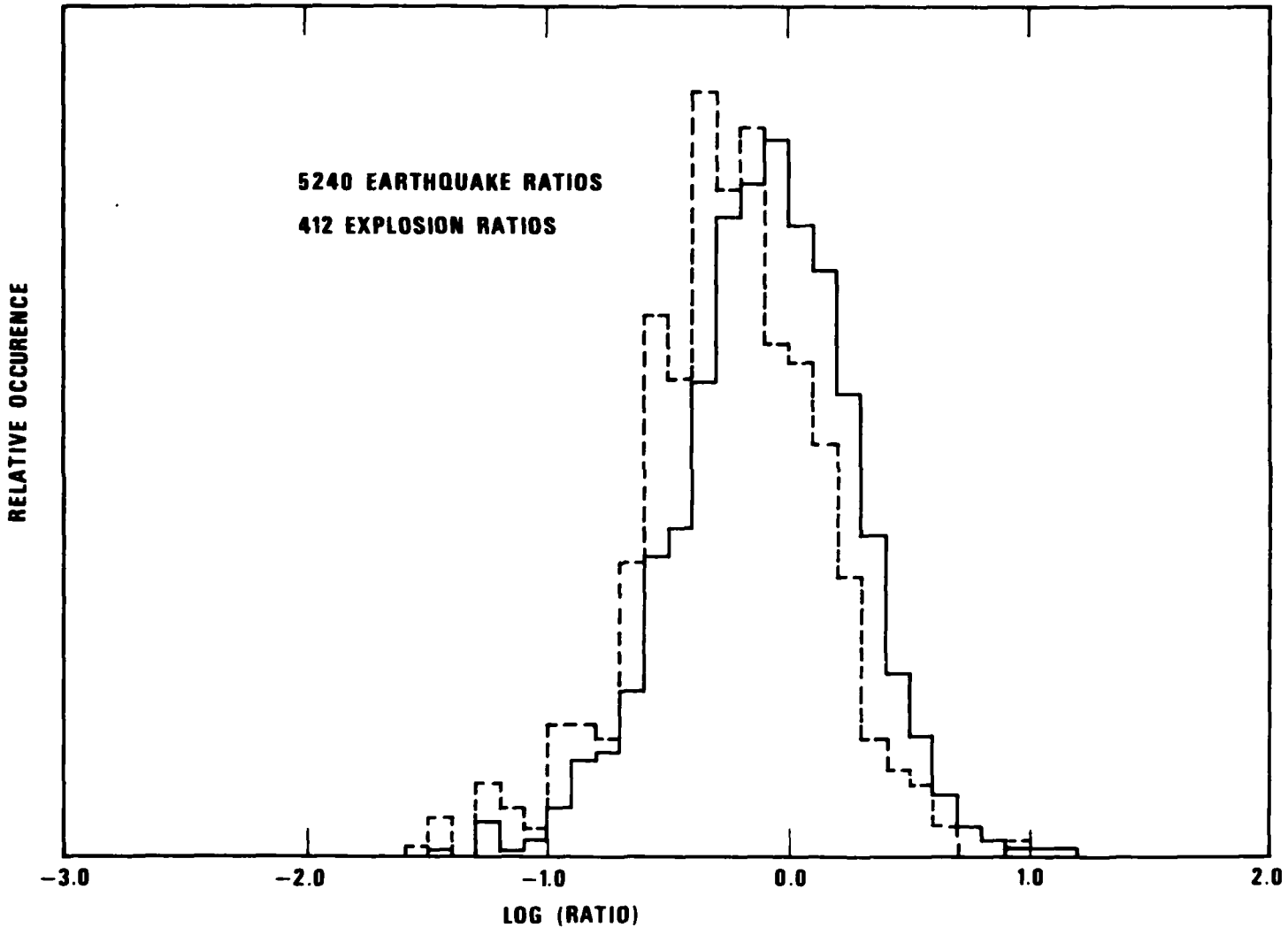

Figure 2 LQ/LR amplitude ratios for NTS explosions and global earthquakes.

M_s versus m_b

This discriminant not only gives excellent results in separating earthquakes and explosions, with a low probability of misidentification (Ericsson, 1970; Weichert and Basham, 1973), but it is also easy to estimate routinely. Normal application involves calculating m_b from the short-period P-wave amplitude near the first arrival and M_s from the long-period LR amplitude near a period of 20 seconds. A number of variations have been investigated, including: 1) AR-- a measure of the envelope area of the LR wave (Brune and Pomeroy, 1963); 2) ERZ-- an integral of the energy spectrum of the LR wave (Lambert et al., 1969); 3) M_o-- a measure of the source moment from long-period signals (Hanks and Thatcher, 1972); 4) M_s (40)-- an estimate of M_s at a period near 40 seconds rather than 20 seconds (Savino et al., 1971). Since these variations are nearly equivalent to the normal M_s-versus-m_b discriminant in that they all represent the generation of long-period LR waves relative to short-period P waves, they will not be discussed separately.

Reasons for the success of M_s versus m_b can be organized into four categories: 1) source geometry; 2) source location; 3) time dimensions of the source; and 4) spatial dimensions of the source. Table I lists these categories along with some of the more important references contributing to the understanding of each.

Beginning with elementary concepts, first considered are the effects on M_s-versus-m_b of the geometry of simple force systems representative of explosions and earthquakes. The uniform compression of an explosion in a cavity can be modeled with three mutually perpendicular and equal couples without

---

Ericsson, U. A. (1970). Event identification for test ban control. Bull. Seism. Soc. Am., 60, 1521-1546.

Weichert, D. H., and P. W. Basham (1973). Deterrence and false alarms in seismic discrimination. Bull. Seism. Soc. Am., 63, 1119-1132.

Hanks, T. C., and W. Thatcher (1972). A graphical representation of seismic source parameters. J. Geophys. Res., 77, 4393-4405.

TABLE I

Possible Causes of the M_S-m_b Separation

Cause	Proponents	Additional Discussions
Source Equivalent Forces	Gilbert (1973) Douglas et al. (1971) Leet (1962)	Press et al. (1963) Douglas et al. (1972b) Tsai and Aki (1971) Rodean (1971)
Source Time Function	Davies and Smith (1968) Marshall (1970) Molnar (1971) Peppin and McEvilly (1974)	Peppin (1976) McEvilly and Peppin (1972) Liebermann and Pomeroy (1969) Savino et al. (1971) Tsai and Aki (1971) Aki (1972) Muller (1973) Aki et al. (1974) Kogeus (1968) Toksöz et al. (1964)
Source Depth	Hudson and Douglas (1975)	Douglas et al. (1971) Douglas et al. (1972b)
Source Dimensions	Liebermann and Pomeroy (1969) Liebermann and Pomeroy (1970) Wyss et al. (1971) Evernden (1975)	Peppin (1976) Aki (1972)

moment (Love, 1944; Maruyama, 1963). An earthquake can be modeled with two such couples with equal, but opposite, moment (Maruyama, 1963; Burridge and Knopoff, 1964). The far-field amplitudes for these sources will be expressed in terms of the quantity moment.

The relative excitation of P waves for the two types of sources will be computed on the basis of the long-period portion of the spectra. Thus, the result will have validity only for m_b measured at frequencies lower than the corner frequencies that characterize each spectrum. For an earthquake, the source modeled (as described above) gives the far-field P-wave spectral amplitude as (Randall, 1973; Dahlen, 1974)

$$\hat{u}_p^Q (\omega \to o) = \frac{M_o^Q R_{\theta\phi}}{4\pi\rho\alpha^3 r}$$

in a homogeneous infinite medium, where M_o^Q is the moment of one of the two equivalent, orthogonal couples, ρ is density, α is compressional velocity, r is distance, and $R_{\theta\phi} = \sin 2\theta \cos\phi$ is the radiation pattern with θ and ϕ the polar and meridian angles of a spherical coordinate system with ϕ in the plane of the fault. For an explosion model, the far-field spectral amplitude is (Muller, 1973)

$$\hat{u}_p^X (\omega \to 0) = \frac{M_o^X}{4\pi\rho\alpha^3 r}$$

Love, A. E. H. (1944). A Treatise on the Mathematical Theory of Elasticity. New York, Dover Publications.

Maruyama, T. (1963). On the force equivalents of dynamic elastic dislocation with reference to the earthquake mechanism. Bull. Earthquake Res. Inst., 41, 467-486.

Burridge, R., and L. Knopoff (1964). Body force equivalents for seismic dislocations. Bull. Seism. Soc. Am., 54, 1875-1888.

Randall, M. J. (1973). The spectral theory of seismic sources. Bull. Seism. Soc. Am., 63, 1133-1144.

Dahlen, F. A. (1974). On the ratio of P-wave to S-wave corner frequencies for shallow earthquake sources. Bull. Seism. Soc. Am., 64, 1159-1180.

Muller, G. (1973). Seismic moment and long-period radiation of underground nuclear explosions. Bull. Seism. Soc. Am., 73, 847-857.

where M_o^X is the strength of one of three mutually perpendicular dipoles. If the moments of the two sources are equal a simple ratio is defined:

$$\frac{\hat{u}_p^Q\ (\omega\to 0)}{\hat{u}_p^X\ (\omega\to 0)} = R_{\theta\phi}\ \frac{(\rho\alpha^3)^X}{(\rho\alpha^3)^Q}$$

Of special interest is the rms value of $R_{\theta\phi}$, that is, a value representing a fairly uniform sampling of the focal sphere by a network of stations estimating m_b for the earthquake. Thus, $R_{\theta\phi}^2$ is integrated over the surface of a sphere (Appendix I) to get $\overline{R_{\theta\phi}^2} = 4/15$ for P waves. In practice $R_{\theta\phi}$ is undoubtedly overestimated because stations near nodes do not detect the P wave. Thus, the result for events of equal moment is

$$\hat{u}_p^Q\ (\omega\to 0) \approx .52\ \hat{u}_p^X\ (\omega\to 0)\ \frac{(\rho\alpha^3)^X}{(\rho\alpha^3)^Q} \qquad (1)$$

The difference in Rayleigh-wave excitation for the two sources, due to source type alone, can be calculated by taking the theoretical excitation expression for a double-couple from Ben-Menahem and Harkrider (1964)

$$\hat{w}_R^Q = M_o^Q k^{\frac{1}{2}} A_R \frac{W_h}{W_o} \left| \chi(\theta,\lambda,\delta,h) \right| \frac{1}{(2\pi r)^{\frac{1}{2}}}$$

where W are vertical displacements on a plane-layered earth model, k is wavenumber, A_R is the spectral amplitude response of a layered medium, and $|\chi(\theta,\lambda,\delta,h)|$ is the radiation-pattern factor at a particular azimuth θ for a fault with slip angle λ and dip angle δ at a depth h. The corresponding explosion expression, given by Harkrider (1964), can be approximated for a source near the surface by

$$\hat{w}_R^X \approx 2\pi P_o\ a^3 k^{\frac{1}{2}} A_R\ \epsilon_h \frac{1}{(2\pi r)^{\frac{1}{2}}}$$

Ben-Menahem, A., and D. G. Harkrider (1964). Radiation patterns of seismic surface waves from buried dipolar point sources in a flat stratified earth. J. Geophys. Res., 69, 2605-2620.

Harkrider, D. G. (1964). Surface waves in multilayered elastic media, I. Rayleigh and Love waves from buried sources in a multilayered elastic half-space. Bull. Seism. Soc. Am., 54, 627-679.

where P_o is the residual pressure, a is the radius of the inelastic-elastic boundary near the source, and ε_h is Rayleigh-wave ellipticity at the shallow source depth h. The elementary relation between pressure P_o in the cavity of radius a and the moment of the explosion is given by Love (1944, p. 187)

$$M_o^X = \frac{P_o\, a^3 \pi \alpha^2}{\beta^2}$$

Thus, we have for the explosion

$$\hat{w}_R^X \approx 2M_o^X k^{\frac{1}{2}} A_R \frac{\varepsilon_h \beta^2}{\alpha^2} \frac{1}{(2\pi r)^{\frac{1}{2}}}$$

Again, assuming equal M_o for the two types of sources, the ratio of Rayleigh-wave amplitudes is

$$\frac{\hat{w}_R^Q}{\hat{w}_R^X} \approx \frac{1}{2} \left| \frac{W_h}{W_o} \chi_R(\theta,\lambda,\delta,h) \right|_{h = h^Q} \left| \frac{\alpha^2}{\varepsilon_h \beta^2} \right|_{h = h^X} \quad (2) \qquad (2)$$

This relation is given in equivalent form for a homogeneous half-space by Douglas et al. (1974a). Just as for the earthquake P wave, the rms of the radiation pattern factor χ_R is adopted, which is given in Ben-Menahem and Harkrider (1964). To get rms χ_R one integrates the expression for all values of slip angle λ and dip angle δ, as well as θ; from Appendix I the result of this integration for a surface source at a period of 20 seconds where M_s is commonly estimated is

$$\overline{\left|\chi_R(\theta,\lambda,\delta)\right|}_{h = 0} \approx \frac{\varepsilon_o}{2} \sqrt{\frac{7}{2} - \frac{8\beta^2}{\alpha^2} + \frac{16\beta^4}{3\alpha^4}}$$

Substituting this in equation (2), using $\alpha = 6.03$ and $\beta = 3.53$ for a Gutenberg earth model, and letting $\varepsilon_o = .67$ for 20-second Rayleigh waves in a Gutenberg earth model, one obtains

$$\hat{w}_R^Q \approx .86\, \hat{w}_R^X \qquad (h \approx 0) \qquad (3)$$

This equation is an approximation for near-surface sources modeled by simple equivalent force systems, and it does not include depth effects or effects

---

Douglas, A., J. B. Young, and J. A. Hudson (1974a). Complex P-wave seismograms from simple earthquake sources. Geophys. J., 37, 141-150.

due to extended time or space dimensions for the source. Combining equations (1) and (3) and taking logarithms, the theoretical $M_s - m_b$ difference is produced for events having arbitrary moments, not necessarily equal, and near the surface in the same medium:

$$(M_s - m_b)^Q \approx (M_s - m_b)^X + .22$$

or for events of equal m_b

$$M_s^Q \approx M_s^X + .22 \qquad (4)$$

This result differs from Gilbert's (1973), who, in a derivation that was elegant but still dependent upon several crucial but not obviously reasonable approximations, predicted $M_s^Q \approx M_s^X + .52$. The derivation here is considered more appropriate because it takes into account the exact theoretical excitation for Rayleigh waves in a layered earth model due to simple point sources. Explosions generate nearly as large Rayleigh waves (factor of 1.7 less) as do typical shallow earthquakes because, although the earthquake mechanism produces additional S waves and, therefore, presumably more Rayleigh waves, much of this additional S is instead converted to Love waves. If equation (4) is approximately true, then a need exists to find through other considerations realistic causes of the large M_s difference which is usually observed to be roughly one magnitude unit or more between earthquakes and explosions of equivalent m_b. Note that an alternative is to consider the cause of the m_b difference at equivalent M_s. Although the procedure followed in the derivation of equation (4) was to take the logarithm of the rms amplitude whereas, in practice, M_s and m_b are calculated by taking the arithmetic mean of the logarithms of the amplitudes, the result should not be affected greatly by considering instead this second method of calculation, which must be treated numerically rather than analytically.

Effects of Source Depth on M_s versus m_b

To evaluate how depth of source affects the $M_s - m_b$ relation through the body-wave and Rayleigh-wave amplitude, equations (1) and (2) can be generalized to any depth by using the appropriate depth-dependent parameters. The explosion source will be kept at the surface while evaluating $|\chi_R(\theta,\lambda,\delta,h)|$, given

in Appendix I, for some discrete depths in a Gutenberg earth model used by Ben-Menahem and Harkrider (1964). The rms radiation will be used again for Rayleigh waves since interest lies in gross dependence on depth. Also evaluated is the rms Love-wave radiation as expressed in Appendix I. According to Harkrider, the actual excitation ratio of Love and Rayleigh waves for a double-couple point source is dependent on the factors A_L, A_R, k_R, and k_L, thus

$$\frac{\hat{V}_L^Q}{\hat{W}_R^Q} = \frac{k_L^{\frac{1}{2}} A_L \frac{V_h}{V_o} \mid \chi_L(\Theta) \mid}{k_R^{\frac{1}{2}} A_R \frac{W_h}{W_o} \mid \chi_R(\Theta) \mid}$$

The results of these computations for a period of 20 seconds are listed in Table II. The factor $k_L^{1/2} A_L / k_R^{1/2} A_R$ is .86 for this case. Figures 3, 4, and 5 illustrate the essential $M_s - m_b$ character as the earthquake becomes more deeply located. Figures 3 and 4 show that the near equivalence of M_s values for a surface explosion and a surface earthquake of equal moment still holds at earthquake depths of 30 km and that the LQ/LR ratio for earthquake is on the order of one near the surface but nearer two at depth. This result provides evidence that much of the S-wave excitation of earthquake sources is converted into Love waves, making it unavailable to increase Rayleigh-wave amplitude relative to that of an explosion. Figure 4 illustrates the strong influence of the $\rho\alpha^3$ factor on P-wave amplitude. Bouchon (1976) and Hudson and Douglas (1975) have emphasized this effect in regards to $M_s - m_b$ discrimination and yield estimation. Figure 5 illustrates the predicted effect of depth on the $M_s - m_b$ discriminant in a realistic Gutenberg earth model. All explosion calculations here were made for zero depth, but evaluation for this earth model of the full explosion factor of Harkrider (1964) to depths of 4 or 5 kilometers would not alter this figure's predictions by more than 20%. Figure 5 indicates that earthquake depth does not improve the $M_s - m_b$ discriminant much and that, in fact, for a certain range of shallow depths, the rms Rayleigh-wave excitation of earthquakes is diminished. Note that the Gutenberg model contains no low-velocity sediment layers near the surface. (Later in this report a model appropriate to the Southwestern United States, that has such layers, will be examined.)

Bouchon, M. (1976). Teleseismic body wave radiation from a seismic source in a layered medium. Geophys. J., 47, 515-530.

Hudson, J. A., and A. Douglas (1975). On the amplitudes of seismic waves. Geophys. J., 42, 1039-1044.

TABLE II

Theoretical Calculations of Surface-Wave and Body-Wave Excitation in a Gutenberg Earth Model

QUAKE DEPTH (km)	1	2	3	4	5	6
0.	0.516	0.354	0.395	0.894	0.858	0.221
1.	0.516	0.354	0.330	0.072	0.727	0.149
2.	0.516	0.354	0.283	1.250	0.629	0.086
3.	0.516	0.354	0.246	1.440	0.550	0.028
4.	0.516	0.355	0.223	1.595	0.501	-0.013
5.	0.516	0.356	0.216	1.647	0.484	-0.028
6.	0.516	0.357	0.220	1.627	0.489	-0.024
7.	0.516	0.359	0.233	1.542	0.515	-0.001
8.	0.516	0.360	0.254	1.418	0.559	0.034
9.	0.516	0.362	0.274	1.323	0.593	0.060
10.	0.516	0.365	0.297	1.227	0.632	0.088
11.	0.516	0.367	0.323	1.136	0.676	0.117
12.	0.516	0.370	0.352	1.051	0.724	0.147
13.	0.516	0.373	0.375	0.994	0.752	0.163
14.	0.516	0.377	0.401	0.941	0.782	0.180
15.	0.516	0.381	0.428	0.891	0.812	0.197
16.	0.516	0.386	0.457	0.844	0.844	0.213
17.	0.516	0.391	0.481	0.813	0.859	0.221
18.	0.516	0.397	0.506	0.784	0.874	0.229
19.	0.516	0.403	0.534	0.756	0.889	0.236
20.	0.516	0.411	0.564	0.729	0.905	0.244
21.	0.479	0.412	0.564	0.731	0.873	0.260
22.	0.446	0.413	0.565	0.731	0.844	0.277
23.	0.415	0.415	0.568	0.730	0.816	0.294
24.	0.387	0.416	0.572	0.727	0.791	0.311
25.	0.361	0.418	0.579	0.723	0.767	0.328
26.	0.349	0.422	0.591	0.713	0.753	0.334
27.	0.349	0.428	0.610	0.701	0.745	0.330
28.	0.349	0.434	0.630	0.690	0.738	0.325
29.	0.349	0.442	0.652	0.678	0.731	0.321
30.	0.349	0.450	0.676	0.666	0.723	0.317
31.	0.349	0.460	0.703	0.654	0.716	0.312
32.	0.349	0.470	0.732	0.642	0.709	0.308
33.	0.349	0.483	0.765	0.631	0.702	0.303
34.	0.317	0.469	0.733	0.640	0.646	0.309
35.	0.288	0.457	0.704	0.650	0.595	0.315
36.	0.263	0.447	0.678	0.659	0.549	0.320
37.	0.240	0.439	0.656	0.669	0.506	0.324
38.	0.220	0.431	0.636	0.678	0.468	0.328
39.	0.202	0.425	0.618	0.687	0.433	0.332
40.	0.185	0.419	0.603	0.696	0.400	0.334
41.	0.185	0.418	0.609	0.687	0.390	0.324

TABLE II (Continued)

Theoretical Calculations of Surface-Wave and
Body-Wave Excitation in a Gutenberg Earth Model

42.	0.185	0.417	0.616	0.677	0.381	0.313
43.	0.185	0.416	0.624	0.667	0.371	0.302
44.	0.185	0.415	0.633	0.657	0.361	0.290
45.	0.185	0.414	0.642	0.645	0.352	0.279
46.	0.185	0.413	0.652	0.634	0.342	0.267
47.	0.186	0.412	0.660	0.624	0.333	0.254
48.	0.187	0.413	0.668	0.618	0.324	0.240
49.	0.188	0.413	0.676	0.612	0.315	0.226
50.	0.189	0.414	0.684	0.605	0.306	0.211

1 P-WAVE SPECTRAL AMPLITUDE RATIO u_p^Q/u_p^X

2 ROOT MEAN SQUARE OF 20-SECOND LOVE WAVE RADIATION PATTERN χ_L

3 ROOT MEAN SQUARE OF 20-SECOND RAYLEIGH WAVE RADIATION PATTERN χ_R

4 RATIO (rms χ_L/rms χ_R)

5 RAYLEIGH WAVE SPECTRAL AMPLITUDE RATIO (rms w_R^Q/rms w_R^X)

6 M_s-m_b DIFFERENCES: $(M_s-m_b)^Q - (M_s-m_b)^X$

Note: Explosion is near surface.

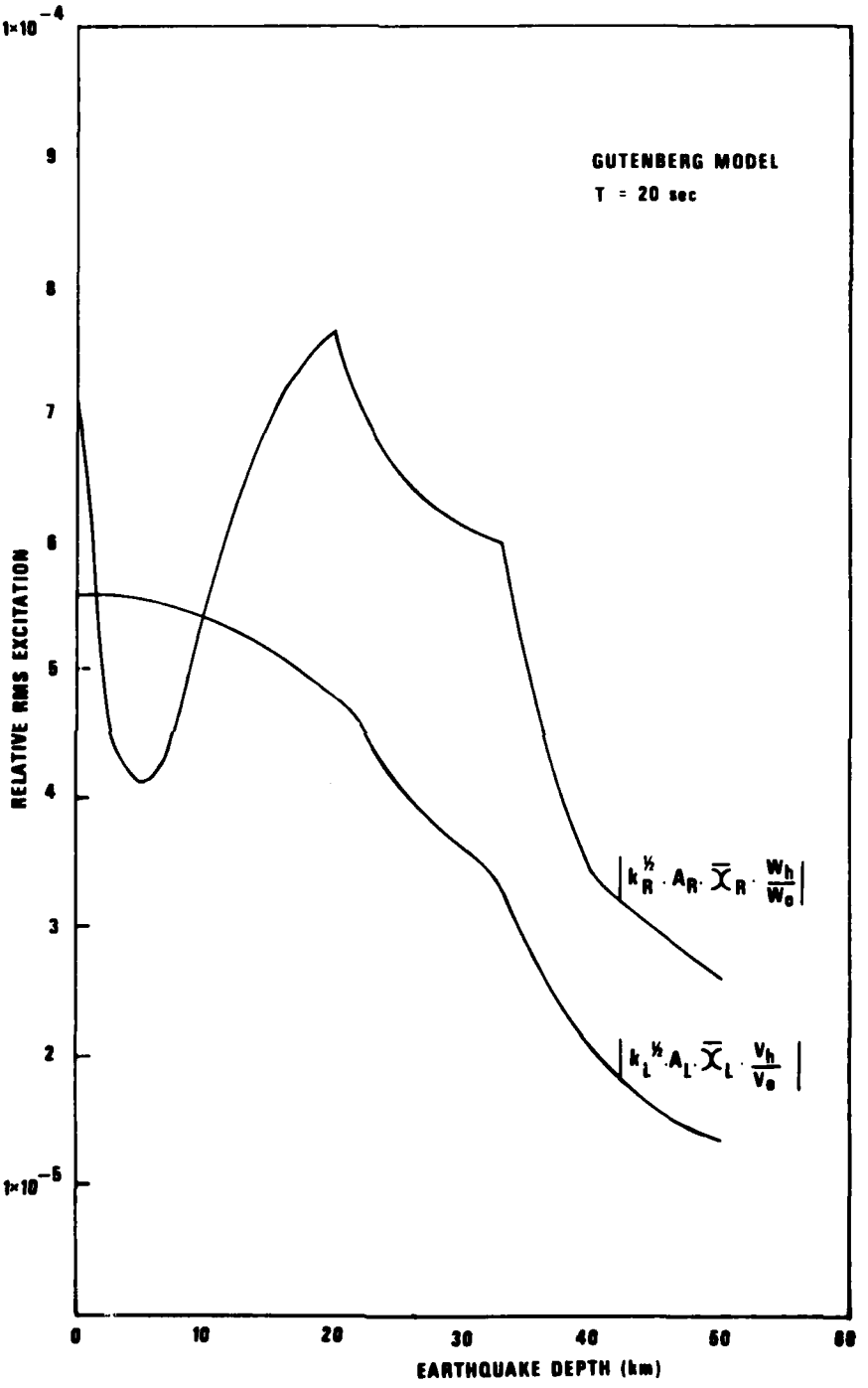

Figure 3 Predicted LQ and LR rms excitation versus depth for an earthquake in a Gutenberg earth model.

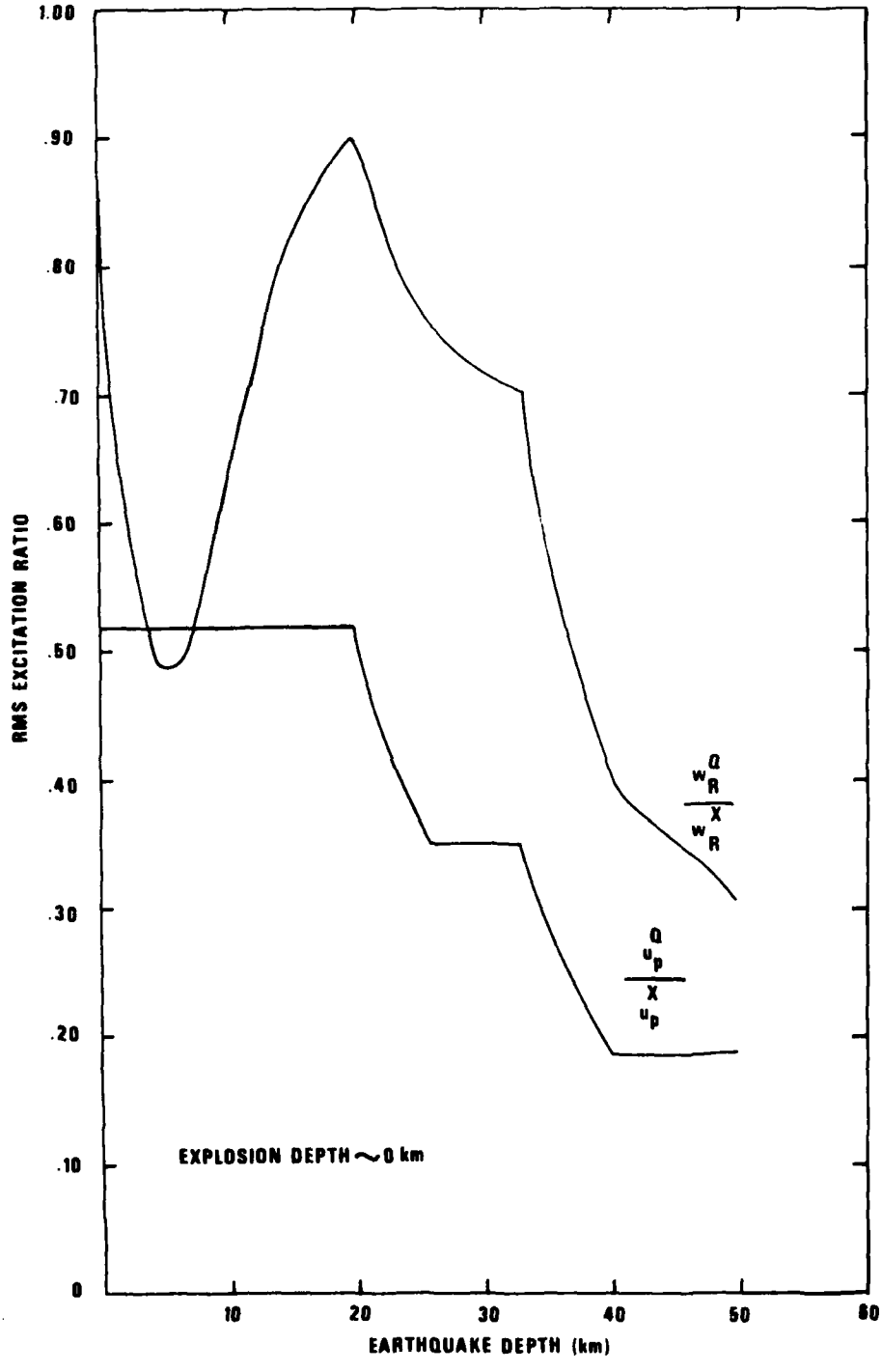

Figure 4 Ratio of earthquake surface-wave and body-wave rms excitation to that of an equivalent-moment explosion near the surface versus depth in the Gutenberg earth model.

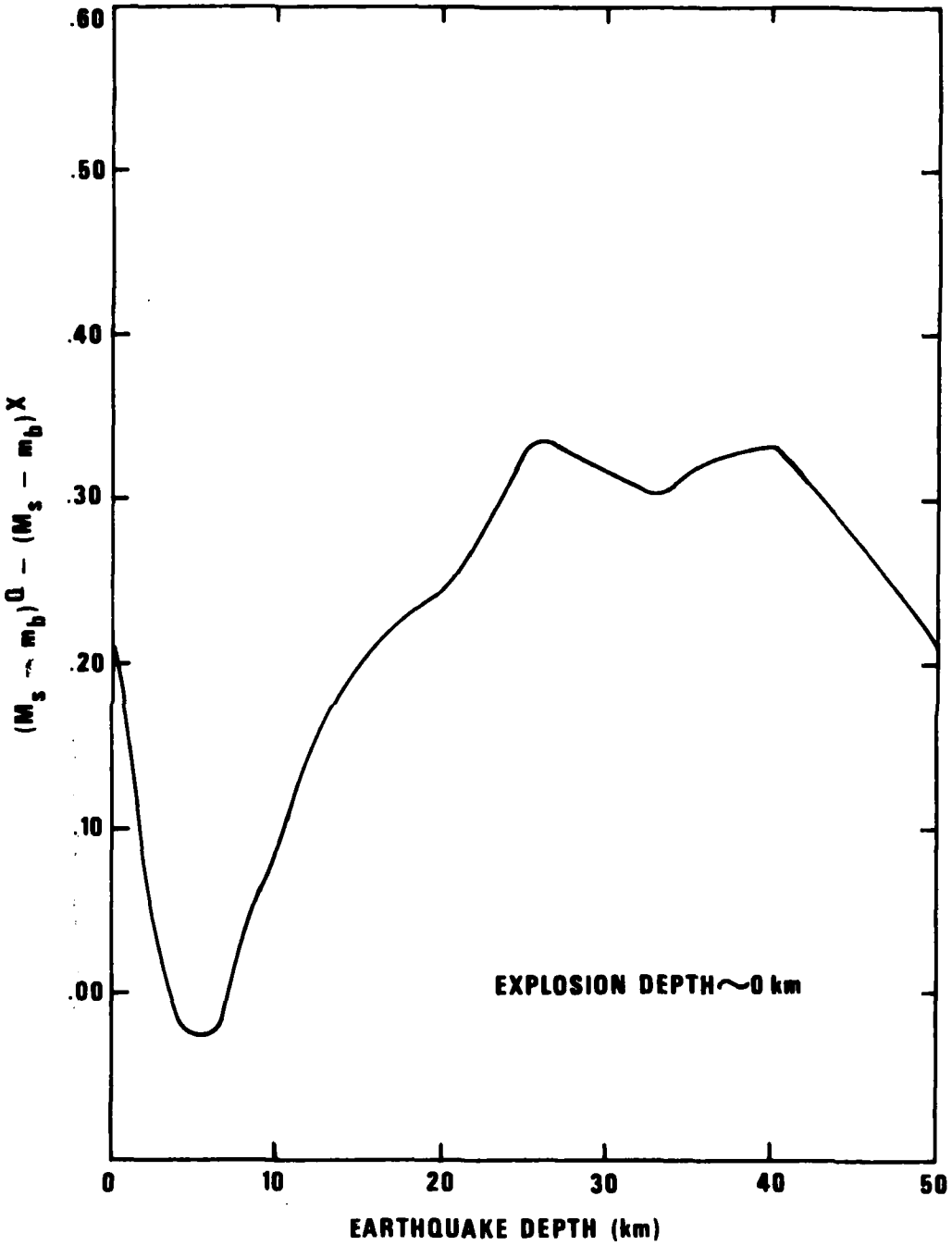

Figure 5 Predicted M_S-m_b difference versus depth between earthquakes and explosions of equal moment in a Gutenberg earth model.

The effect of the pP interaction on m_b must also be considered, but only for very shallow events. This is true because m_b is typically measured within the first five seconds of a P-wave signal, and so the free-surface effect on m_b measured from short-period recordings can be neglected for events deeper than roughly ten kilometers. Assuming zero-degree incidence for explosions, the free-surface reflection is simply the P signal reversed in polarity and equal in amplitude. Clearly, since the P radiation pattern is uniform from an explosion and the basic signal pulse is only one cycle, the pP can raise or lower m_b only if it arrives within this first cycle. Douglas et al. (1971) have adequately discussed the effect: for zero time delay of the pP (explosion right at the surface), the P signal will be cancelled. For a time delay equal to roughly one-half cycle, the P signal will be reinforced and nearly doubled in amplitude. Figure 6 shows a progression of cases using a signal synthesized for a 10 kt shot as recorded by a short-period Benioff seismometer over a path with $t^* = .74$. Because of inelastic effects near the detonation, the cancelling of P motion for zero-depth explosions is unrealistic; and, in fact, the equivalent source approaches a downward point force applied at the surface, rather than a uniform compressional force (Kisslinger et al., 1961). Douglas et al. (1971) also indicated the effect of the free surface on earthquake m_b. Here the situation is more complicated because, for events shallow enough to have pP recorded within the first five seconds of the direct P, the m_b measurement will undoubtedly reflect the larger of the two waves. Thus, receivers on or near a node of the P-wave radiation pattern may be situated so that the pP is large and thus still report a normal or high m_b for the earthquake. Therefore, free-surface reflection will produce some anomalies in m_b for shallow earthquakes. Averaged over a well-distributed network, the surface reflection effect for earthquakes should be to increase m_b at most one or two tenths, and at worst it will do no more than increase the explosion m_b by three tenths. In summary, depth effects on P-wave shape cannot significantly contribute to separation of earthquakes and explosions on $M_s - m_b$ plots.

Douglas, A., J. A. Hudson, and V. K. Kembhavi (1971). The relative excitation of seismic surface and body waves by point sources. J. Geophys. Res., 23, 451-460.

Kisslinger, C., E. J. Mateker, and T. V. McEvilly (1961). SH waves from explosions. Nature, 253, 242-245.

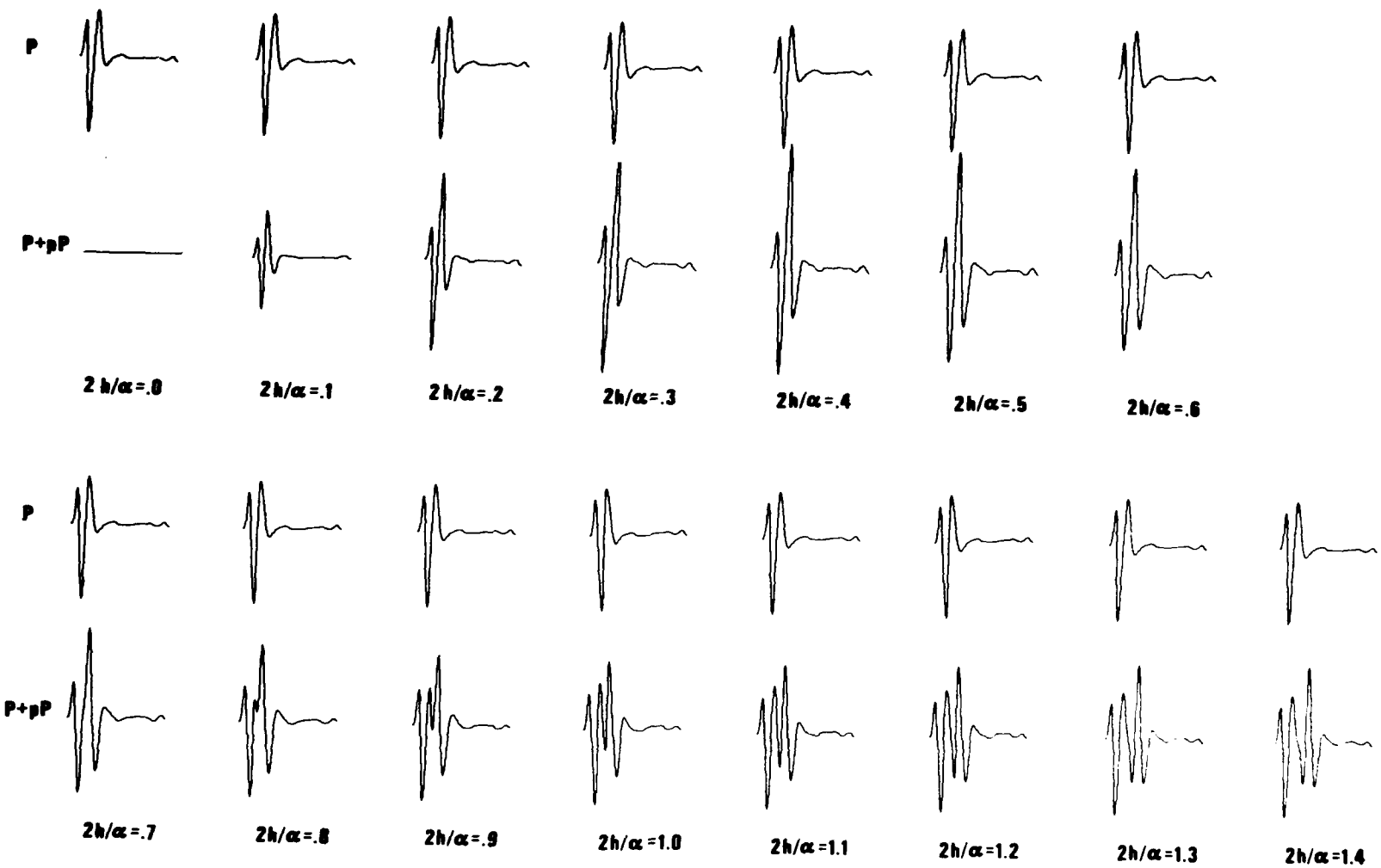

Figure 6 Effect of detonation depth on signal amplitude--perfect reflection of pP is assumed.

Effect of Source Dimension on $M_s - m_b$

This section focuses on the effects which the finite size of the source has on the spectra of seismic signals from explosions and earthquakes. Foremost among these effects is the corner frequency in the spectrum indicative of the spatial extent of the source. Appropriate expressions derived for both cases must contain source dimension so that their effect on discrimination is readily perceived. Thus, the explosion and earthquake expressions should be obtained in as nearly an equivalent form as possible.

For the explosion, the solution for far-field displacement is easily attained because of the radial symmetry of the problem. Jeffreys (1931), Blake (1952), Sharpe (1942), and Rodean (1971), among others, have already performed a solution of the wave equation subject to Cauchy boundary conditions at the cavity radius (or equivalent elastic radius). The common solution is in terms of the pressure on the cavity radii, and so it is not directly comparable to earthquake models which usually express the far-field displacement in terms of displacement at the source. As shown in Appendix II, the explosion result can also be expressed in terms of a step source displacement

$$|u(r,\omega)| = \frac{a D_o}{r} \left(\omega^2 + \frac{\alpha^2}{a^2}\right)^{-\frac{1}{2}} \tag{5}$$

With a corner frequency at $\omega = \alpha/a$, the high-frequency asymptote is ω^{-1}. At low frequencies the value of the flat portion of the spectrum is

$$|\hat{u}(r,0)| = \frac{a^2 D_o}{\alpha r} \tag{6}$$

Jeffreys, H. (1931). On the cause of oscillatory movements in seismograms. Monthly Notices of the Royal Astronomical Society, 8, 408-416.

Blake, F. C. (1952). Spherical wave propagation in solid media. J. Acoust. Soc. Amer., 24, 211-215.

Sharpe, J. A. (1942). The production of elastic waves by explosion pressures, Part I. Geophys., 7, 144-154.

Rodean, H. C. (1971). Nuclear-Explosion Seismology. USAEC Division of Technical Information, Oak Ridge, Tennessee.

Letting $\alpha^2 = \lambda + 2\mu$, this can be rearranged to give

$$4\pi\rho\alpha^3 r|\hat{u}(r,0)| = M_o$$

where $M_o = 4\pi a^2 D_o \rho\alpha^2$, an expression agreeing with Aki et al. (1974) and Muller (1973).

For an earthquake, a finite source will be introduced as a circular plane where the slip occurs instantaneously as a step function of time. The formal expression for the spectrum of the far-field P-wave displacement is given by Molnar et al. (1973), which, for future convenience, is herein divided by a factor of $\sin^2\theta$:

$$|\Omega(r,\omega)| = \frac{\mu R_{\theta\phi} D_o a^2}{2\rho\alpha^3 r(\omega a \cdot \sin\theta/\alpha)^2}\left[\frac{\alpha}{\omega a\cdot\sin\theta}\sin\left(\frac{\omega a\cdot\sin\theta}{\alpha}\right) - \cos\left(\frac{\omega a\cdot\sin\theta}{\alpha}\right)\right]$$

Where the polar axis for θ is perpendicular to the circular fault plane and $R_{\theta\phi}$ is the radiation pattern for P waves from a double couple without moment. Here, displacement is assumed to be variable over the fault rather than constant in an effort to more closely model the actual mechanism according to

$$D_{a'}(t) = D_o \frac{(a^2-a'^2)^{\frac{1}{2}}}{a} H(t)$$

where a' ($\leq a$) is the radius at which $D_{a'}(t)$ is calculated. The long-period asymptote of the earthquake spectrum is

$$|\Omega(r,0)| = \frac{\mu R_{\theta\phi} D_o a^2}{6\rho\alpha^3 r}$$

Using $A=\pi a^2$ for the fault area, this can be rearranged to obtain

$$\frac{4\pi\rho\alpha^3 r|\Omega(r,0)|}{R_{\theta\phi}} = \frac{2}{3}\mu A D_o$$

Aki, K., M. Bouchon, and P. Reasenberg (1974). Seismic source function for an underground nuclear explosion. Bull. Seism. Soc. Am., 64, 131-148.

The right-hand side is exactly the moment of each couple of the equivalent double-couple point source if we replace $\frac{2}{3}D_o$ by $\bar{D}_o$, the average displacement on the fault, which can be obtained by integrating equation (7) over the fault plane. This relation between the far-field long-period portion of the spectrum and the seismic moment holds for any fault shape whose area is A and any fault displacement whose average value is $\bar{D}_o$ (Savage, 1972; Randall, 1973; Dahlen, 1974). The corner frequency occurs at roughly $\omega a \cdot \sin\theta/\alpha \approx 1$. The minimum corner frequency, when $\sin\theta = 1$, is $\omega \approx \frac{\alpha}{a}$; and it increases as $\sin\theta \to 0$ until the spectrum becomes white, corresponding to an impulsive P wave observed on a line perpendicular to the fault. For high frequencies, the spectrum is roughly given by:

$$|\hat{u}(r,\omega)| \propto \cos\left(\frac{\omega a}{\alpha}\right)/\left(\frac{\omega a}{\alpha}\right)^2$$

The high-frequency asymptote of the spectrum is thus proportional to ω^{-2}. For the even simpler model with constant displacement D_o over the entire fault, the spectrum can be shown to decay as $\omega^{-3/2}$ at high frequencies. Recall that the corner frequency of the explosion model with step displacement is α/a and that the high-frequency asymptote is ω^{-1}.

The effects of a finite source on explosion and earthquake far-field P-wave spectra have been partially determined. The finite source models already examined specified a step function for displacement over the source area, normal to a spherical surface for the explosion and parallel to a circular surface for an earthquake. The spectra of the finite sources have flat low-frequency portions and corner frequencies at roughly $\omega = \frac{\alpha}{a}$, the main difference being an ω^{-2} to $\omega^{-3/2}$ falloff for earthquakes versus ω^{-1} for explosions. This difference can be attributed to the geometrical shape of the two sources that govern the rate of growth of the far-field P displacement pulse. The spherical shape of the explosion model leads to a higher-order discontinuity in the far-field pulse than the circular shape of the earthquake model.

Savage, J. C. (1972). Relation of corner frequency to fault dimensions. J. Geophys. Res., 77, 3788-3795.

Other fault shapes have been considered which give different falloffs (Haskell, 1964; Savage 1974; Savage, 1966); as little as ω^{-1} falloff can be predicted from a rectangular fault, when the observing station is aligned along a parallel to one edge. Thus, the shape of the source is important in predicting the asymptotic behavior of the far-field spectrum, but spectral amplitude difference between the earthquake model with instantaneous rupture and the explosion model are not great enough to enable effective discrimination to be based upon this aspect alone because attenuation in the earth has a large effect on shaping the higher-frequency portion of body-wave spectra. However, such attenuation effects could be removed in a strictly regionalized study, where both types of events were located within a homogeneous province.

Effect of Source Time Function on $M_s - m_b$

Next considered are source time functions other than a step. A ramp function to a final static value related to the seismic moment is probably a satisfactory first-order approximation for earthquakes. Brune (1970), Dahlen (1974), and Haskell (1964), among others, have all considered this type of function. Its effect is to introduce another ω^{-1} falloff in the spectrum of the P-wave, with a corner frequency equal roughly to the inverse of the rise time at the source. That this rise time should relate to the fault dimension divided by the rupture velocity is theoretically appealing because the motion of the fault should continue until the rupture reaches the edges and dies out. Archuleta and Brune (1975), in model experiments, demonstrated that such a

Haskell, N. A. (1964). Total energy and energy spectral density of elastic wave radiation from propagating faults. Bull. Seism. Soc. Am., 54, 1811-1841.

Savage, J. C. (1974). Relation between P- and S-wave corner frequencies in the seismic spectrum. Bull. Seism. Soc. Am., 64, 1621-1628.

Savage, J. C. (1966). Radiation from a realistic model of faulting. Bull. Seism. Soc. Am., 56, 577-592.

Brune, J. N. (1970). Tectonic stress and the spectra of seismic shear waves from earthquakes. J. Geophys. Res., 75, 4997-5010.

Archuleta, R. J., and J. N. Brune (1975). Surface strong motion associated with a stick-slip event in a foam rubber model of earthquakes. Bull. Seism. Soc. Am., 65, 1059-1072.

time function occurs in a simply fractured and stressed material. Enough variations can arise in considering different rupture velocities and fault shapes, including position of the observer relative to the fault plane, that making general predictions from more realistic models becomes difficult. Dahlen's (1974) theoretical model is especially well-constructed though; and it offers some simplicity in its final form, predicting that the corner frequency due to rise time and the corner frequency due to finiteness of the source are identical. Taking the rupture velocity to be equal to V everywhere and assuming a Poisson medium, the corner frequency for Dahlen's work is

$$\omega_c^Q = \left[\frac{4\pi\mu V^2 \dot{D}}{M_o} \left(1 - \frac{1}{3}\sin^2\theta\right)\right]^{1/3}$$

where $\dot{D}$ is the velocity of particle movement between the fault planes or slope of the ramp time function. The high-frequency asymptote is ω^{-3} for his model. Using $\dot{D} = .5VD_o/a$, $M_o = \mu A \cdot \bar{D}$, $A = \pi a^2$, and $\bar{D} = \frac{2}{3}D_o$, one can reduce this expression to roughly $1.4V/a < \omega_c < 1.9V/a$, depending on θ, or $\omega_c \approx \frac{\alpha}{a}$.

For the explosion, we take our spectrum given by equation (5) for a step function at the source and generalize to any time function by replacing D_o by $\omega D_o |D(\omega)|$ where $|D(\omega)|$ is the amplitude spectrum of an arbitrary source-time function D(t) whose final value is scaled to unity.

Now specify D(t) to be a ramp function similar to our earthquake model, with rise time a/α. Rodean (1971, p. 58) has shown that this form is a reasonable first-order approximation to the source function. This form is reasonable because it is theoretically appealing to have each point on the cavity wall (or elastic radius limit) move outward until effects from all other points of the source boundary, but which are not occluded by the cavity itself, pass by after traveling a distance a at velocity α. With this assumption

$$\omega D_o |D(\omega)| \to D_o \qquad \omega \to 0$$

$$\omega D_o |D(\omega)| \to D_o / (a\omega/\alpha) \qquad \omega \to \infty$$

Substituting this equation into equation (5) for D_o shows that the low-frequency asymptote is again related to the moment, as in equation (6), and that

the high-frequency asymptote is proportional to ω^{-2} and that the corner frequency $\omega \approx \alpha/a$ is identical to that of the simple earthquake model. Although the analytical approach was different in each case, Mueller and Murphy (1971) and von Seggern and Blandford (1972) have previously predicted the ω^{-2} spectrum for far-field P waves from explosions.

Thus far rather idealized sources have been employed, at least in the case of the earthquake model. The major theoretical findings relevant to $M_s - m_b$ discrimination show that, given similar ramp displacement functions at the source, the earthquake spectrum will fall off more rapidly beyond the corner frequency than the explosion one, ω^{-3} versus ω^{-2}. This fact, however, will not alter the $M_s - m_b$ predictions if the corner frequency is in fact larger than roughly 1 cps, which is the typical frequency of teleseismic P waves as recorded by the WWSSN and past and present VELA stations. The m_b at which the corner frequency is 1 cps can be found by using the following data: Mueller and Murphy (1971) showed empirical evidence that $a \approx 10^{-1} Y^{1/3}$ km for explosions in hard rock where Y is in kilotons. Assuming $\omega_c \approx \frac{\alpha}{a}$, the corner frequency can be expressed as

$$\omega_c^X \approx 10\alpha/Y^{1/3}$$

Assume $\alpha \approx 3.5$ km/sec as a velocity for a typical hard rock detonation medium; this gives $\omega_c \approx 35/Y^{1/3}$ or $f_c \approx 6/Y^{1/3}$. Therefore, the corner frequency for explosions lies above 1 cps until roughly Y = 200 kt or roughly $m_b = 6$ as determined empirically (Evernden, 1970); and up to that yield m_b is measured on the flat portion of the spectrum. That the $M_s - m_b$ relation is nearly linear with slope 1.0 (Springer and Hannon, 1973) from small yields to one megaton

---

von Seggern, D., and R. Blandford (1972). Source time functions and spectra for underground nuclear explosions. Geophys. J., 31, 83-97.

Mueller, R. A., and J. R. Murphy (1971). Seismic characteristics of underground nuclear detonations, Part I. Seismic spectrum scaling. Bull. Seism. Soc. Am., 61, 1675-1692.

Evernden, J., (1970). Magnitude versus yield of explosions. J. Geophys. Res., 75, 1028-1032.

Springer, D. L., and W. J. Hannon (1973). Amplitude-yield scaling for underground nuclear explosions. Bull. Seism. Soc. Am., 63, 477-500.

confirms that the explosion corner frequency is beyond 1 cps until very large yields. Thus, a point-source theory for explosions is a good approximation in studying the $M_s - m_b$ difference for all but the largest detonations. Similarily, if the simple coherent fault model which has been introduced was applicable, then the earthquake corner frequency would be beyond 1 cps until a similarly high magnitude. A point-source theory would also apply to $M_s - m_b$ determinations for earthquakes, resulting in little difference between them and explosions. Thus, the observed large $M_s - m_b$ difference between earthquakes and explosions at $m_b < 6$ has not been explained by requiring finite sources and simple dynamics.

At this point, two possibilities remain for enhancing the theoretical $M_s - m_b$ difference between earthquakes and explosions: 1) in contrast to earthquakes, the source time function for explosions may have a very short rise time and may have a significant peak before it reaches its static value and 2) the source dimensions for an earthquake may be significantly larger than those of an explosion of the same m_b. The first explanation is most often referred to as differences in the source time function, and the second as differences in source dimensions.

Several researchers have utilized the source time function explanation (see Table I). However, in these cases separating this phenomenon from the effect of source dimensions that actually control the rise time of the source function is conceptually difficult. One prediction related to the time function states that if the rupture propagation on a fault is lowered causing the slope of the ramp time function to be lower while the ramp is lengthened, this subsonic faulting will tend to lower the earthquake corner frequency and enhance $M_s - m_b$ discrimination.

Another aspect of the source time function is the possibility of a significant peak in the explosion spectrum. This possibility is suggested by many close-in observations of displacements around an underground nuclear detonation (Werth et al., 1963;

Werth, G. C., R. F. Herbst, and D. L. Springer (1962). Amplitudes of seismic arrivals from the M discontinuity. J. Geophys. Res., 67, 1587-1610.

Perret, 1972; Healy et al., 1971). These close-in observations often showed overshoots in the displacement that are several times the apparent static or residual value. Since cable breaks or instrument failure typically truncate the recordings within two seconds of detonation, residual displacement cannot be inferred accurately. This is unfortunate because shape of the time function out to tens of seconds is, of course, important for predicting Rayleigh-wave amplitudes. In cases of purely elastic response, overshoots of such magnitude are not predicted by theoretical calculations for a cavity in a whole space, but are apparently allowable for cavities near the surface of a half-space (Holzer, 1965; Aboudi, 1972). Caution must be taken to separate that overshoot part of the source function which is due to the surface reflection effect from that due to inelastic behavior since the first should affect both shallow explosions and earthquakes. The limit of inelastic effects in the case of a shallow explosion leads to cratering, and the corresponding close-in displacements exhibit large overshoots. However, even for normal depth of burial scaled to the yield, overshoot by a factor of two may be realistic in certain media. For example, note the source time function for the NTS MAST explosion calculated with a finite-difference stress code by Barker et al. (1976). It is suggested here that observed overshoots in close-in data are due largely to inelastic behavior, if the measurements are

---

Perret, W. R. (1972). GASBUGGY seismic source measurements. Geophysics, 37, 301-312.

Healy, J. H., C. Y. King, and M. E. O'Neill (1971). Source parameters of the SALMON and STERLING nuclear explosions from seismic measurements. J. Geophys. Res., 76, 3344-3355.

Holzer, F. (1965). Measurement and calculations of peak shock-wave parameters from underground nuclear detonations. J. Geophys. Res., 70, 893-905.

Aboudi, J., (1972). The response of an elastic halfspace to the dynamic expansion of an embedded spherical cavity, Bull. Seism. Soc. Am., 62, 115-128.

Barker, T. G., T. C. Bache, J. T. Cherry, N. Rimer, and J. M. Savino (1976). Prediction and matching of teleseismic ground motion (body and surface waves) from the NTS MAST explosion. Report No. SSS-R-76-2727, Systems, Science, and Software, La Jolla, California.

near the surface, plus an elastic surface-reflection contribution which is best described by numerical computer codes. Thus, the effect on $M_s - m_b$ of possible overshoots in the source time function for explosions is most likely less than 0.3. The very linear $M_s - m_b$ relation for explosions (Evernden et al., 1971; Springer and Hannon, 1973; Peppin and McEvilly, 1974) seems to reinforce this argument because if a large overshoot occurred, it would result in a large hump in the far-field spectrum that would pass through the narrow frequency band in which m_b is measured as the yield was increased, thus leading to a noticably non-linear $M_s - m_b$ relation.

Note, however, that considerable empirical evidence exists, mostly from Rayleigh waves (Toksöz et al., 1964; Helmberger and Harkrider, 1972; Aki et al., 1974), for the presence of a large overshoot in the source function. Most of these investigators suggest a decaying time function in the form $kt^b e^{-ct}$. However, the decay rate that they required cannot be accommodated by theoretical calculations or observations for the pressure inside a post-shot cavity (Olsen, 1967, 1970). This is true because the physical properties do not allow a significant pressure decay, unless there is venting or a cavity collapse. Contrary to the Rayleigh-wave studies just mentioned,

---

Evernden, J. F., W. J. Best, P. W. Pomeroy, T. V. McEvilly, J. M. Savino, and L. R. Sykes (1971). Discrimination between small-magnitude earthquakes and explosions. J. Geophys. Res., 76, 8042-8055.

Toksöz, M. N., A. Ben-Menahem, and D. G. Harkrider (1964). Determination of source parameters of explosions and earthquakes by amplitude equalization of seismic surface waves. 1. Underground nuclear explosions. J. Geophys. Res., 69, 4355-4366.

Helmberger, D. V., and D. G. Harkrider (1972). Seismic source descriptions of underground explosions and a depth discriminant. Geophys. J., 31, 45-66.

Olsen, C. W. (1967). Time history of the cavity pressure and temperature following a nuclear detonation in alluvium. J. Geophys. Res., 72, 5037-5041.

Olsen, C. W. (1970). Soil strain near a nuclear detonation. Bull. Seism. Soc. Am., 60, 1999-2014.

Tsai and Aki (1971) have concluded from Rayleigh waves that the source time functions for explosions and earthquakes are nearly identical. Also, Peppin's (1976) close-in spectra for many NTS explosions showed no apparent overshoot. Numerous corrections are made in reducing far-field signal spectra back to the source however, and all investigators must admit the possibility that these corrections are not precisely known.

Another aspect of the source time function is that earthquake sources are coherent only for periods longer than their fault length divided by the wave velocity. Spectral amplitudes for periods less than this can be predicted only by statistical or stochastic methods, and they are necessarily greater for an incoherent model of faulting. Haskell (1964, 1966) first presented this concept in an analytical fashion, and Aki (1967) worked from Haskell's model to show that such incoherent behavior results in predicted spectra for earthquakes that agree with several types of empirical data from large magnitude events. The phenomenon of incoherence should affect $M_s - m_b$ discrimination for events whose source dimensions are on the order of 5 km or larger since this is the dimension related to m_b measurement at 1 cps. Liebermann and Pomeroy (1970) gave varied evidence that this magnitude lies at 4.5 to 5.0. However, on the basis of the success of the $M_s - m_b$ discriminant alone, one should be reluctant to admit any significant effect for incoherence since its effect is to raise, not lower, the spectral high-frequency level.

The question of whether earthquake and explosion $M_s - m_b$ lines converge at low magnitudes is a disputed one which usually rests on empirical observations at very low signal-to-noise ratios. It has been shown here that no theoretical reason exists to support a $M_s - m_b$ difference between explosions and

---

Haskell, N. A., (1966). Total energy and energy spectral density of elastic wave radiation from propagating faults. Part II. A statistical source model. Bull. Seism. Soc. Am., 56, 125-140.

Aki, K. (1967). Scaling law of seismic spectrum. J. Geophys. Res., 72, 1217-1231.

Liebermann, R. C., and P. W. Pomeroy (1970). Source dimensions of small earthquakes as determined from the size of the aftershock zone. Bull. Seism. Soc. Am., 60, 879-890.

earthquakes that is more than roughly one-half magnitude unit at low magnitudes. To support a larger difference, one must hypothesize a combination of subsonic faulting for an earthquake and perhaps some significant overshoot in the explosion source-time function. Thus, $M_s - m_b$ discrimination is a tenuous proposition for small events, a contention that Peppin's (1976) data supports for low-magnitude explosions and earthquakes at the NTS since it shows incomplete separation of source type by Pg vs. LR measurements.

Surface-Wave Spectra

Derr (1970) and von Seggern and Lambert (1970), who studied a large number of explosions and earthquakes, have shown that the discrimination capability in surface waves alone is minimal. Even assuming significant differences in the source time function between the two types of seismic events, the propagation and radiation pattern corrections are so variable that differences in observed spectra cannot reliably be attributed to one source type or another. Source depth can, however, have a persistent effect on observed Rayleigh-wave spectra if the earthquakes are all deeper than explosions in the same area because generation of longer periods is enhanced relative to shorter periods as a source is moved downwards. Tsai and Aki (1971) and Marshall (1970) discussed this possible means of discrimination. The M_s difference between 20-second and 40-second estimates has been shown by Savino et al. (1971) to be larger for earthquakes than for explosions in general. These results are most likely due to depth, and Marshall and Basham (1972) even employ the 40-sec versus 20-sec Rayleigh-wave ratio to determine a depth correction for M_s. Tsai and Aki (1971) showed that deep crustal earthquakes in the Southwest United States can be identified as such on the basis of Rayleigh-wave spectra. At best, Rayleigh-wave spectra can only be described as an aid to discrimination rather than as a reliable discriminant in itself.

Derr, J. S. (1970). Discrimination of earthquakes and explosions by the Rayleigh-wave spectral ratio. Bull. Seism. Soc. Am., 60, 1653-1668.

Marshall, P. D. (1970). Aspects of the spectral difference between earthquakes and underground explosions. Geophys. J., 20, 397-416.

Marshall, P. D., and P. W. Basham, (1972). Discrimination between earthquakes and underground explosions employing an improved M_s scale. Geophys. J., 28, 431-458.

Body-Wave Spectra

Although discrimination on the basis of short-period P-wave spectra has been demonstrated by several studies (Frantti, 1963; Bakun and Johnson, 1970; Weichert, 1971; Briscoe and Walsh, 1967; Anglin, 1971; Manchee, 1972; Lacoss, 1969; Dahlman et al., 1974), physical reasons for success of this discriminant have only recently become apparent. Because pP will cancel P at low frequencies and because the spectrum falls off as ω^{-2} for explosions versus ω^{-3} for earthquakes, the amplitude at high frequencies of explosion P waves is enhanced relative to that of earthquakes. The definition of spectral ratio, such as that of Lacoss (1969) for instance, takes advantage of this inherent difference. However, this discrimant may not rest on a firm base because the high-frequency portion of the spectrum (> 1 cps) is greatly affected by various propagation effects which may dominate source characteristics. Von Seggern and Blandford (1976) surveyed spectral ratios from globally-distributed earthquakes. Their results are reproduced in Figure 7, which shows nearly as much scatter as typical $M_s - m_b$ plots for earthquakes. The few presumed explosions are not clearly separated in this work. Therefore, unless events are in proximity, there

---

Frantti, G. E. (1963). Energy spectra for underground explosions and earthquakes. Bull. Seism. Soc. Am., 53, 997-1005.

Bakun, W. H., and L. R. Johnson (1970). Short-period spectral discriminants for explosions. Geophys. J., 22, 147-152.

Weichert, D. H. (1971). Short-period spectral discriminant for earthquake - explosion differentiation. Z. Geophys., 37, 147-152.

Briscoe, H. W., and J. Walsh (1967). Ratios of spectral densities. SDSTS, 30 June 1967, Lincoln Laboratory, Lexington, Massachuetts.

Anglin, F. M. (1971). Discrimination of earthquakes and explosions using short-period seismic array data. Nature, 233, 51-52.

Dahlman, O., H. Israelson, A. Austegard, and G. Hornstrom (1974). Definition and identification of seismic events in the USSR in 1971. Bull. Seism. Soc. Am., 64, 607-636.

Manchee, E. B. (1972). Short-period seismic discrimination. Nature, 239, 152-153.

von Seggern, D. H., and R. R. Blandford (1976). Observed variation in the spectral ratio discriminant from short-period P waves. Report No. SDAC-TR-76-12, Teledyne Geotech, Alexandria, Virginia.

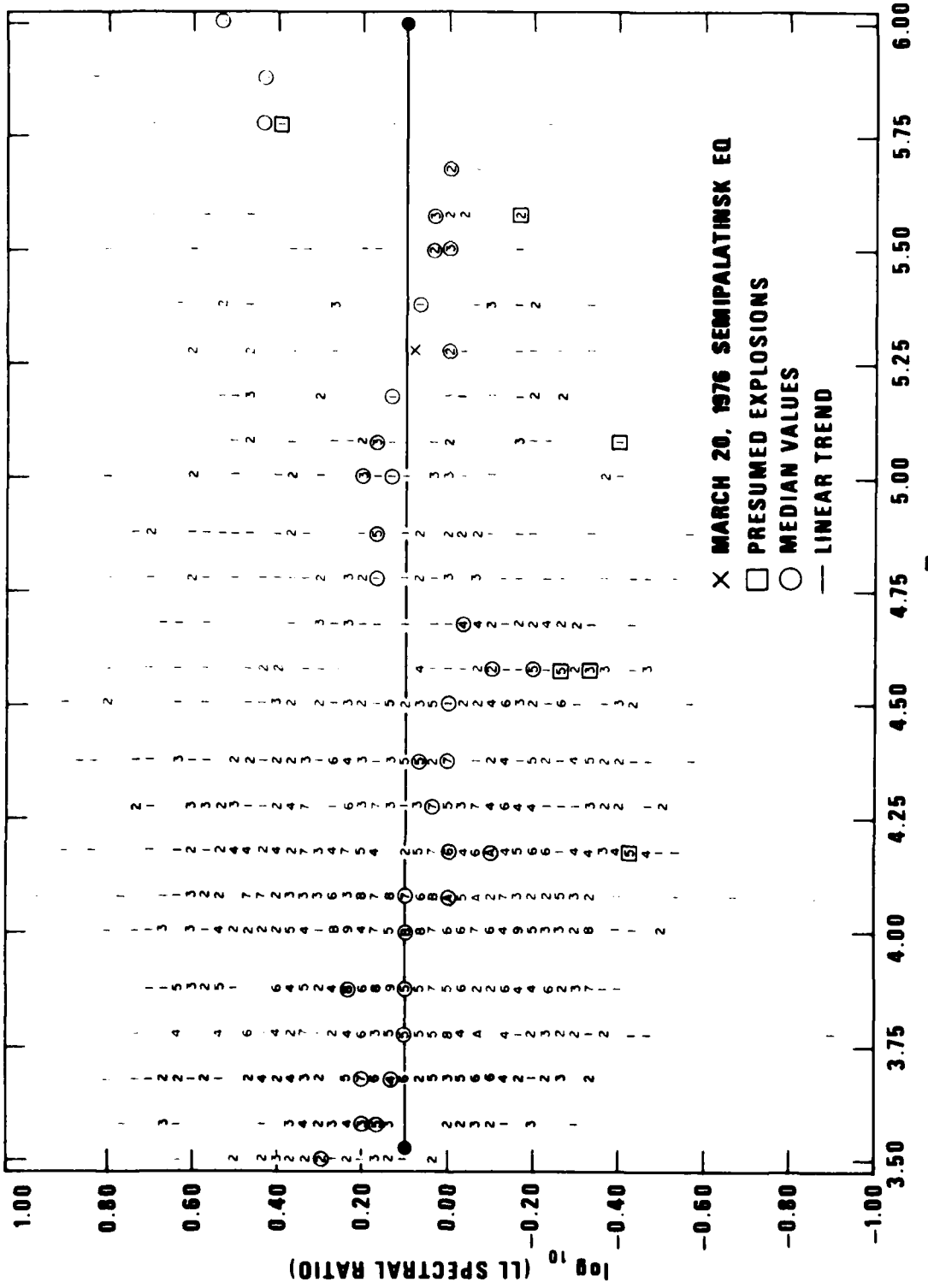

Figure 7 Spectral ratios from P-waves recorded at LASA from a global sample of earthquakes.

is no certainty that observed differences are indicative of source type. This problem relates to the problem of large scatter in m_b, which can be attributed either to Q differences (Ward and Toksöz, 1971; Solomon, 1972a; and Douglas et al., 1974a) or to the focusing effects of lateral inhomogeneities (Davies and Julian, 1972). If m_b is so highly dependent on path, then spectral ratios also may be, especially if higher frequencies are employed.

A better approach with short-period spectral ratios is to emphasize the frequencies below 1 cps. Here, the explosion spectrum should decrease rapidly as a result of the effect of the free surface, which theoretically applies a factor of ω to the P-wave spectrum up to a frequency characteristic of the source depth (Douglas et al., 1971). The notably small long-period P waves from explosions (von Seggern, 1972; Evernden, 1969) are evidence of this effect. The effect on the earthquake P spectrum is more complex because of the radiation pattern. However, if the earthquakes are generally deeper than the explosions, then their spectra are expected to remain at the level predicted by a whole-space model down to lower frequencies than that for shallow explosions. Molnar (1971) and Wyss et al. (1971) observed this difference in explosion and earthquake spectra and suggested it as a discriminant. Such a discriminant is related to depth determination by spectral methods (mentioned above) and will be subject to possible pitfalls associated with that procedure. In general, a P-wave spectral ratio employing as wide a frequency band as possible should be a good discriminant, but less reliable than $M_s - m_b$.

Ward, R. W., and M. N. Toksöz (1971). Causes of regional variation of magnitudes. Bull. Seism. Soc. Am., 61, 649-670.

Solomon, S. C. (1972a). Seismic wave attenuation and partial melting in the upper mantle of North America. J. Geophys. Res., 77, 1483-1502.

Douglas, A., J. B. Young, and J. A. Hudson (1974a). Complex P-wave seismograms from simple earthquake sources. Geophys. J., 37, 141-150.

Davies, D., and B. R. Julian (1972). A study of short period P-wave signals from LONGSHOT. Geophys. J., 29, 185-202.

Wyss, M., T. C. Hanks, and R. C. Liebermann (1971). Comparison of P-wave spectra of underground explosions and earthquakes. J. Geophys. Res., 76, 2716-2729.

Complexity of the Recorded Signal

Early comparisons of time traces for explosions and earthquakes revealed the earthquake signals to be more complex in appearance. Carpenter (1964) offered an explanation in terms of the crustal transfer function at the source which, theoretically, should provide more numerous and stronger secondary arrivals within thirty seconds after the initial P arrival for an earthquake at depth than for an explosion near the surface. In opposition to this idea, Douglas et al. (1974a) showed that a thick low-velocity layer in the crust is required to generate complex earthquakes. Douglas et al. (1973), in a thorough discussion of the reasons for complexity, concluded that Q along the path may be the major influence and that differences in complexity between explosion and earthquake signals are most often explained by their emanating from regions of greatly different Q, that is, stable versus tectonic provinces. Citing LONG SHOT in their analysis, Davies and Julian (1972) show that shadowing effects of dipping plates can cause explosion signals to appear highly complex. Overall, for explosions and earthquakes in the same area, complexity is expected to be a poor discriminant. In fact, Evernden (1969) and Ericsson (1970) showed it to be of little value in comparison to $M_s - m_b$. In studies of short-period discrimination which employ spectral ratios and complexity together (Anglin, 1971; Dahlman et al., 1974), little of the discriminating power can be attributed to the complexity measure. Greenfield (1971) pointed out the complexity of explosion signals from Novaya Zemlya, attributing it to mode conversion from Rayleigh waves to P waves in the vicinity of the source. Clearly, complexity caused in this manner relates to the source region and not to the nature of the source and thus offers no discrimination capability. Complexity, then, is by far the most tenuous discriminant.

Higher-Mode Surface Waves

Shurbet (1969) reported on the difference in higher-mode Rayleigh-wave excitation of an explosion at NTS and a nearby earthquake.

Greenfield, R. J. (1971). Short-period P-wave generation by Rayleigh-wave scattering at Novaya Zemlya. J. Geophys. Res., 76, 7988-8002.

Shurbet, D. H. (1969). Excitation of Rayleigh waves. J. Geophys. Res., 74, 5339-5341.

Forsyth (1976) studied Asian events and found that higher modes could aid in identifying earthquakes. Observations such as these could be important for discrimination, but thus far no detailed study has been undertaken for events in the United States. This omission is due largely to the higher detection threshold for Rayleigh modes other than the fundamental mode (on the order of one magnitude unit); such thresholds are in agreement with theory (Harkrider, 1970) that predicts that the excitation of higher modes is only a fraction of the fundamental mode excitation for shallow focal depths in the Southwestern United States, as shown in Figure 8.

Forsyth, D. W. (1976). Higher-mode Rayleigh waves as an aid to seismic discrimination. Bull. Seism. Soc. Am., 66, 827-842.

Harkrider, D. G., (1970). Surface waves in multilayered elastic media. II. Higher mode spectra and spectral ratios from point sources in plane layered earth models. Bull. Seism. Soc. Am., 60, 1937-1988.

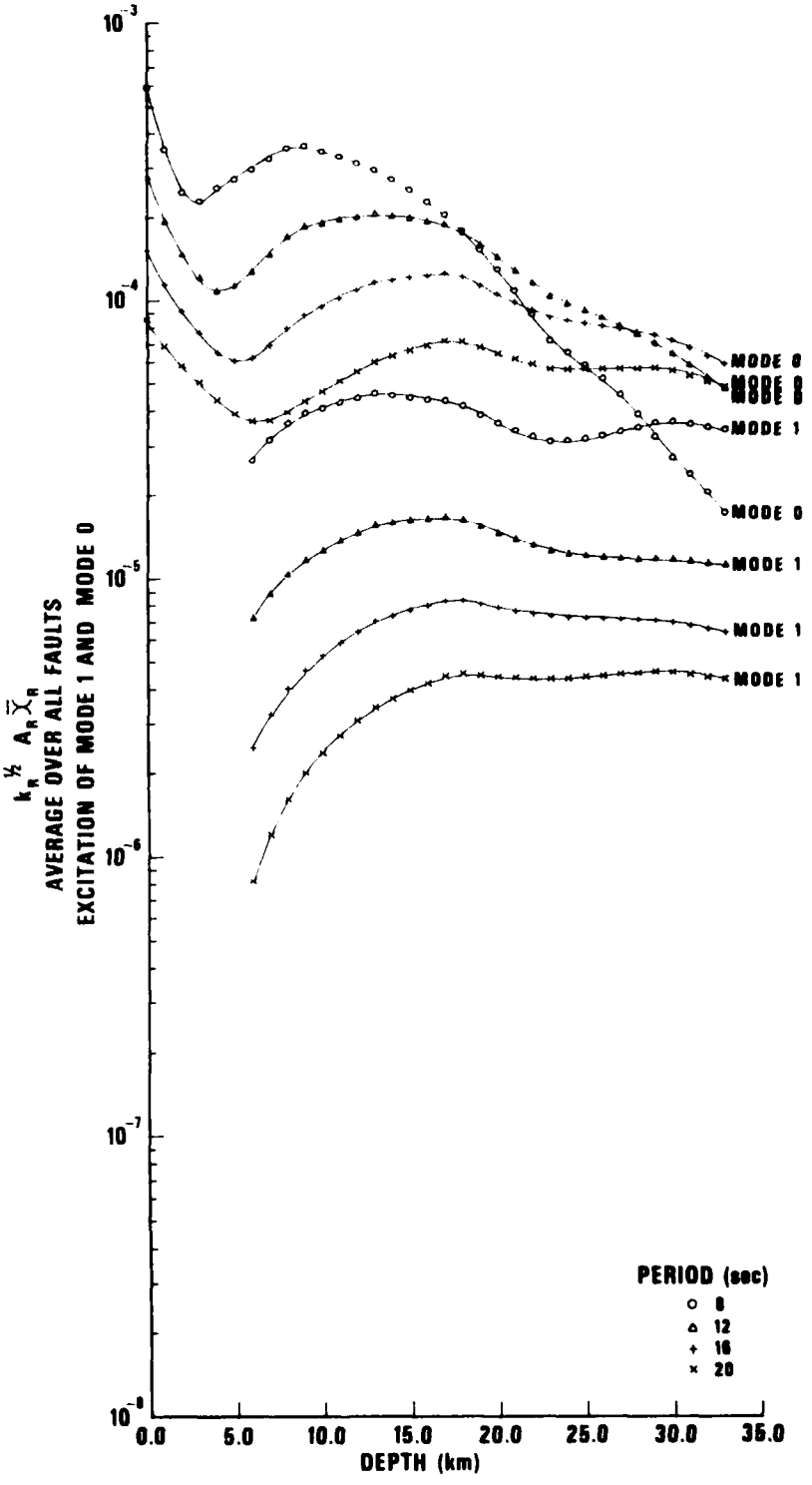

Figure 8 Theoretical excitation of fundamental-mode and higher-mode Rayleigh waves versus depth of focus in the Southwestern United States.

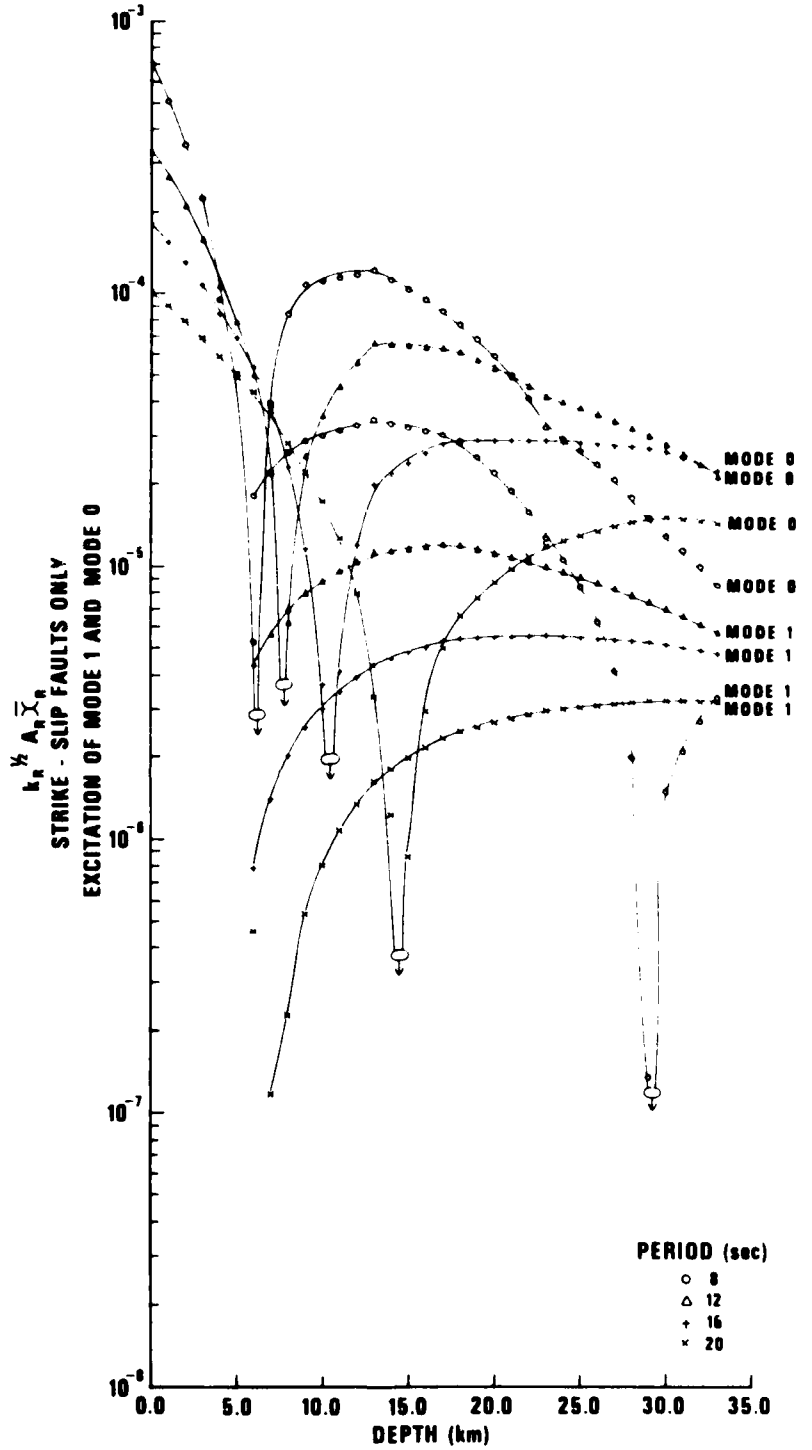

Figure 8 (cont.) Theoretical excitation of fundamental-mode and higher-mode Rayleigh waves versus depth of focus in the Southwestern United States.

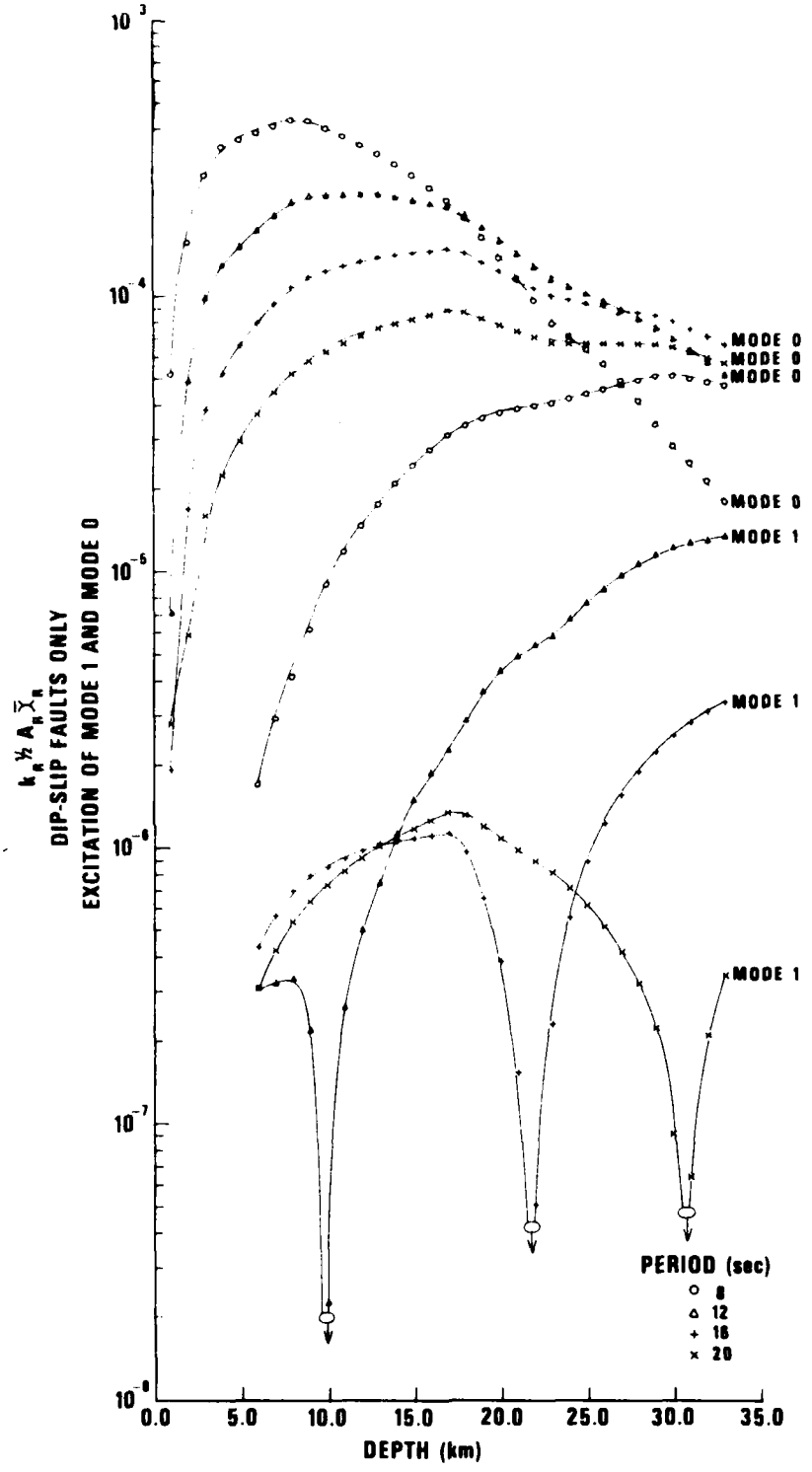

Figure 8 (cont.) Theoretical excitation of fundamental-mode and higher-mode Rayleigh waves versus depth of focus in the Southwestern United States.

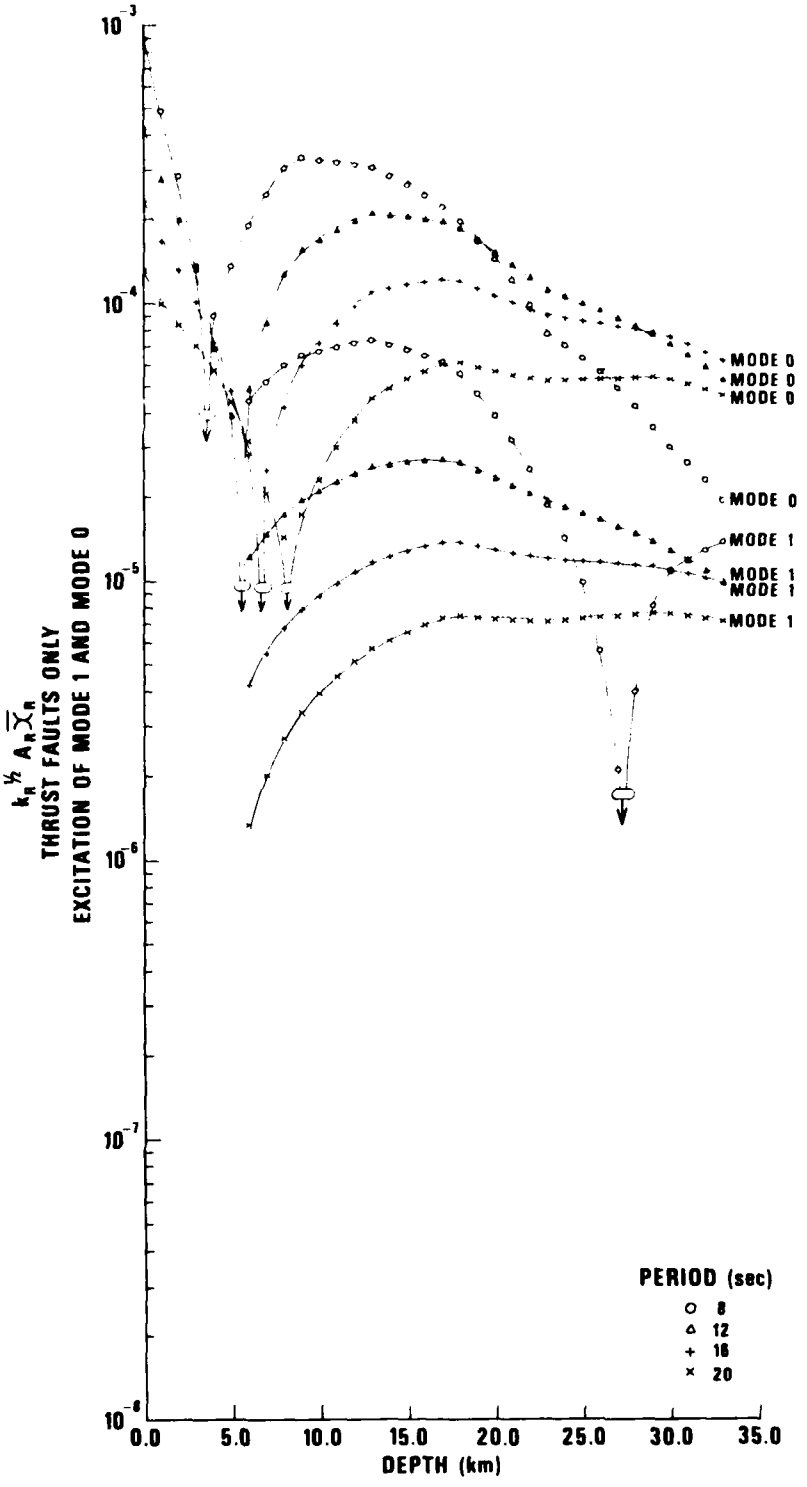

Figure 8 (cont.) Theoretical excitation of fundamental-mode and higher-mode Rayleigh waves versus depth of focus in the Southwestern United States.

NATURE OF THE CRUST AND UPPER MANTLE IN THE WESTERN UNITED STATES

General Geologic History

The geological history of the Western United States is as complex as that of any region on the globe. For purposes of this report, this history will be described only briefly, focusing only on those generally broad current features that may be relevant to discrimination of events within the region. Specific and limited geological features that can affect signals emanating from or propagating through them will be discussed later when selected events are actually analyzed.

A detailed account of the region's geological history can be found in King (1969). The presence of Precambrian and Paleozoic rocks throughout the area indicate that this has long been part of a continental plate, even though shallow seas have often covered it extensively in the past. The most conspicuous recent Cenozoic activities have been a broad upwarping of the whole region, major block faulting from the Sierra Nevadas eastward through the Colorado Rockies, and strike-slip faulting associated with the San Andreas transform fault (Hamilton and Meyers, 1966). Figure 9 shows the major physiographic regions of the Western United States. The area under study here is roughly bounded by 30°N-42°N and 104°W to the California coast. In the following sections each of the five major physiographic provinces shown in this figure are discussed in terms of their general static structure. A discussion of tectonic movements, seismicity, and fault mechanisms follows in another section.

Basin and Range

Knowledge of the present tectonics of the Basin-and-Range (B-R) activity holds the key to understanding the surrounding provinces. This province is anomalous in its surface features, but it is even more so at depths where the existence of an upper mantle akin to that under oceanic ridges or that behind island arcs is firmly established by geophysical evidence.

King, P. B., (1969). The tectonics of North America - a discussion to accompany the tectonic map of North America. Geological Survey Professional Paper 628. U.S. Geological Survey, Dept. of Interior, Washington, D. C.

Hamilton, W., and W. B. Meyers (1966). Cenozoic tectonics of the Western United States. Rev. of Geophys., 4, 509-549.

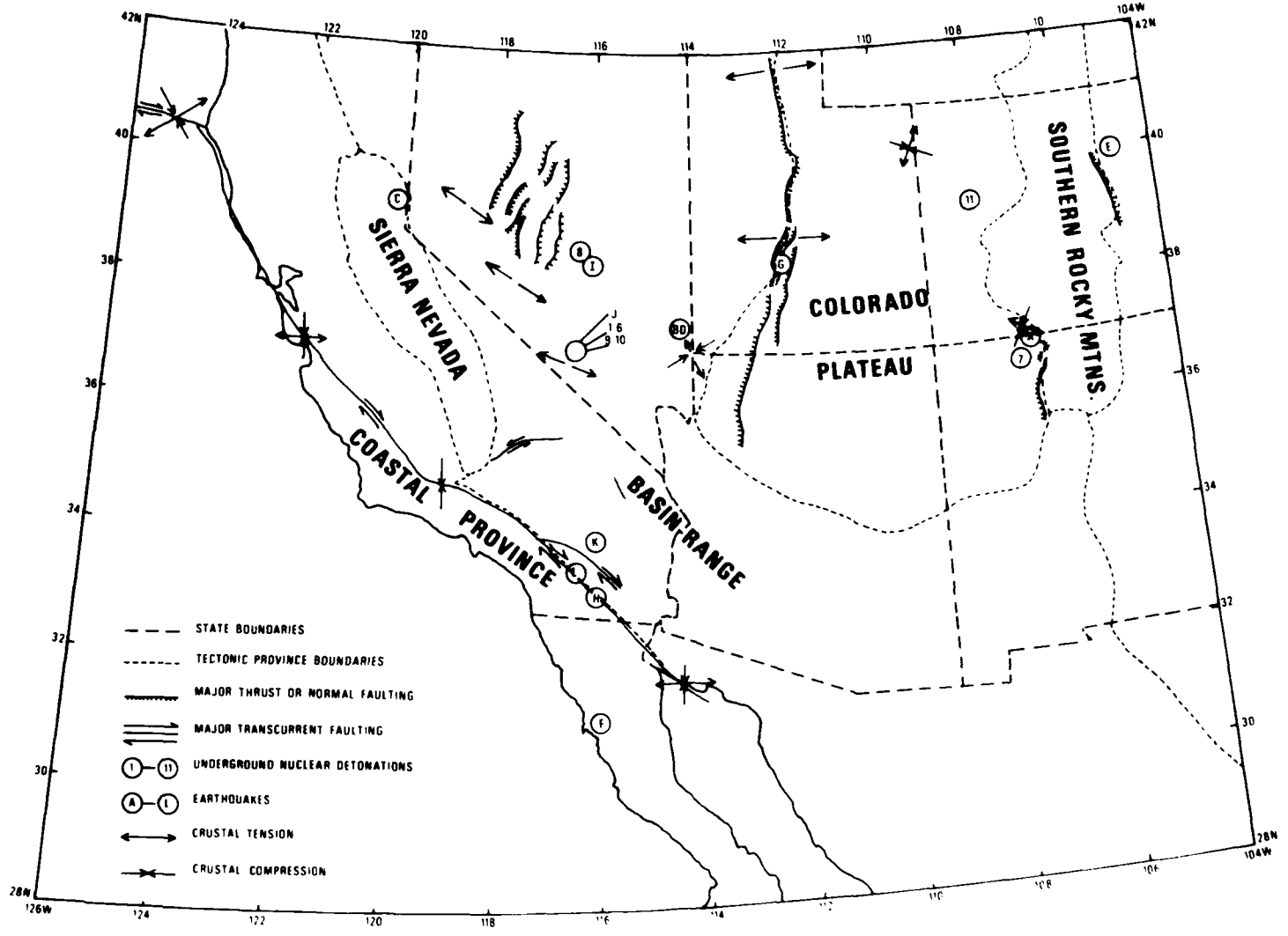

Figure 9 Physiographic regions of the Southwestern United States and schematic of tectonic forces.

The crust is relatively thin for continental areas; refraction surveys show it to be roughly 30 km or less (Prodehl, 1970; Pakiser, 1963). The crust thins toward the Gulf of California to rougly 20 km at the northern end (Thatcher and Brune, 1973). The eastern border of the province is fairly well defined along, or just east of, the Wasatch Front where the crust begins to thicken rapidly to 40 km or greater beneath the Colorado Plateau (Braile et al., 1974). The western border is marked by the Sierra Nevada orogeny, where the crust exceeds 40 km in depth (Oliver et al., 1961; Mikumo, 1965; Eaton, 1963).

The thinness of the crust, widespread block faulting, and crustal extension in the Basin and Range province are intimately associated with an anomalous upper mantle concentrated beneath this region. The salient characteristics of this anomalous upper mantle are low velocities, high attenuation, high heat flow, and high conductivity. Early evidence of anomalously low velocities under the Basin and Range province came from surface-wave group-

---

Prodehl, C. (1970). Seismic refraction study of crustal structure in the Western United States. Geophys. J., 81, 2629-2646.

Pakiser, L. C. (1963). Structure of the crust and upper mantle in the Western United States. J. Geophys. Res., 68, 5747-5756.

Thatcher, W., and J. N. Brune (1973). Surface waves and crustal structure in the Gulf of California region. Bull. Seism. Soc. Am., 63, 1689-1698.

Braile, L. W., R. B. Smith, G. R. Keller, R. M. Welch, and R. P. Meyer (1974). Crustal structure across the Wasatch front from detailed seismic refraction studies. J. Geophys. Res., 79, 2669-2677.

Oliver, H. W., L. C. Pakiser, and M. F. Kane (1961). Gravity anomalies in the Central Sierra Nevada, California. J. Geophys. Res., 66, 4265-4271.

Mikumo, T. (1965). Crustal structure in central California in relation to the Sierra Nevada. Bull. Seism. Soc. Am. 55, 65-83.

Eaton, J. (1963). Crustal structure from San Francisco, California, to Eureka, Nevada, from seismic refraction measurements. J. Geophys. Res., 68, 5789-5806.

velocity measurements of Press (1960) and Alexander (1963). Biswas and Knopoff (1974) recently confirmed this using phase velocities of surface waves, and their data also showed that the mantle is of nearly normal continental character eastward of the Basin and Range province. Early evidence from low P_n velocities (Herrin and Taggart, 1962) also indicated a deeper anomalous zone under the Basin and Range province. Other important evidence for low velocities in the upper mantle here came from studies of P-wave travel-time delays (Cleary and Hales, 1966; Herrin and Taggart, 1968) and S-wave travel-time delays (Hales and Roberts, 1970; Yasar and Nuttli, 1974). The P-wave delays are not so great as the S-wave delays, but they do indicate a low-velocity zone for compressional waves which is not well established by using surface waves. Many models of the Basin-Range upper-mantle velocities have been derived from detailed studies of P-wave amplitudes and arrival times (Archambeau et al., 1969;

Press, F. (1960). Crustal structure in California-Nevada region. J. Geophys. Res., 65, 1939-1051.

Alexander, S. S. (1963). Surface wave propagation in the Western United States. Ph.D. Thesis, California Institute of Technology, Pasadena.

Biswas, N. N., and L. Knopoff (1974). The structure of the upper mantle under the United States from the dispersion of Rayleigh waves. Geophys. J., 36, 515-539.

Herrin, E., and J. Taggart (1962). Regional variations in P_n velocities and their effect on the location of epicenters. Bull. Seism. Soc. Am., 52, 1037-1046.

Cleary, J., and A. L. Hales (1966). An analysis of the travel times of P wave to North American stations in the distance range 32° to 100°. Bull. Seism. Soc. Am., 56, 467-489.

Herrin, E., and J. Taggart (1968). Regional variations in P travel times. Bull. Seism. Soc. Am., 58, 1325-1337.

Hales, A. L., and J. L. Roberts (1970). The travel times of S and SKS. Bull. Seism. Soc. Am., 60, 461-489.

Yasar, T., and O. W. Nuttli (1974). Structure of the shear-wave low-velocity channel in the Western United States. Geophys. J., 37, 353-364.

Archambeau, C. B., E. A. Flinn, and D. G. Lambert (1969). Fine structure of the upper mantle. J. Geophys. Res., 74, 5825-5865.

Julian and Anderson, 1968; Wiggins and Helmberger, 1973; Massé et al., 1972), from apparent velocities of P (Niazi and Anderson, 1965; Johnson, 1967), and from apparent velocities of S (Kovach and Robinson, 1969). These models exhibit significant differences in the exact structure of the low-velocity zone. York and Helmberger (1973) attempted to map the lateral structure by using P-PL travel times. Altogether, the data delineates a low-velocity zone (LVZ) for both P and S waves which begins at or very near the Moho (there is very little or no high-velocity "lid" over the LVZ) and extends to a depth of between 150 and 250 km. S-wave velocities may be as low as 3.85 km/sec in this zone (Yasar and Nuttli, 1974), although a range of 4.0-4.3 km/sec is usually inferred, compared with normal upper-mantle velocities of 4.4.-4.6 km/sec. P-wave velocities are not so anomalous as the S velocities, but they are typically inferred to be .2 km/sec less than normal upper-mantle P velocities under continents. These velocity anomalies abate considerably to the east under the Colorado Plateau and where the LVZ become thinner and has a thicker lid (Archambeau et al., 1969).

Other evidence of an anomalous zone in the Basin and Range province is the relatively high heat flow (Roy et al., 1968; Sass et al., 1971; Warren et al., 1969) and relatively high electrical conductivity (Porath and Gough, 1971; Gough, 1973), both of which have been associated roughly with the depths of

---

Julian, B. R., and D. L. Anderson (1968). Travel times, apparent velocities and amplitudes of body waves. Bull. Seism. Soc. Am., 58, 339-366.

Wiggins, R. A., and D. V. Helmberger, (1973). Upper mantle structure of the Western United States. J. Geophys. Res., 78, 1870-1880.

Roy, R. F., E. R. Decker, D. D. Blackwell, and F. Birch (1968). Heat flow in the United States. J. Geophys. Res., 73, 5207-5221.

Sass, J. H., A. H. Lachenbruch, R. J. Munroe, G. W. Greene, and T. H. Moses (1971). Heat flow in the Western United States. J. Geophys. Res., 76, 6376-6413.

Warren, R. E., J. G. Sclater, V. Vacquier, and R. F. Roy (1969). A comparison of terrestrial heat flow and transient geomagnetic fluctuations in the Southwestern United States. Geophysics, 34, 463-478.

Porath, H., and D. I. Gough (1971). Mantle conductive structures in the Western United States from magnetometer array studies. Geophys. J., 22, 261-275.

Gough, D. I. (1973). The geophysical significance of geomagnetic variation anomalies. Phys. Earth. Planet. Int., 7, 379-388.

the LVZ. Gravity and magnetic surveys show no appreciable anomalies over this region.

For this study, the most important feature is the pronounced low Q zone associated with the LVZ in the Basin and Range province. Mapping of P-wave magnitude residuals (Cleary, 1967; Evernden and Clark, 1970) showed lower amplitudes in the Western United States, but they were not necessarily confined to the Basin and Range. Der et al. (1975), in a study using short-period P and S waves, found high attenuation in the Western United States relative to that in the Eastern United States. The same gross pattern is seen from long-period P and S waves (Solomon and Toksöz, 1970). Using S_n waves, Molnar and Oliver (1969) mapped attenuation in the uppermost mantle of the Western United States and found that the Basin and Range province has relatively high attenuation. Mitchell (1975) showed higher attenuation in the Western United States using surface waves. The values of Q estimated for the upper mantle under the Basin and Range province varied considerably, depending upon how much of the actual path lay in this anomalous region. Der and McElfresh (1977) estimated an average Q of 100-200 for the uppermost 200 km of the mantle under the Western United States, as compared to roughly 1600 in the Eastern United States where

---

Cleary, J. (1967). Analysis of the amplitudes of short-period P waves recorded by Long Range Seismic Measurements Stations in the distance range 30° to 102°. J. Geophys. Res., 72, 4705-4712.

Der, Z. A., R. P. Massé, and J. P. Gurski (1975). Regional attenuation of short-period P and S waves in the United States. Geophys. J., 40, 85-106.

Solomon, S. C., and M. N. Toksöz (1970). Lateral variation of attenuation of P and S waves beneath the United States. Bull. Seism. Soc. Am., 60, 819-838.

Molnar, P., and J. Oliver, (1969). Lateral variation of attenuation in the upper mantle and discontinuities in the lithosphere. J. Geophys. Res., 74, 2648-2682.

Mitchell, B. J. (1975). Regional Rayleigh-wave attenuation in North American. J. Geophys. Res., 80, 4904-4916.

Der, Z. A., and T. W. McElfresh (1977). The relationship between anelastic attenuation and regional amplitude anomalies of short-period P waves in North America. Bull. Seism. Soc. Am., 67, 1303-1317.

a normal continental upper mantle exists. Also with short-period P waves, Veith and Clawson (1972) postulated a Q of 110 for a LVZ of 100 km thickness while Helmberger (1973) postulated an even lower Q on the order of 50 in the LVZ.

To account for the presence of such low Q, partial melting of the asthenosphere has been suggested by, among others, Solomon (1972a) and Archambeau et al. (1969). The cause of this low-Q character and other associated phenomena (described above) has been set forth in a variety of theories, most of which relate to active tectonics associated with moving plates. Menard (1960), for example, suggested that the active oceanic ridge in the Gulf of California continues into the B-R province. Cook (1969) elaborated on this concept, pointing out the physiographic similarities of the B-R to oceanic rifts and the similarity of low P velocities and high attenuation between the two. Scholz et al. (1971) thought this hypothesis was incompatible with, among other things, the volcanic pattern throughout the region and suggested instead that the B-R province is more akin to many interarc basins around the Pacific (Barazangi et al., 1975) where attenuation is also high and velocities low. The crustal extension seen in the B-R province is characteristic of both ocean rifts and interarc basins. This interarc basin hypothesis requires a subduction zone. While no convincing evidence exists of a contemporary active zone

---

Veith, K. F., and G. E. Clawson (1972). Magnitude from short-period P-wave data. Bull. Seism. Soc. Am., 62, 435-452.

Helmberger, D. V. (1973). On the structure of the low velocity zone. Geophys. J., 34, 251-263.

Solomon, S. C. (1972a). Seismic wave attenuation and partial melting in the upper mantle of North America. J. Geophys. Res., 77, 1483-1502.

Menard, H. W. (1960). The East Pacific Rise. Science, 132, 1737-1746.

Cook, K. L. (1969). Active rift system in the Basin and Range province. Tectonophysics, 8, 469-511.

Scholz, C. H., M. Barazangi, and M. L. Sbar (1971). Late Cenozoic evolution of the Great Basin, Western United States, as an ensialic interarc basin. Bull. Geol. Soc. Amer., 82, 2979-2990.

Barazangi, M., W. Pennington, and B. Isacks, (1975). Global study of seismic wave attenuation in the upper mantle behind island arcs using pP waves. J. Geophys. Res., 80, 1079-1092.

west of the B-R province, a prior active one, which has been overridden by westward movement of the North American plate, has ample support from a number of different workers (Atwater, 1970; Hamilton and Meyers, 1966; Shaw et al., 1971).

Pacific Coast and Sierra Nevada

The Pacific Coast (P-C) province is separated from the B-R province by the Sierra Nevada orogeny along the eastern border of middle to southern California. The demarcation becomes less clear physiographically in southern California, but King (1969) has asserted that the Sierra Nevada orogeny extends down into the Baja Peninsula, thus providing the necessary division. (To the north the division with the B-R province becomes even less clear, but this area is beyond our study.) The Sierra Nevada has a crustal "root" down to at least 40 km. In contrast the crustal structure of the Pacific Coast is generally shallow, about 20-25 km (Press, 1960; Mikumo, 1965; Healy, 1963). This thickness is slightly thinner than that of the B-R crust; but it does not have the low P_n velocities of the B-R province (Herrin and Taggart, 1962; Pakiser, 1963), indicating that at least the lid over the LVZ has been restored in this region relative to the B-R. Evidence for a LVZ under the Pacific Coast province is not so complete as for the B-R province, but the high attenuation inferred from short-period waves, as referenced above for the B-R province, apparently continues nearly unabated into the P-C province. However, P-wave delay times, as referenced above for the B-R province, disappear westward toward the coast.

Atwater, T. (1970). Implications of plate tectonics for the Cenozoic tectonic evolution of Western North America. Bull. Geol. Soc. Am. 81, 3513-3536.

Hamilton, W., and W. B. Meyers (1966). Cenozoic tectonics of the Western United States. Rev. of Geophys., 4, 509-549.

Shaw, H. R., R. W. Kistler, and J. F. Evernden (1971). Sierra Nevada plutonic cycle: Part II, tidal energy and a hypothesis for orogenic-epeirogenic periodicities. Geol. Soc. Am. Bull., 82, 869-896.

Healy, J. H. (1963). Crustal structure along the coast of California from seismic-refraction measurements. J. Geophys. Res., 68, 5777-5787.

Colorado Plateau

At the Wasatch Front, the crust begins to thicken eastward (Keller et al., 1975) to values of 40-45 km for the Colorado Plateau (Prodehl, 1970). The Wasatch Front, however, is not the boundary for high attenuation, high heat flow, or high conductivity, because these characteristics persist eastward under the Colorado Plateau and into the southern Rockies. The upper-mantle velocity profile for the Colorado Plateau is distinct from the B-R province because P_n velocities are normal (Herrin and Taggart, 1962) and there is a thicker lid and less pronounced velocity anomalies in the upper mantle (Archambeau et al., 1969; Biswas and Knopoff, 1974; York and Helmberger, 1973). Whether those anomalous features are a remnant of past orogenic activity (King, 1969), the first westward indications of the overriding of an oceanic rift (Cook, 1969), or the outermost effects of the formation of the ensialic interarc basin (Scholz et al., 1971) remains an open question. The area as a whole is relatively aseismic (Smith and Sbar, 1974), a fact that further attests to its stability and cohesiveness.

Southern Rockies

This province is the easternmost border of the tectonic cycles that have churned the Western United States and, as such, it is the most eastward expression of the anomalous upper mantle that characterizes provinces to the west. The crustal thickness is about 50 km (Pakiser, 1963), which is only slightly greater than for the Colorado Plateau. The anomalous geophysical aspects of high conductivity and heat flow seem to persist eastward from the B-R province into this province (Reitzel et al., 1970; Porath and Gough, 1971). The nature of the LVZ under this province is not well defined although it is certainly

---

Keller, G. R., R. B. Smith, and L. W. Braile (1975). Crustal structure along the Great Basin - Colorado Plateau transition from seismic refraction studies. J. Geophys. Res., 80, 1093-1098.

Smith, R. B., and M. Sbar (1974). Contemporary tectonics and seismicity of the Western United States, with emphasis on the intermountain seismic belt. Bull. Geol. Soc. Amer., 85, 1205-1218.

Reitzel, J. S., D. I. Gough, H. Porath, and C. W. Anderson III (1970). Geomagnetic deep sounding and upper mantle structure in the Western United States. Geophys. J., 19, 213-236.

extant to some degree in the southern portion, which is a northward extention of the Rio Grande rift system with its anomalous upper-mantle velocities (York and Helmberger, 1973).

EARTHQUAKES IN THE SOUTHWESTERN UNITED STATES

Tectonic Forces

The development of plate tectonics as the unifying theory for interpreting the global distribution of seismicity in relation to prominent physiographic features within and around the ocean margins (Isacks et al., 1968) has generated reinterpretations of the present structure and activity of the Western United States. At least four relatively distinct interpretations of the anomalous zone centered under the B-R province, all associated with plate tectonics, have been recently presented: 1) Cook (1969) set forth the rift theory holding that the North American plate has overridden the East Pacific rise which now supposedly lies beneath the Basin and Range province; 2) Atwater (1970) argued that the Basin and Range province is a result of broad right-lateral movement in the Western United States, centered in the San Andreas and associated faults, but not entirely accommodated there; 3) Shaw et al. (1971) suggested that earth tidal power generated a thermal source behind an subduction zone on the West Coast, which has now been assimilated, leaving the remnant thermal source under the Basin and Range province; 4) Scholz et al. (1971) claimed that release of compressive stress, due to the termination of an active subduction zone on the West Coast, enabled a mantle diapir created by the subduction zone to initiate crustal extension in the Basin and Range province in a way similar to several interarc basins in the Pacific Ocean. All these hypotheses are satisfactory in explaining observed seismicity of the Southwestern United States because each recognizes the two dominant patterns shown on Figure 9 -- transform motion along the San Andreas fault zone and crustal extension in the Basin and Range province. The presentation of Scholz et al. (1971), as well as that of Smith and Sbar (1974) and Bolt et al. (1968), gives a particularly thorough interpretation of present seismic activity in the region of this study.

Seismicity

Figure 10 shows the distribution of the seismic activity in the Southwestern United States over the past fifteen years, as recorded in the NEIS

Isacks, B., J. Oliver, and L. R. Sykes (1968). Seismology and the new global tectonics. J. Geophys. Res., 73, 5855-5900.

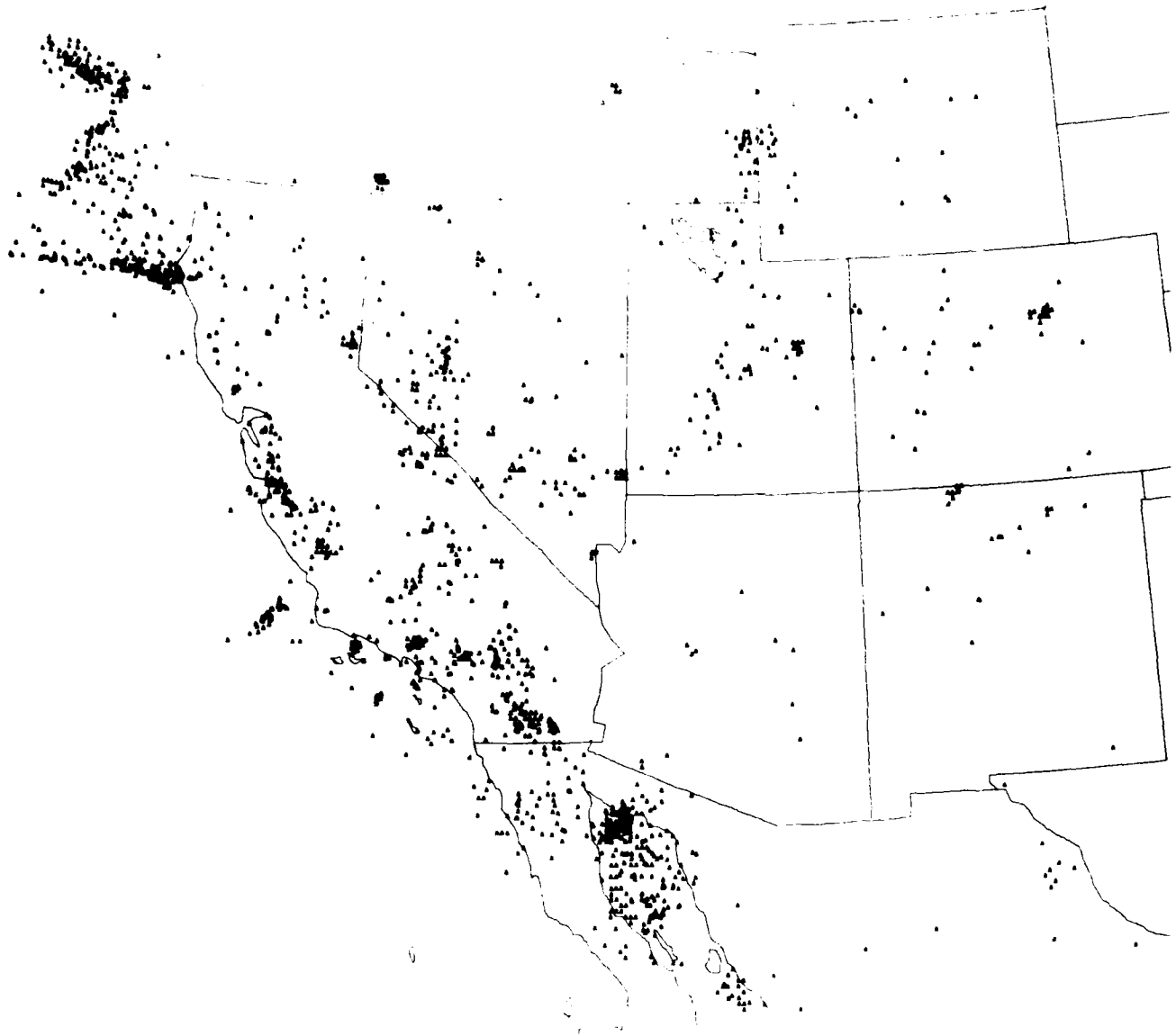

Figure 10 Seismicity of the Southwestern United States from 1961-1975, with m_b > 3.5 (NEIS epicenter files).

epicenter file. All earthquakes with $m_b > 3.5$ have been plotted, except within the Nevada Test Site, where most earthquakes are known to be associated with explosions (Hamilton et al., 1972). Explosions at NTS have also been eliminated, along with the few other scattered events known to be explosions in the Southwestern United States. Three concentrated seismic zones appear to exist. The first zone is the NW-SE lineation associated with the transform motion of the San Andreas fault in western California. A second occurs in eastern California and western Nevada. A third prominent zone is the intermountain seismic belt running N-S along the Wasatch Front in Utah.

The first zone along western California contains events with primarily right-lateral strike-slip motion (Allen et al., 1965; Bolt et al., 1968). This observation is consistent with Wilson's (1965) hypothesis that the San Andreas system is a transform fault linking the East Pacific Rise and the Gorda Ridge. This motion reflects an average slip rate of roughly 4 mm/year (Bolt et al., 1968), which is compatible with geodetic determinations (Savage and Burford, 1973) and with known spreading rates for the East Pacific Rise and Gorda Rise. The only major deviation from this right-lateral strike-slip trend is along the Transverse Ranges and the Garlock Fault (see Figure 9), where thrust and steep reverse faults with a left-lateral component have

---

Hamilton, R. M., B. E. Smith, F. G. Fisher, and P. J. Paponek (1972). Earthquakes caused by underground nuclear explosions on Pahute Mesa, Nevada Test Site. Bull. Seism. Soc. Am., 62, 1319-1341.

Allen, C. R., P. St. Amand, C. F. Richter, and J. M. Nordquist (1965). Relationship between seismicity and geologic structure in the southern California region. Bull. Seism. Soc. Am., 55, 753-795.

Bolt, B. A., C. Lomnitz, and T. V. McEvilly (1968). Seismological evidence on the tectonics of central and northern California and the Mendocino Escarpment. Bull. Seism. Soc. Am., 58, 1725-1767.

Wilson, J. T., (1965). A new class of faults and their bearing on continental drift. Nature, 207, 343-347.

Savage, J. C., and R. O. Burford (1973). Geodetic determination of relative plate motion in central California. J. Geophys. Res., 78, 832-845.

been identified (Allen et al., 1965). For southern California, Thatcher and Hanks (1973) and Wyss and Brune (1971) provided evidence for a considerable range of source mechanisms, dimensions, and stress so that a generalization about this area is not possible though localized similarities do occur. Northern Baja California and the northern Gulf of California are similarly varied. However, Thatcher (1972) pointed out gross differences between most Baja and Gulf earthquakes in this area. The differences are smaller source dimensions and moments for the Baja events and larger stress drops for them, one or two orders of magnitude perhaps. Thatcher's work shows that several of these Baja earthquakes are difficult to discriminate by $M_s - m_b$ from NTS explosions. It also shows that there are a number of exceptions where Baja events have large source dimensions like the Gulf events.

The second zone of concentrated seismicity, the "Nevada seismic zone," reflects both the crustal extension produced by the anomalous upper mantle under the B-R province and the broad right-lateral plate motion of the North American plate against the Pacific plate. This motion interacts with the fairly rigid Sierra Nevada batholith (Gumper and Scholz, 1971) producing a varied stress pattern. Nearly all earthquake mechanisms east and north of this seismic zone are of dip-slip nature (Smith and Sbar, 1974; Gumper and Scholz, 1971; Ryall and Malone, 1971; Stauder and Ryall, 1976) which is compatible with simple block faulting in the B-R province. The crustal extension required for this phenomenon is affirmed by strain and geodetic measurements

---

Thatcher, W., and T. C. Hanks (1973). Source parameters of southern California earthquakes. J. Geophys. Res., 78, 8547-8576.

Thatcher, W. (1972). Regional variation of seismic source parameters in the northern Baja California area. J. Geophys. Res., 77, 1549-1565.

Gumper, F. J., and C. Scholz (1971). Microseismicity and tectonics of the Nevada seismic zone. Bull. Seism. Soc. Am., 61, 1413-1432.

Ryall, A., and S. D. Malone (1971). Earthquake distribution and mechanism of faulting in the Rainbow Mountain-Dixie Valley - Fairview Peak Area, central Nevada. J. Geophys. Res., 76, 7241-7248.

Stauder, W., and A. Ryall (1967). Spatial distribution and source mechanism of microearthquakes in central Nevada. Bull. Seism. Soc. Am., 57, 1317-1345.

(Meister et al., 1968; Priestly, 1974). Overall, focal mechanisms and these physical measurements suggest that the extension is in the NW-SE direction, with the E-W component becoming progressively larger eastward. The total extension in the late Cenozoic era is at least 100 km and, according to Scholz et al. (1971), it may be as much as 300 km.

In the Nevada Seismic Zone, but toward the California-Nevada border, more complex tectonics exist. Gumper and Scholz (1971) determined that in addition to normal faulting, left-lateral strike-slip motion existed over a broad area near 38° N, 118°-119° W. Gumper and Scholz asserted that this area was a transform between two lines of crustal extension to the north and south of roughly 38°N, with the northern seismicity offset to the east. In addition, Gumper and Scholz found a right-lateral component to several of the predominant dip-slip mechanisms of this area. Although many fault mechanisms have been determined in this area, data on stress drops and source dimensions for earthquakes in this zone are sparse.

The third concentrated zone in the region under study is the "intermountain seismic belt," described in detail by Smith and Sbar (1974) and Sbar et al. (1972). This zone encompasses the physiographic boundary known as the Wasatch Front in central Utah and continues northward beyond the region under study. Dip-slip motion on steeply-dipping fault planes is indicated by composite focal-mechanism solutions for various parts of this zone. Smith and Sbar assert that this can be explained either as differential vertical movement of the B-R province relative to the Colorado Plateau, a manifestation of crustal extension characteristic of the B-R province to the west, or as evidence that the B-R province is a subplate moving westward relative to North America. They have also correlated a number of earthquake swarms in this

---

Meister, L. J., R. O. Burford, G. A. Thompson, and R. L. Kovach (1968). Surface strain changes and strain energy release in the Dixie Valley - Fairview Peak Area, Nevada. J. Geophys. Res., 73, 5981-5994.

Priestley, K. (1974). Crustal strain measurements in Nevada. Bull. Seism. Soc. Am., 64, 1319-1328.

Sbar, M. L., M. Barazangi, J. Dorman, C. H. Scholz, and R. B. Smith (1972). Tectonics of the intermountain seismic belt, Western United States, microearthquakes, seismicity, and composite fault plane solutions. Bull. Geol. Soc. Amer., 83, 13-28.

zone with areas of high heat flow and characteristic geothermal features. The westward-trending lower part of this zone in southern Utah and eastern Nevada appears to have left-lateral strike-slip motion, which is further evidence of westward motion of the B-R province relative to the Colorado Plateau. Almost no data is available on source dimensions and stress drops for earthquakes in this zone.

In addition to the natural seismicity in the Western United States, examples exist of artificial seismicity. The artificial seismicity associated with NTS shots is well known. Also, earthquakes have been associated with fluid injection near Denver, Colorado (described by Healy et al., 1968). Effective stress and drops for these events have been determined by Wyss and Molnar (1972). Their calculations suggest small stress drops and normal source dimensions relative to values expected for their magnitude (M_L).

Depth of Focus

Many authors (e.g., Brace and Byerlee, 1970; Cook and Smith, 1967; Tocher, 1958) have affirmed that all seismicity in the Southwestern United States is shallow. All accurately located earthquakes have been within the crust, the majority at depths of less than 15 km. No present seismic evidence exists for continued motion of the subduction zone, which has been postulated to be active on the West Coast during the Cenozoic Era. In the B-R province, Smith and Sbar (1974) reported a rather abrupt cutoff in seismicity related to a crustal low-velocity zone starting at depth of roughly 15 km (Braile et al., 1974;

Healy, J. H., W. W. Rubey, D. T. Griggs, and C. B. Rayleigh (1968). The Denver earthquakes. Science, 161, 1301-1310

Wyss, M., and P. Molnar (1972). Efficiency, stress drop, apparent stress, effective stress, and frictional stress of Denver, Colorado, earthquakes. J. Geophys. Res., 77, 1433-1438.

Brace, W. F., and J. D. Byerlee (1970). California earthquakes, why only shallow focus. Science, 156, 1573-1575.

Cook, K. L., and R. B. Smith (1967). Seismicity in Utah, 1850 through June 1965. Bull. Seism. Soc. Am., 57, 689-718.

Tocher, D. (1958). Earthquake energy and ground breakage. Bull Seism. Soc. Am., 48, 147-153.

Mueller and Landisman, 1971). Shurbet and Cebull (1971) elaborated on this idea, postulating that such a crustal layer is undergoing extension and that it is the origin of the graben-and-horst character of the B-R province. It is most reasonable that the extension be due to an anomalous upper mantle, and that, if seismicity indeed abates below 15 km, then the lower crust must be deformed plastically along with the upper mantle.

In sum, the shallowness of seismicity in the Western United States means that location alone is of little importance in discriminating events in this region unless master events were widely employed to narrow the depth confidence limits produced by a high-quality network of teleseismic stations. However, use of master events may not be the solution because Blandford (1975) found a 20-km standard deviation for depth estimates of master-controlled NTS explosions when well-distributed networks of teleseismic stations were used.

Mueller, S., and M. Landisman (1971). An example of the unified method of interpretation for crustal seismic data. Geophys. J., 23, 365-371.

Shurbet, D. H., and S. E. Cebull (1971). Crustal low-velocity layer and regional extension in the Basin and Range province. Bull. Geol. Soc. Am., 82, 3241-3244.

Blandford, R. R. (1975). Use of source-region-station-time corrections at NTS for depth estimation. Report No. SDAC-TR-75-4, Teledyne Geotech, Alexandria, Virginia.

DATA SELECTED FOR DISCRIMINATION STUDY

The twenty-three seismic events described below were selected from known events in the Southwestern United States. Eleven were explosions and twelve were earthquakes. This sample was considered sufficient to produce clear results and also to supply many important and interesting particular features for study. In order to take advantage of the continuous recording of several sites in the Long Range Seismic Measurements (LRSM) network of the VELA-Uniform program, the events were restricted to the years 1966-1969. The magnitude range, 4.8 to 6.5 m_b, of these events insures that most signals recorded by the North American LRSM network are of good signal/noise ratio. Low-magnitude events were intentionally rejected since this study is not one of detection and signal enhancement but one of multi-dimensional discrimination based upon the best available data. However, results attained here for medium-magnitude events are expected to apply in most aspects to events of lower magnitude. The only significant deviations at lower magnitudes would result from different scaling of source dimensions and time functions between earthquakes and explosions for lower magnitudes versus medium magnitudes.

Data for the eleven explosions listed in Table III were taken from Springer and Kinnaman (1971). Eight of these explosions were at the Nevada Test Site and represented various yields, depths, locations, and mediums. Several, such as PILE DRIVER, GREELEY, and BENHAM, had a considerable component of tectonic strain release (Toksöz and Kehrer, 1972a); these explosions were deliberately included to empirically assess the degree of adverse effect on discrimination entailed in this phenomenon. Only three nuclear explosions-- FAULTLESS, GASBUGGY, and RULISON-- were detonated outside NTS in the desired time period; they were included to spread the explosion sources over a wide area of the Southwestern United States. The locations of all these explosions have been plotted on Figures 9 and 11.

Springer, D. L., and R. L. Kinnaman (1971). Seismic source summary for U. S. underground nuclear explosions, 1961-1970. Bull. Seism. Soc., Am., 61, 1073-1098.

TABLE III

Selected Events for Discrimination Study

EARTHQUAKES

SYMBOL	NAME	DATE	ORIGIN TIME	LATITUDE	LONGITUDE	m_b	DEPTH (km)	PLACE
A	Dulce, N.M. EQ	01/23/66	01:56:38.8	37.000N	107.000W	5.5	14	New Mexico
B	Caliente EQ	08/16/66	18:02:36.6	37.400N	114.200W	5.6	33	Nevada
C	Truckee EQ	09/12/66	16:41:02.1	39.400N	120.100W	5.7	11	California
D	Caliente AS	09/22/66	18:57:36.5	37.400N	114.200W	5.3	33	Nevada
E	Denver EQ	08/09/67	13:25:06.2	39.900N	104.700W	5.3	5	Colorado
F	Baja EQ	09/21/67	00:01:54.1	31.200N	115.900W	5.1	33	Baja Cal.
G	Utah EQ	10/04/67	10:20:14.0	38.500N	112.100W	5.2	18	Utah
H	Borrego Mtn. EQ	04/09/68	02:28:58.9	33.100N	116.100W	6.1	20	California
I	Nevada EQ	05/22/68	13:21:55.7	38.576N	116.186W	5.1	13	Nevada
J	BENHAM AS	12/21/68	00:14:25.2	37.325N	116.506W	4.9	4	Nevada
K	29 Palms EQ	01/23/69	23:01:01.0	33.887N	116.040W	4.9	18	California
L	Coyote Mtn. EQ	04/28/69	23:20:42.9	33.350N	116.350W	5.7	20	California

EXPLOSIONS

SYMBOL	NAME	DATE	O.T.	LAT.	LONG.	m_b	DEPTH (m)	PLACE	MEDIUM	(YIELD (kt)
1	DURYEA	04/14/66	14:13:43.1	37.242	116.431	5.21	544	Pahute Mesa	Rhyolite	65
2	PILE DRIVER	06/02/66	15:30:00.1	37.227	116.056	5.55	463	North of Yucca Flats	Granite	56
3	HALFBEAK	06/30/66	22:15:00.1	37.216	116.299	6.03	819	Pahute Mesa	Rhyolite	300
4	GREELEY	12/20/66	15:30:00.1	37.302	116.408	6.26	1215	Pahute Mesa	Tuff	825
5	COMMODORE	05/20/67	15:00:00.0	37.130	116.064	5.68	746	Yucca Flats	Tuff	250
6	SCOTCH	05/23/67	14:00:00.0	37.275	116.370	5.56	977	Pahute Mesa	Tuff	150
7	GASBUGGY	12/10/67	19:30:00.1	36.678	107.208	5.26	1292	New Mexico	Shale	29
8	FAULTLESS	01/19/68	18:15:00.1	38.634	116.215	6.51	975	Hot Creek Valley	Tuff	(Intermediate)
9	BOXCAR	04/26/68	15:00:00.0	37.295	116.456	6.42	1158	Pahute Mesa	Rhyolite	1200
10	BENHAM	12/19/68	16:30:00.0	37.231	116.474	6.40	1402	Pahute Mesa	Tuff	1100
11	RULISON	09/10/69	21:00:00.0	39.406	107.948	4.62	2573	Colorado	Sandstone	40

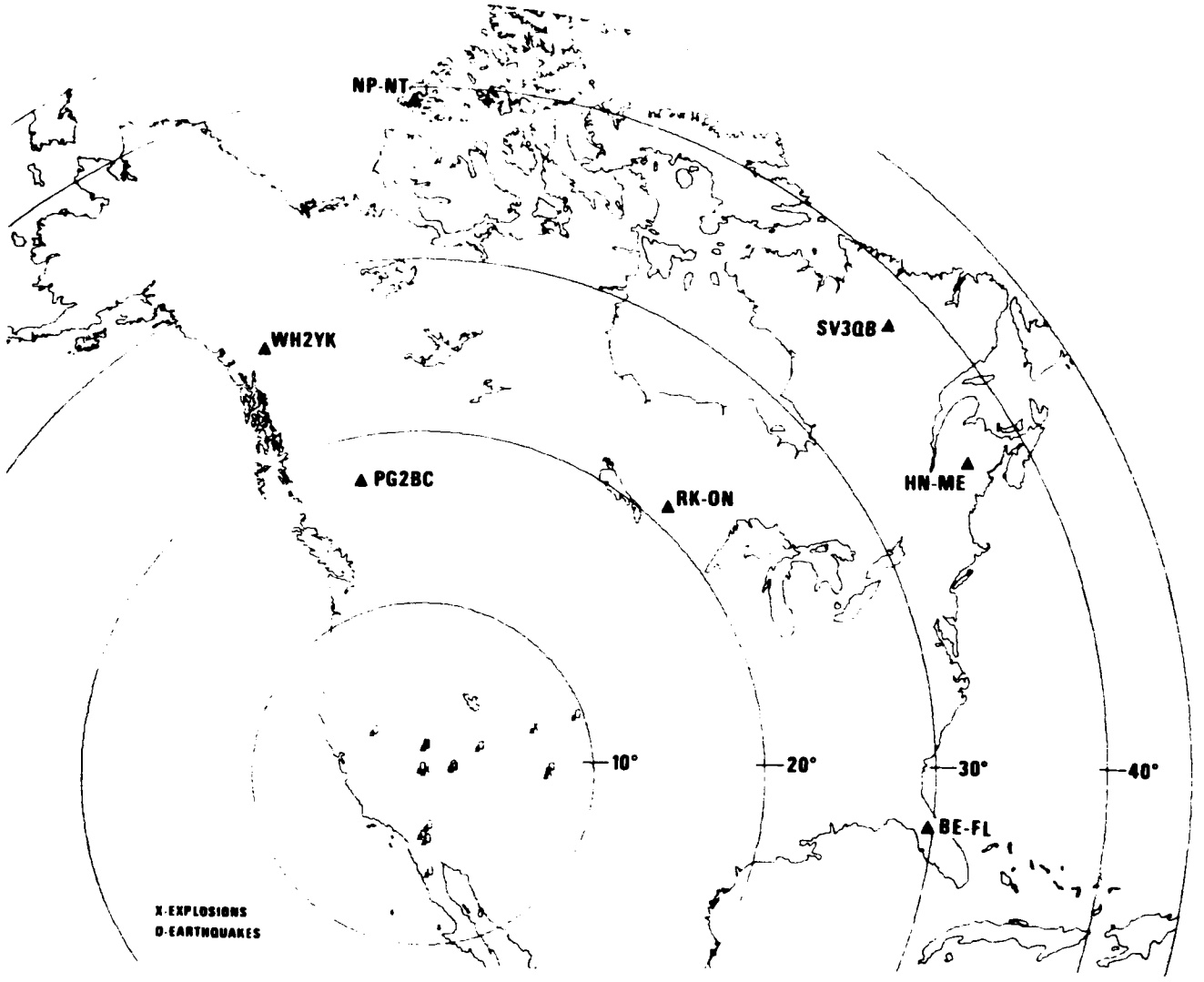

Figure 11 Locations of stations and events used in this study.

The twelve earthquakes selected are also listed in Table III; the epicenter data is from the NEIS list. The symbols associated with the earthquakes and explosions in this Table are used throughout this report. As seen in Figures 9 and 11, the earthquakes are reasonably well distributed over the region of study. Four of these earthquakes are in Nevada and will provide the most direct comparison with explosions. Each of these events have themselves been the subject of separate studies or part of a group of events studied or examined in another published work. Their presence in such studies was one criterion for inclusion in this study. Another criterion used for earthquake selection was that they should only slightly separate from NTS explosions in published $M_s - m_b$ plots. All of this previous information fits into this regional study and aids in sustaining its conclusions.

A subset of the LRSM network, namely WH-YK, NP-NT, RK-ON, SV3QB, HN-ME, BE-FL, and PG-BC, plotted in Figure 11, was chosen for this study. Each station of this subset was operational for most, or all, the time encompassing the selected events. The stations were chosen because they are teleseismic or nearly teleseismic from the selected events. This situation eases problems associated with multiple arrivals due to travel-time triplications or problems inherent in head-wave interpretations. Teleseismic distances tend to simplify magnitude determination compared to regional distances. Although this selected subset provides nearly as wide an azimuthal distribution of teleseismic stations as possible over North America, relative to events in the Southwestern United States, the coverage still is barely more than one quadrant. All the seismograms were re-examined to produce the amplitude data for this report. Other data, in the form of spectral ratios and complexities, was obtained from digitized recordings. The data base pertinent to discrimination of these events is listed in Table IV. The magnitude data of this list was computed according to the common relations

$$m_b = \log(A/T) + B$$
$$M_s = \log(A/T) + 1.66 \log\Delta + 0.3$$

TABLE IV

Seismic Discrimination Data for Selected Southwestern United States Events

DATA USED IN STUDY OF 11 EXPLOSIONS AND 12 EARTHQUAKES IN SOUTHWEST U.S.

COLUMN (1) : STATION NAME
(2) : EPICENTER-TO-STATION DISTANCE (DEGREES)
(3)-(4) : EPICENTER-TO-STATION AND STATION-TO-EPICENTER AZIMUTHS (DEGREES)
(5)-(8) : BODY-WAVE MAGNITUDES DETERMINED FROM SHORT-PERIOD P, SHORT-PERIOD S, LONG-PERIOD P, AND LONG-PERIOD S
(9)-(10) : SURFACE-WAVE MAGNITUDES DETERMINED FROM LOVE WAVES AND RAYLEIGH WAVES
(11)-(12) : SPECTRAL RATIOS DETERMINED FROM SHORT-PERIOD AND LONG-PERIOD SPECTRA
(13) : LOGARITHM OF SHORT-PERIOD SIGNAL COMPLEXITY
(14) : POLARITY OF FIRST MOTION

NOTE CONVENTION (SEE FOOTNOTES) REGARDING MINUS SIGNS

EVENT = 1 DUPUYA

STN	DELTA	E-S AZ	S-E AZ	SPP	SPS	LPP	LPS	LQ	LR	SP SR	LP SP	LG CORR	SGN
BE	29.8	96.	295.	-5.05	-5.09	-4.59	-4.15	-3.79	4.42		0.0707		
HN	36.6	60.	273.	5.54	-5.42	-4.53	-4.19	4.27	3.65	0.0266	-1.9768	0.226	
HP	39.0	358.	176.	4.66	-4.35	-4.96	-4.57	4.34	4.20	0.0490	1.6387	0.415	
PG	17.3	307.	163.	4.93	-5.25					0.0304		0.664	
RK	21.1	82.	238.	5.39	-4.36	-5.31	-3.27	3.59		0.0215	-1.6847	0.691	
SV	37.7	86.	263.	4.92	-4.95	-5.43	-4.39	-3.62	3.75	-0.0436		0.385	

EVENT = 2 PILEDRIVER

STN	DELTA	E-S AZ	S-E AZ	SPP	SPS	LPP	LPS	LQ	LR	SP SR	LP SR	LG CORR	SGN
BE	29.5	96.	295.	5.61	-5.05	-3.50	3.94	4.35	4.51	0.0451	2.0403	0.317	
HN	36.4	60.	273.	5.67	-4.53	-3.56	-3.09	5.05	4.06	0.0187	1.5981	0.401	
HP	39.0	358.	176.	5.66	4.06	-3.77	-4.10	4.79	4.73	0.0964	1.6061	0.606	
PG	17.3	307.	162.	5.68	-4.74	3.90	4.30	4.60	3.80	0.0509		1.093	
RK	20.9	82.	238.		-3.37	3.78	4.05	4.30	4.06	-0.0667	1.5857	0.373	
SV	37.5	86.	262.	5.27	4.94	-4.27	4.36		4.30	0.0542	1.6569	1.118	

EVENT = 3 HALFBEAK

STN	DELTA	E-S AZ	S-E AZ	SPP	SPS	LPP	LPS	LQ	LR	SP SR	LP SR	LG CORR	SGN
BE	29.7	96.	295.	6.02	-5.24	-4.41	5.08		5.37	0.0095	0.0239	0.538	
HN	36.5	60.	273.	6.21	-5.63	-3.82	4.80	5.11	5.05	0.0128	0.0388	0.366	
PG	17.2	307.	163.	5.94	-5.59	3.96	4.31	5.41	4.69	0.0114	2.0870	1.133	
RK	21.0	82.	238.	6.14	-4.68	3.50	4.31	5.10	4.75	0.0209	2.1572	0.386	
SV	37.5	86.	263.	6.11	-5.14	-5.20	-4.66		4.45	0.0161	-1.3211	0.618	

EVENT = 4 GRPELEY

STN	DELTA	E-S AZ	S-E AZ	SPP	SPS	LPP	LPS	LQ	LR	SP SR	LP SP	LG CORR	SGN
BE	29.8	96.	295.	6.48	-5.68	-4.85	5.38		5.88	0.0261	2.0662	0.870	
HN	36.6	60.	273.	6.67	-5.56	-4.37	-4.88	6.23	5.38	0.0049	2.0755	0.518	
HP	39.0	358.	176.	6.33	-5.70	-4.11	5.59		5.45	-0.0191	2.1198	0.554	
PG	17.2	307.	163.	6.58	-5.53	4.29	5.06	5.93	6.96	0.0037	1.9316	0.958	
RK	21.1	82.	238.	6.27	-5.21	5.01	4.38	5.88	4.98	0.0101	2.1196	0.000	
SV	37.6	86.	263.	6.60	-5.70	-4.62	-4.88	5.68	5.26	0.0063	1.8039	0.652	
GN	26.2	339.	144.	5.58	-5.13	-4.78	5.77	5.99	5.55	0.0107	1.6206	0.025	

TABLE IV (Continued)

Seismic Discrimination Data for Selected Southwestern United States Events

EVENT = 5 COMMODORE

STN	DELTA	E-S AZ	S-E AZ	SPP	SPS	LPP	LPS	LQ	LR	SP SR	LP SR	LG COMP	SGN
NN	16.4	60.	273.	6.07	-5.06	-4.40	-4.82	5.04	4.87	0.0100	1.2287	0.478	
WP	19.1	355.	176.	6.00	-5.60	-4.09	-4.29	4.83	5.28	0.0303	1.8712	0.402	
PG	17.4	347.	163.	5.61	-5.26	-3.39	-4.40	4.77	4.99	0.0109		1.060	
RK	21.0	42.	237.	6.02	-4.86	-3.59	-4.13	4.22	3.95	0.0126	1.8740	0.395	
SV	37.5	45.	260.	5.64	-4.76	-4.09	-4.51	4.58	4.91	0.0315	-2.2444	0.519	
GN	26.4	339.	144.	5.07	-4.36	-4.02	4.98	4.78	4.94	0.0139	1.1755	0.725	

EVENT = 6 SCOTCH

STN	DELTA	E-S AZ	S-E AZ	SPP	SPS	LPP	LPS	LQ	LR	SP SR	LP SR	LG COMP	SGN
NN	16.6	60.	273.	5.82	-4.57	-4.39	-4.18	4.90	4.53	0.0231	1.0035	0.185	
WP	19.0	356.	176.	5.56	-4.90	-4.53	-4.82	5.62	5.10	0.1537	1.5115	0.622	
PG	17.2	347.	163.	5.34	-5.32	-4.11	-4.59	5.24	4.45	0.0337	1.8856	0.760	
RK	21.1	42.	238.	6.06	-4.55	-3.61	-4.14	5.19	4.11	0.0427	0.0022	0.685	
SV	37.6	45.	260.	5.68	-4.70	-4.41	-4.76	5.00		0.0174	1.6890	0.616	
GN	26.2	339.	144.	5.04	-4.27	-4.01	5.87	4.85	5.09	-0.0297	1.5381	0.959	

EVENT = 7 GASBUGGY

STN	DELTA	E-S AZ	S-E AZ	SPP	SPS	LPP	LPS	LQ	LR	SP SR	LP SR	LG COMP	SGN
NN	10.5	58.	246.	-5.15	-4.97	-4.70	-3.60	3.64	3.64		-1.3737		
WP	39.9	355.	164.	4.82	-4.82		-4.88	-3.68		0.0563		0.387	
PG	20.3	333.	182.	4.56	-4.89	-3.55	-3.57	3.90	3.61	0.0969	1.5188	0.589	
RK	17.1	30.	216.	4.38	-4.86	-4.12	-4.34	3.48	3.61	0.1336	-1.5781	0.372	
SV	32.8	43.	253.	4.32	-5.04	-4.15	-4.24	3.79	3.83	0.0321		0.653	
GN	29.8	332.	130.	4.15	-5.29	-4.79	-4.72	3.91	3.98				

EVENT = 8 PAULTLESS

STN	DELTA	E-S AZ	S-E AZ	SPP	SPS	LPP	LPS	LQ	LR	SP SR	LP SR	LG COMP	SGN
BE	30.1	90.	297.	6.57	-5.46		4.58		5.10		1.2155		
NN	36.1	61.	275.	6.41	-5.58	-4.58	4.63	5.26	5.72	0.0228	1.6137	0.013	
WP	35.6	358.	176.	6.09	-5.96	-5.23	5.38	5.63	5.75	0.0118	-1.8730	0.687	
PG	33.9	347.	162.	6.27	-6.07	4.58	5.76	5.27	5.21	0.0060	1.8738	0.606	
RK	28.2	85.	241.	6.32	-5.08	4.25	4.88	5.12	5.80	0.0324	2.0613	1.208	
SV	36.8	47.	265.	6.54	-5.69	4.35	4.89	5.13	4.77	0.0101	1.8317	1.097	
GN	24.9	339.	144.	6.17	-5.20	-4.56	5.38	5.11	5.83	0.0018	1.5605	0.762	

EVENT = 9 BOXCAR

STN	DELTA	E-S AZ	S-E AZ	SPP	SPS	LPP	LPS	LQ	LR	SP SR	LP SR	LG COMP	SGN
NN	36.7	60.	273.	6.66	-5.36	-5.27	5.23		5.75	0.0116	0.7001	0.809	
WP	39.0	358.	176.	6.37	-5.66	-4.23	5.37		5.92	0.0109	1.1352	0.691	
PG	37.2	347.	163.	6.70	-5.70	4.28	5.50		5.31	0.0051	1.4861	1.069	
RK	31.1	42.	238.	6.73	-5.35	4.32	5.13		5.20	0.0060	1.4523	0.975	
SV	37.7	46.	263.	6.04	-5.48	-4.21	5.18	5.16	5.60	0.0201	1.6885	0.691	
GN	26.2	339.	144.	5.74	-5.09	-4.07	6.02	5.19	5.65	0.0208	1.3621	0.927	

TABLE IV (Continued)

Seismic Discrimination Data for Selected Southwestern United States Events

EVENT = 10 PENNAM

STN	DELTA	P-S AZ	S-P AZ	SPP	SPS	LPP	LPS	LQ	LR	SP SR	LP SR	LG COMP	SGN
NN	3.7	60.	223.	6.08	-5.35	-4.72	5.34	6.11	5.85	0.0097	0.8451	0.557	
WP	10.0	358.	178.	6.80	-5.77	-4.64	6.50		6.11	0.0117	1.8635	0.815	
PG	17.3	345.	163.	6.68	-5.86	-4.79	6.09		5.24	0.0047	1.7056	1.014	
BK	21.1	42.	233.	6.86	-6.17	-4.93	5.14		5.25	0.0065	2.4298	1.001	
SV	26.3	336.	144.	5.92	-5.44	-4.75	7.00		5.68	0.0221	1.2997	0.905	

EVENT = 11 WILLISON

STN	DELTA	P-S AZ	S-P AZ	SPP	SPS	LPP	LPS	LQ	LR	SP SR	LP SP	LG COMP	SGN
NN	29.8	63.	271.	5.08	-4.96	-4.23	4.51	4.18	4.10	0.0140	2.1519	0.808	
WP	17.2	358.	165.	4.76	-4.68	-4.17	4.74		4.13	0.0270	2.3547	0.812	
PG	17.6	350.	180.	4.89	-4.93	-4.59	-5.02	3.71	3.57	0.1325		0.519	
BK	19.2	36.	226.	4.97	-5.75	-3.72	-4.84	3.62	3.67	0.3466	0.8520	1.101	

EVENT = A 1/23/66

STN	DELTA	P-S AZ	S-P AZ	SPP	SPS	LPP	LPS	LQ	LR	SP SR	LP SP	LG COMP	SGN
BE	22.3	103.	297.	-5.12	-5.00	5.59	5.33	4.97	4.99		1.6923		
NN	30.2	58.	266.	-4.86	-4.23	-4.92	4.92	4.95	4.99	0.0091	1.0766		-
WP	10.6	355.	164.	5.16	-4.35	-4.55	-4.69	4.63	4.46	0.0158	-1.6688	0.873	*
PG	20.1	332.	181.	5.07	-3.53	-4.28	3.96	4.53	4.82	0.0270	-1.6889	1.238	*
BK	16.8	30.	210.	4.69	-5.58	-4.04	5.22		4.91	0.1004	1.0768	0.587	-
SV	32.5	63.	253.	5.16	-4.30	-5.18	4.78	5.20	5.13	0.0179	1.6222	0.583	

EVENT = B 8/16/66

STN	DELTA	P-S AZ	S-P AZ	SPP	SPS	LPP	LPS	LQ	LR	SP SR	LP SR	LG COMP	SGN
BE	28.0	98.	296.	4.90	-4.36		4.95		5.19		-2.1057		-
NN	35.0	66.	272.	5.69	-4.73	4.29	5.20		5.61	0.0181	1.1629	0.322	-
WP	10.0	356.	173.	5.39	-4.56		6.01	6.01	5.59		0.9181		-
PG	17.6	343.	157.	5.60	-4.76	4.26	5.62		5.02	0.0273	1.2648	1.563	*
BK	19.8	80.	239.	5.83	-4.29		4.88	5.43	5.32	0.0256		1.188	*
SV	36.3	85.	261.	6.71	-4.65	-4.51	5.28			0.0129		0.253	-

EVENT = C 9/12/66

STN	DELTA	P-S AZ	S-P AZ	SPP	SPS	LPP	LPS	LQ	LR	SP SR	LP SR	LG COMP	SGN
BE	32.9	96.	298.		4.85	6.09	5.88	5.61	5.91		-0.5911		*
NN	36.8	0.	180.	5.62	5.07	4.54	6.27	5.30	5.60	0.0189	-1.0214	0.962	-
WP	14.7	354.	172.	5.73	-5.95	5.35	6.67		5.19	0.0051	1.5097	1.323	-
PG	21.7	49.	248.	5.45	5.64	4.79	4.91	5.30	5.60	0.0283	0.8224	1.060	
SV	38.1	88.	268.	6.19	-4.90	-4.66	5.50	5.64	5.94	0.0225	1.1653	1.029	

EVENT = D 9/22/66

STN	DELTA	P-S AZ	S-P AZ	SPP	SPS	LPP	LPS	LQ	LR	SP SR	LP SR	LG COMP	SGN
BE	28.0	98.	296.	-4.56	4.58	-5.15	5.03	5.26	4.95		1.9746		
NN	30.9	358.	173.	4.46	-5.67	-4.65	4.99		5.32		-0.9069		-
PG	17.6	343.	157.	4.13	-4.52	3.80	5.61		4.67	0.2934	1.9898	1.243	*
BK	19.8	80.	235.	5.03	-4.26	4.26	4.76		4.88	0.0601	0.6987	1.913	
SV	36.3	85.	261.	4.37	-4.88	-4.74	5.05	5.68	5.25		1.2175		

TABLE IV (Continued)

Seismic Discrimination Data for Selected Southwestern United States Events

EVENT = E 9/9/67

STN	DELTA	E-S AZ	S-E AZ	SPP	SPS	LPP	LPS	LQ	LR	SP SR	LP SR	LG COMP	SGN
NN	27.3	64.	270.	4.32	-4.39	4.49	4.71	4.85	4.72		1.3726		*
BP	36.9	354.	169.	5.24	-4.86		4.25	4.87		0.2357		0.316	-
PG	18.5	325.	132.	4.43	-3.91	3.47	3.97	4.23	3.93	0.0140	1.0139	1.020	
RK	13.4	31.	210.	5.35	-6.32	4.09	5.51	4.63	4.35	0.0747	1.3533	1.289	*
SV	29.2	46.	265.			-4.43	4.74		4.17		0.1778		
BN	24.8	328.	120.	5.13	-4.56	-4.23	-3.94	4.29	3.77	0.0416	1.7188		

EVENT = F 9/27/67

STN	DELTA	E-S AZ	S-E AZ	SPP	SPS	LPP	LPS	LQ	LR	SP SR	LP SR	LG COMP	SGN
BP	35.1	358.	175.		-4.62	-4.74	4.12	5.05	4.82				
RK	25.6	33.	228.	5.02				3.55	3.68	-0.0453	-1.2352	1.362	
SV	31.8	40.	255.	-4.78	-4.73	-3.86	-4.13	4.26	4.25		-1.1389		
BN	32.1	342.	148.					4.95	4.22		1.7715		

EVENT = G 10/8/67

STN	DELTA	E-S AZ	S-E AZ	SPP	SPS	LPP	LPS	LQ	LR	SP SR	LP SR	LG COMP	SGN
NN	33.6	62.	272.	-5.10	-4.96	-4.10	4.89				3.9955		
BP	37.0	357.	170.	5.26	-4.83	-4.81	5.15	5.05	4.73	0.0120	-2.7621	0.719	-
PG	17.0	330.	151.	5.23	-5.23	4.89	5.35		4.74	0.0230	2.2913	0.668	
RK	17.9	40.	230.	4.76	-5.28	3.85	4.78		4.01	0.0267	3.0978	1.049	-
SV	30.2	46.	260.	-4.98	-5.46	-4.32	4.84	5.01	4.69				
BN	26.5	330.	136.	5.42	-4.85	5.41	5.57	5.20	4.91				*

EVENT = H 4/9/68

STN	DELTA	E-S AZ	S-E AZ	SPP	SPS	LPP	LPS	LQ	LR	SP SR	LP SP	LG COMP	SGN
NN	38.6	55.	267.	6.72	6.50	5.41	6.28			0.0020		0.828	
BP	43.2	350.	175.		-6.06	5.93	6.59			0.0433		1.139	-
PG	21.6	349.	165.	5.81	5.41					0.0298		1.057	
RK	24.1	36.	231.	6.94	6.27	5.59				0.0565		1.102	-
SV	40.5	42.	256.	6.50	6.58	4.92	-5.70						
BN	30.3	341.	147.	5.58		6.30		6.54	6.58	0.0261	-0.7625	1.134	-

EVENT = I 5/22/68

STN	DELTA	E-S AZ	S-E AZ	SPP	SPS	LPP	LPS	LQ	LR	SP SR	LP SR	LG COMP	SGN
NN	35.8	61.	275.	6.44	-6.07	6.13	-4.26	6.33	6.10		0.9598		-
BP	37.7	350.	175.	6.43	-5.66	-6.24	6.63	5.08	6.57	0.0133	0.9666	0.969	*
PG	16.0	346.	161.	6.51	-6.76	-5.33	5.73	6.00	5.06	0.0152	-1.7929	1.163	*
RK	20.6	46.	240.	6.27	-5.76	-5.75	5.69	6.16	5.65		-1.1304		*
SV	38.4	47.	264.	-6.56	-5.12	-6.20	6.52	6.18	6.05				
BN	25.1	338.	163.	5.98	-5.19	-6.25	6.69	6.34	6.26	0.2061			

TABLE IV (Continued)

Seismic Discrimination Data for Selected Southwestern United States Events

EVENT = J 12/21/69

STN	DELTA	E-S AZ	S-P AZ	SPP	SPS	LPP	LPS	LQ	LR	SP SR	LP SR	LG CORR	SGN
HN	36.7	60.	273.	-5.73	-5.59	-4.06	-3.99	4.54	3.66		-1.5265		
BP	38.0	358.	176.	-4.60	-4.32	-5.31	-5.14	4.48	-4.34				
PG	17.2	340.	161.	4.68	-4.93	-3.36	-4.72	3.87	3.41		-1.0785		*
BR	21.1	42.	239.	4.82	-3.88	-1.99	3.74	3.80	3.53	0.0206	-2.2115	0.981	
BH	26.2	338.	144.	4.19	-4.41	-4.14	5.11	4.12	3.83		1.1343		*

EVENT = K 1/23/69

STN	DELTA	E-S AZ	S-P AZ	SPP	SPS	LPP	LPS	LQ	LR	SP SR	LP SR	LG CORR	SGN
HN	36.1	56.	268.	-4.50	-5.42	-4.68	-4.11	5.05	4.22		0.5786		
BP	42.4	358.	175.	4.38	4.85	-4.92	-4.80	5.23	-4.59				-
PG	20.6	340.	160.	4.47	-4.23	-3.98	3.78	4.86	3.96	0.1009	1.6935	0.616	
BR	23.5	37.	232.	4.66	-4.52	-4.07	4.11	4.06	3.63	0.0160	-1.2863	1.018	*
BH	29.6	341.	146.	-4.25	-4.26	-4.40	4.61	4.90	4.20		-2.1677		

EVENT = L 8/28/69

STN	DELTA	E-S AZ	S-P AZ	SPP	SPS	LPP	LPS	LQ	LR	SP SR	LP SR	LG CORR	SGN
HN	30.6	55.	268.	5.57	-4.86	4.29	5.33		5.00				-
BP	42.6	358.	176.	5.21	-4.66	-4.06	5.26		5.50	0.0206	-2.2979	1.698	-
PG	21.1	340.	165.	5.77	-4.86	4.80	5.02		5.28	0.0118		1.709	-
BR	26.1	36.	232.	5.81	-4.22	4.02	5.32		5.65	0.0129		1.291	-
BH	30.0	341.	149.	5.54	-3.56	5.02	5.79	6.11	5.66				-

********** NOTES **********

MINUS SIGNS INDICATE THAT THESE MAGNITUDES ARE MEASUREMENTS OF NOISE LEVELS, NOT SIGNAL DETECTIONS. (FOR SPECTRAL RATIOS, THIS MEANS A SIGNIFICANT PORTION OF THE SPECTRAL BANDS WAS AFFECTED BY NOISE)

ALL S-WAVE DATA (SHORT- AND LONG-PERIOD) IS FOR THE LARGEST OF THE 3 COMPONENTS

NOTE THAT THE VALUES LISTED HERE ARE OF THE SHORT- AND LONG-PERIOD SPECTRAL RATIOS, NOT THEIR LOGARITHMS

NO ATTENUATION CORRECTION HAS BEEN APPLIED TO THE SHORT-PERIOD SPECTRAL RATIOS

NOTE THAT THE VALUES LISTED HERE ARE OF THE LOGARITHMS OF THE SIGNAL COMPLEXITIES

BP 10 : LQ BASED ON BEAR-BY STATION ABC (MOULD BAY, CANADA), FOR WHICH M(LQ)-M(LR)=0.5

EVENT 11 : ALL SPS AND LPS MEASUREMENTS AT ALL STATIONS VERY UNCERTAIN

BP B : LQ BASED ON ABC, FOR WHICH M(LQ)-M(LR)=0.82

EVENT C : ALL LQ BASED ON TSAI & AKI (BSSA,60,P.1193) LQ30/LR2=2 FROM SPECTRA AT 4 STATIONS, SO M(LQ)-M(LR)=0.30

GN M : LQ ASSUMED = LR; CF. MS=6.7 FROM MASHORT & ANDERSON (BSSA,OCT. 75)

where

A - one-half the peak-to-trough maximum amplitude on the recording, reduced to nm,

T - period in seconds,

Δ - distance in degrees,

B - Gutenberg-Richter distance-correction terms for P and S phases.

For the event magnitudes to be shown in later plots, the magnitude estimation technique of Ringdal (1976) has been employed. This technique tends to eliminate upward bias, relative to the true magnitude, of an event magnitude which is averaged over only a few recording stations for small events. The technique will be explained in detail in a later section. If no signals of a particular type were recorded for an event, then an event magnitude will be plotted as the average of the station magnitudes based on noise measurements. This approach tends to overestimate the true magnitude, but there is no simple and satisfactory alternative.

The complexity values in Table IV were computed in the manner shown by Lambert et al. (1969). Essentially, they represent the inverse of the power in the first 5 seconds of P arrival divided by that in the following 30 seconds of coda (higher complexity value means more coda). The spectral ratios were computed on the raw spectrum of the P and LR signals. For P waves, the first 6.4 seconds of signal data, sampled at 20 pts/sec, were tapered and transformed. For LR waves, the data in the group-velocity window from roughly 3.7 to 2.8 km/sec, sampled at 1 pt/sec, were tapered and transformed. The P-wave spectral ratio was computed as the sum of the Fourier amplitude coefficients from 1.56 to 1.87 Hz over that from 0.47 to 0.78 Hz, and the LR-wave ratio used 0.0459 to 0.0718 Hz over 0.0283 to 0.0449 Hz. In both cases, the spectral ratio represents high over low frequencies. Spectral ratios regarded as inaccurate due to interfering noise in any of these bands, are indicated in Table IV.

The focal mechanisms of the selected events are plotted in Figure 12, and the source of each focal mechanism determination is listed in Table V. Several earthquakes had more than one proposed mechanism, and the mechanism that seemed best was chosen. Note that some published mechanisms adopted here rested on scant data and could be significantly in error. Three events

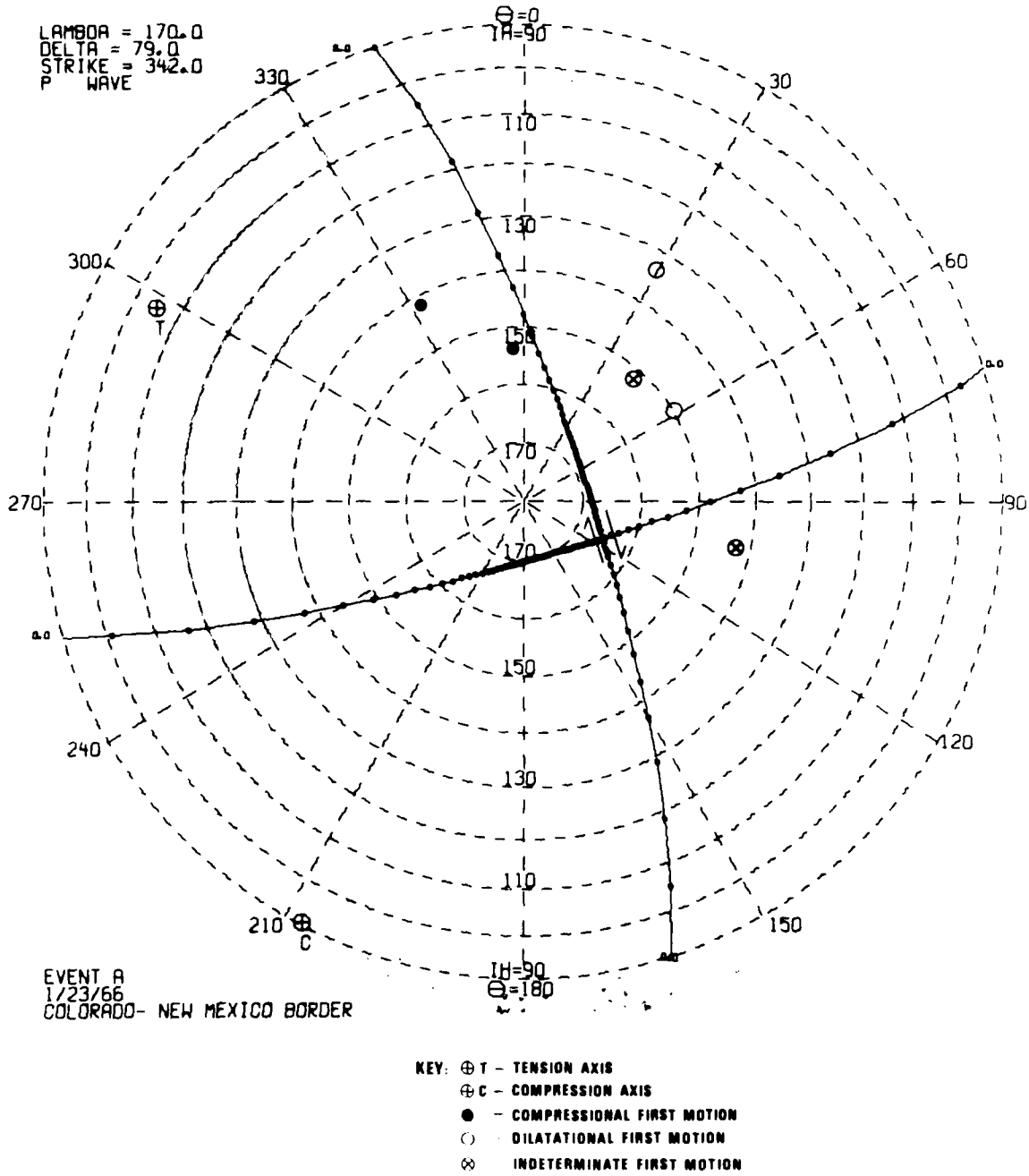

Figure 12 Focal mechanism of the earthquakes selected for this study.

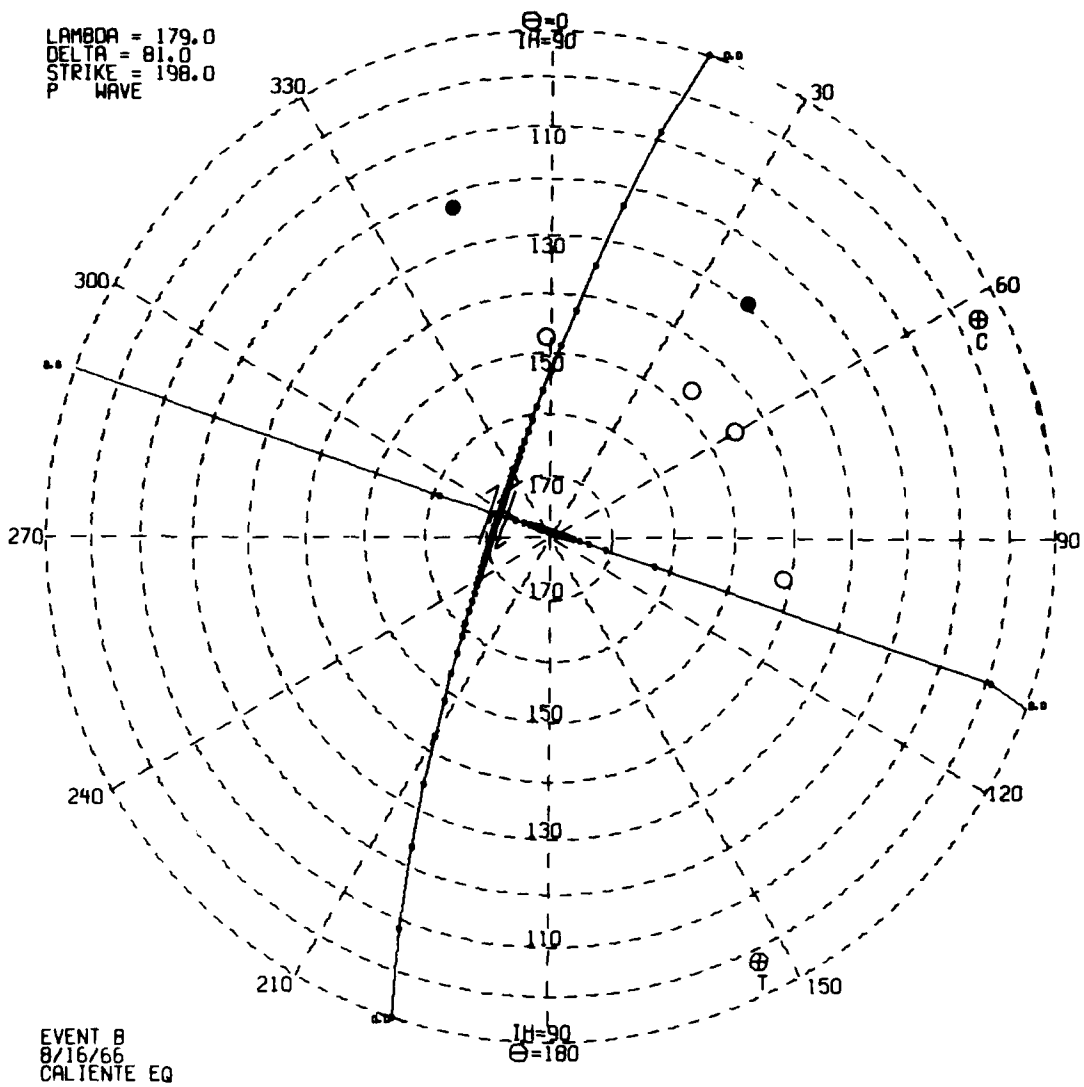

Figure 12 (cont.) Focal mechanism of the earthquakes selected for this study.

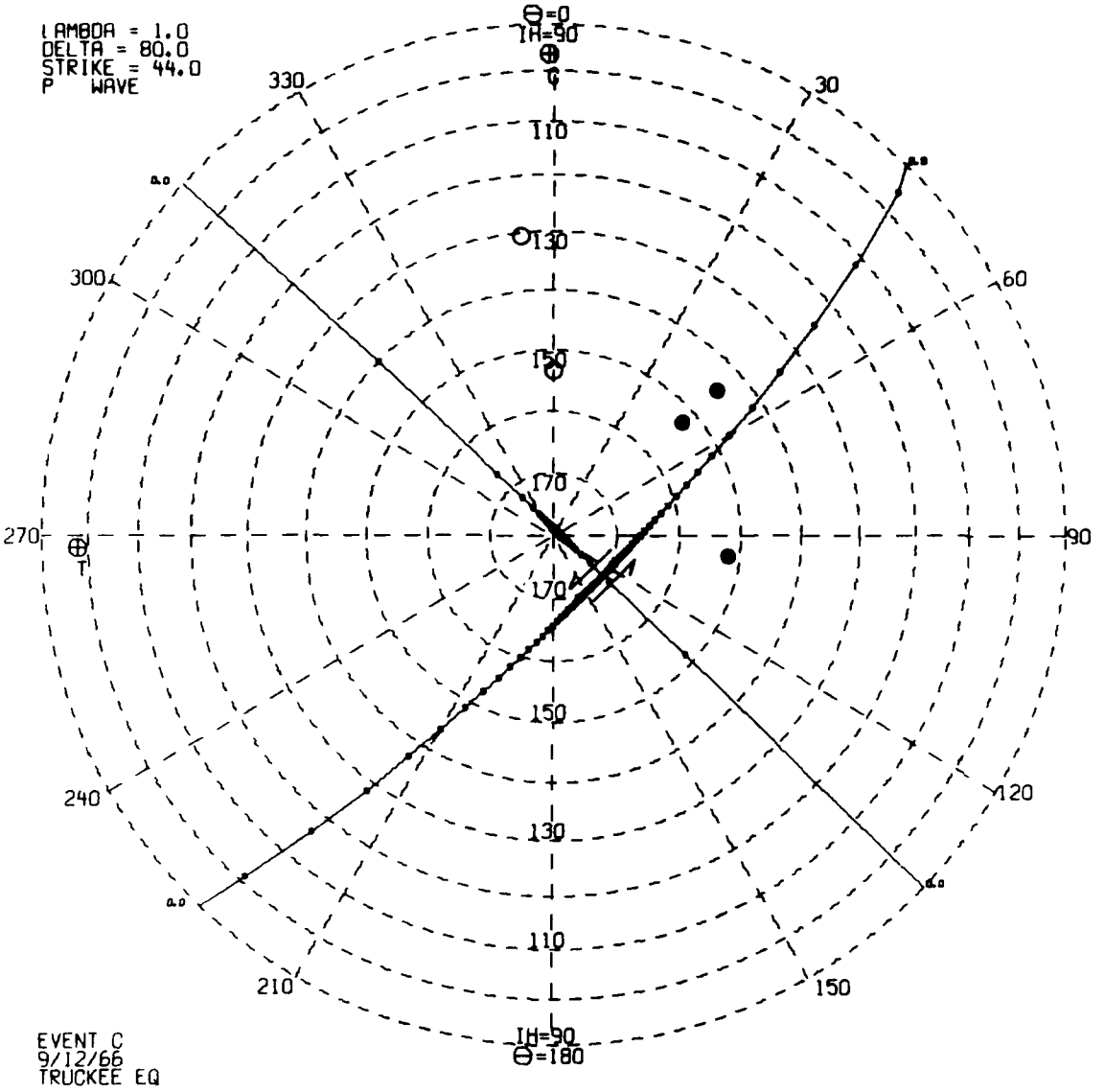

Figure 12 (cont.) Focal mechanism of the earthquakes selected for this study.

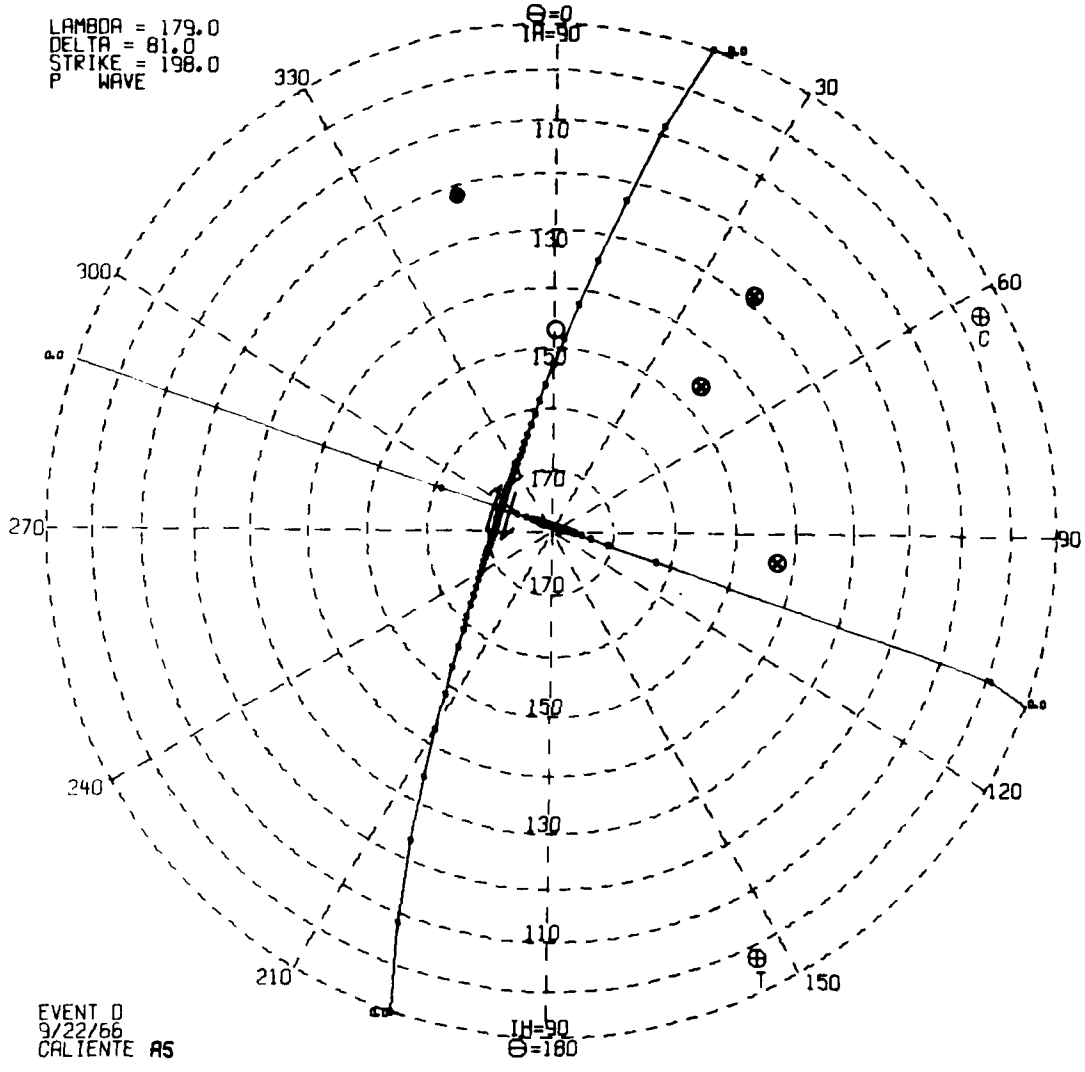

Figure 12 (cont.) Focal mechanism of the earthquakes selected for this study.

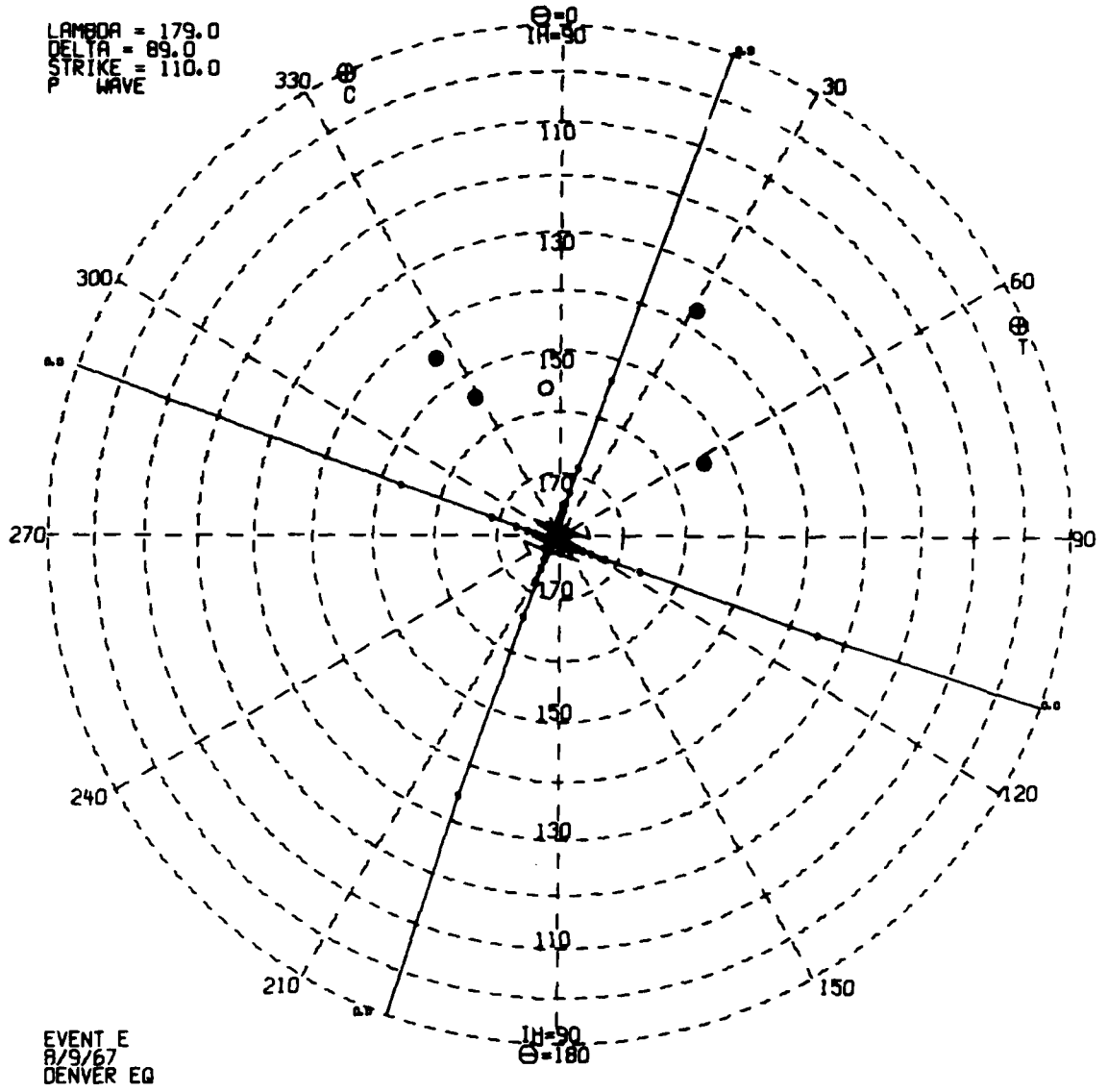

Figure 12 (cont.) Focal mechanism of the earthquakes selected for this study.

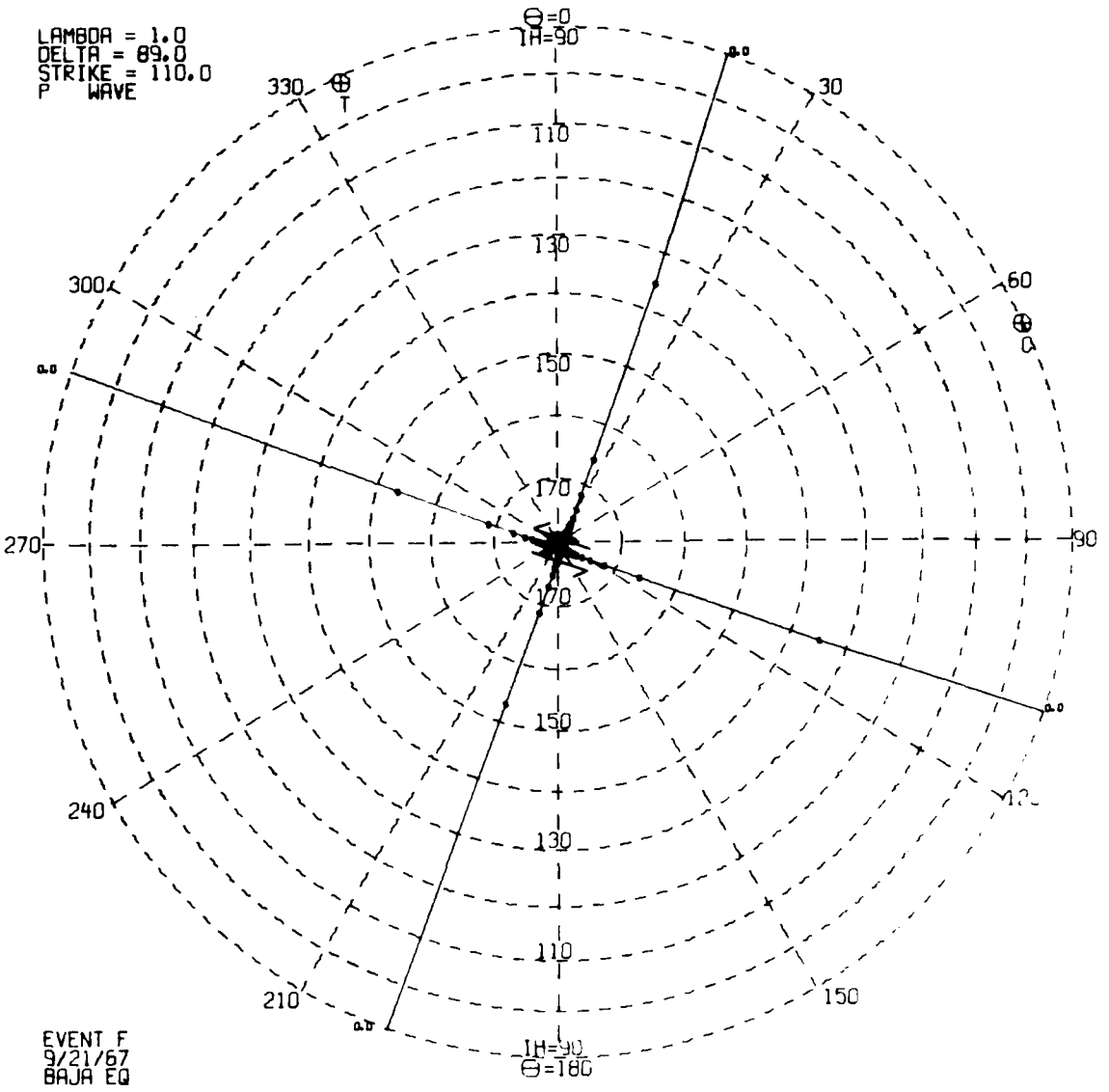

Figure 12 (cont.) Focal mechanism of the earthquakes selected for this study.

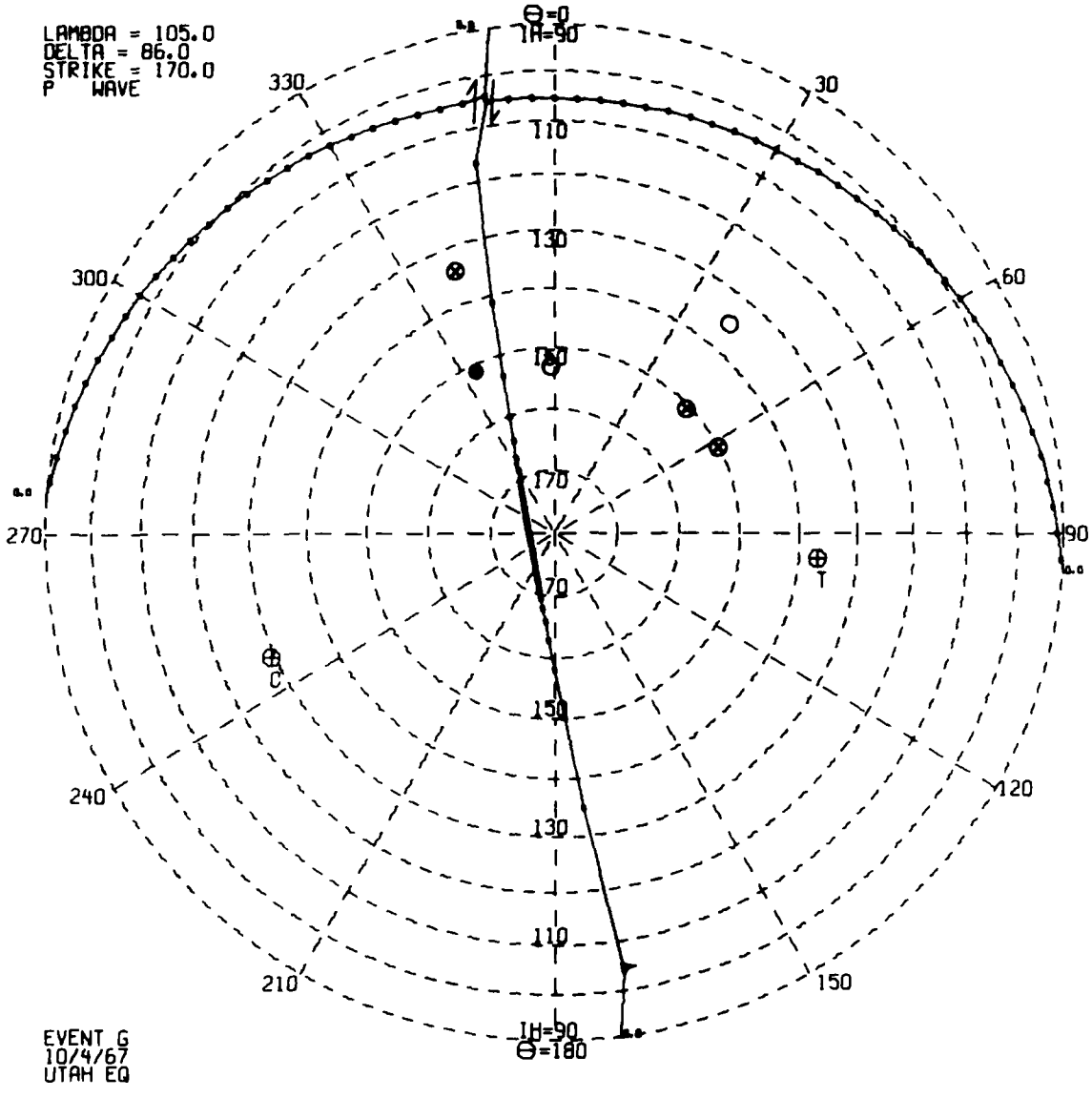

Figure 12 (cont.) Focal mechanism of the earthquakes selected for this study.

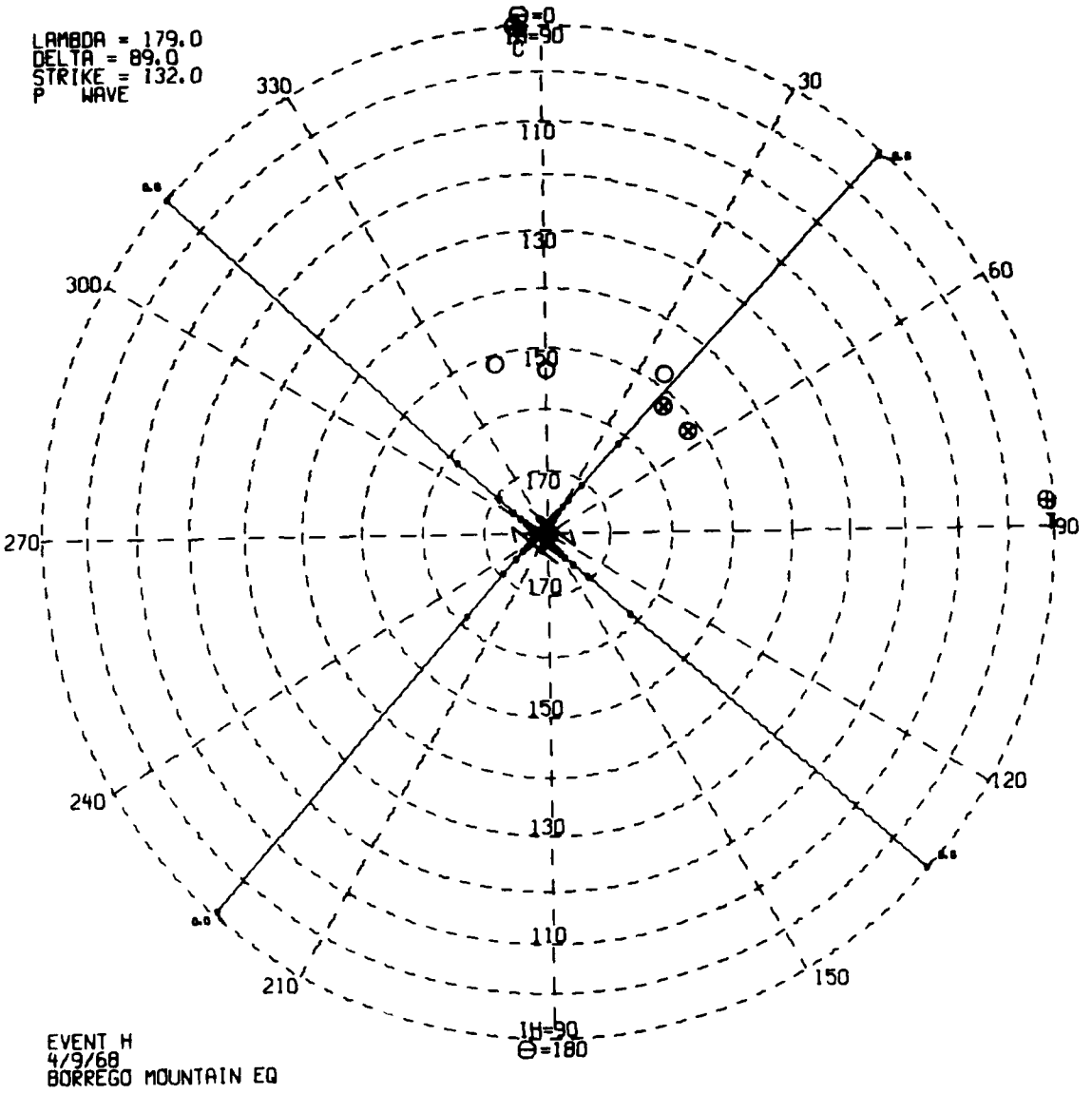

Figure 12 (cont.) Focal mechanism of the earthquakes selected for this study.

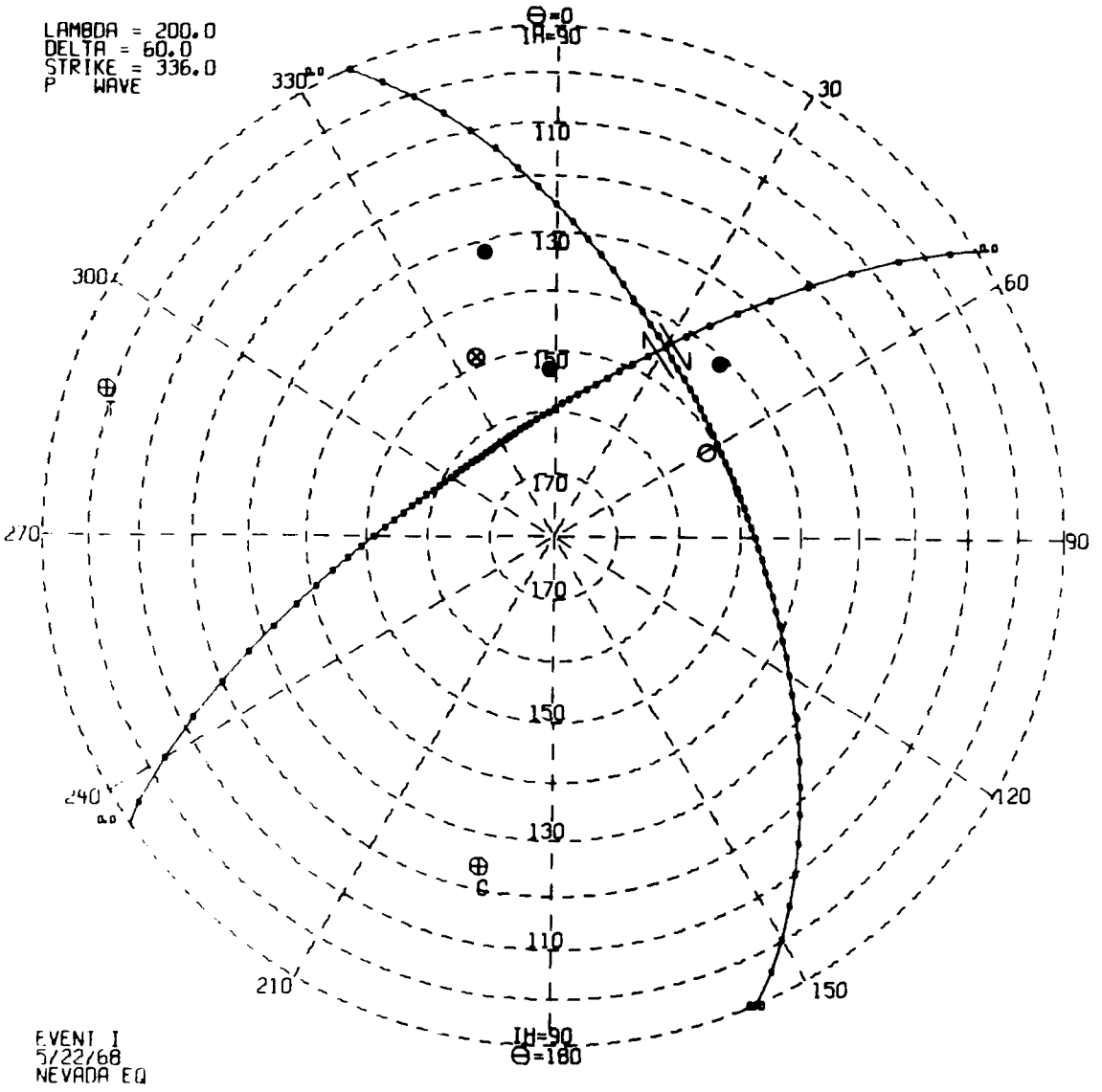

Figure 12 (cont.) Focal mechanism of the earthquakes selected for this study.

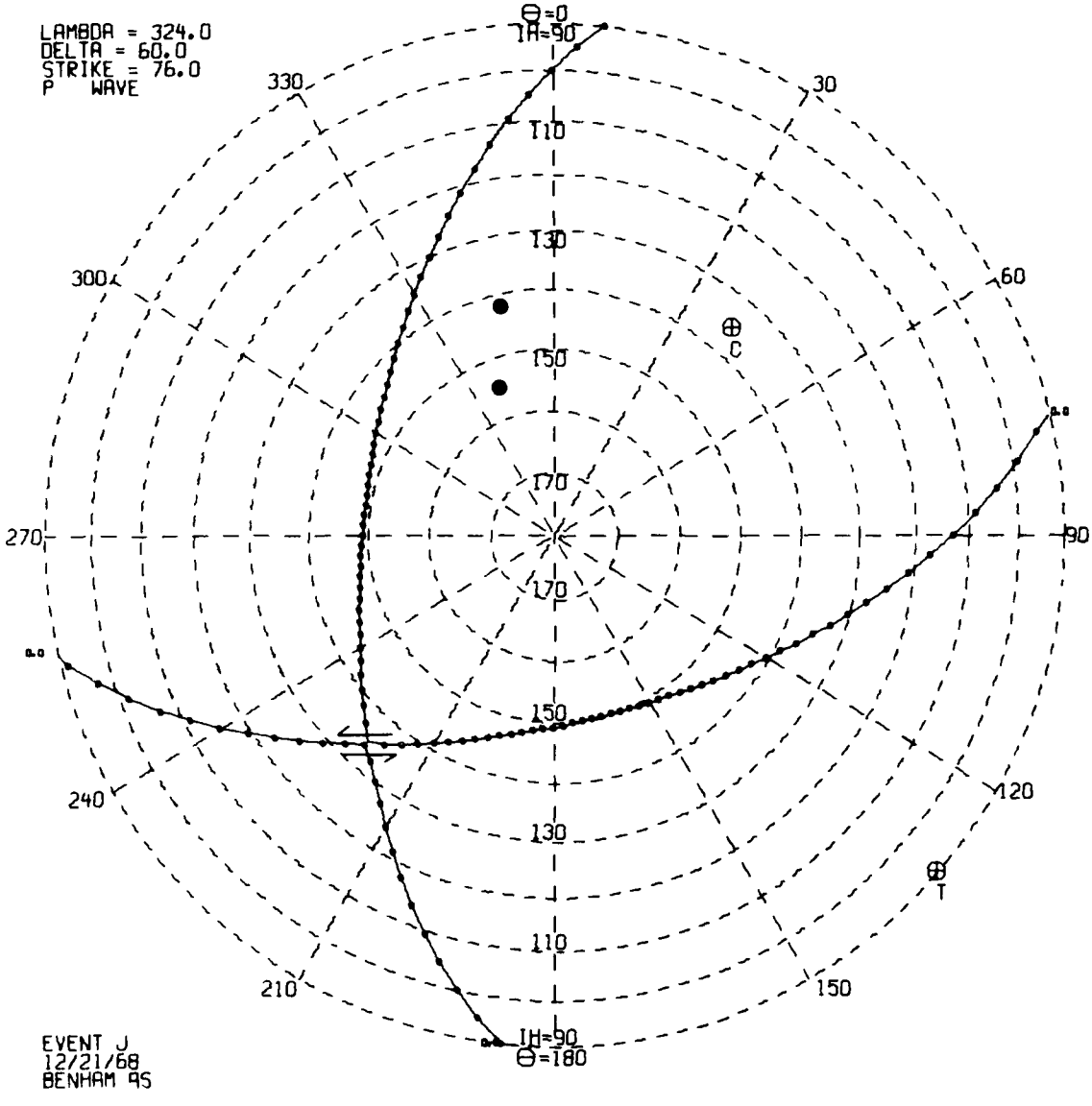

Figure 12 (cont.) Focal mechanism of the earthquakes selected for this study.

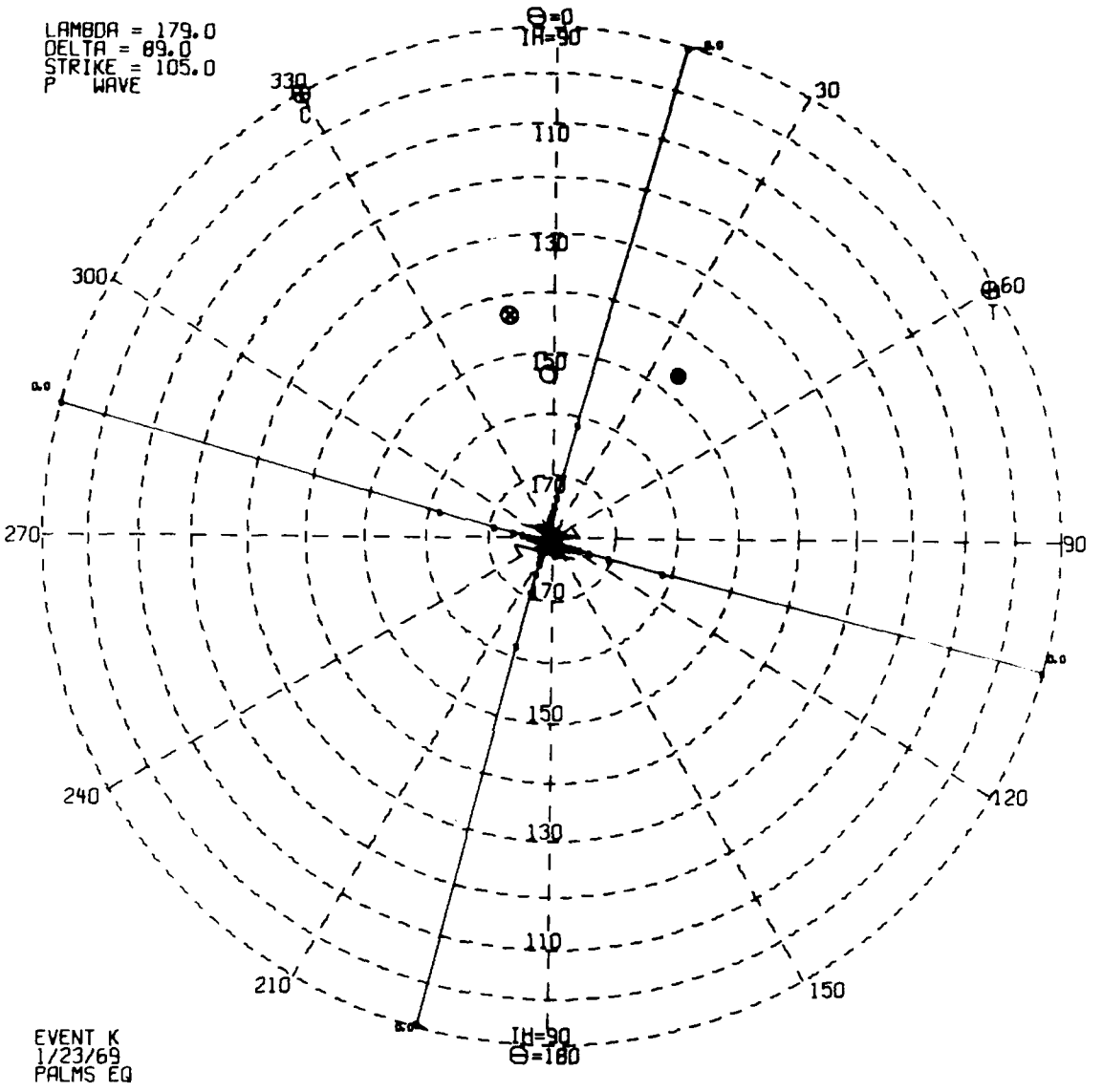

Figure 12 (cont.) Focal mechanism of the earthquakes selected for this study.

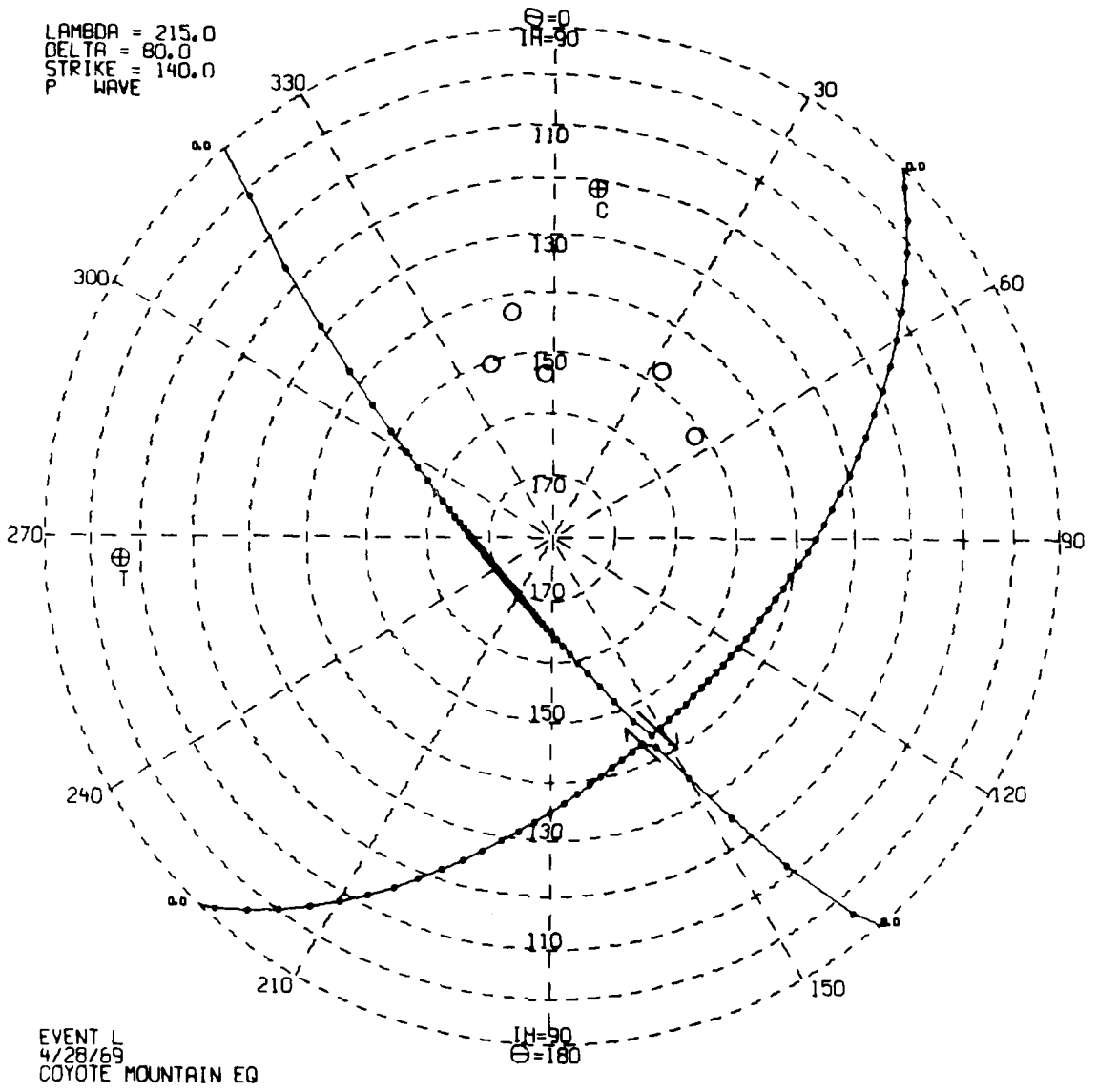

Figure 12 (cont.) Focal mechanism of the earthquakes selected for this study.

TABLE V

Sources of Information on the Focal Mechanisms of Earthquakes Selected for this Study

Event	Name	Reference
A	Dulce, N.M. EQ	Smith and Sbar (1974)
B	Caliente EQ	Tsai and Aki (1971)
C	Truckee EQ	Tsai and Aki (1970)
D	Caliente AS	assumed to be same event B
E	Denver EQ	Major and Simon (1968)
F	Baja EQ	assumed on basis of nearby fault motion
G	Utah EQ	Smith and Sbar (1974)
H	Borrego Mtn. EQ	Hanks and Wyss (1972)
I	Nevada EQ	assumed on the basis of nearby fault mechanism solutions
J	BENHAM AS	Savino et al. (1971)
K	29 Palms EQ	assumed on the basis of fault orientation and ISC first motions
L	Coyote Mtn. EQ	Thatcher and Hamilton (1973)

have no published mechanisms, and the mechanics of faulting were inferred from association of the events with known faults or proximity to earthquakes with known mechanisms. First-motion data plotted in these figures is from our analysis of the seven LRSM stations and will be discussed later in this report.

SOURCE EFFECTS

In this section aspects of the source responsible for identifiable differences in the recorded signals of our selected events are discussed within a context of discrimination which employs commonly regarded measures such as $M_s - m_b$, spectral ratios, shear-wave generation, and complexity. The variety of tectonic processes occurring within the source region implies that the selected earthquakes cannot be characterized uniformly. In regard to the explosions, a more nearly uniform source behavior is anticipated.

Polarity of First Motion

In the focal-mechanism diagrams of Figure 12, data from the seven LRSM stations are added. Except for larger events, where long-period P waves were often recorded, this first motion data is from short-period instruments. In most cases, this data is consistent with the known or assumed fault mechanisms, and the exceptions merely demonstrate the well-known inadequacy of first motion taken from short-period recordings. Because of epicenter-to-station distance and because of the signal-to-noise ratio, few of the observed first motions would have satisfied the criteria set forth by the Technical Working Group II of the Geneva Conference (U.S. Joint Committee on Atomic Energy, 1960). For ten of the twelve earthquakes, at least one apparent dilatational first motion was found among the stations; such data cannot constitute positive discrimination of source type, but merely a strong diagnostic. Furthermore, an examination of P signals on these LRSM recordings of the eleven explosions revealed several P signals that could be described objectively as dilatational first motions.

S Waves

Earlier work of von Seggern (1972) already demonstrated with real data that measurement of the excitation of S waves relative to P waves should present a reliable discriminant. In Figures 13 and 14 are short-period S and long-period S magnitudes plotted against routine m_b. Many of the events are

---

U.S. Joint Committee on Atomic Energy (1960). Technical aspects of detection and inspection controls of a nuclear weapon test ban (Summary analysis of hearings before the Special Subcommittee on Radiation and the Subcommittee on Research and Development, April 19-22, 1960). Superintendent of Documents, U.S. Government Printing Office, Washington, D.C.

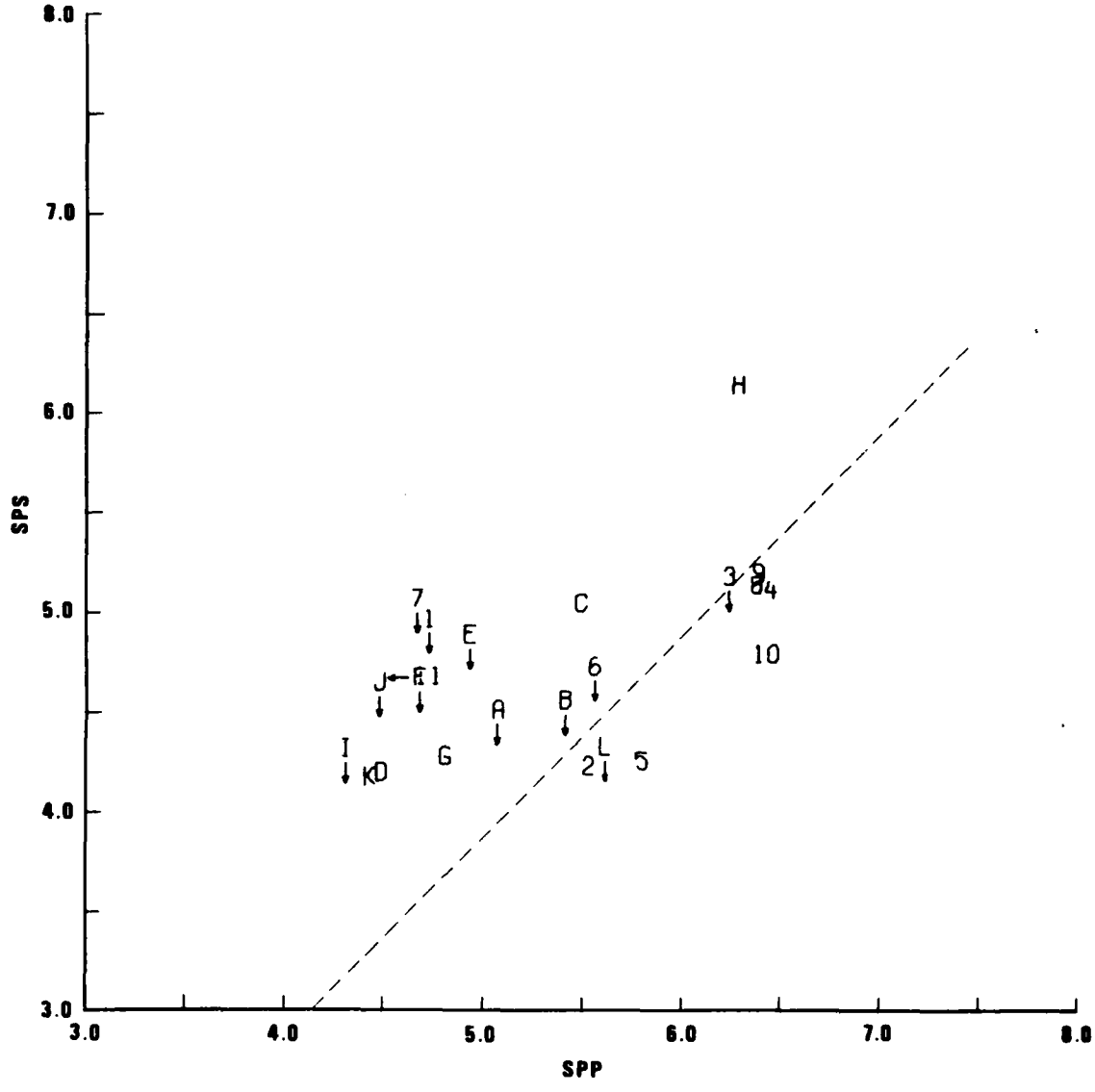

Figure 13 Short-period S magnitude versus short-period P magnitude for selected Southwestern United States events.

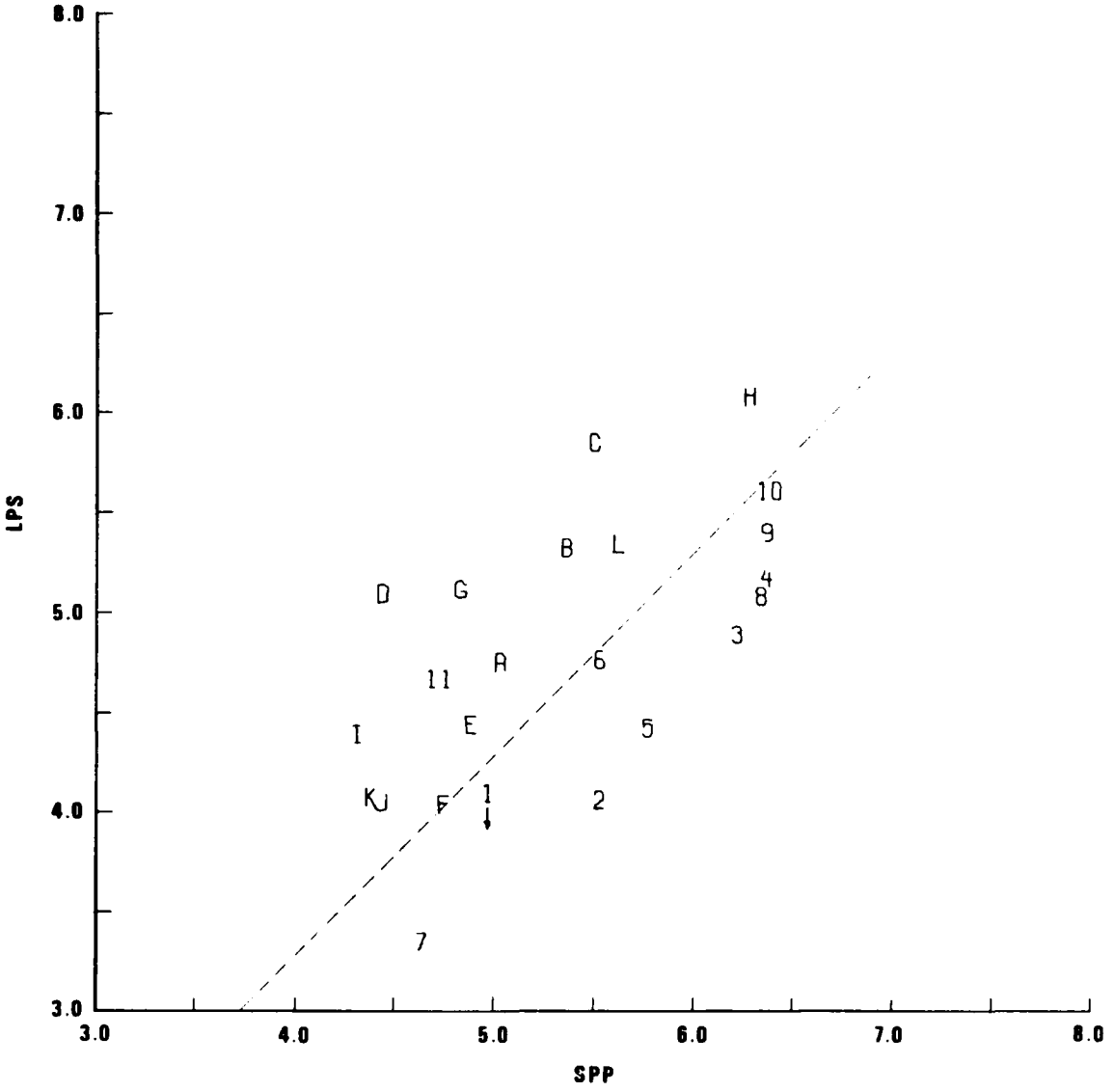

Figure 14 Long-period S magnitude versus short-period P magnitude for selected Southwestern United States events.

represented by noise estimates (see Table IV and VI), and the effective threshold for application of this discriminant is m_b ∿5.0 in the short-period mode and m_b ∿ 4.5 in the long-period mode. These figures show that, when measurable, the short-period and long-period S waves are generally smaller relative to P for the explosions than the earthquakes. There are, however, several exceptions: earthquakes A and B have low short-period S and event L, which is difficult to identify on the basis of $M_s - m_b$ also, is not well identified on the basis of S waves. The Coyote Mountain earthquake, event L, is especially troublesome because, while its short-period S magnitude in Figure 13 is based upon noise measurements, the lack of visible S waves on short-period components for a m_b ∿ 6 earthquake is certainly anomalous. Von Seggern (1972) found no S/P amplitude ratios < 0.1 on LRSM recordings of $m_b \geq 6.0$ earthquakes worldwide; undetected S waves were not treated in von Seggern's study though.

Excitation of LQ

Figure 15 outlines relative LQ/LR excitation of the selected events and shows that no distinct separation between the earthquakes and explosions exists. PILE DRIVER (2) and GREELEY (4) are the events Toksöz and Kehrer (1972a) assigned the largest tectonic component in a study of strain release by underground explosions at the Nevada Test Site. Note that these two explosions were not included in the earthquake population in terms of short-period and long-period S excitation (Figures 13 and 14.) It is postulated that the long-period S-wave amplitude, which is due to tectonic-strain release, is also cancelled by the surface reflection in the same way as is shallow explosion P by $_{n}p$. In addition, the authors think that the tectonic-strain release component is deficient in short-period S waves due to a long time or space dimension for the source. Neither of these arguments prevents the degree of LQ excitation required to explain transverse-component recordings of explosions. RULISON, Event 11, in the more stable Colorado Plateau, has appreciably less LQ than Nevada explosions; and GASBUGGY, Event 7, which lies close to seismic activity in northern New Mexico, appears to excite LQ to the same degree, that is, lower than at NTS. The low LQ amplitudes of RULISON and GASBUGGY provide further evidence that the high LQ excitation of certain NTS explosions is a source-related phenomenon and is not due to propagation-path effects, such as mode conversion. Overall, excitation of shear modes as represented by short-period S, long-

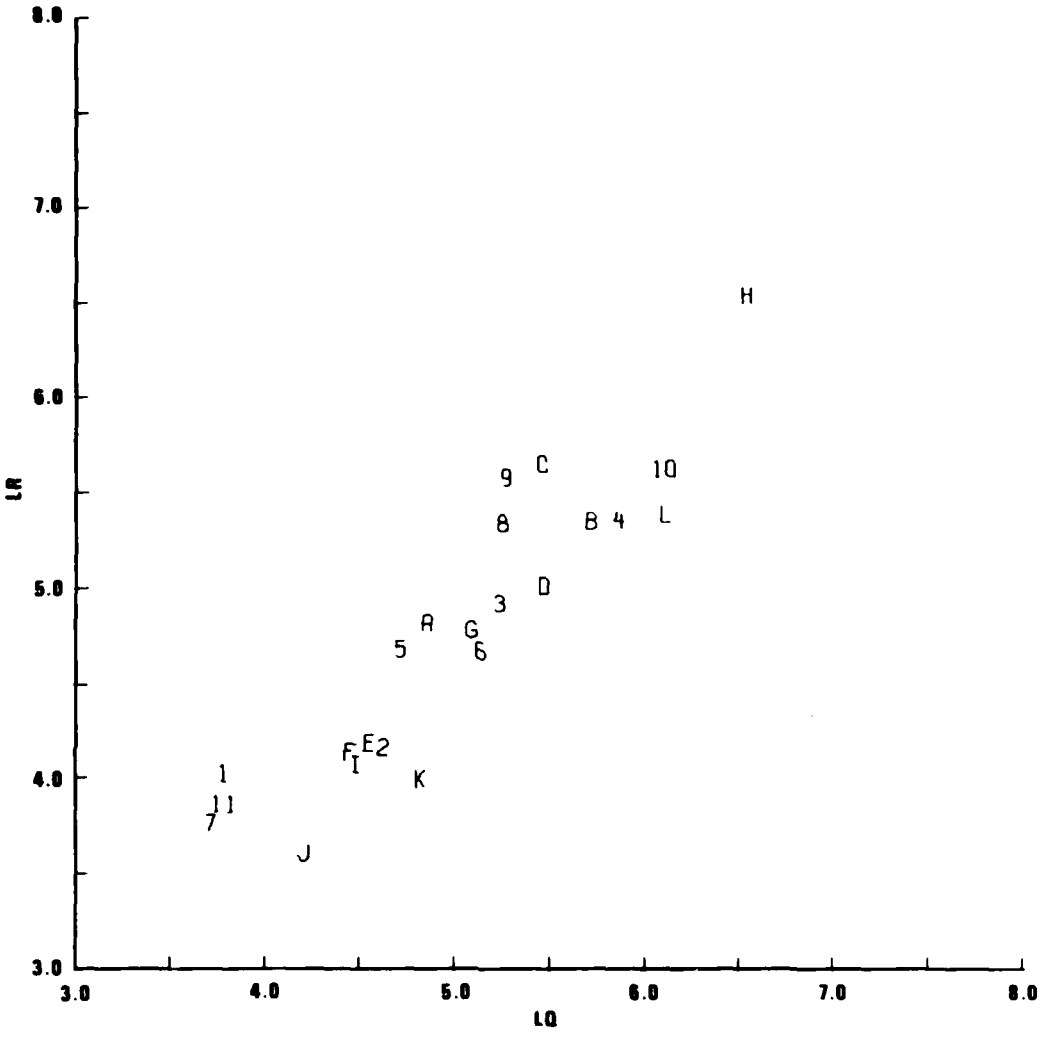

Figure 15 Rayleigh-wave magnitude versus Love-wave magnitude for selected Southwestern United States events.

period S, and LQ, relative to P and LR, betrays whether the source type is double couple or uniform compression. Note that when attempts are made to confuse identification of explosions by the firing of shot arrays to enhance M_s without similarly increasing m_b and to produce pP-like phases (Kolar and Pruvost, 1975), then the low relative excitation of S waves and LQ waves by an explosion will not be changed, and careful analysis of recordings would suggest the possibility of such an evasion attempt.

P-Wave Spectrum and Frequency

Figure 16 shows excitation of long-period P waves relative to short-period P waves, as measured on their respective LRSM components. A fairly clear separation exists between the two classes of events whenever long-period P was detected. Event L, the Coyote Mountain earthquake, is somewhat low and also appeared as rather inefficient in long-period S excitation in Figure 14. The known depth of this earthquake, 10-15 km, precludes pP cancellation of the longer-period portion of the P-wave spectrum (Molnar, 1971; Helmberger and Harkrider, 1972), which is evident for explosions in the data set. The explosions with highest relative long-period P amplitude have the largest yields in the group, and the relative increase of long-period P is due to the decrease in corner frequency with yield. This causes m_b from the short-period P to be measured at frequencies beyond this corner in the spectrum and thus at a lower level than that of a smaller explosion.

Study of the spectra of the P waves provides a fuller understanding of their generation. The P-wave spectra of the selected events from recordings at NP-NT and RK-ON are shown in Figures 17 and 18, respectively. More recordings were recovered for these stations than for the other stations in our group, so comparative analysis was facilitated for them. As shown in Figure 11, NP-NT is teleseismic and somewhat equidistant to all the events while RK-ON has a large range of epicentral distances, some of which entail multiple arrivals. The good S/N ratios at RK-ON for high frequencies is an advantage, however. To estimate the source spectrum $U_s(\omega)$, corrections have been made to the observed spectrum $U_o(\omega)$ according to

$$U_s(\omega) = U_o(\omega)e^{\pi f t^*}/I(\omega)$$

Kolar, O. C., and N. L. Pruvost (1975). Earthquake simulation by nuclear explosions. Nature, 253, 242-245.

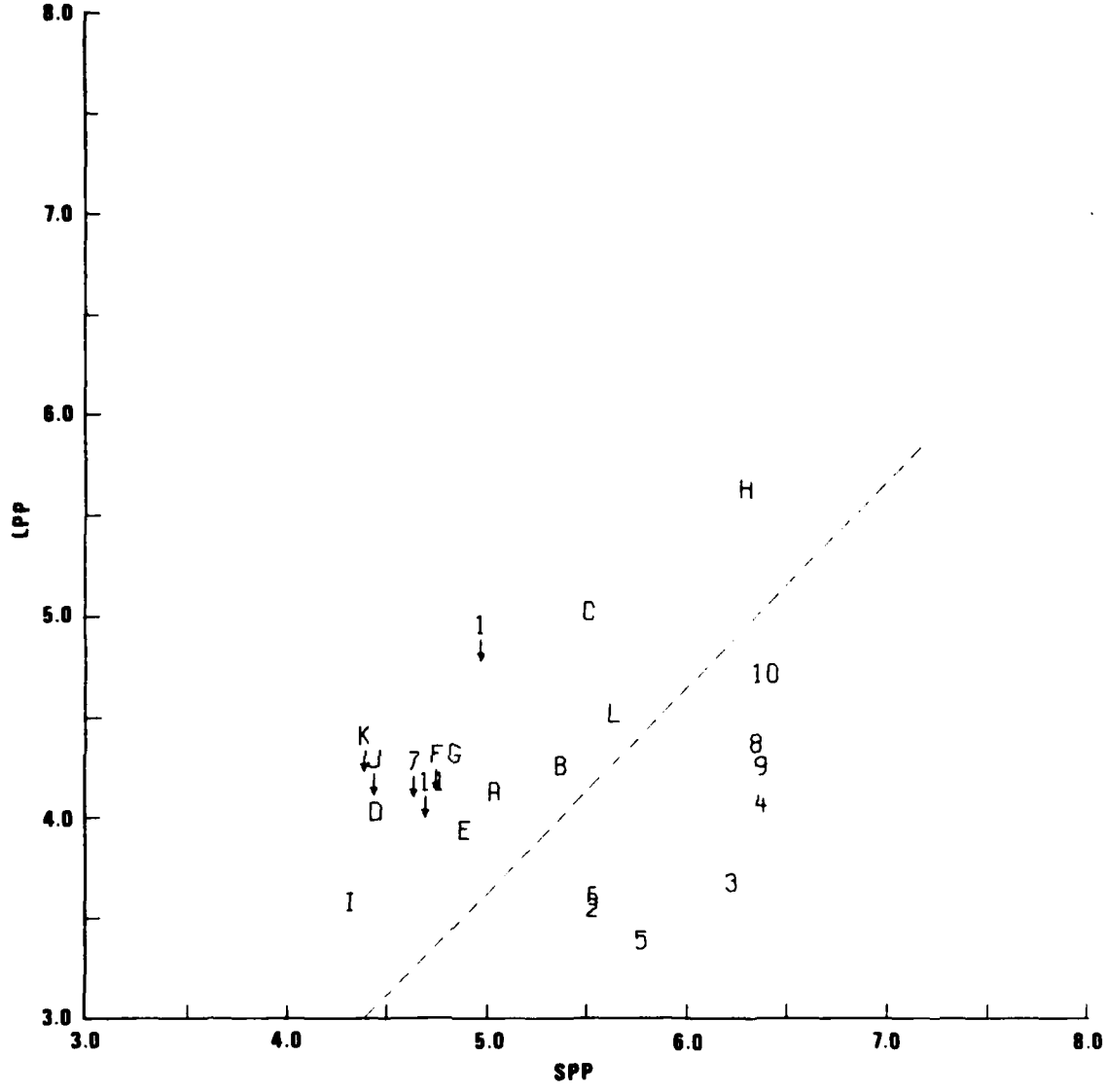

Figure 16 Long-period P magnitude versus short-period P magnitude for selected Southwestern United States events.

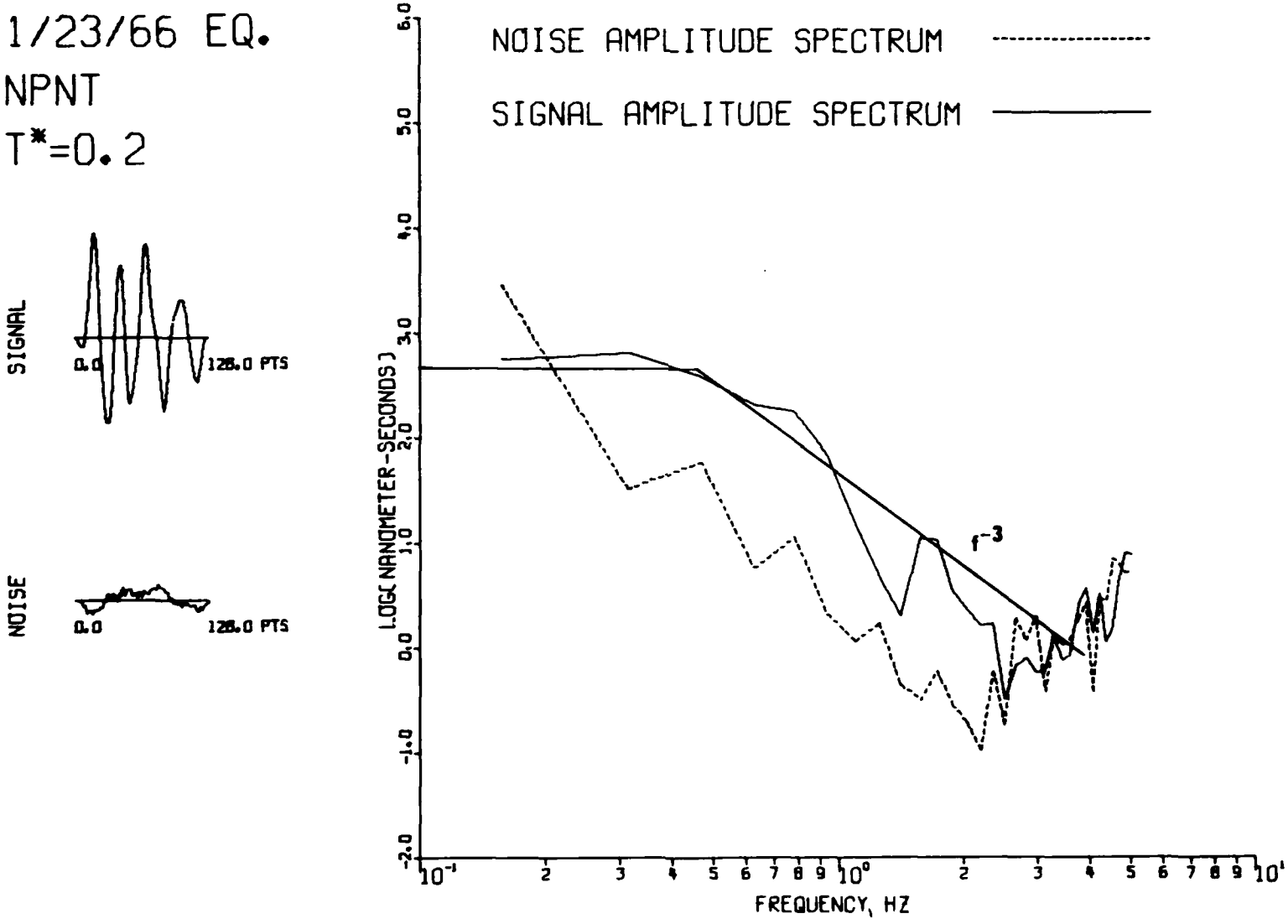

Figure 17 Spectra of P waves from short-period recordings at NP-NT of selected Southwestern United States events.

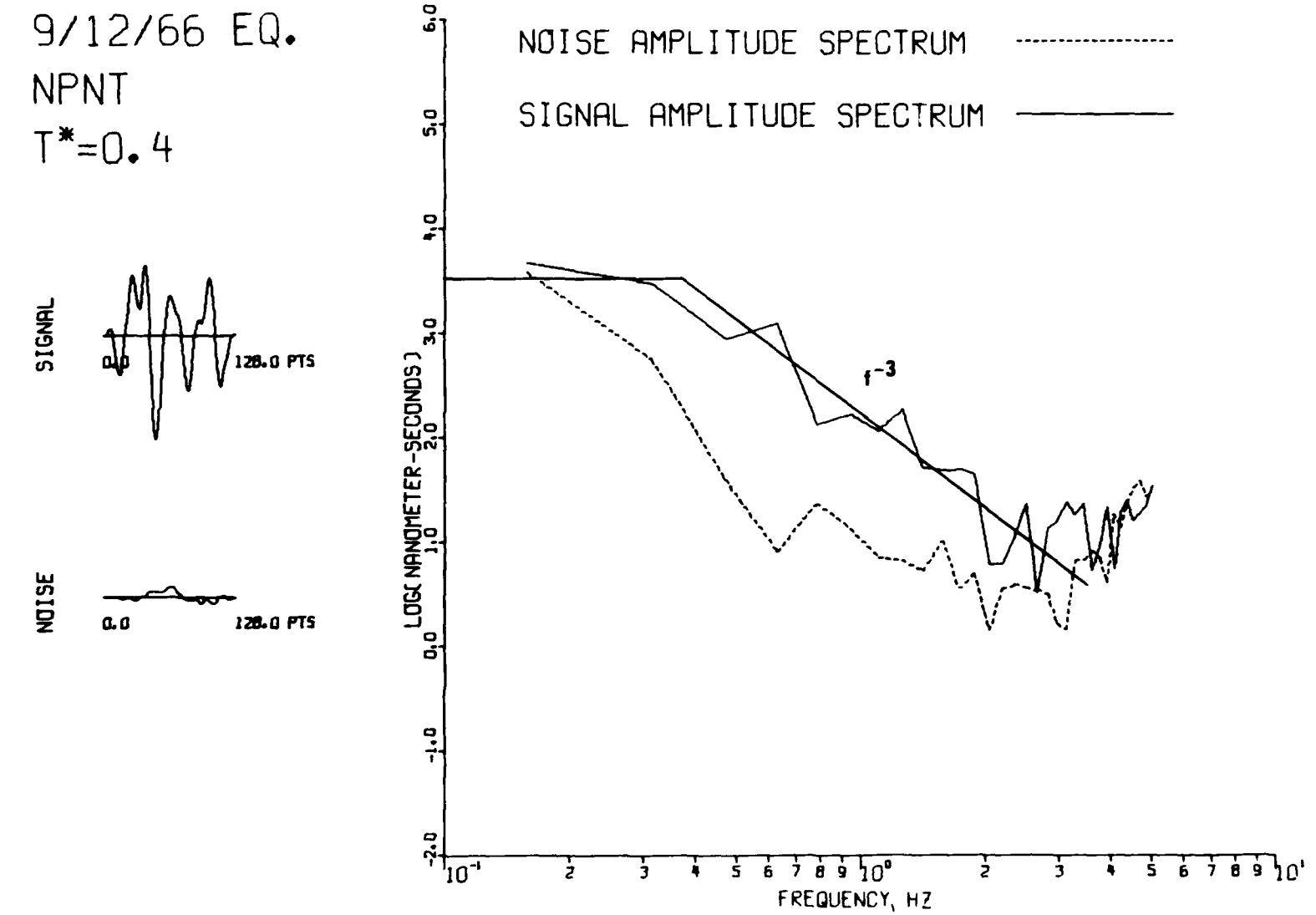

Figure 17 (cont.) Spectra of P waves from short-period recordings at NP-NT of selected Southwestern United States events.

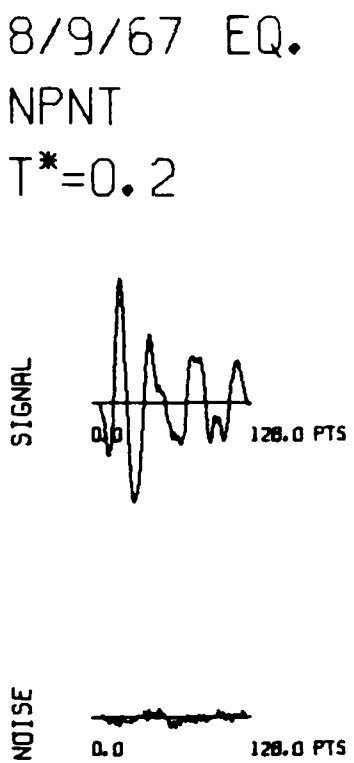

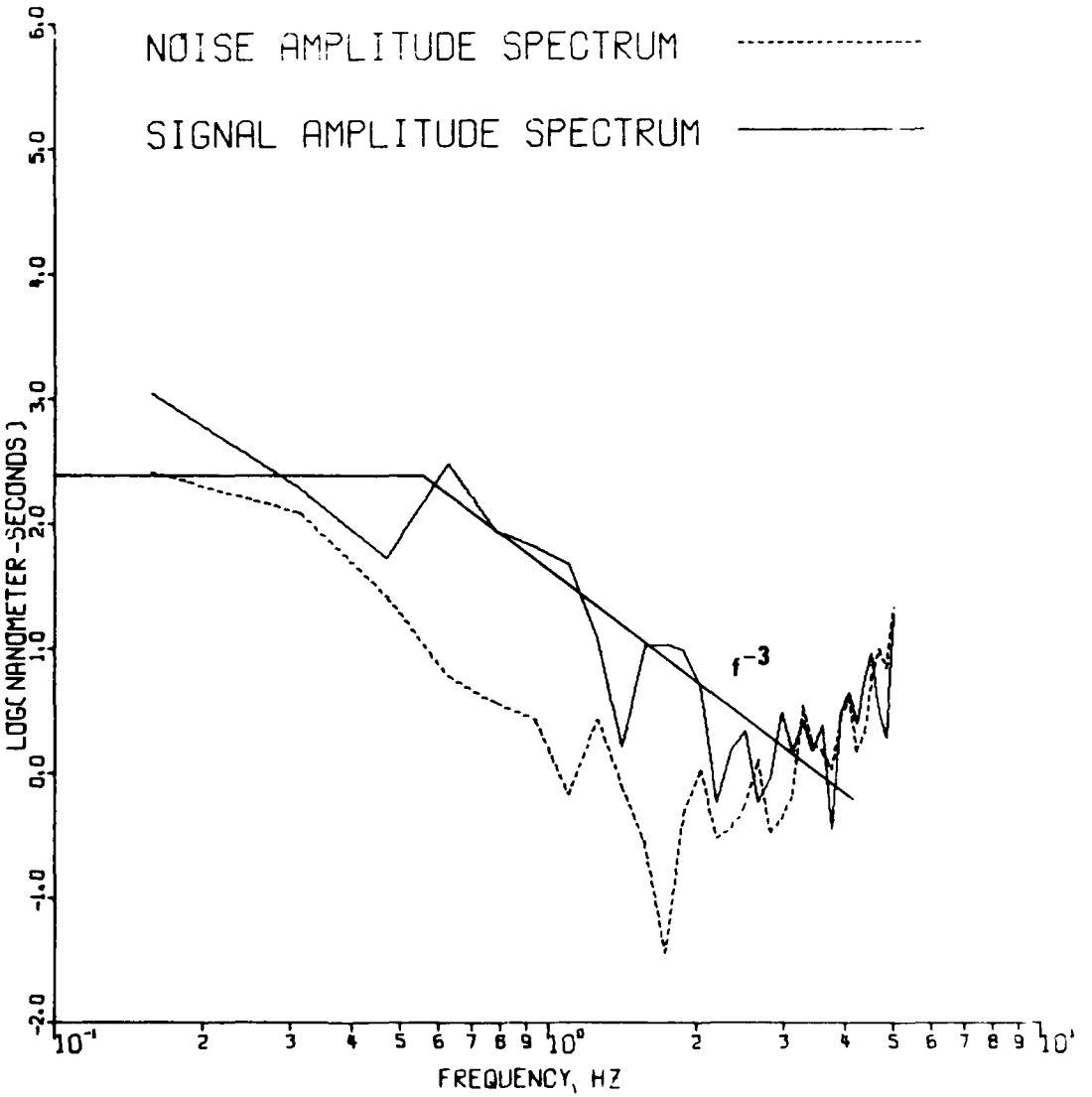

Figure 17 (cont.) Spectra of P waves from short-period recordings at NP-NT of selected Southwestern United States events.

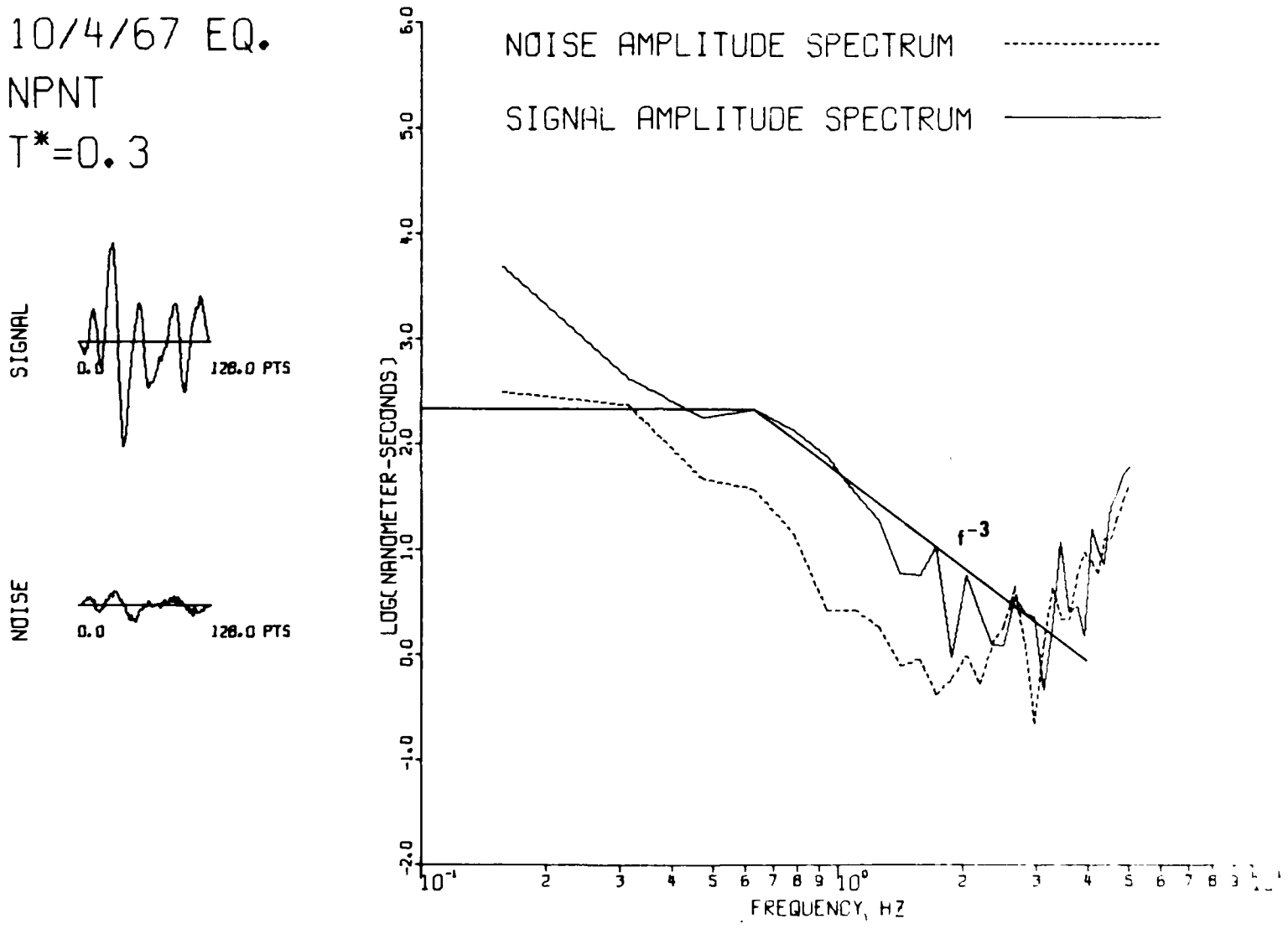

Figure 17 (cont.) Spectra of P waves from short-period recordings at NP-NT of selected Southwestern United States events.

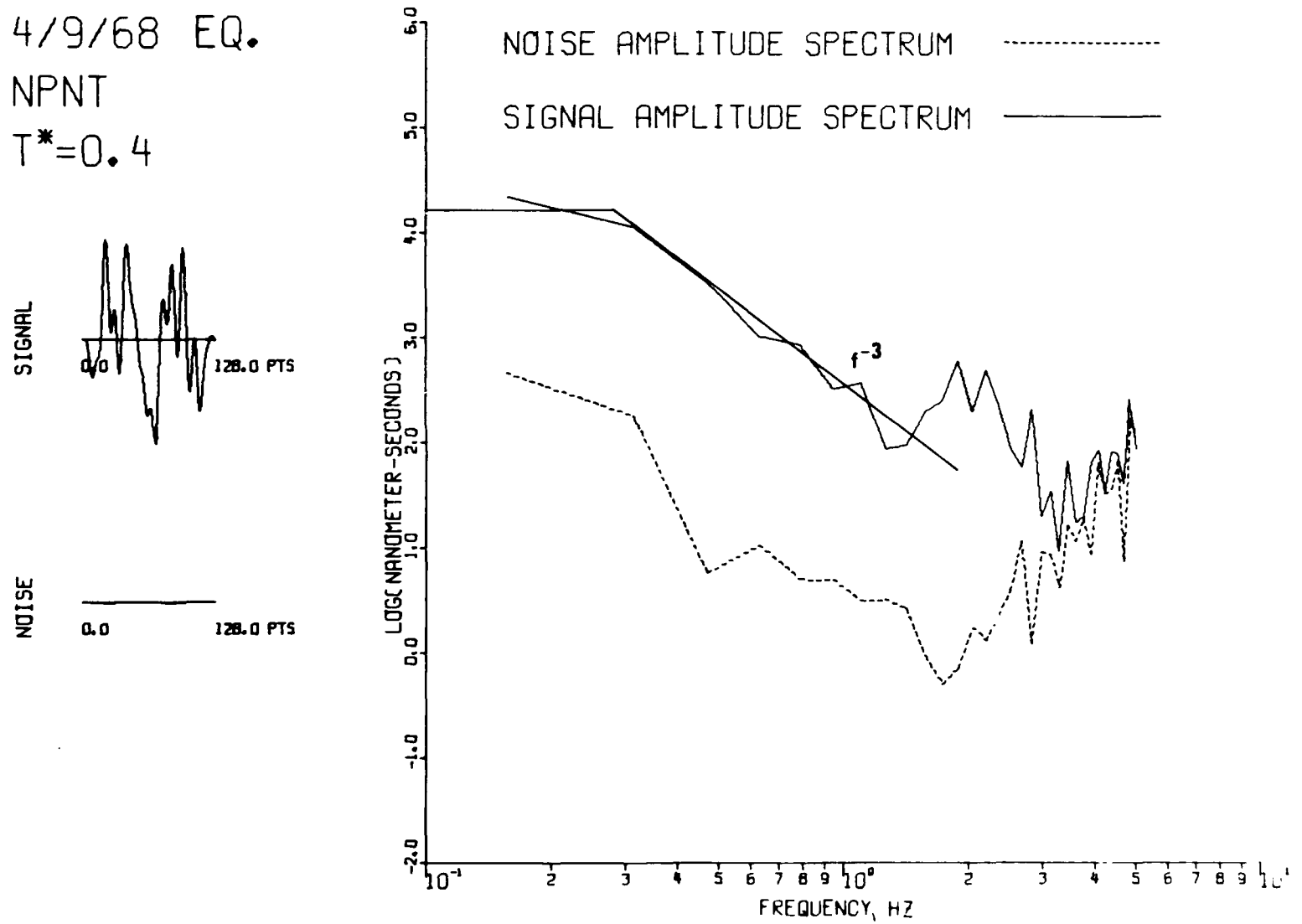

Figure 17 (cont.) Spectra of P waves from short-period recordings at NP-NT of selected Southwestern United States events.

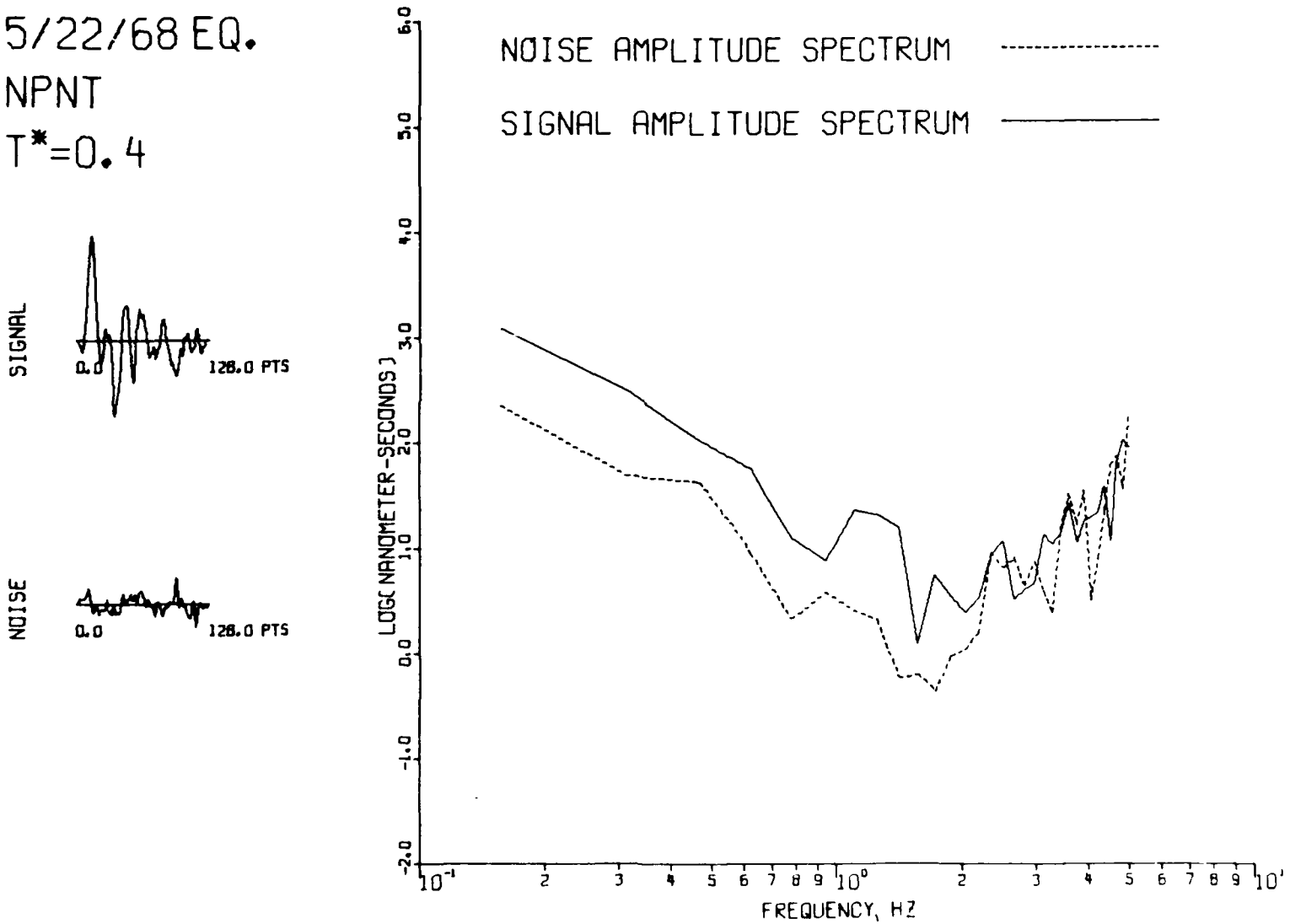

Figure 17 (cont.) Spectra of P waves from short-period recordings at NP-NT of selected Southwestern United States events.

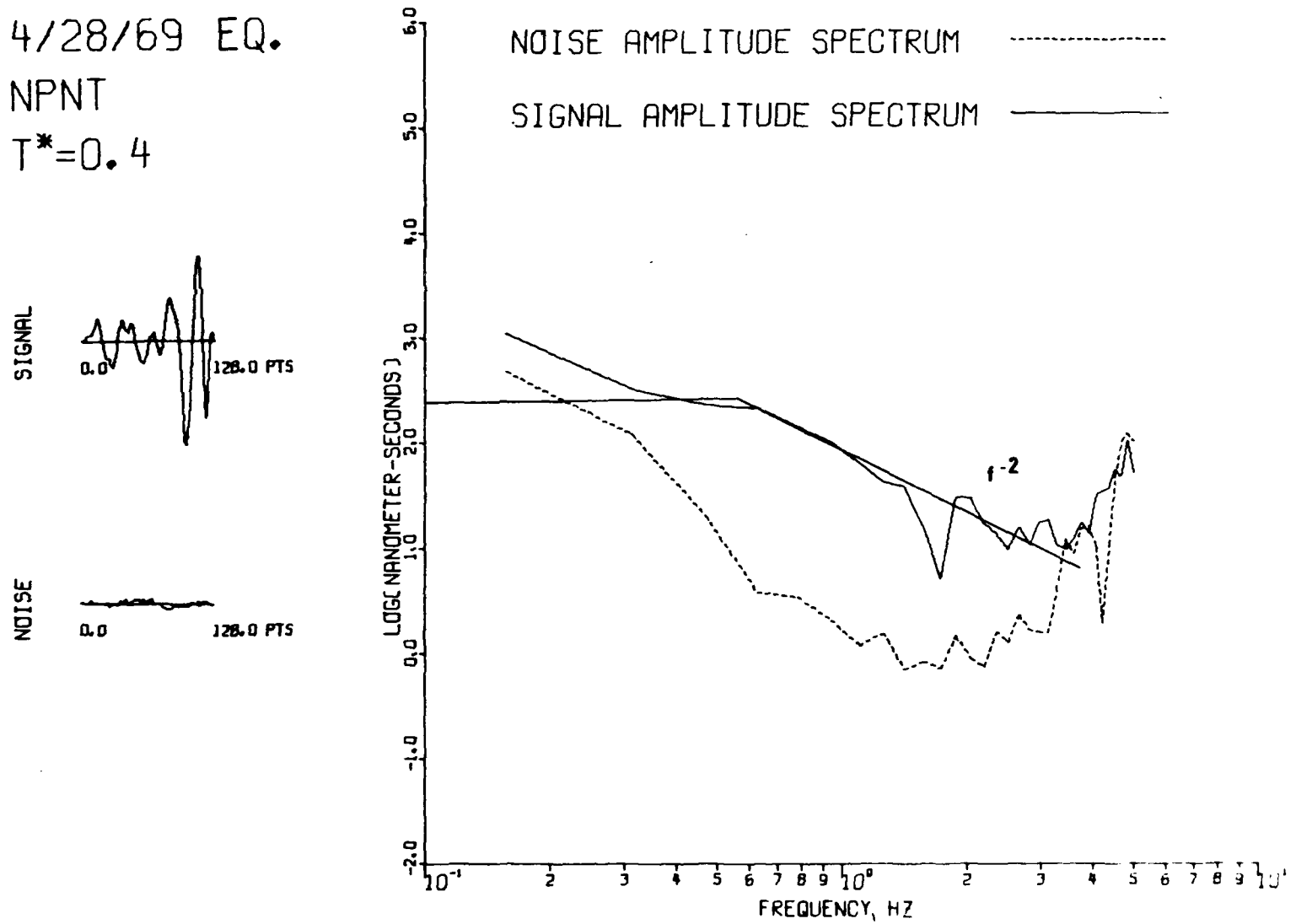

Figure 17 (cont.) Spectra of P waves from short-period recordings at NP-NT of selected Southwestern United States events.

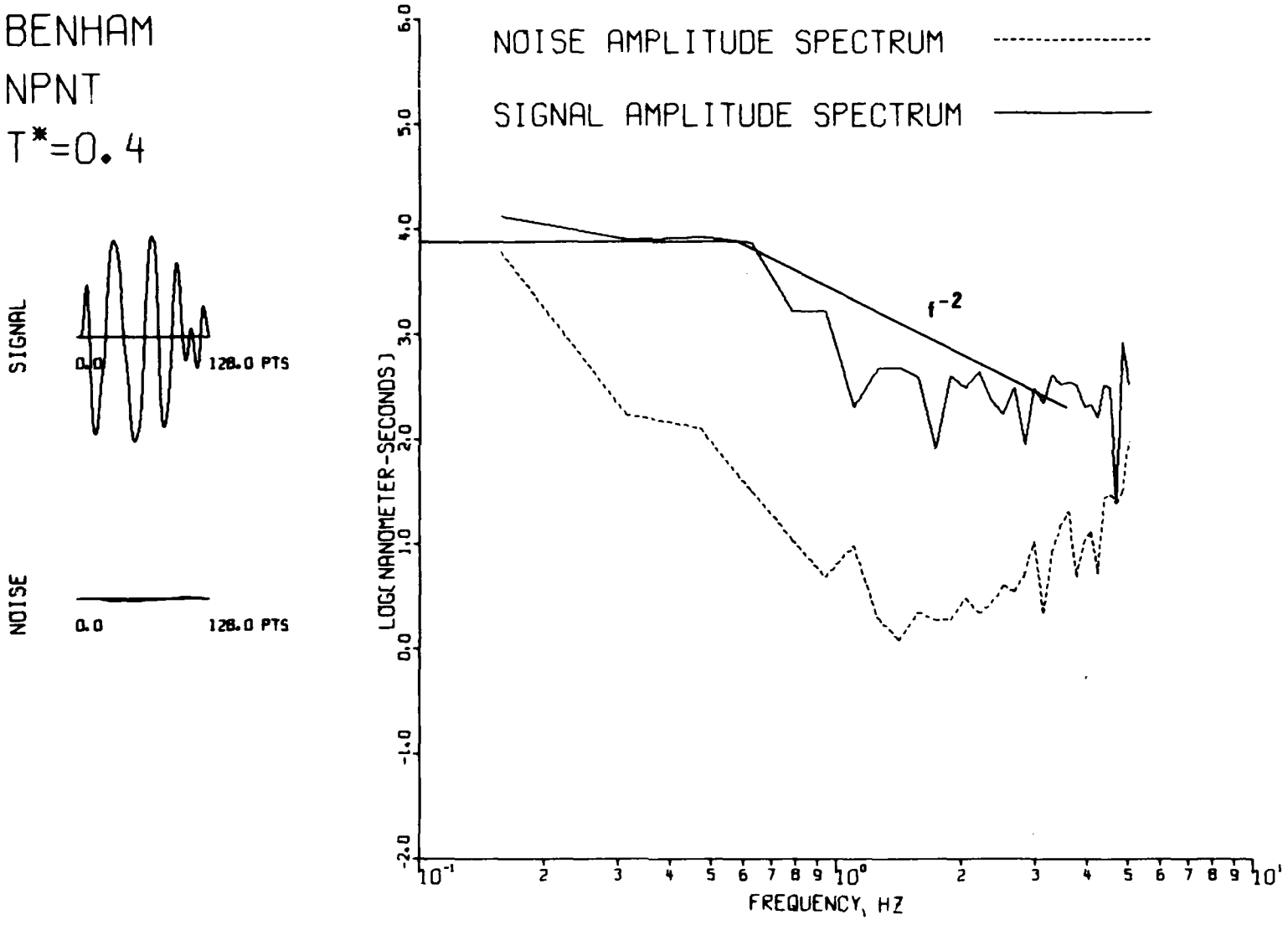

Figure 17 (cont.) Spectra of P waves from short-period recordings at NP-NT of selected Southwestern United States events.

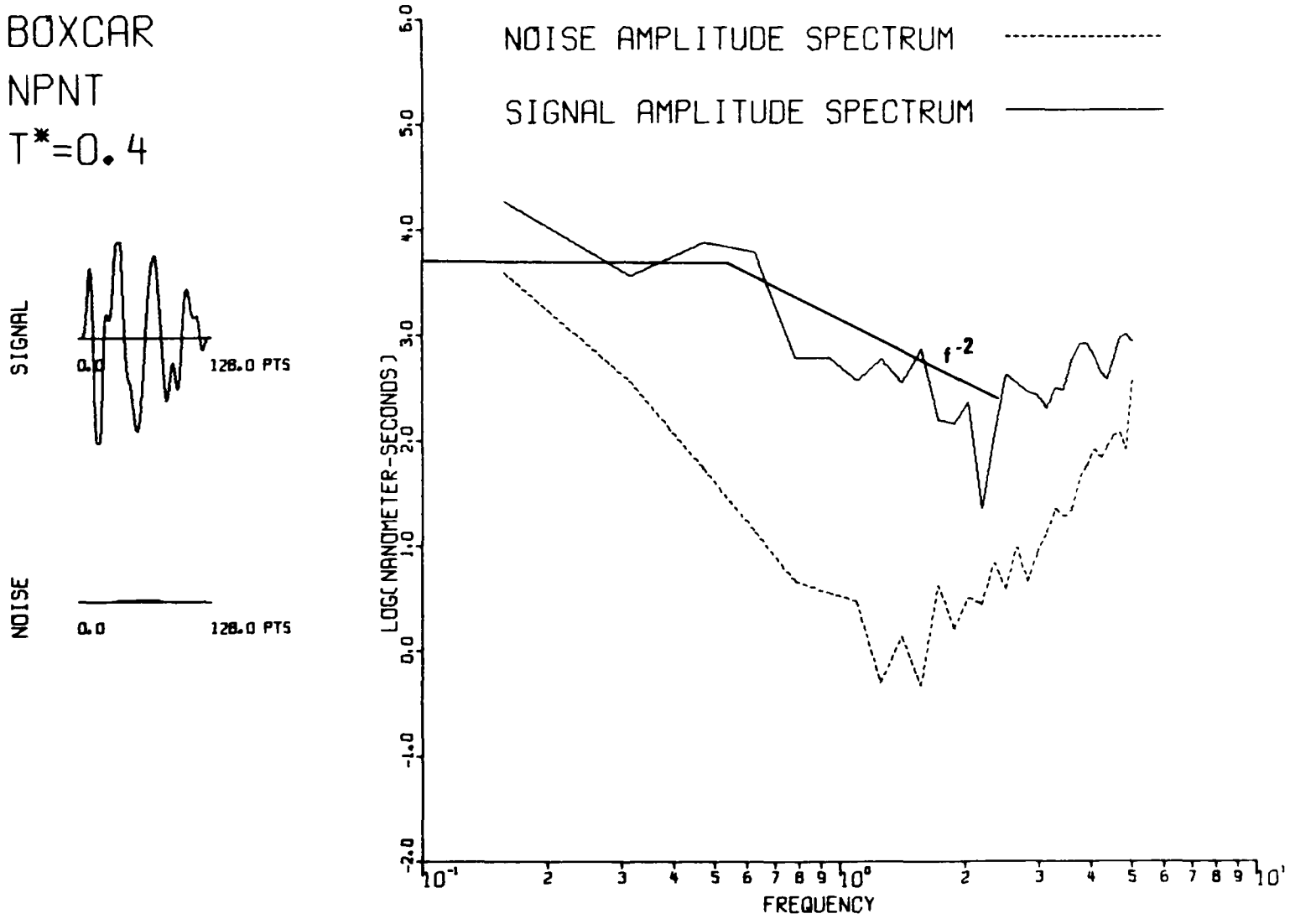

Figure 17 (cont.) Spectra of P waves from short-period recordings at NP-NT of selected Southwestern United States events.

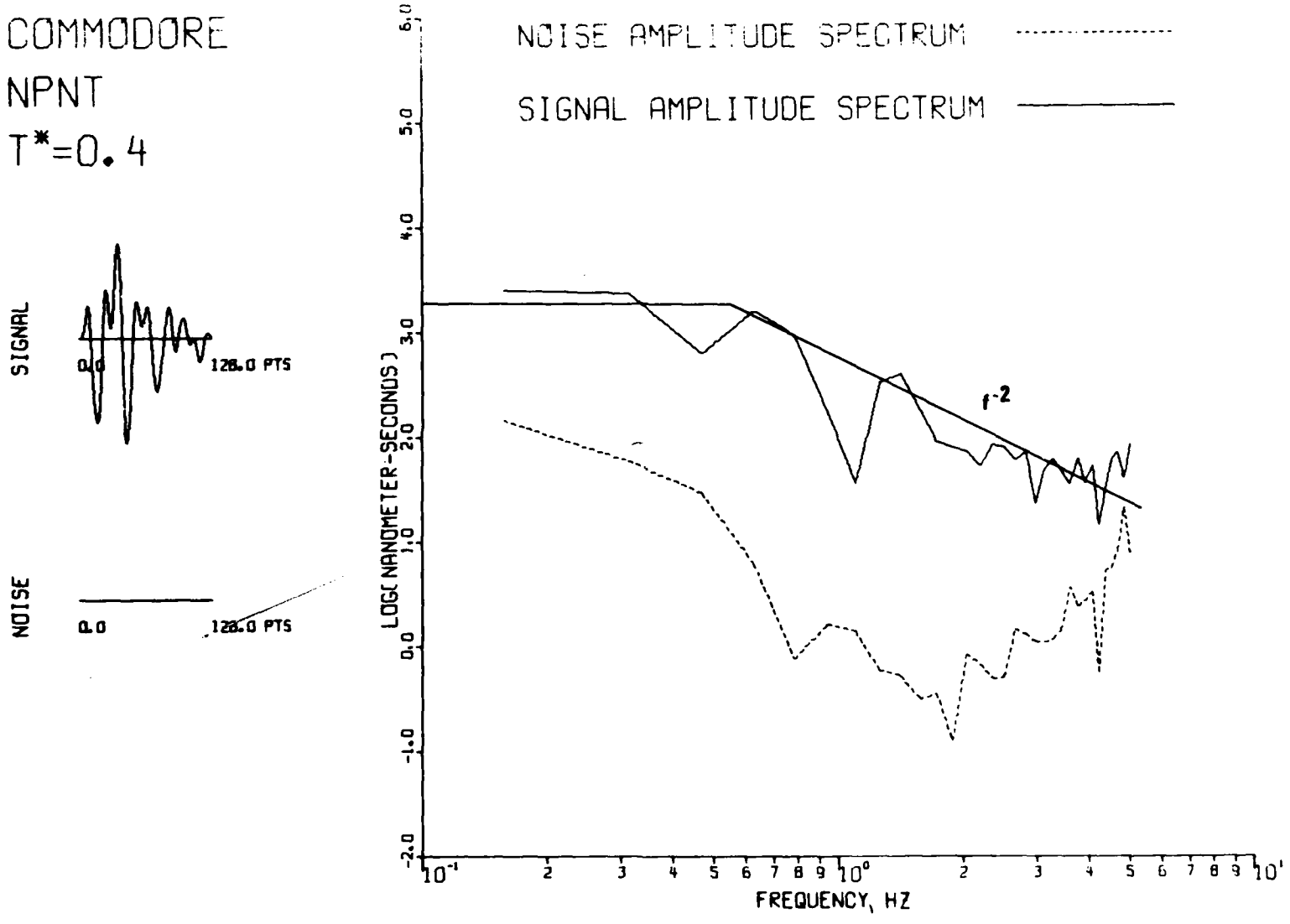

Figure 17 (cont.) Spectra of P waves from short-period recordings at NP-NT of selected Southwestern United States events.

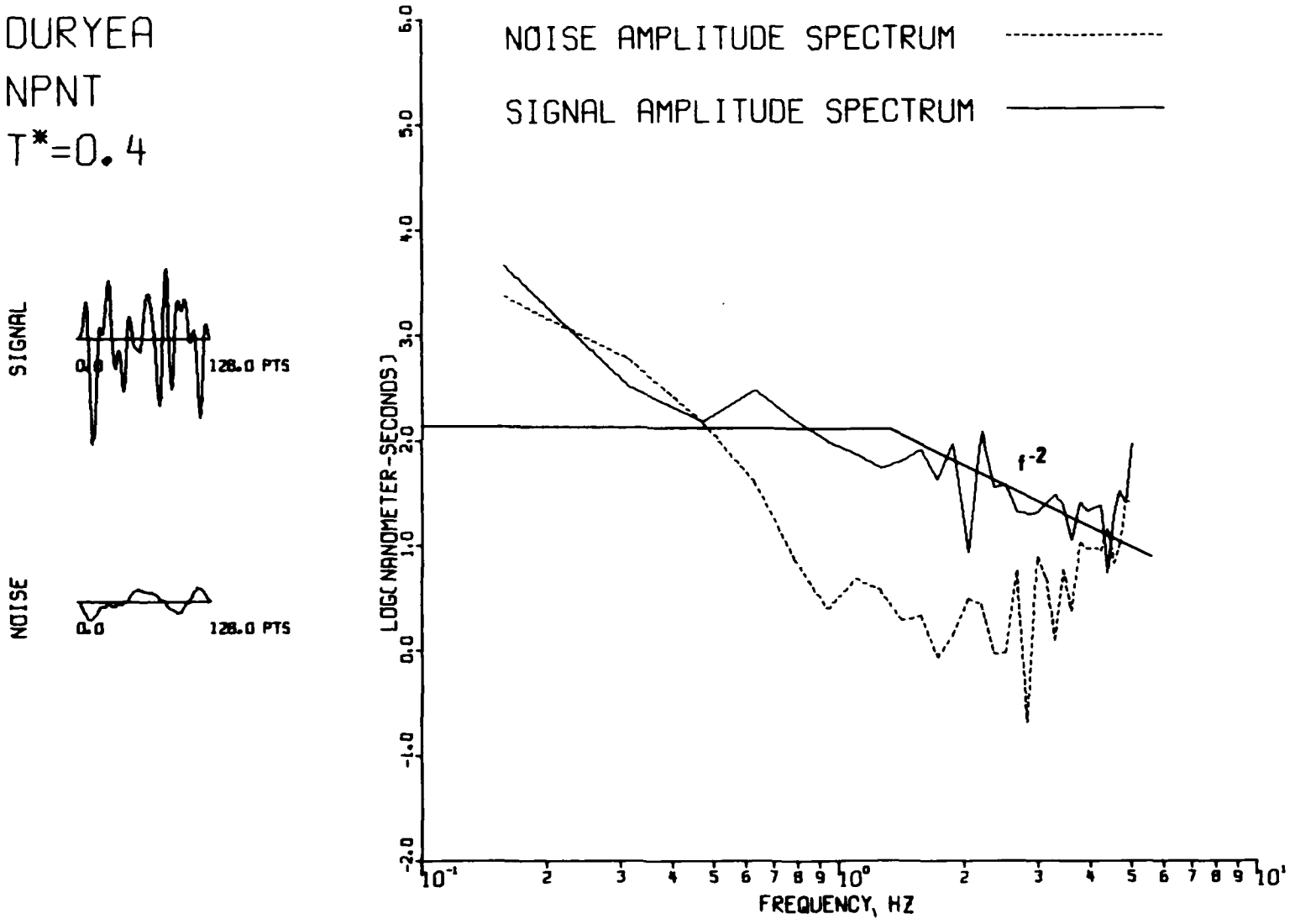

Figure 17 (cont.) Spectra of P waves from short-period recordings at NP-NT of selected Southwestern United States events.

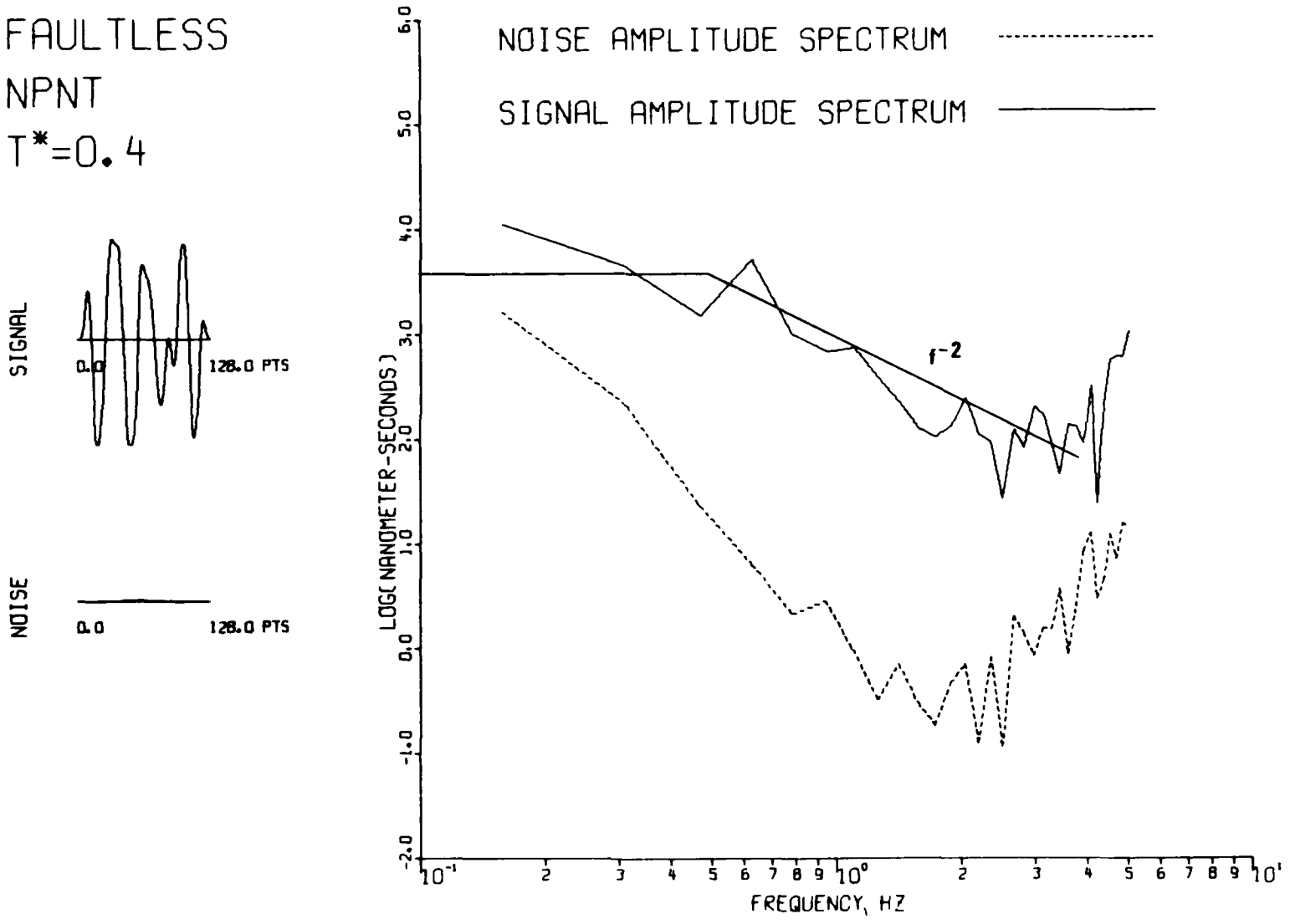

Figure 17 (cont.) Spectra of P waves from short-period recordings at NP-NT of selected Southwestern United States events.

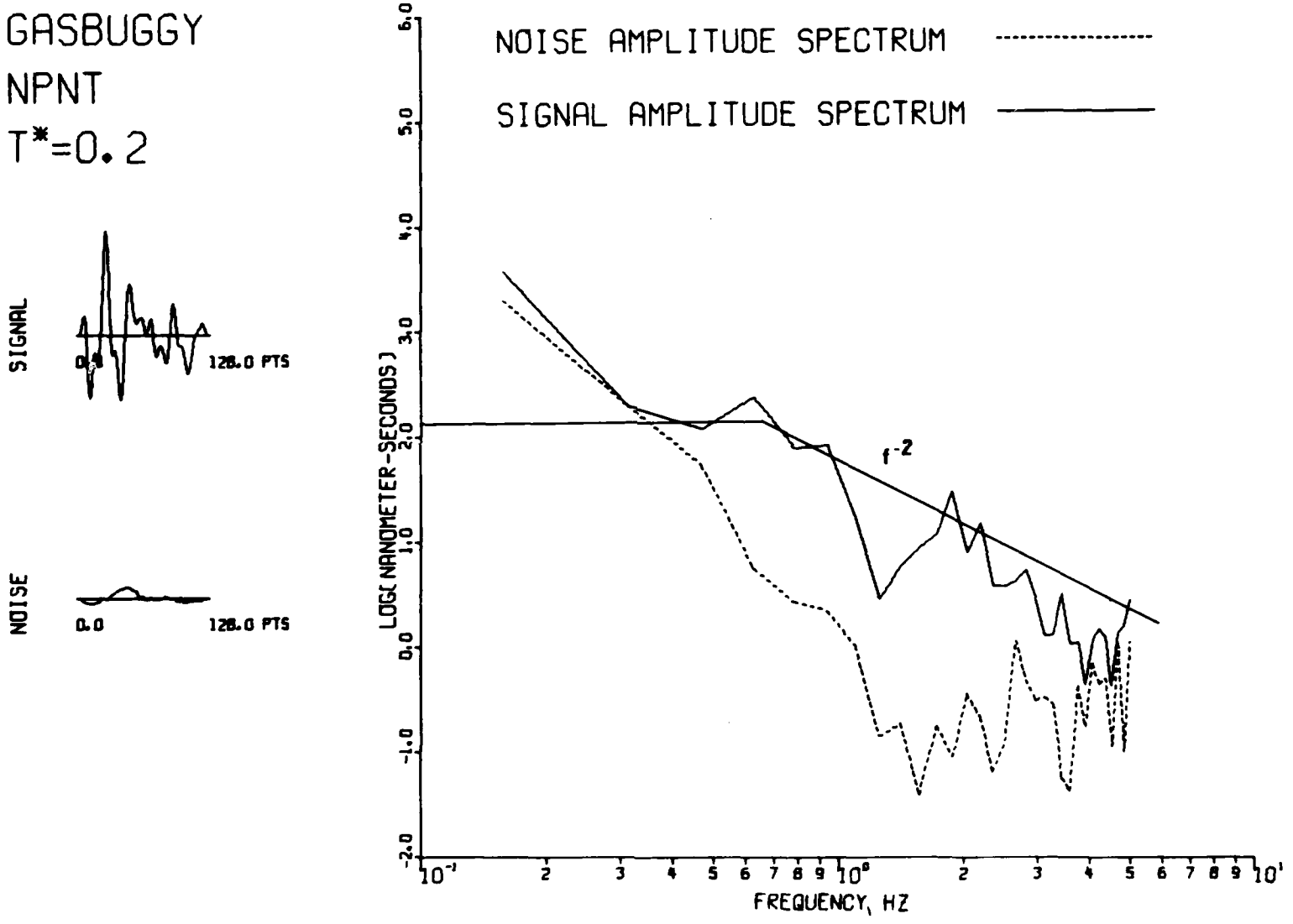

Figure 17 (cont.) Spectra of P waves from short-period recordings at NP-NT of selected Southwestern United States events.

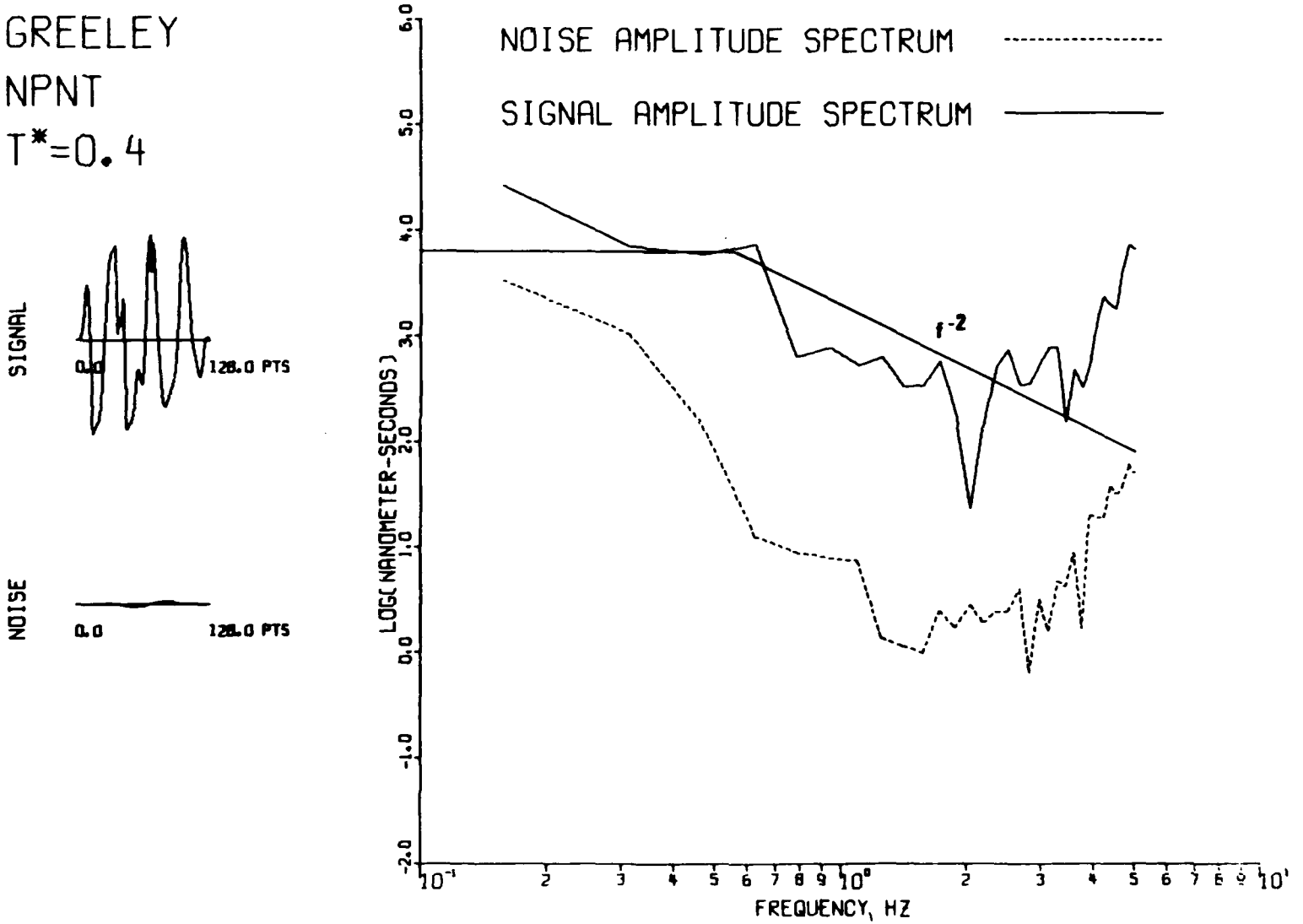

Figure 17 (cont.) Spectra of P waves from short-period recordings at NP-NT of selected Southwestern United States events.

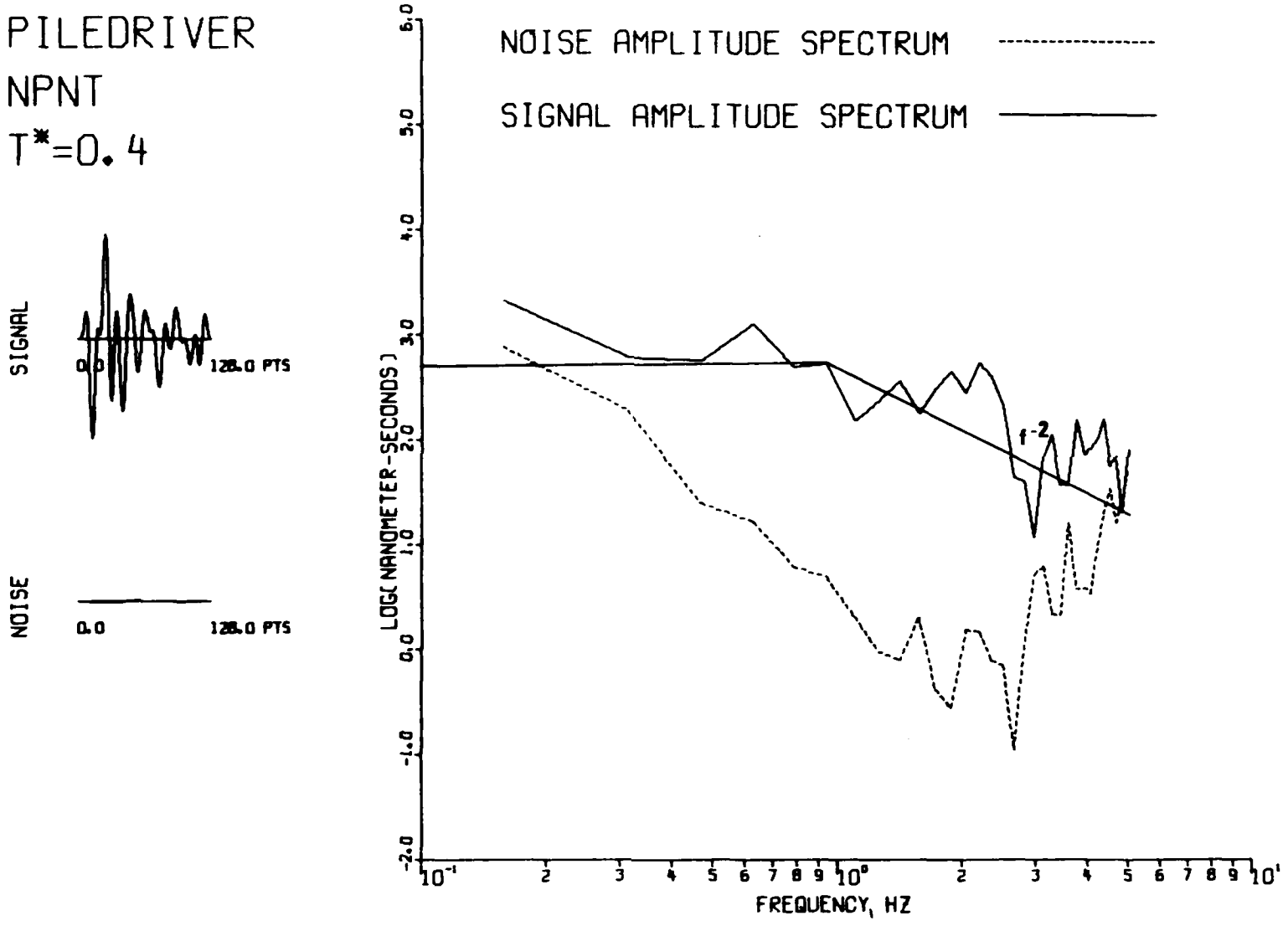

Figure 17 (cont.) Spectra of P waves from short-period recordings at NP-NT of selected Southwestern United States events.

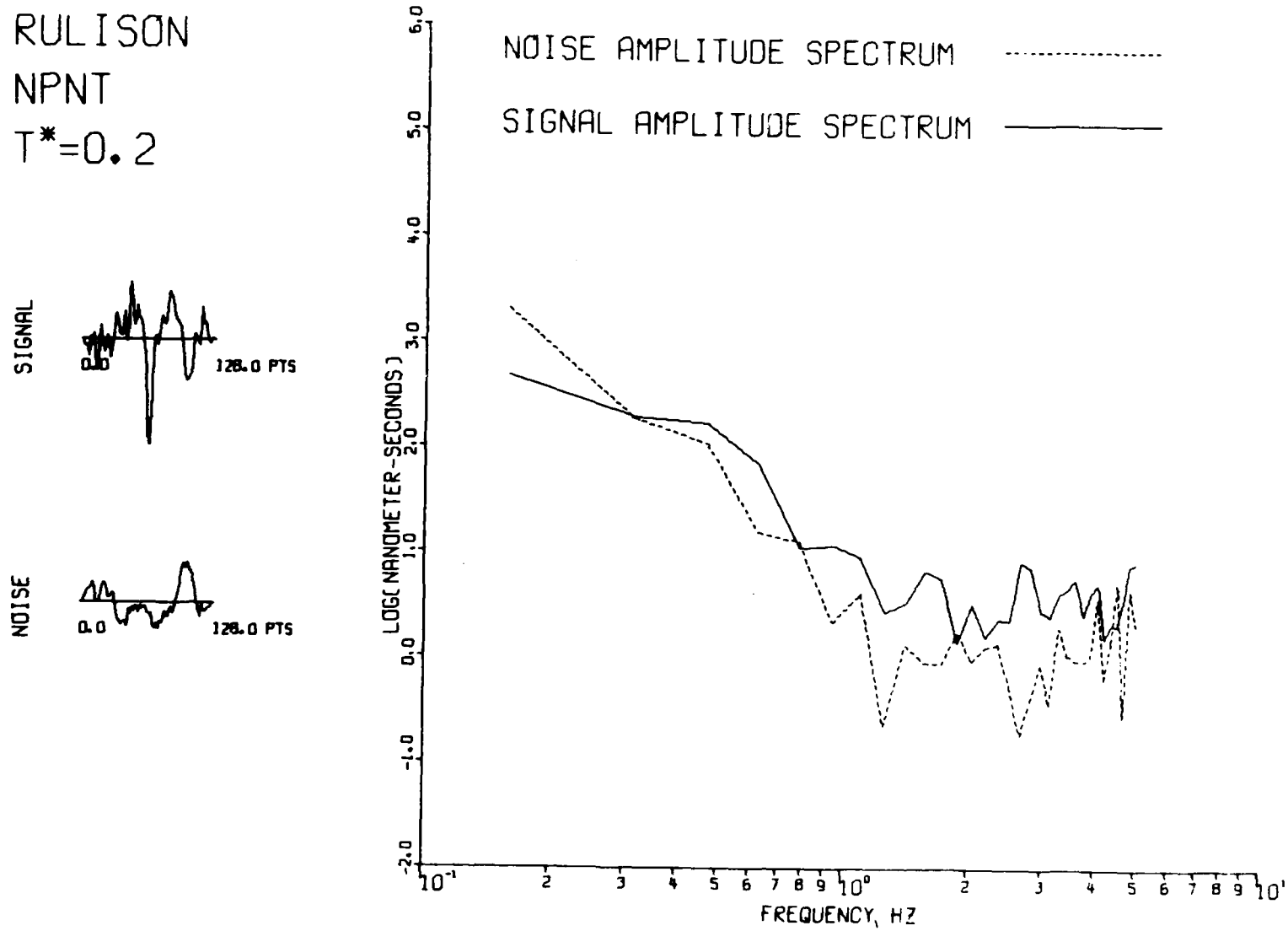

Figure 17 (cont.) Spectra of P waves from short-period recordings at NP-NT of selected Southwestern United States events.

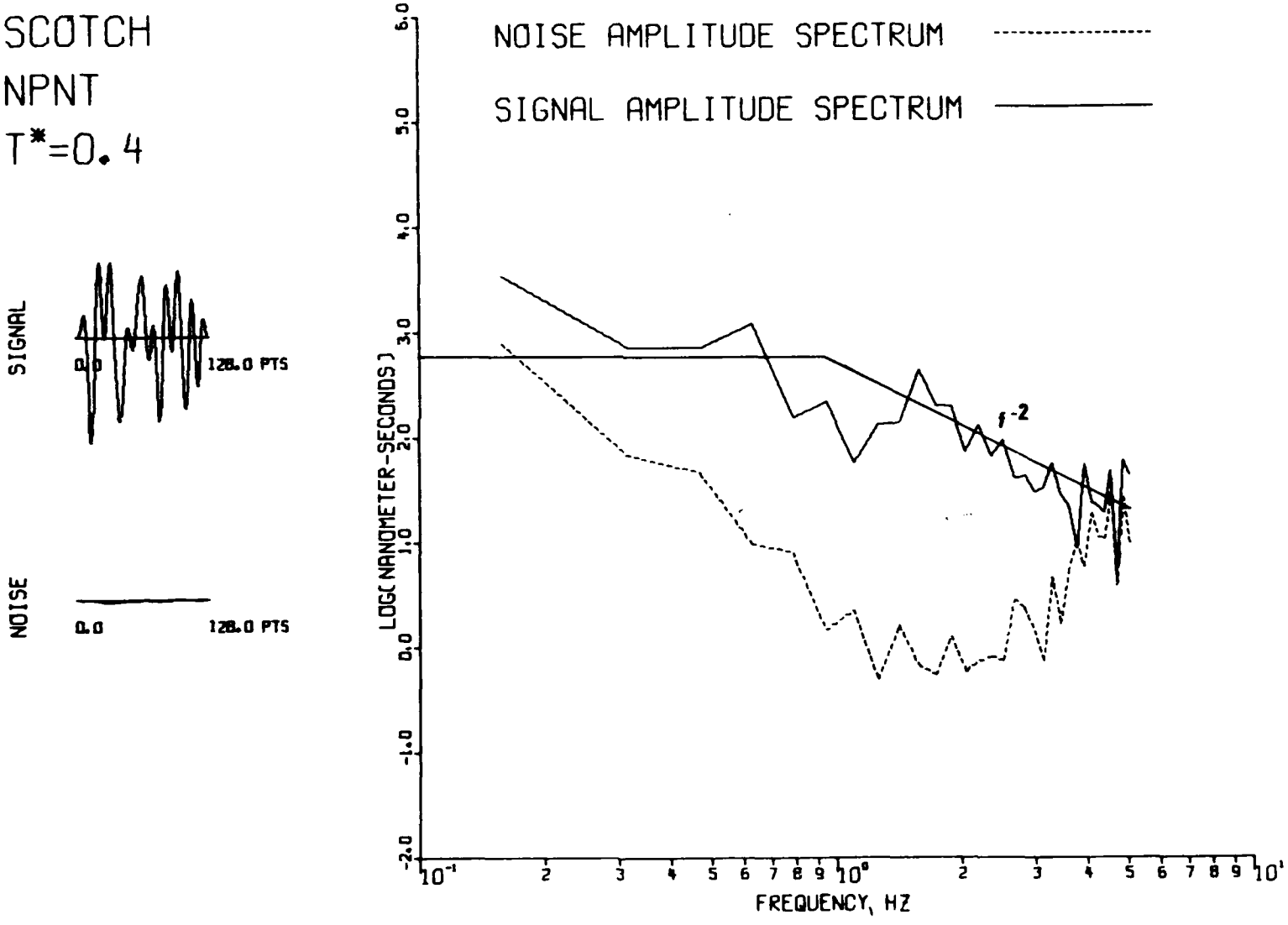

Figure 17 (cont.) Spectra of P waves from short-period recordings at NP-NT of selected Southwestern United States events.

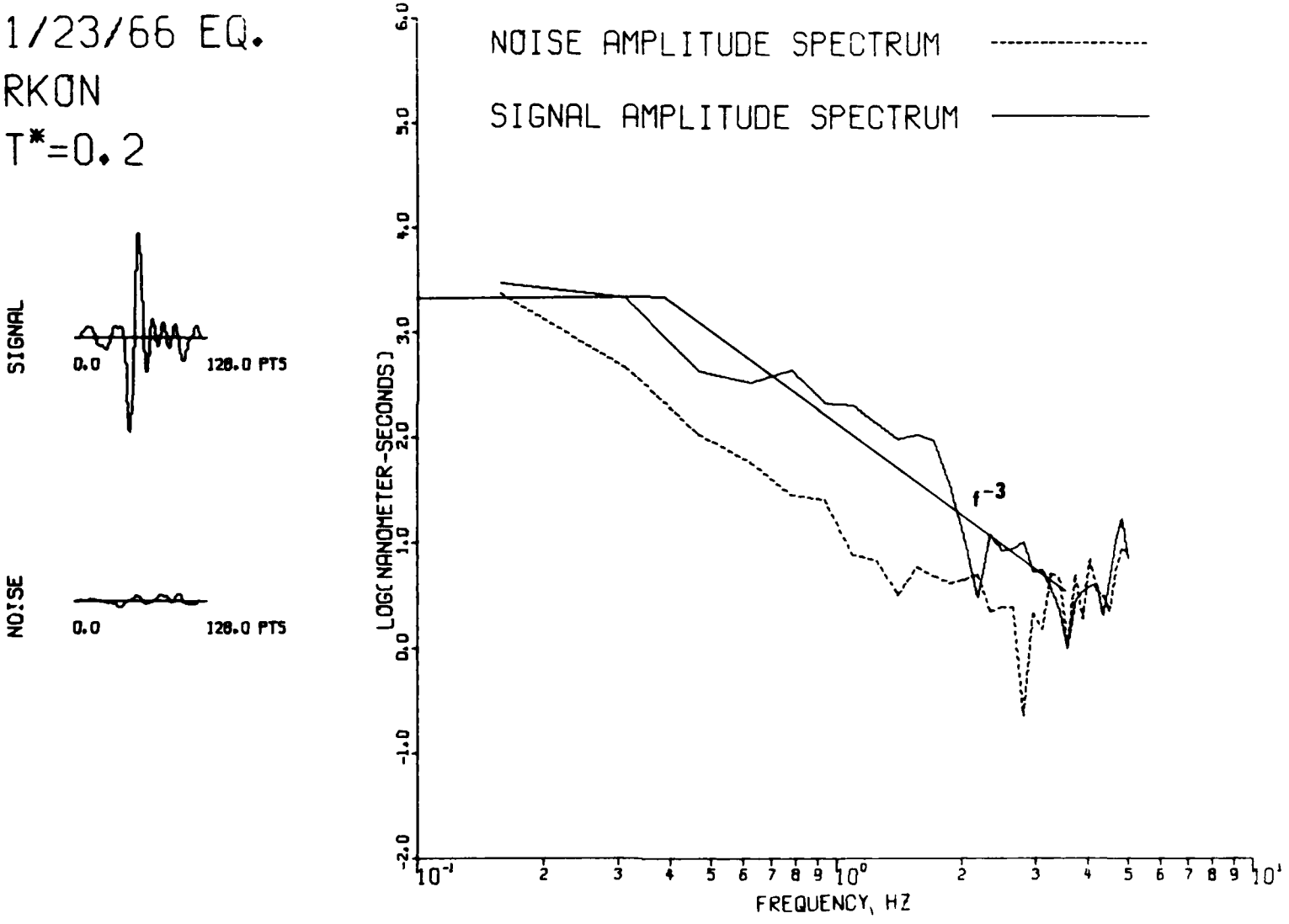

Figure 18 Spectra of P waves from short-period recordings at RK-ON of selected Southwestern United States events.

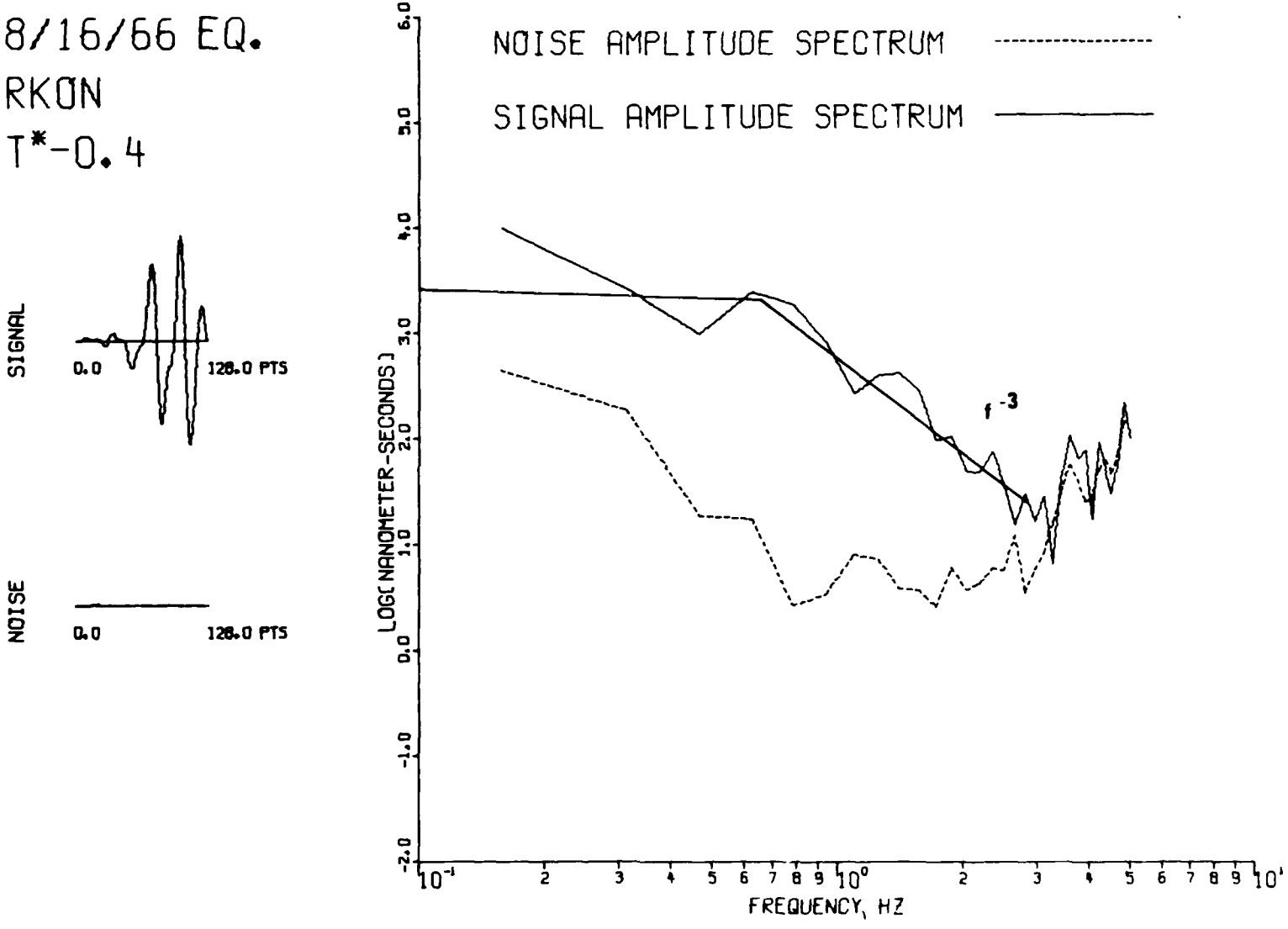

Figure 18 (cont.) Spectra of P waves from short-period recordings at RK-ON of selected Southwestern United States events.

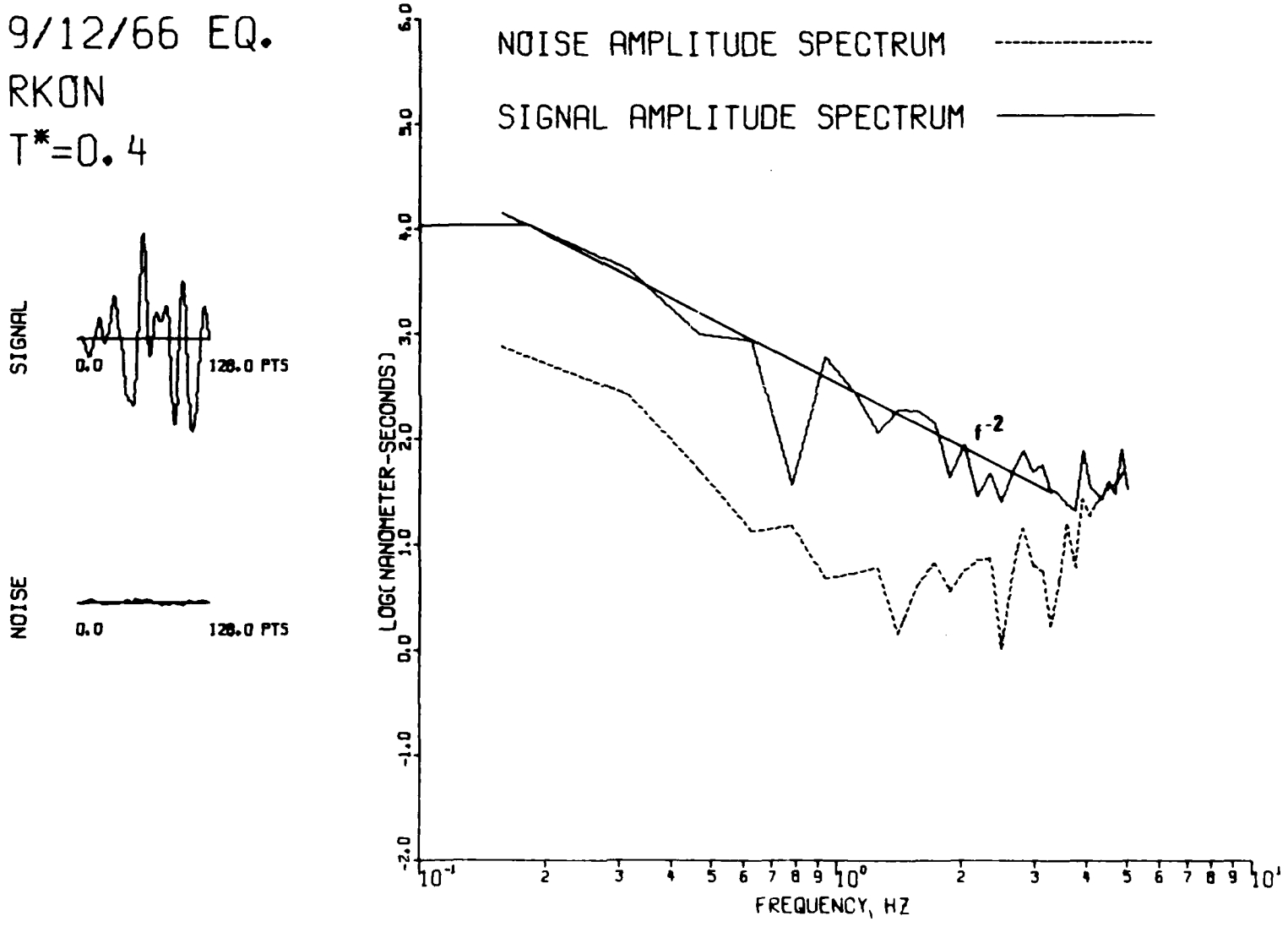

Figure 18 (cont.) Spectra of P waves from short-period recordings at RK-ON of selected Southwestern United States events.

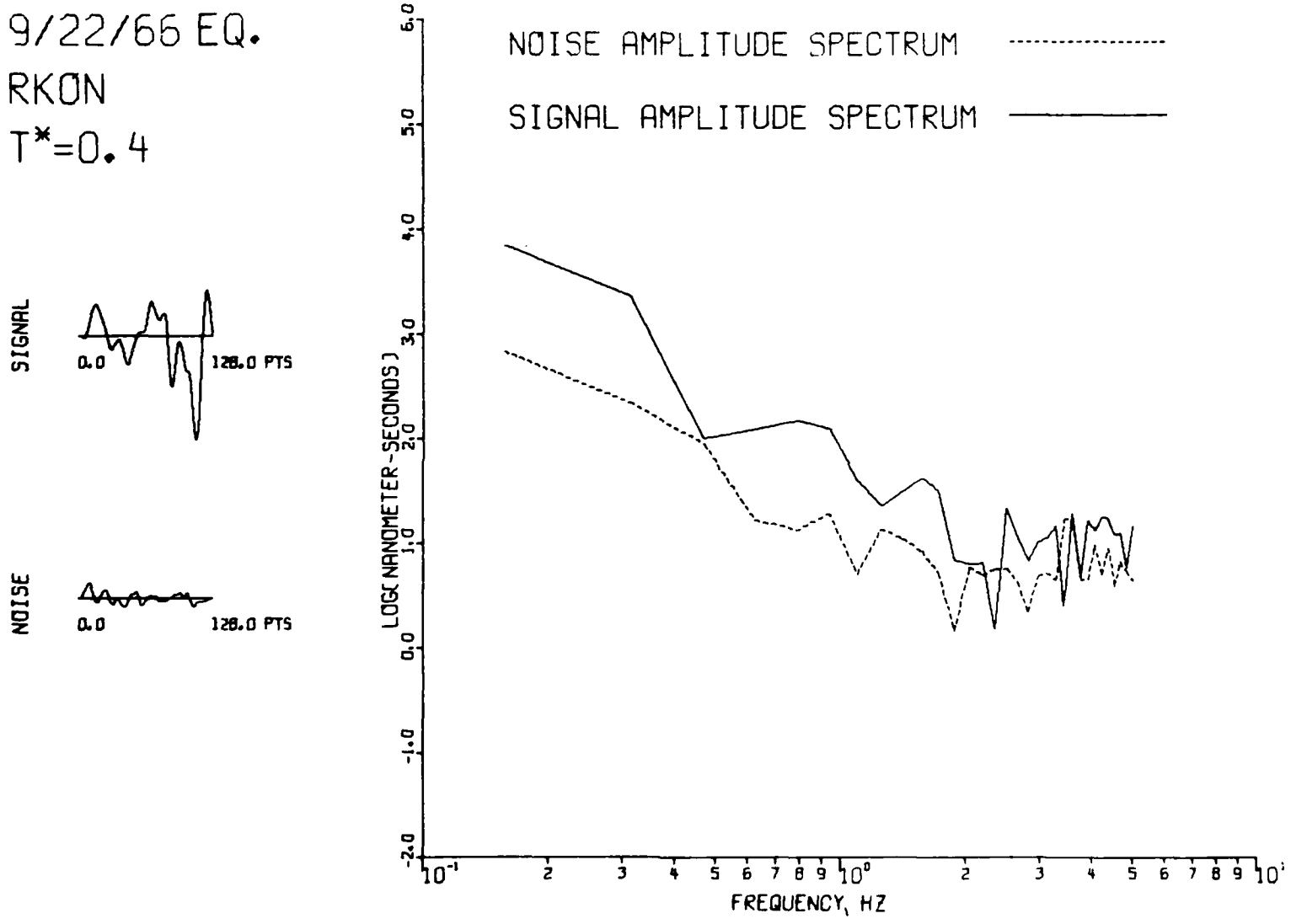

Figure 18 (cont.) Spectra of P waves from short-period recordings at RK-ON of selected Southwestern United States events.

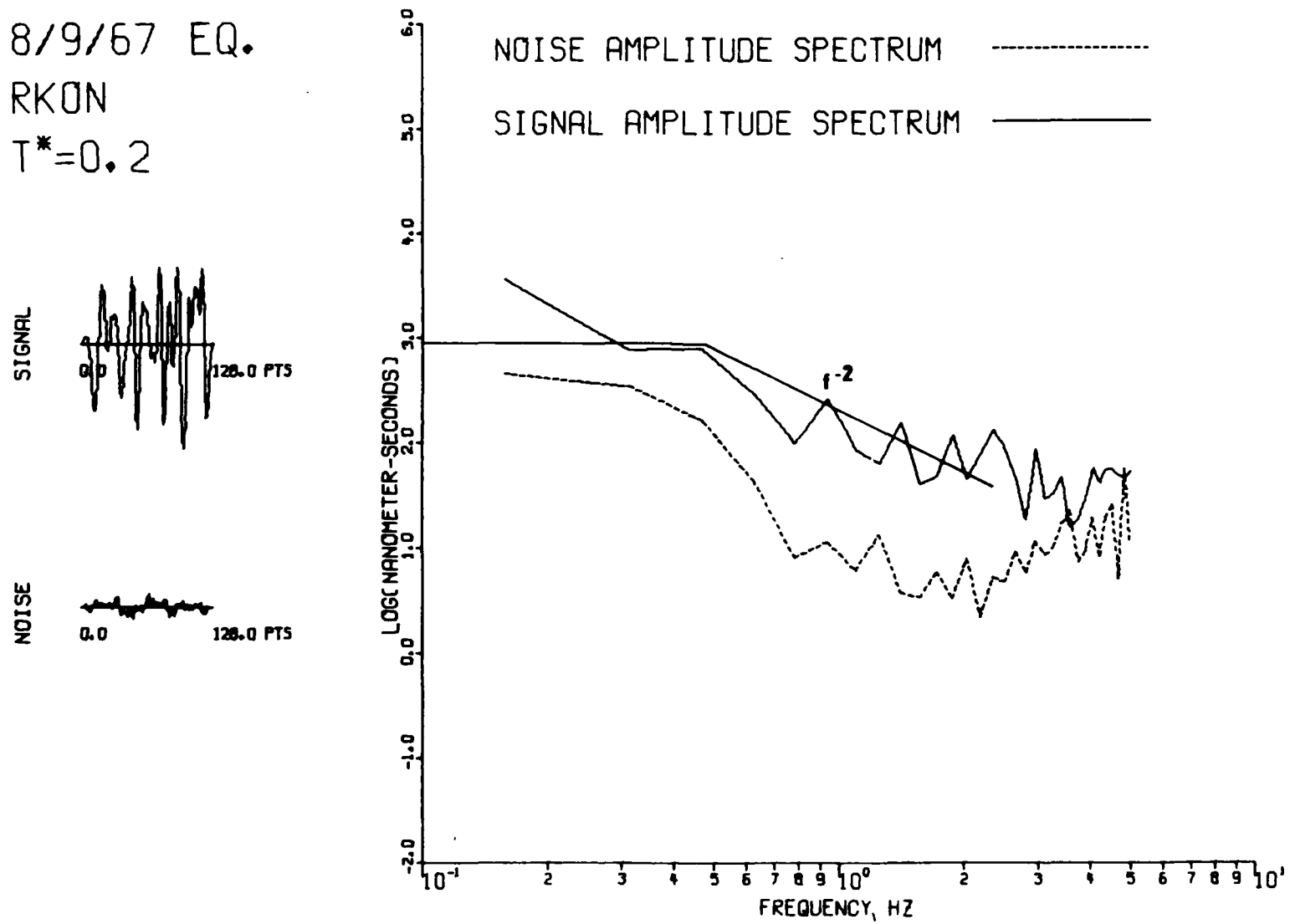

Figure 18 (cont.) Spectra of P waves from short-period recordings at RK-ON of selected Southwestern United States events.

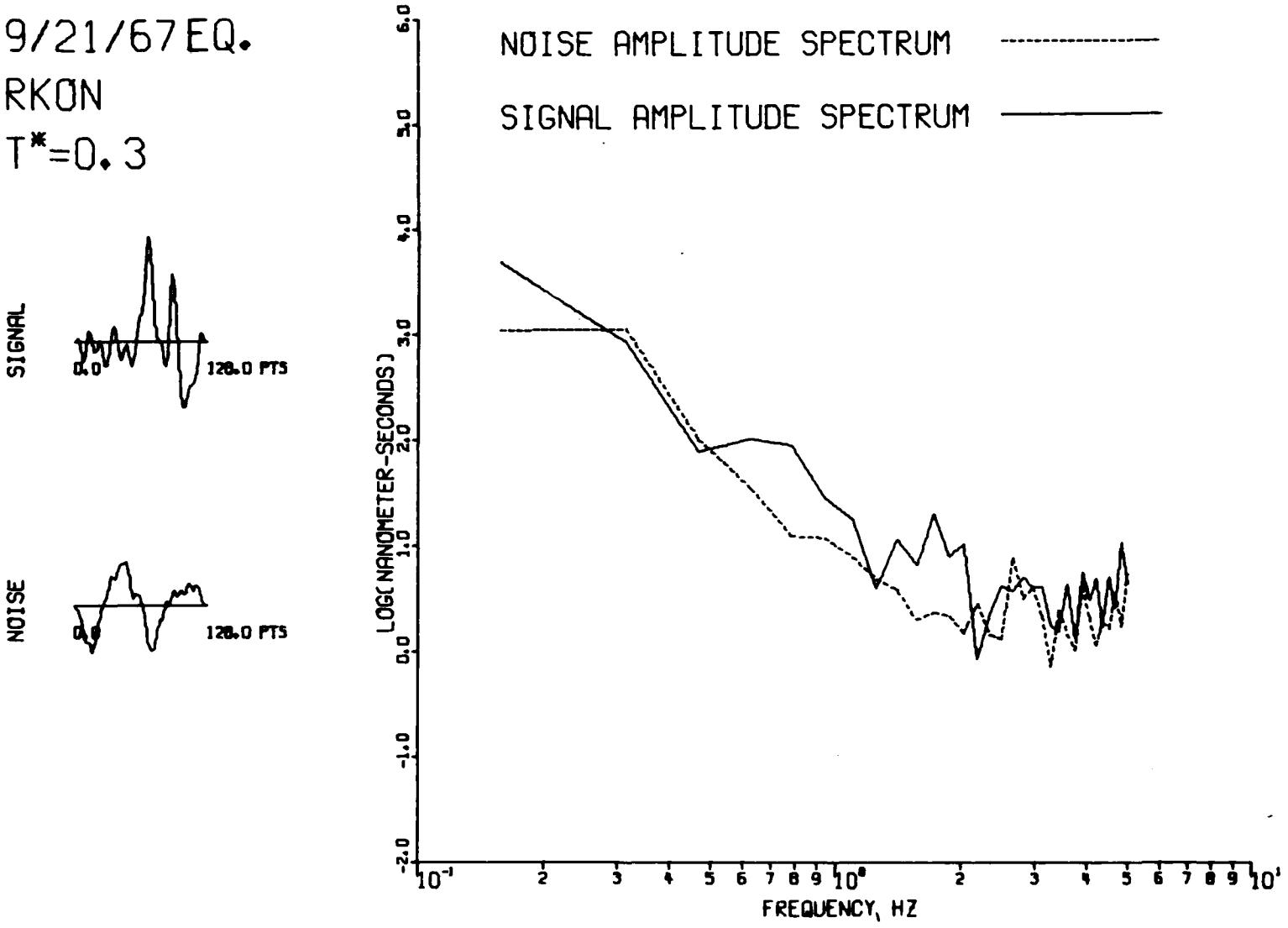

Figure 18 (cont.) Spectra of P waves from short-period recordings at RK-ON of selected Southwestern United States events.

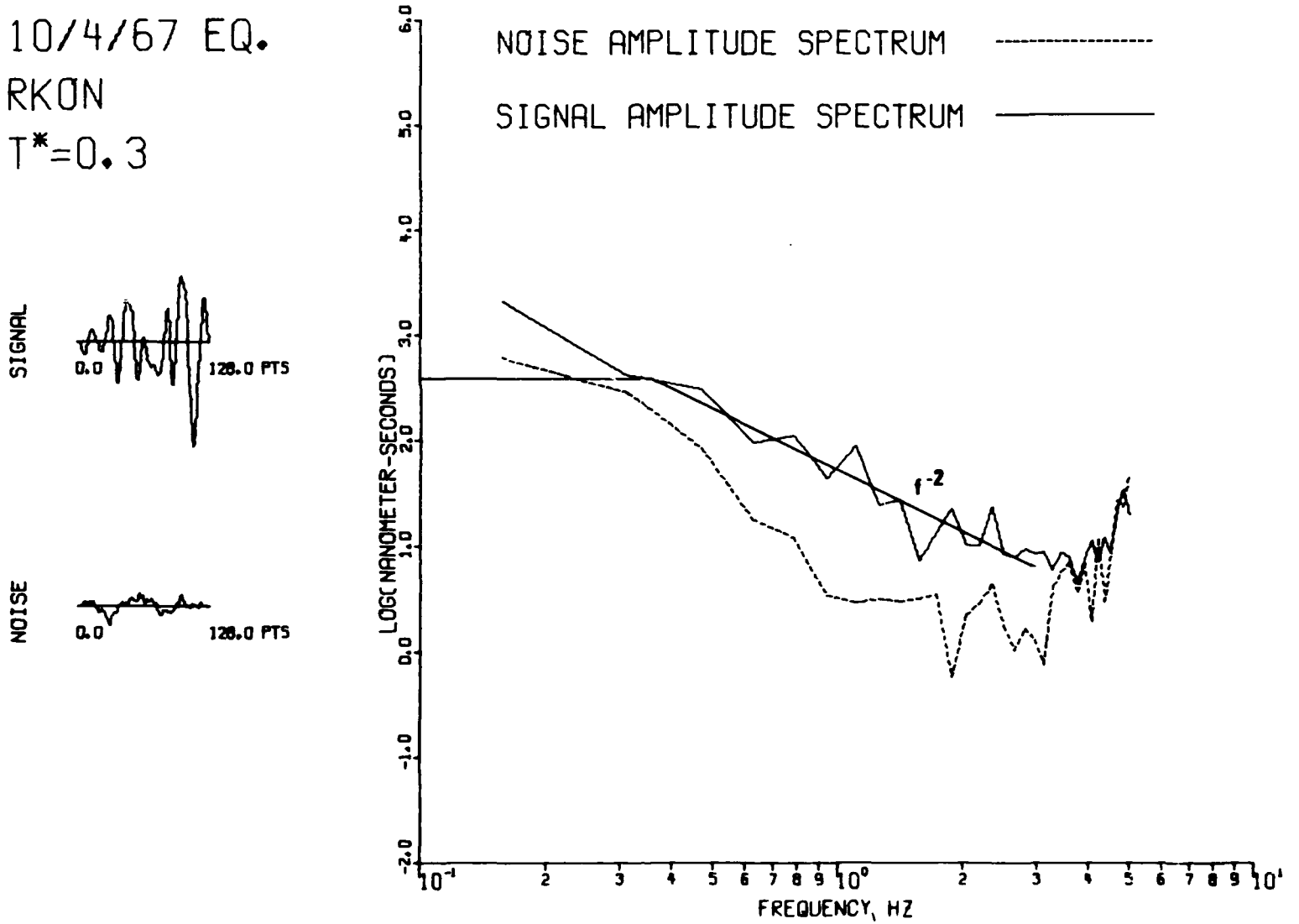

Figure 18 (cont.) Spectra of P waves from short-period recordings at RK-ON of selected Southwestern United States events.

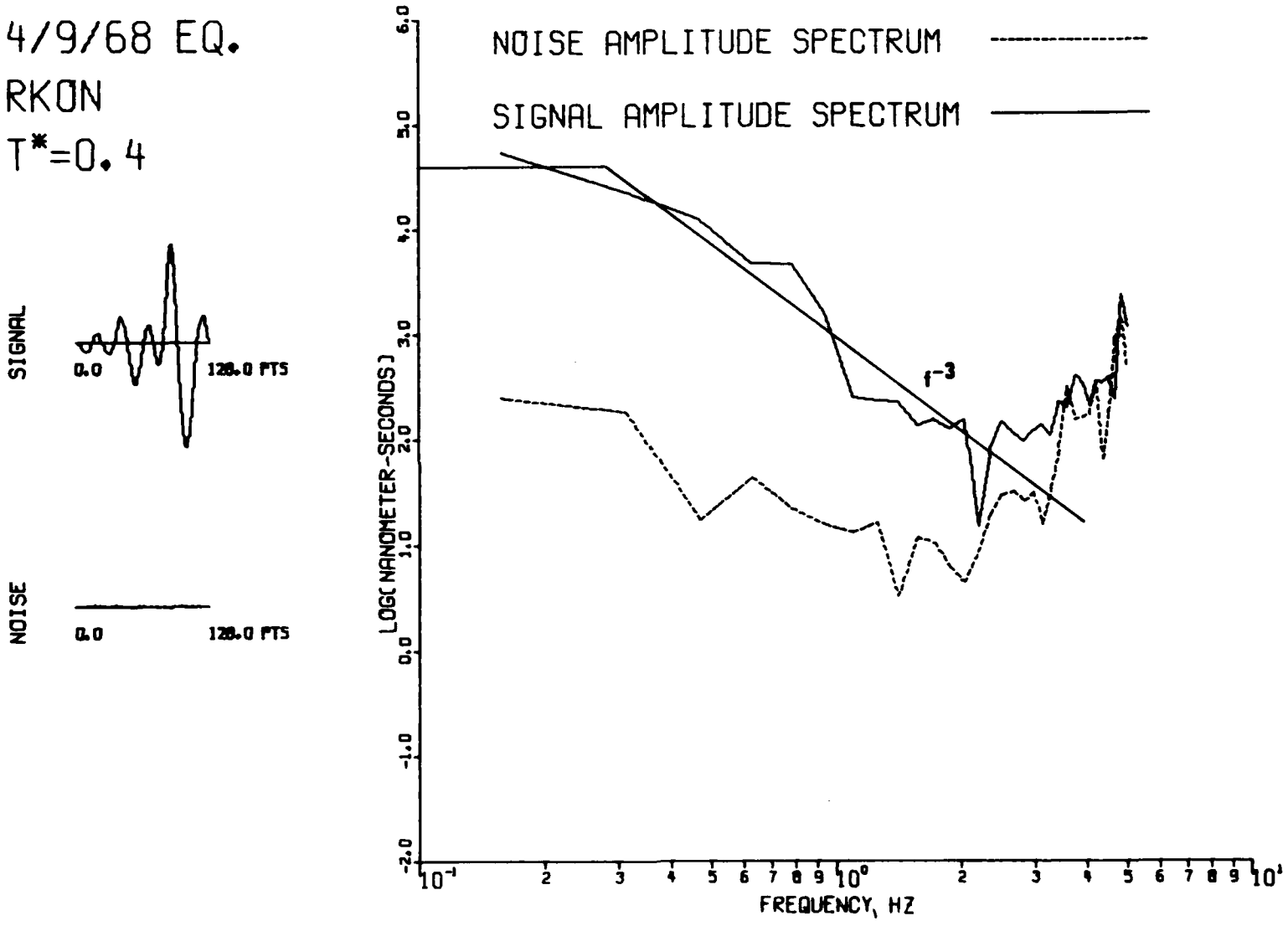

Figure 18 (cont.) Spectra of P waves from short-period recordings at RK-ON of selected Southwestern United States events.

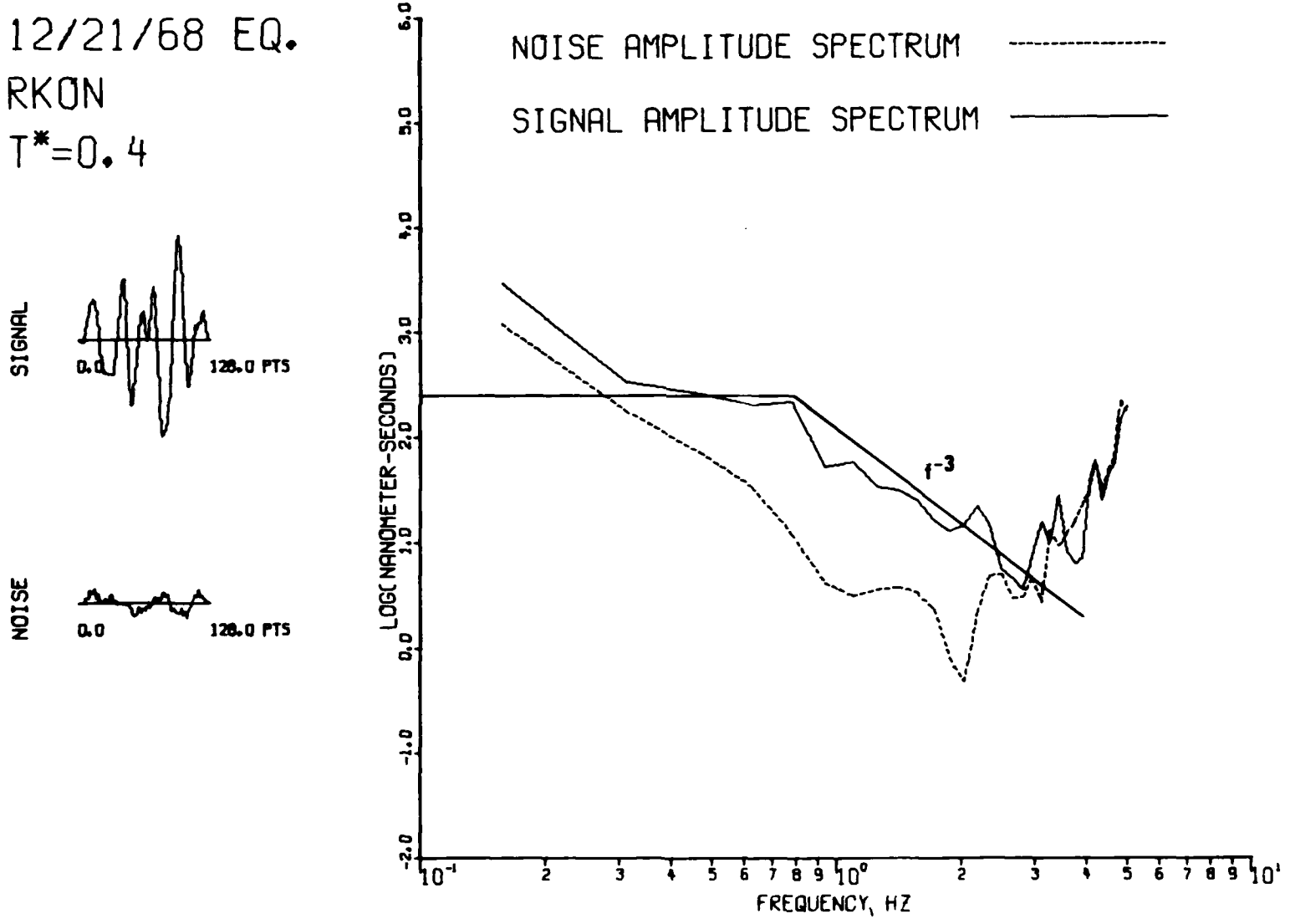

Figure 18 (cont.) Spectra of P waves from short-period recordings at RK-ON of selected Southwestern United States events.

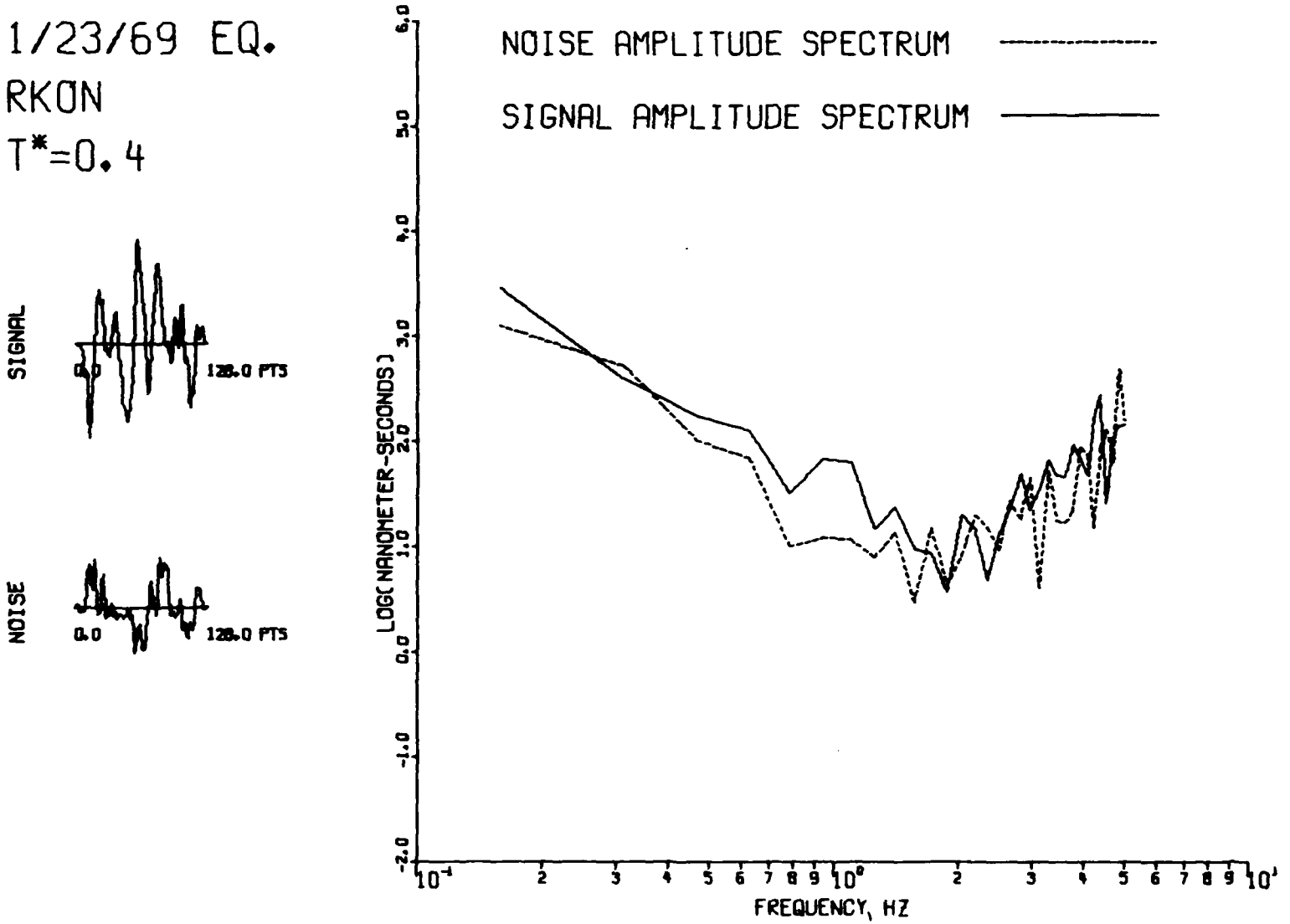

Figure 18 (cont.) Spectra of P waves from short-period recordings at RK-ON of selected Southwestern United States events.

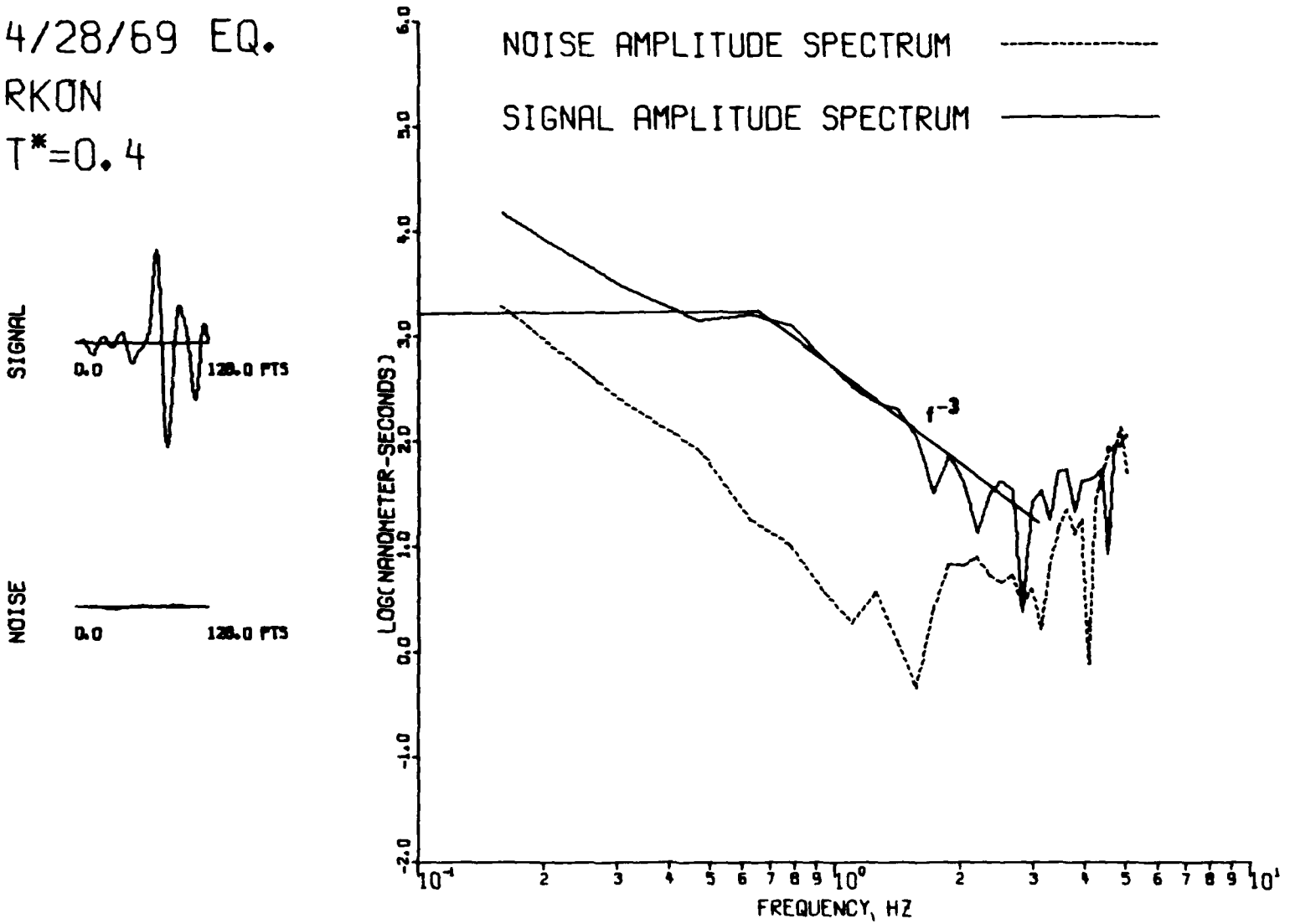

Figure 18 (cont.) Spectra of P waves from short-period recordings at RK-ON of selected Southwestern United States events.

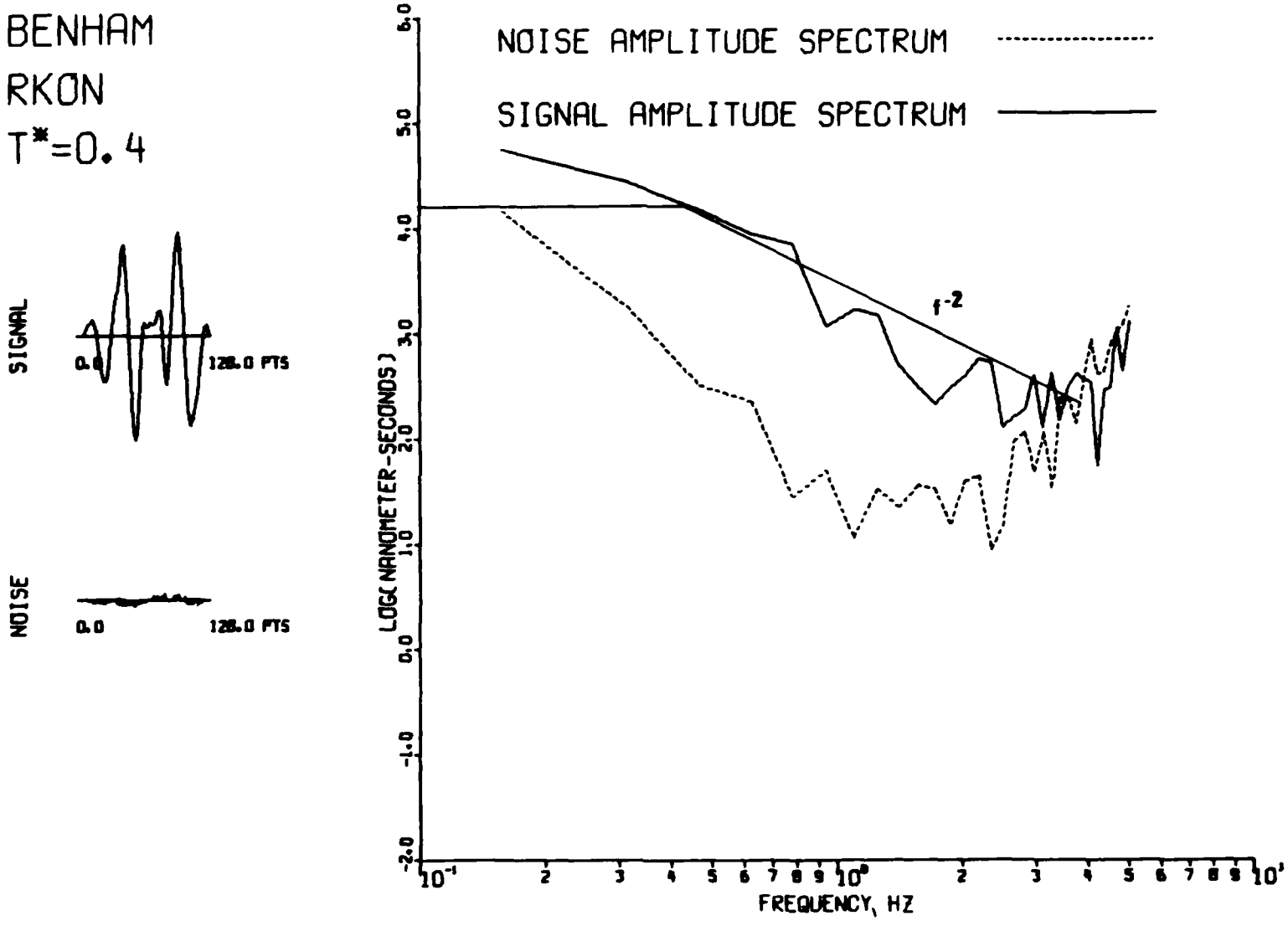

Figure 18 (cont.) Spectra of P waves from short-period recordings at RK-ON of selected Southwestern United States events.

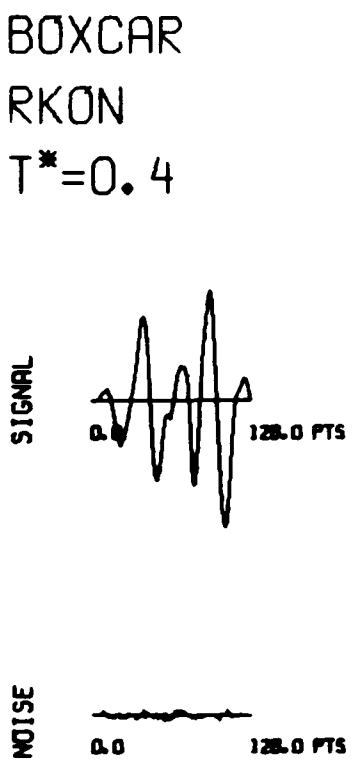

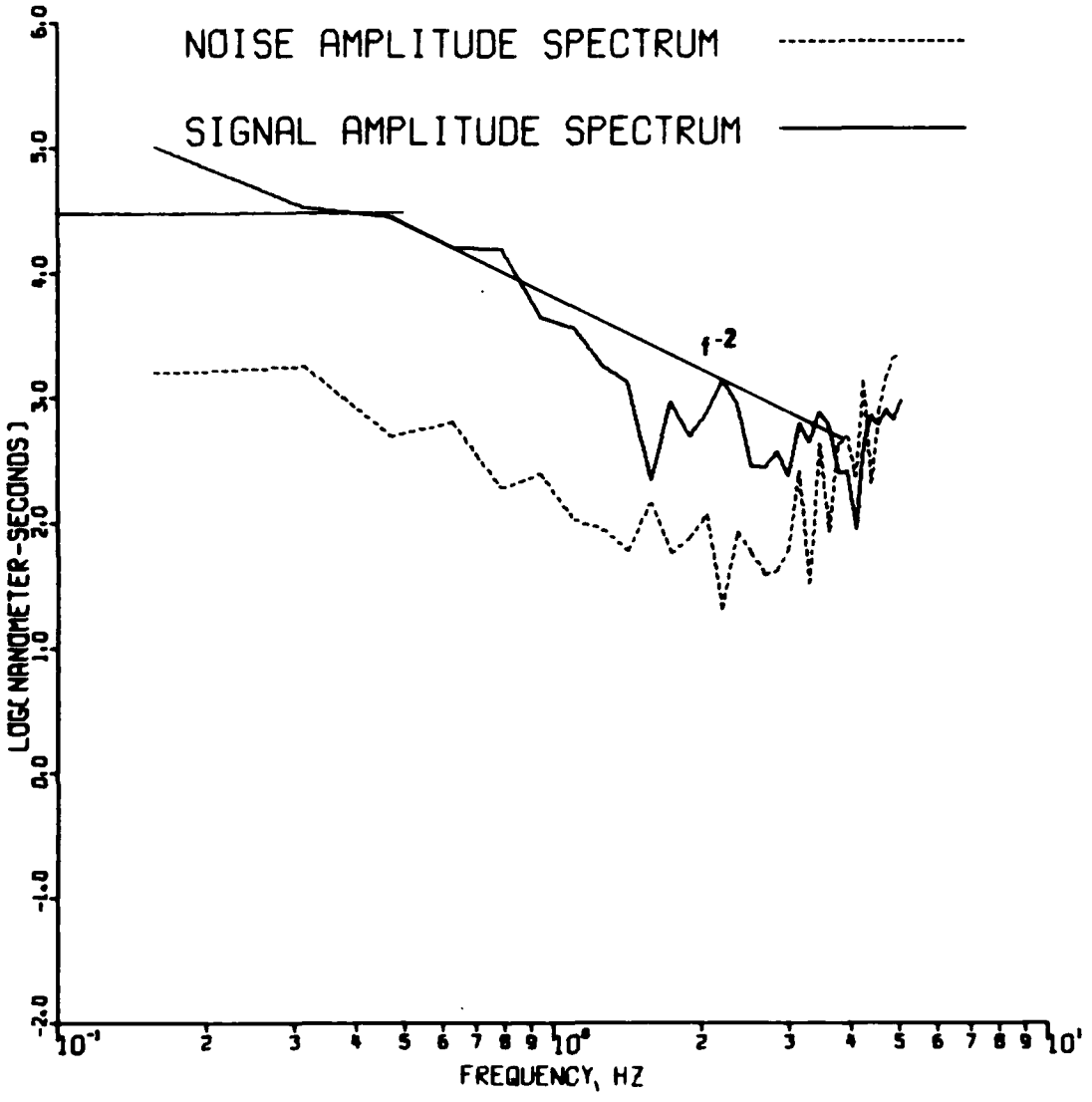

Figure 18 (cont.) Spectra of P waves from short-period recordings at RK-ON of selected Southwestern United States events.

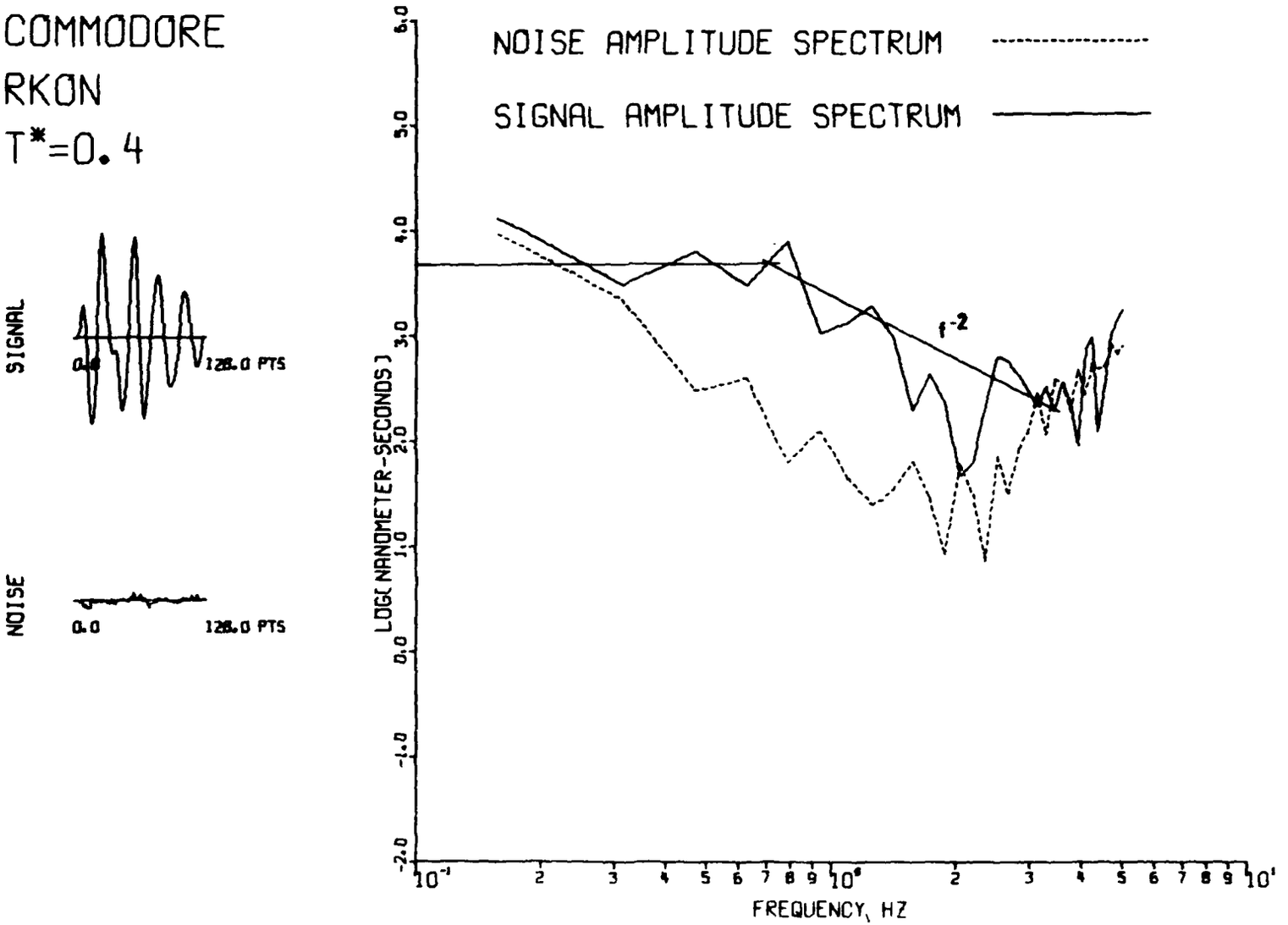

Figure 18 (cont.) Spectra of P waves from short-period recordings at RK-ON of selected Southwestern United States events.

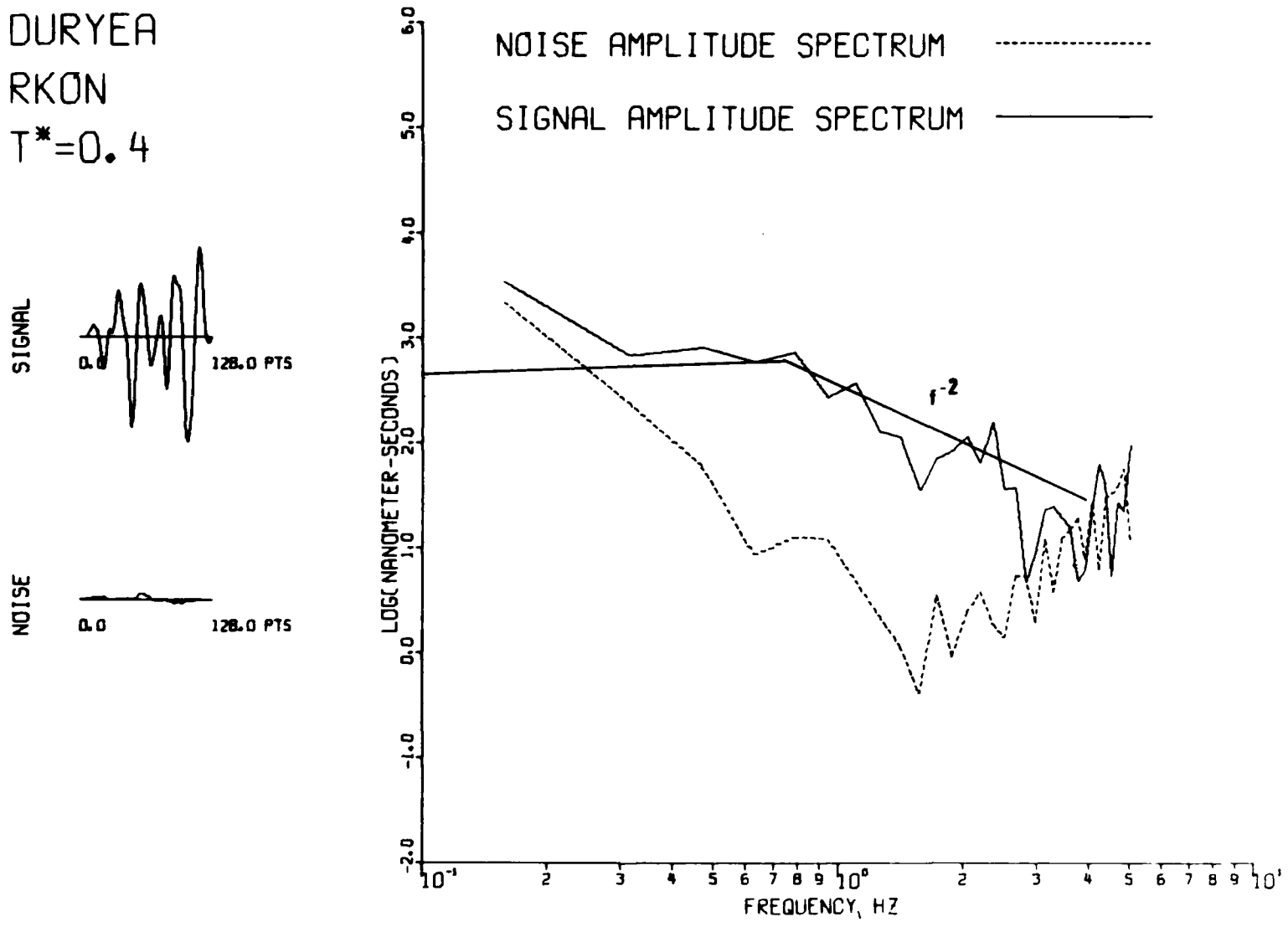

Figure 18 (cont.) Spectra of P waves from short-period recordings at RK-ON of selected Southwestern United States events.

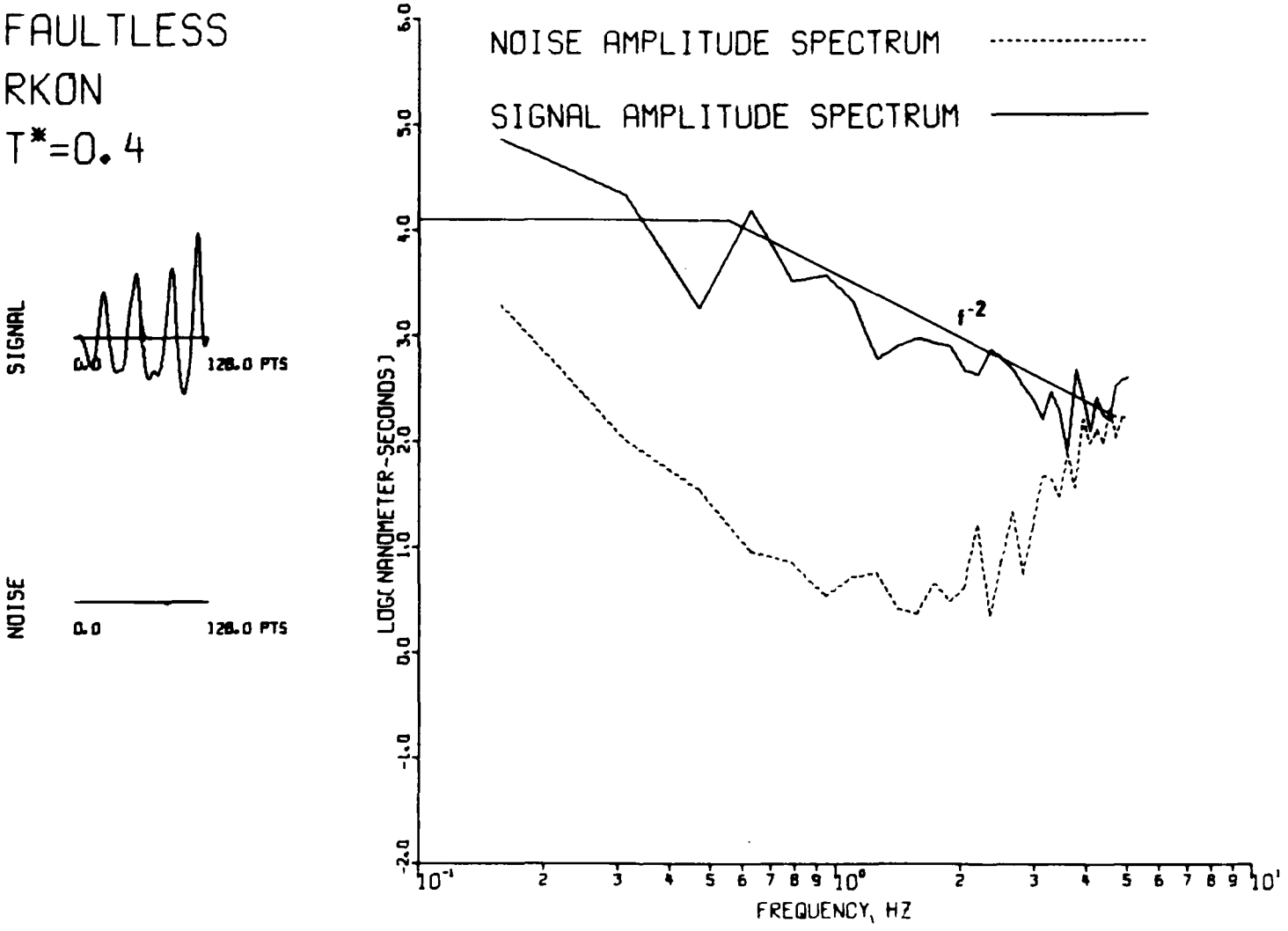

Figure 18 (cont.) Spectra of P waves from short-period recordings at RK-ON of selected Southwestern United States events.

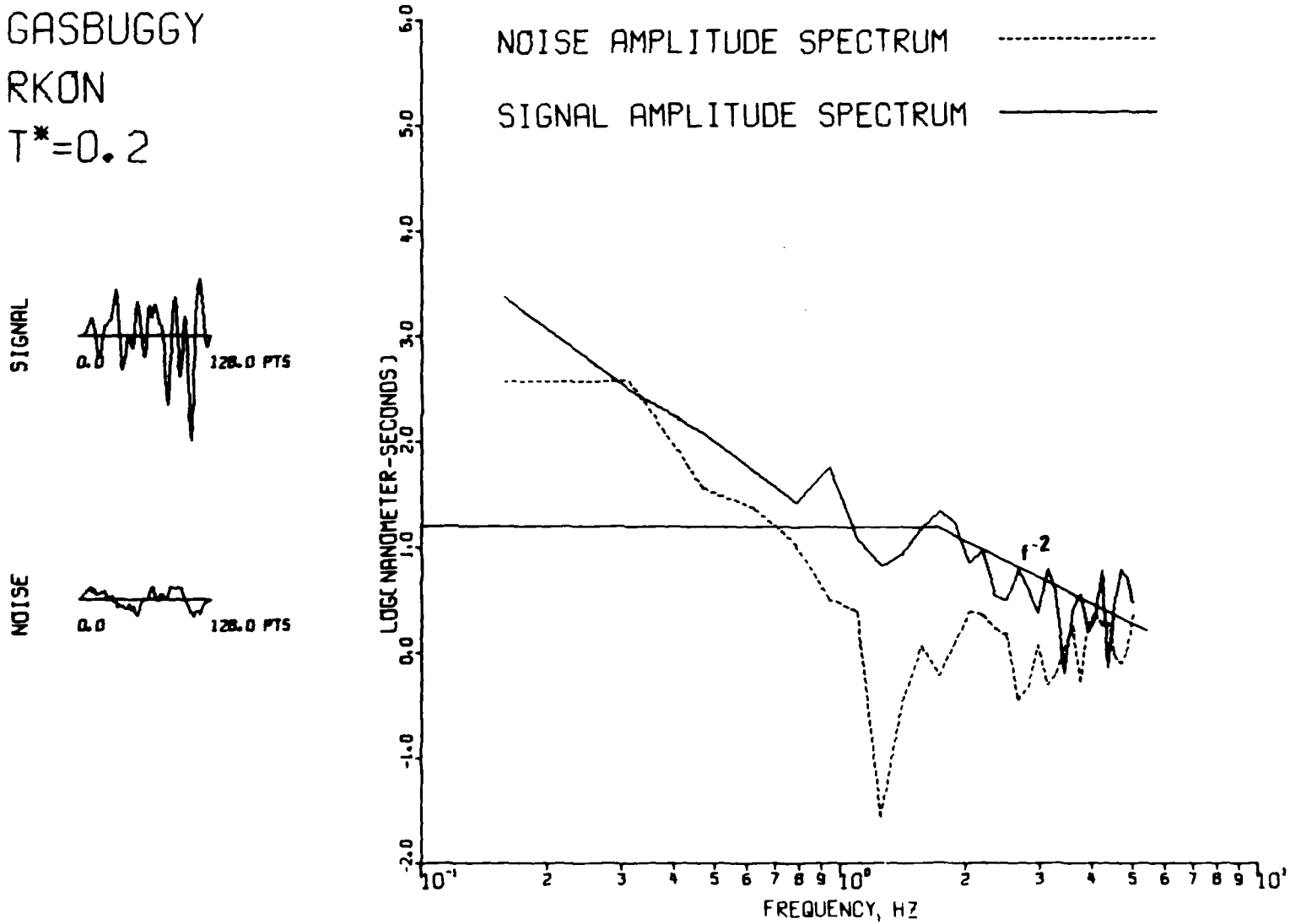

Figure 18 (cont.) Spectra of P waves from short-period recordings at RK-ON of selected Southwestern United States events.

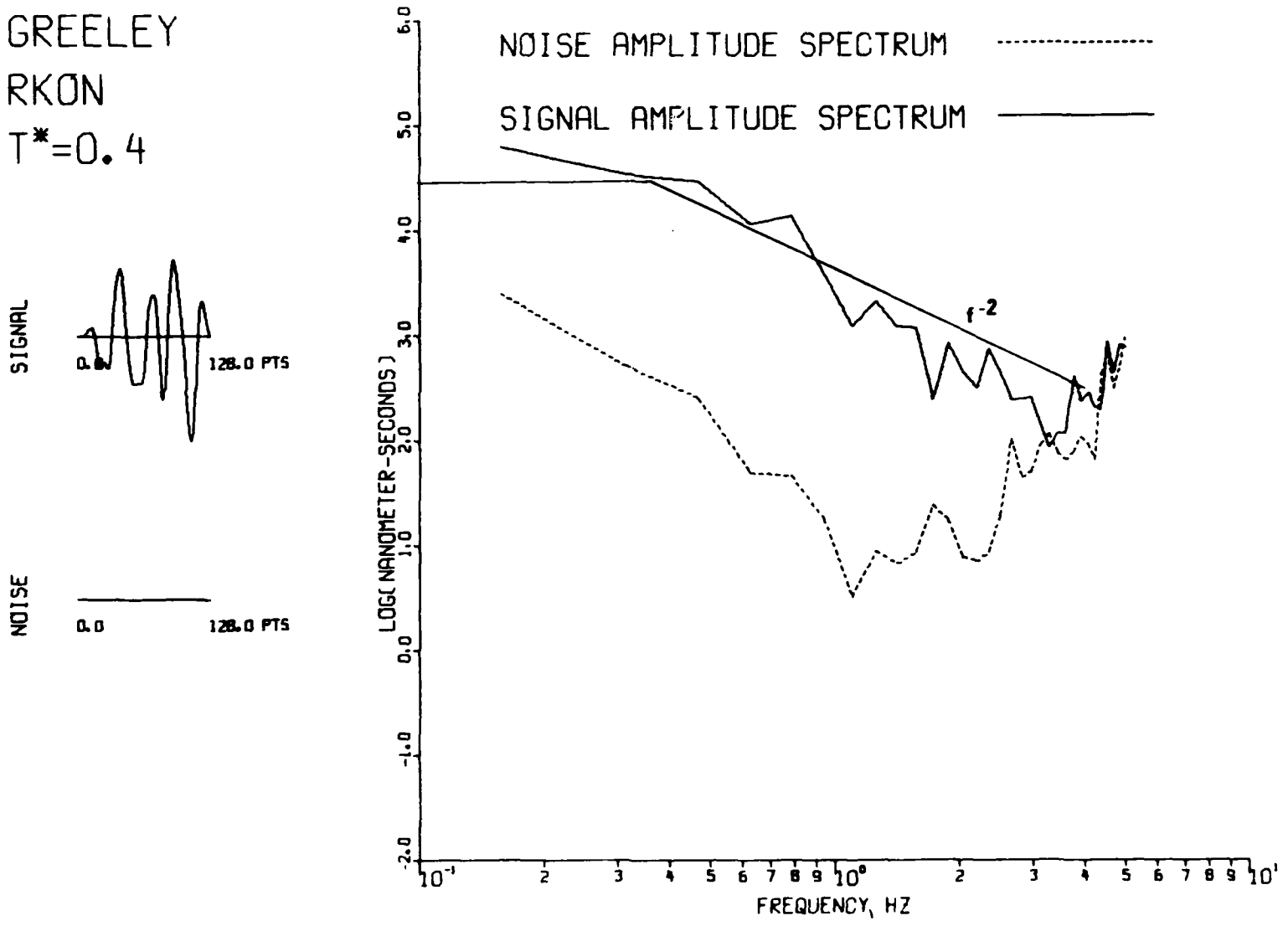

Figure 18 (cont.) Spectra of P waves from short-period recordings at RK-ON of selected Southwestern United States events.

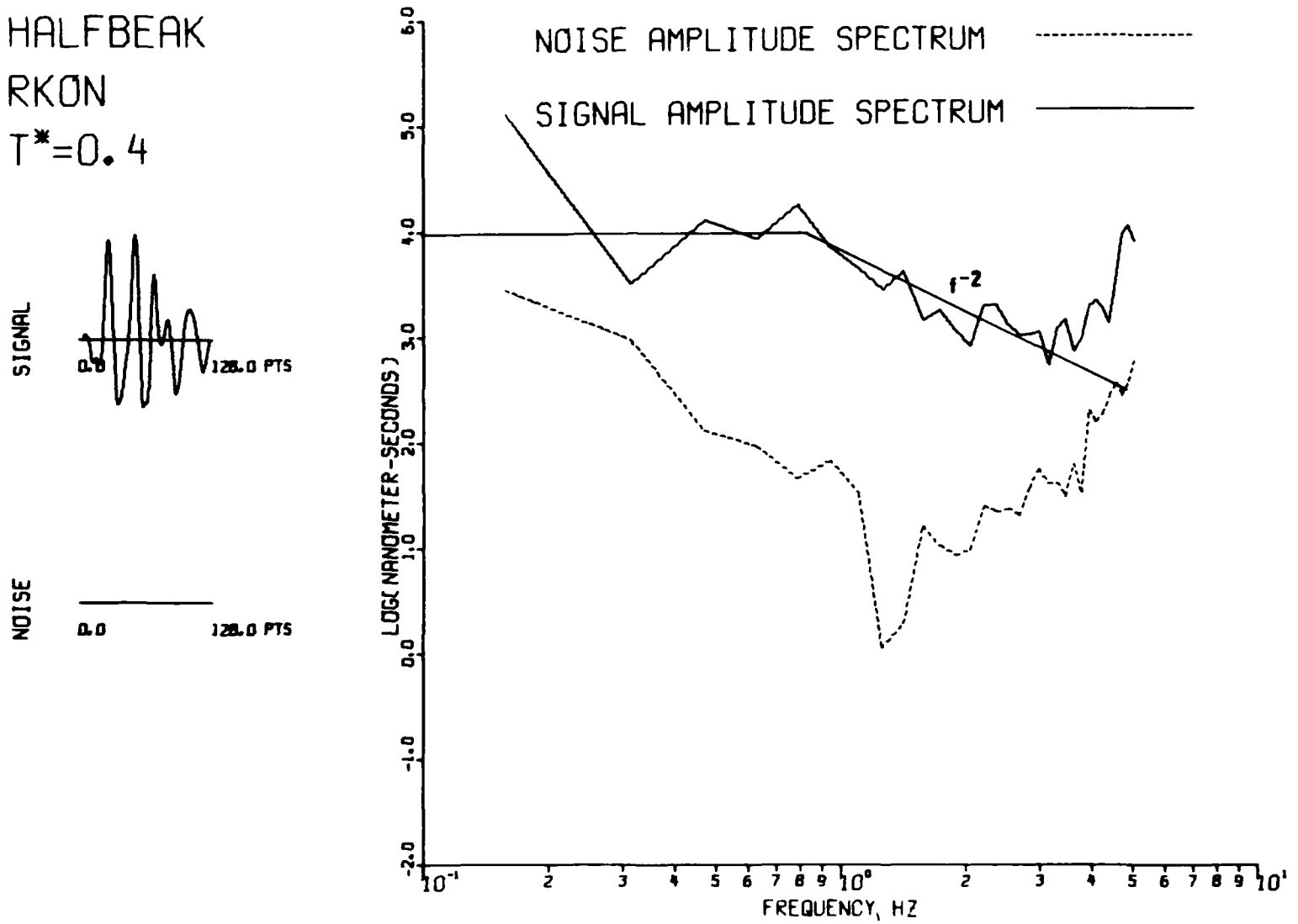

Figure 18 (cont.) Spectra of P waves from short-period recordings at RK-ON of selected Southwestern United States events.

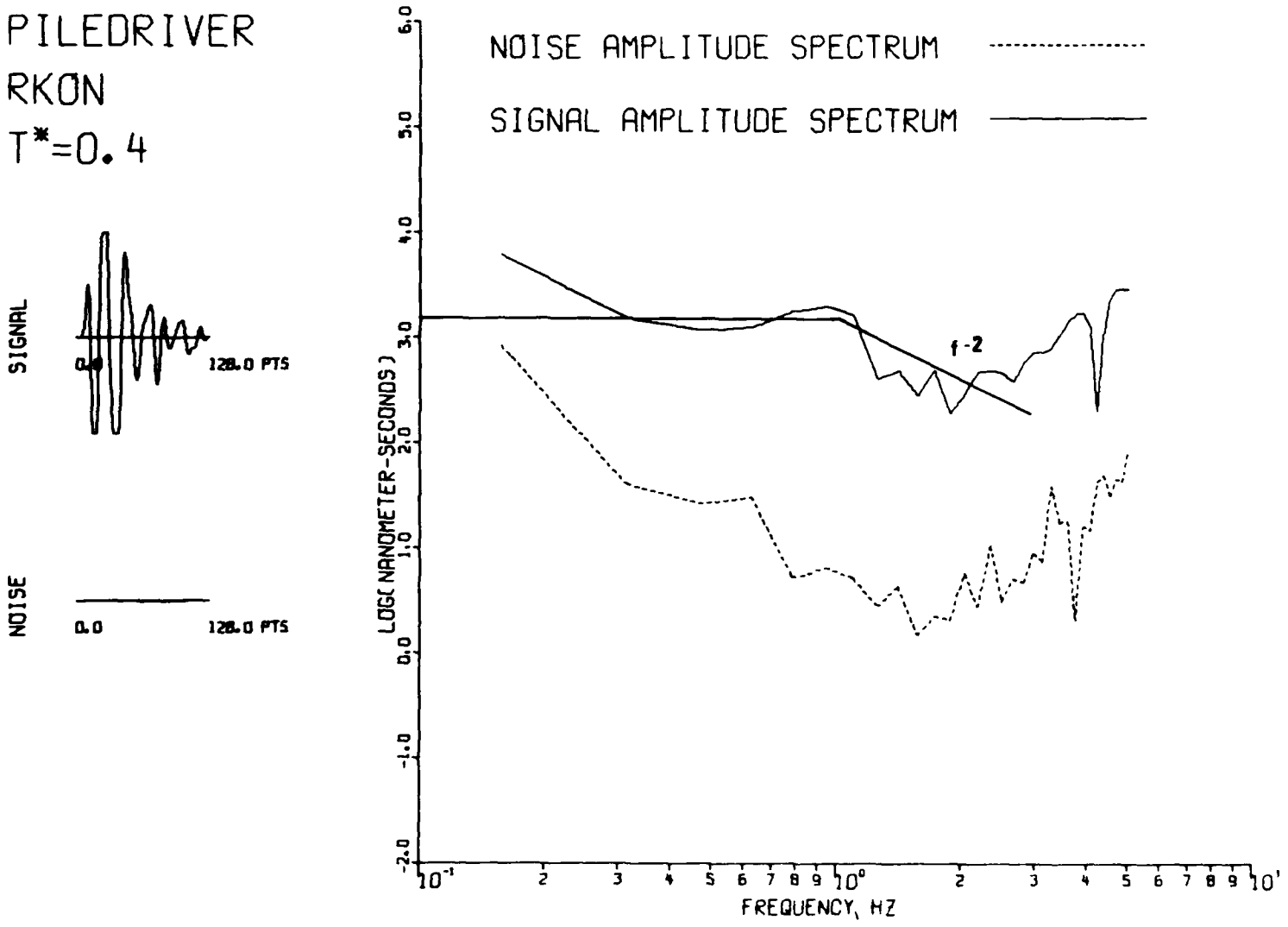

Figure 18 (cont.) Spectra of P waves from short-period recordings at RK-ON of selected Southwestern United States events.

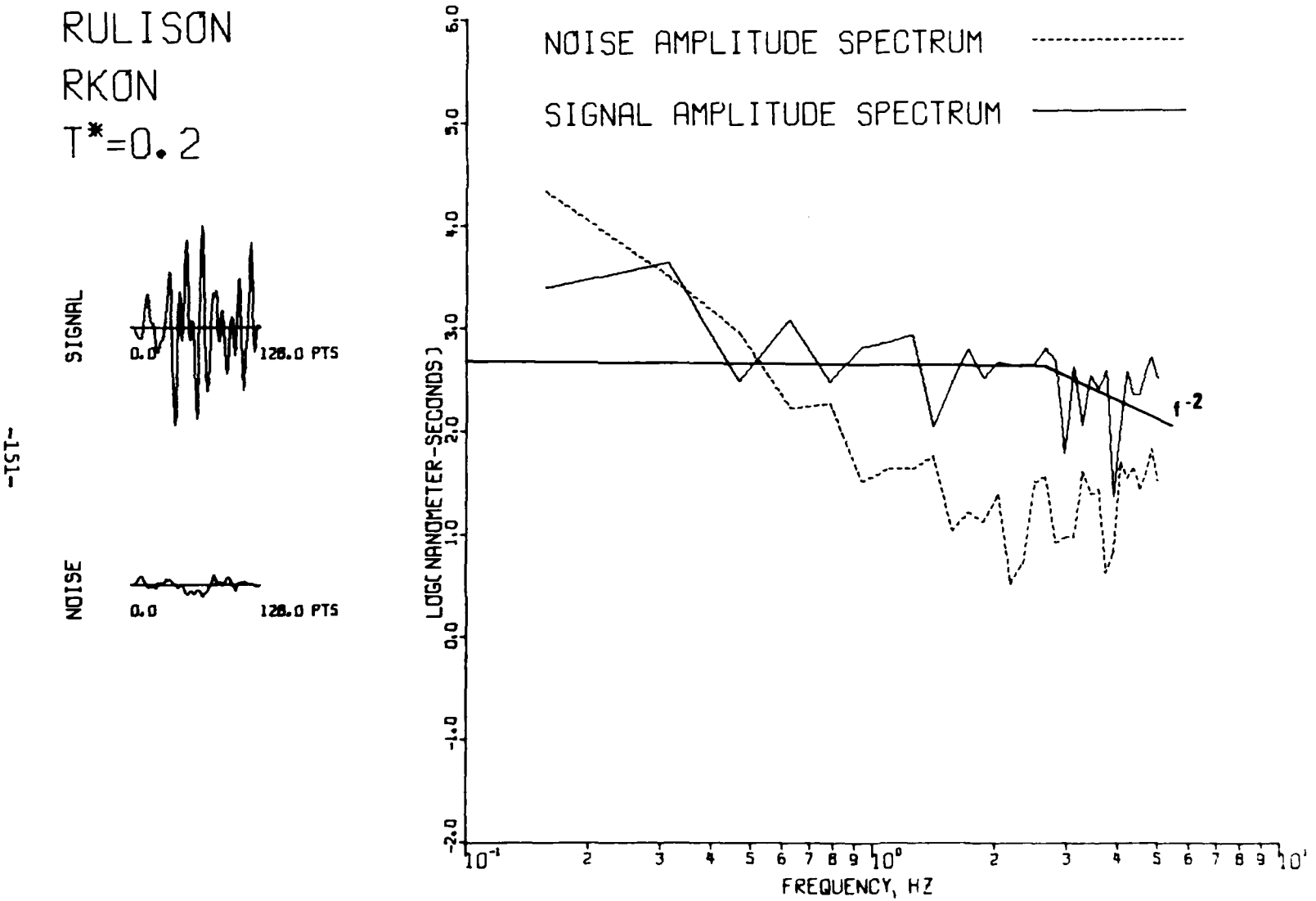

Figure 18 (cont.) Spectra of P waves from short-period recordings at RK-ON of selected Southwestern United States events.

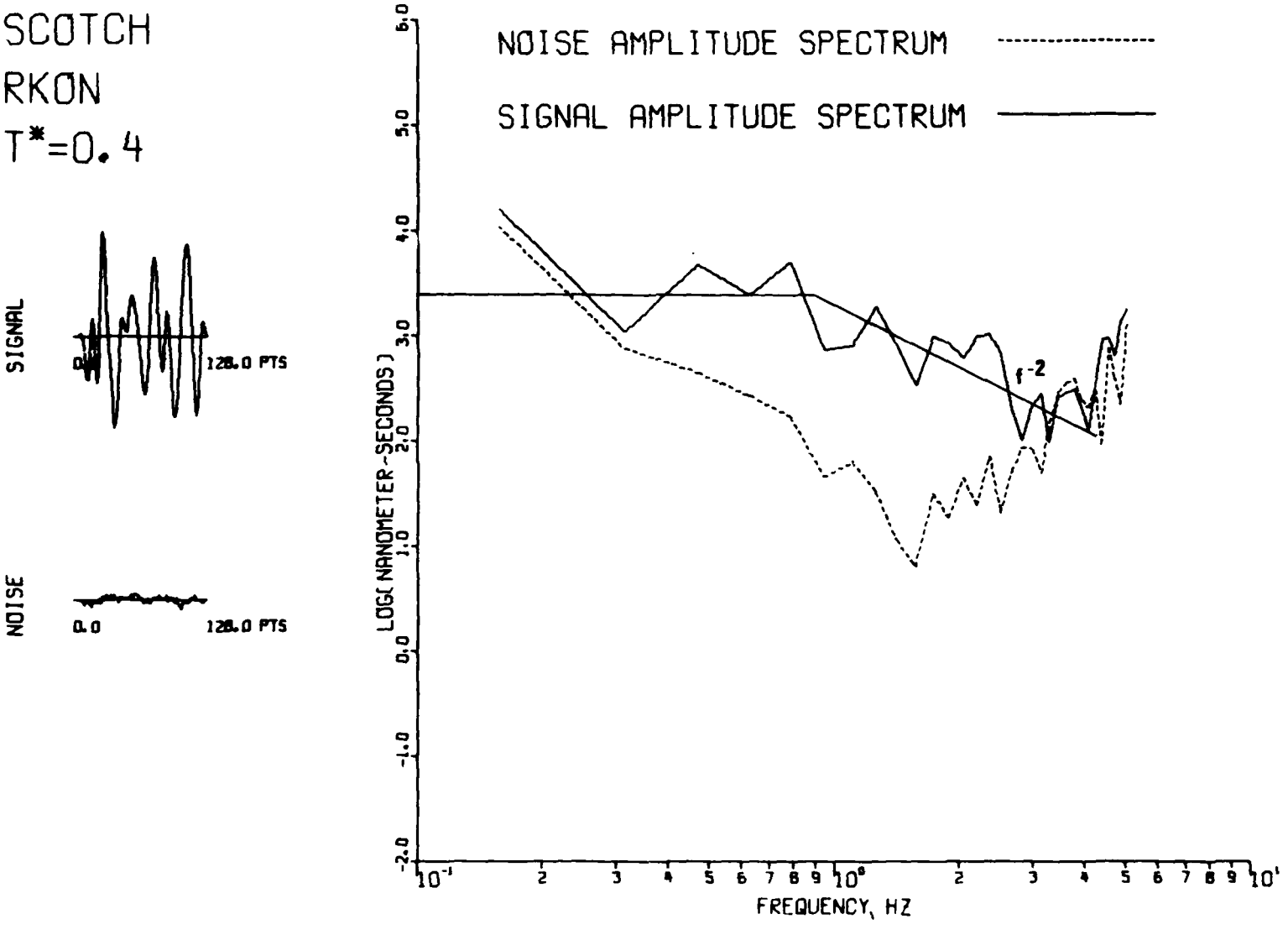

Figure 18 (cont.) Spectra of P waves from short-period recordings at RK-ON of selected Southwestern United States events.

where t* is defined as travel time divided by average Q along the travel path, and $I(\omega)$ is the displacement response of the LRSM seismographs. The chosen values of t* varied according to source region (Der, 1976); they were 0.2 for events east of the Wasatch Front (see Figure 9) and 0.4 for events to the west of it, except for events G and F, which were arbitrarily assigned an intermediate value of 0.3. Spectra of noise samples preceding the first arrival of the P wave were also computed and, to retain the comparative S/N ratio, these spectra were also adjusted by the factor $\exp[\pi ft^*]/I(\omega)$.

The corner frequencies and low-frequency asymptotic levels of these spectra were determined in a visual, but objective, manner. To conform to theorectical predictions of von Seggern and Blandford (1972), high-frequency asymptotic slopes of f^{-2} were uniformly drawn for the explosion spectra. This slope is a good fit in almost all cases, but f^{-3} would be acceptable for some spectra, such as for GREELEY at RK-ON or BENHAM at NP-NT. For the earthquakes, either an f^{-2} or f^{-3} slope was used to fit the high-frequency falloff; either slope can be predicted from various earthquake source theories. Diagrams of the long-period level versus corner frequency are shown in Figure 19, where a fairly clear separation of earthquakes from explosions occurs. Event 1 (DURYEA) fails to separate for RK-ON even though the parameters seem to be well-determined from its spectrum in Figure 18. Event 7 (GASBUGGY) fails to separate at NP-NT, but its spectrum in Figure 17 is close to the noise level and possibly yields an inaccurate spectral shape. Event L (Coyote Mtn. EQ) lies in the earthquake population for both stations. (Previously it was determined that it had rather low S-wave and long-period P-wave excitation, and in the next section we show that its M_S is low.) In the final analysis, the data in Figure 19 could be interpreted to reflect one physical basis for discrimination: that for a given low-frequency level indicative of source size, the characteristic rise time for the earthquake displacement-time function is longer than that for an explosion.

Der, Z. (1976). On the existence, magnitude, and causes of broad regional variations in body-wave amplitudes. SDAC Report No. TR-76-8, Teledyne Geotech, Alexandria, Virginia.

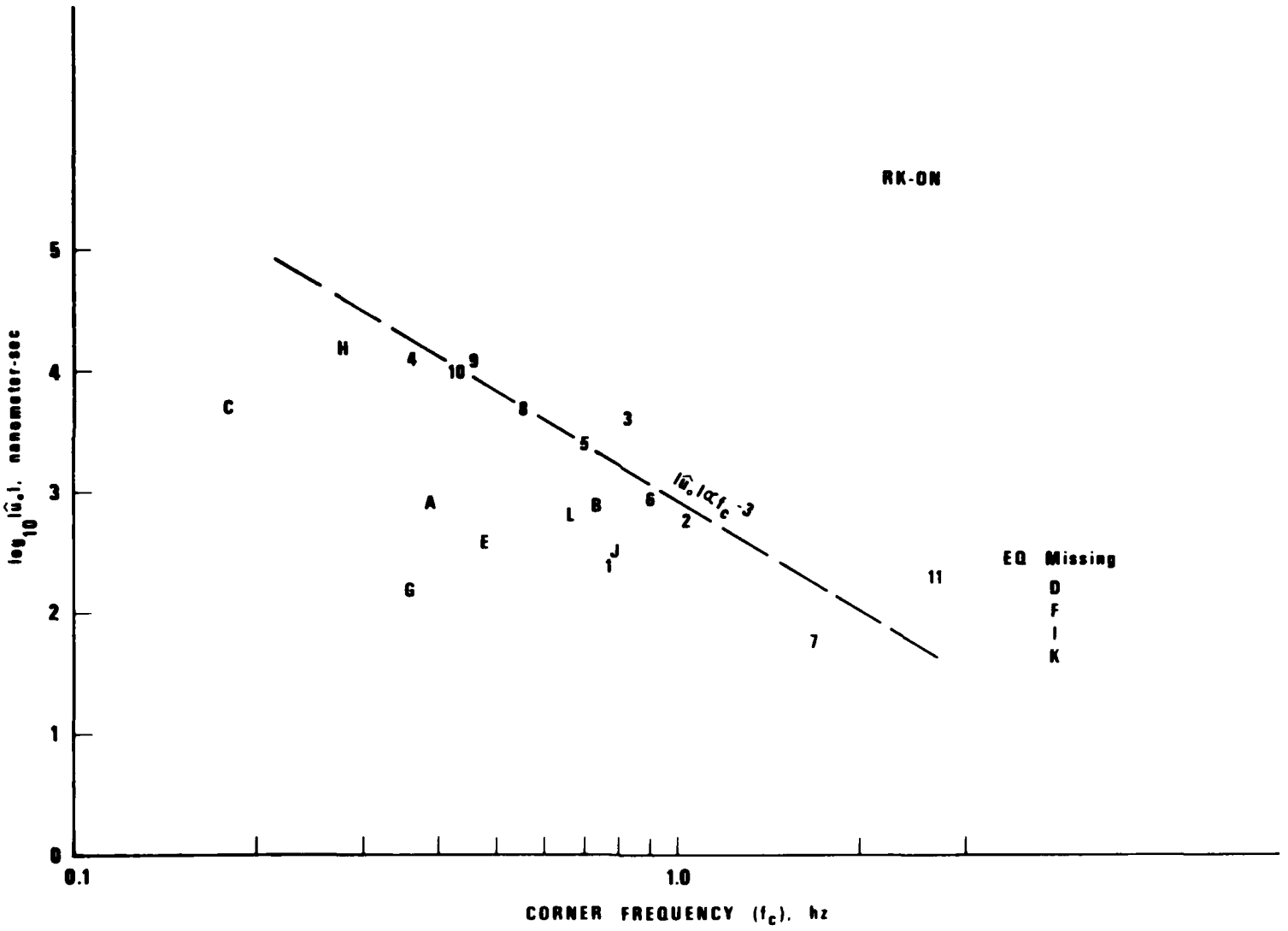

Figure 19 Long-period spectral level $\hat{u}_o$ versus corner frequency for P waves recorded at NP-NT and RK-ON.

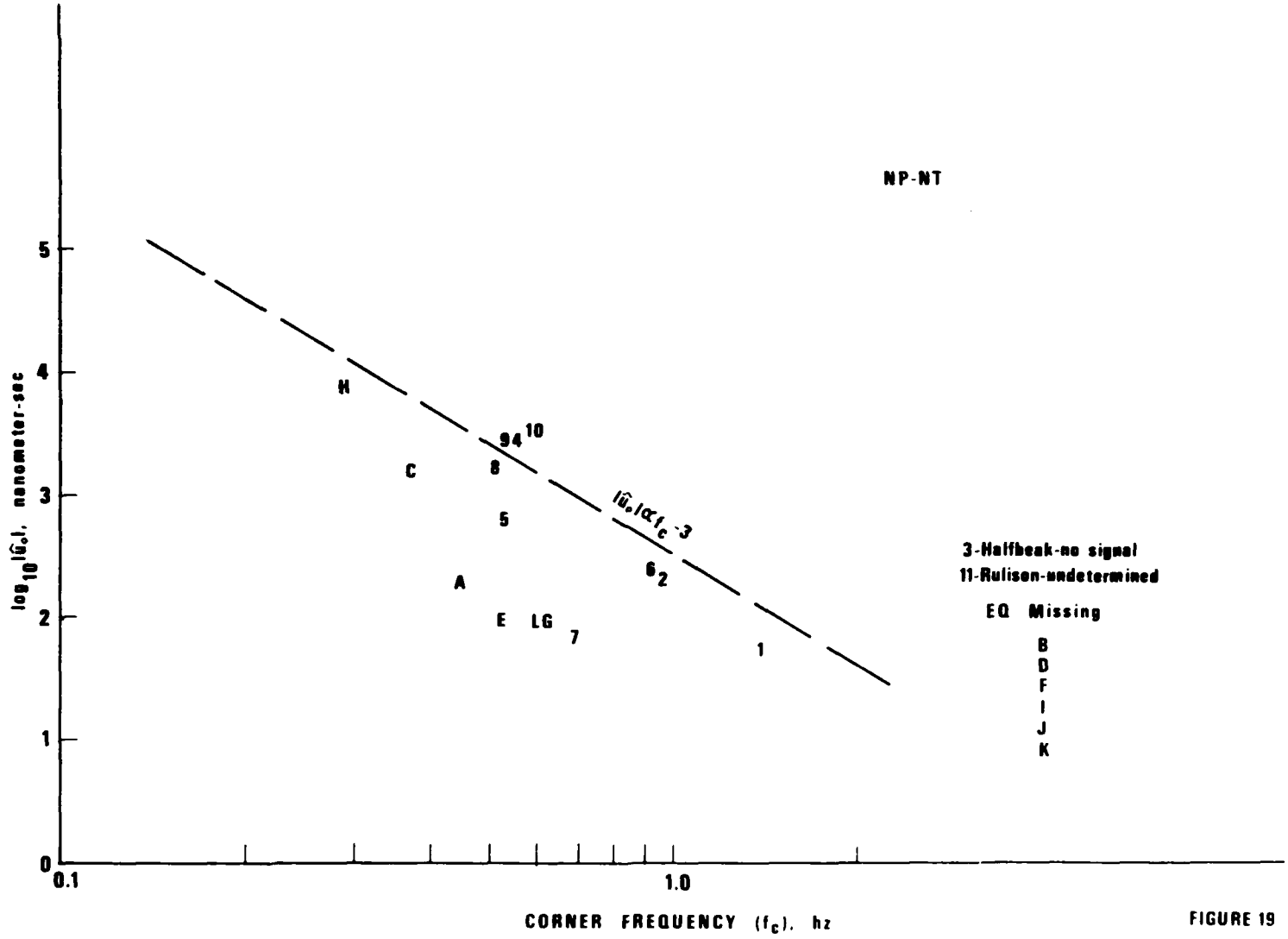

Figure 19 (cont.) Long-period spectral level $\hat{u}_o$ versus corner frequency for P waves recorded at NP-NT and RK-ON.

M_s versus m_b

Figure 20 illustrates the utility of the $M_s - m_b$ plot for distinguishing source type. However, in our group three earthquakes at lower magnitude (E, F, and J) are definitely near the explosion population and a fourth, event L, is somewhat anomalous at a higher magnitude. Because of the importance of the $M_s - m_b$ discriminant, possible causes of such anomalous behavior will be examined in detail.

Thatcher and Hamilton (1973) have previously noted the unusual characteristics of Event L, the Coyote Mountain earthquake. They reported a small source dimension ($\sim$3 km) and a relatively large stress drop ($\sim$80 bars). Source dimensions of the largest explosions in the study sample have been variously estimated to be on the order of 1 km, so that the small difference in source dimension is compatible with the proximity of the Coyote Mountain earthquake to the explosion population in Figure 20. The relatively small source dimension for this earthquake causes the corner frequency in Figure 19 to differ little from the largest explosions in our sample.

Thatcher and Hamilton calculated the seismic moment of the Coyote Mountain earthquake from Rayleigh waves to be roughly 7×10^{24} dyne·cm, while Aki and Tsai (1972) calculated that of event 9, BOXCAR, to be roughly 2×10^{24}. Thus, if moment rather than M_s were plotted in Figure 20, the Coyote Mountain earthquake would separate clearly from the explosions. The observed M_s for this earthquake is low due probably to the focal depth's location near the node of the Rayleigh-wave displacement-depth function in combination with predominantly strike-slip motion. To illustrate this condition, Figure 21 shows the relative Rayleigh-wave excitation of various infinitesimal sources in a layered halfspace chosen to represent the Basin-Range structure. The zeroes for spectral excitation at .05 Hz will change only slightly with various continental structures. Note that if the Coyote Mountain earthquake is a strike-slip fault at depths of 10-13 km (Thatcher and Hamilton, 1973), then the 20-second LR excitation would be roughly five times less than an explosion of equal moment near the surface. In fact, however, the moment ratio is roughly three for the Coyote Mountain earthquake versus BOXCAR, and thus the 20-second excitation should be nearly equal, as the M_s values in Figure 20 indicated.

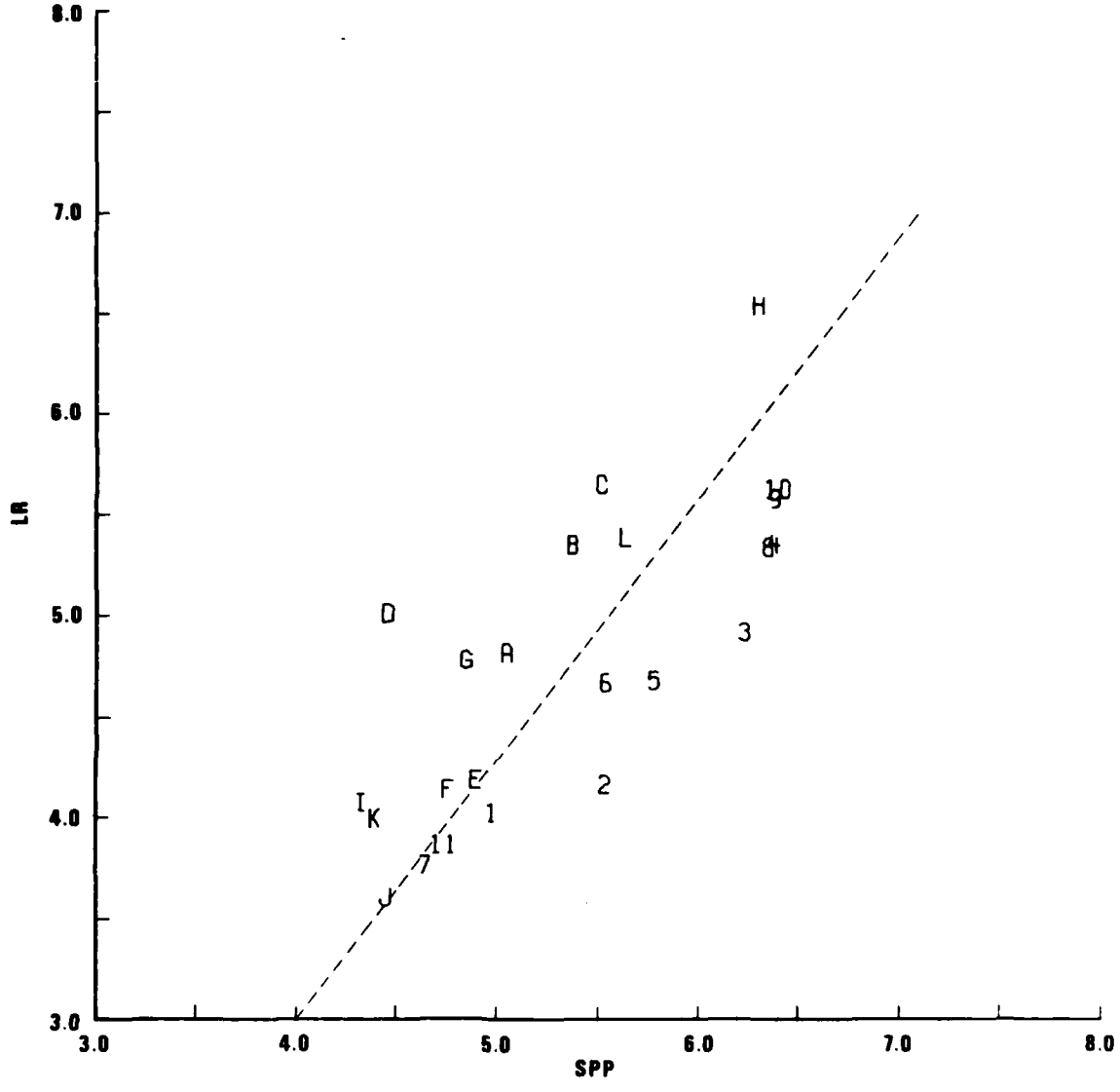

Figure 20 M_s versus m_b for selected Southwestern United States events.

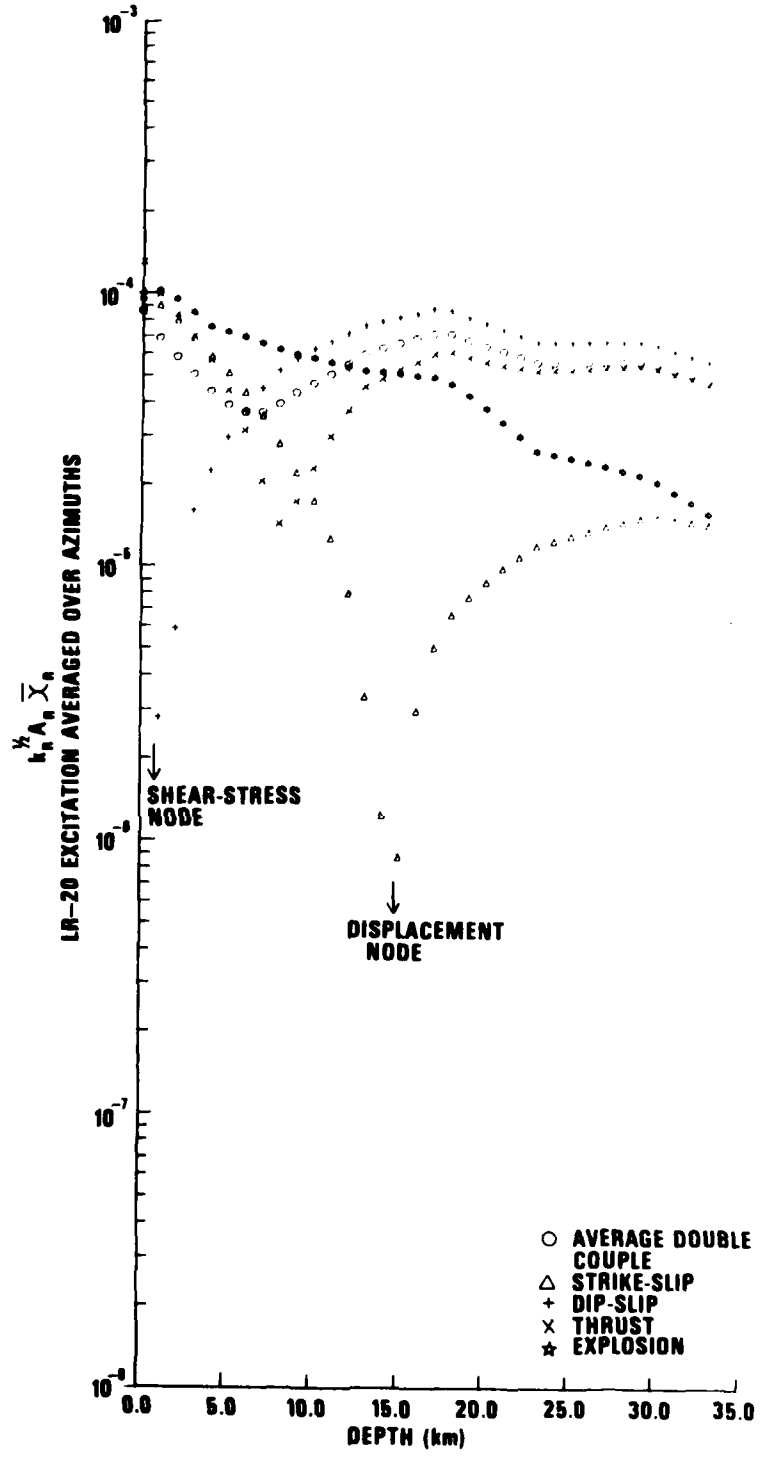

Figure 21 Relative Rayleigh-wave excitation at a period of 20 seconds for various source types in a Basin-Range structure.

Event J, the BENHAM aftershock, is the most important earthquake in our study because of its proximity to the underground explosions at NTS. This fact enables us to ignore path effects in discrimination and to focus on the source contribution itself. Points discussed earlier in the review of discrimination, and the relation of LR and P excitation to focal depth for a Basin-Range structure (shown in Figure 21 and 22), suggest that for small sources discrimination of shallow earthquakes from explosions should be rather difficult on the basis of $M_s - m_b$ alone. Basham et al. (1970), Peppin and McEvilly (1974), and Savino et al. (1971) have all noted that the BENHAM aftershock, reported to have occurred at 3.5 km depth (Hamilton et Healy, 1969), had low M_s. The focal mechanism in Figure 12 is dominated by dip-slip motion on a high-angle fault. Figure 21 shows that excitation tends to zero in dip-slip sources near the surface as the fault plane steepens. Thus, the cause of low M_s for this event has probably been identified but m_b must still be considered. According to Figure 22, the m_b of the BENHAM aftershock should be low relative to an explosion of equal moment in the upper layers at NTS. If a correction for source depth were made to observed m_b, then the BENHAM aftershock would move farther right into the explosion population in Figure 20. Part of the physical basis which holds this earthquake among the explosions is a high corner frequency and small source dimension, a fact represented in the spectral parameters illustrated in Figure 19.

Event E, the Denver earthquake, is interesting because it was probably induced by hydraulic lubrication of pre-existing fractures. It took place in an environment considerably altered from the natural stress state by forced pumping of liquid wastes at the Rocky Mountain Arsenal. This earthquake was at a relatively shallow depth of 5 km, and Major and Simon (1968) determined that it was predominantly strike-slip on a nearly vertical fault. Figure 21

Hamilton, R. M., and L. H. Healy (1969). Aftershocks of the BENHAM nuclear explosions, Bull. Seism. Soc. Am., 59, 2271-2281.

Basham, P. W., D. H. Weichert, and F. M. Anglin (1970). An analysis of the BENHAM aftershock sequence using Canadian recordings. J. Geophys. Res., 75, 1545-1556.

Major, M. W., and R. B. Simon (1968). A seismic study of the Denver (Derby) Earthquakes. Quarterly of the Colorado School of Mines, 63, 9-56.

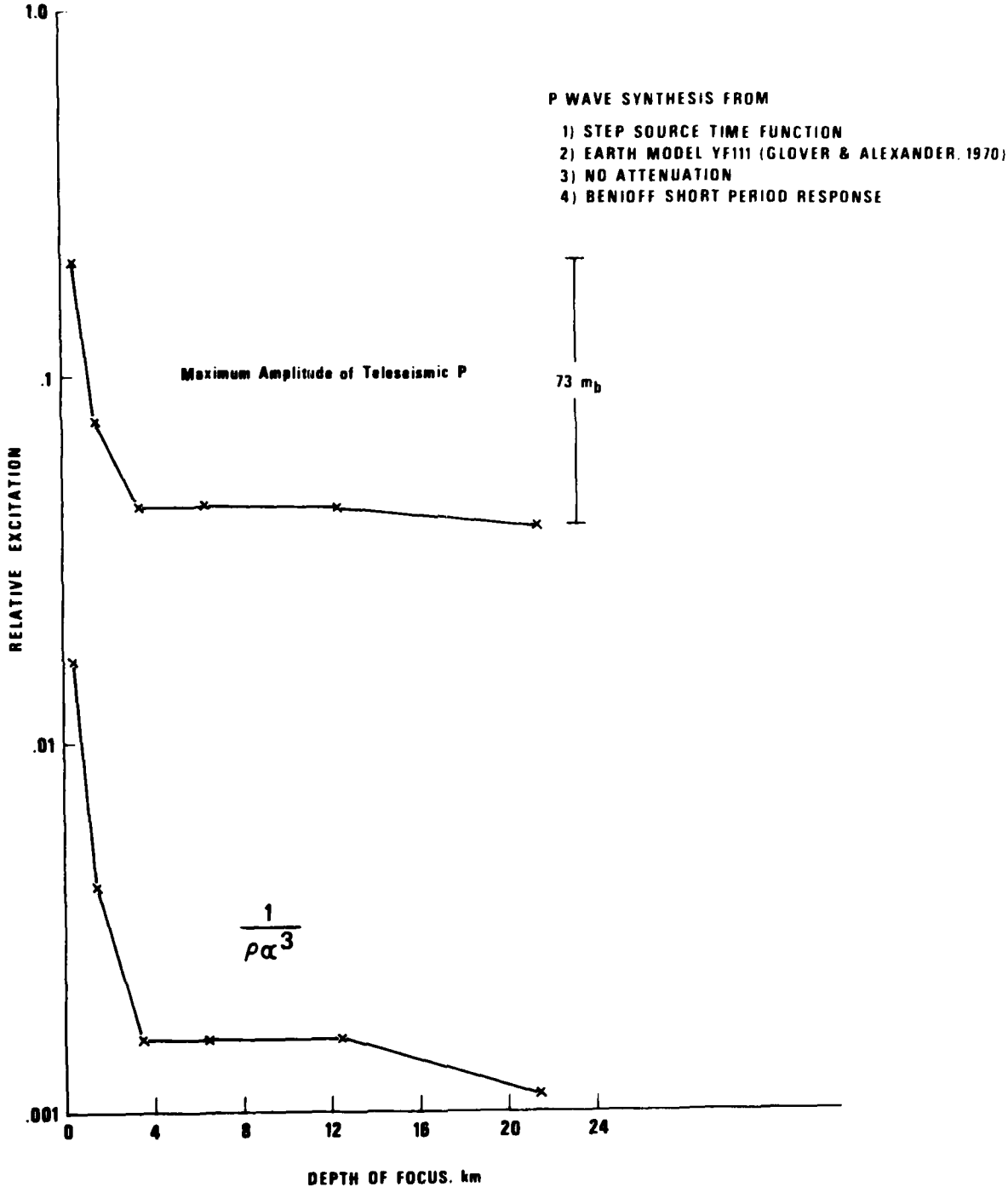

Figure 22 Relative amplitude of teleseismic P waves from dilatational sources of identical moment at various depths in a Basin-Range structure.

indicated that such a mechanism at such depth should not be low on the M_s scale. Therefore, an anomalously high m_b must be the reason why this event falls close to the explosions. Wyss and Molnar (1972) inferred a fault dimension of ∿3 km, which is above average for an earthquake at this magnitude. Indeed, Major and Simon concluded that the fault dimension may be as large as 10 km. The P-wave corner frequency data in Figure 19 supports these interpretations that a source dimension much larger than that of explosions at this magnitude exists. Thus, the anomalous $M_s - m_b$ of this event is not compatible with known source characteristics.

Event F, the Baja California earthquake, is one of many that Thatcher (1972) studied in the surrounding area. The focal depth, taken as 33 km from the NEIS list, is not accurate and it could actually be anywhere within the crust. In the next section, which deals with complexity, event F is shown to have a high P coda, suggesting a focus well below the surface. Also, the mechanism of this event could not be specified and it was arbitrarily assumed to be strike-slip (Table V). Thatcher observed that most of the Baja events in his data set, including this one, had low long-period spectral level for their local magnitude M_L, measured at high frequencies. He concluded that source dimensions for these events are relatively small, nearly like explosions. On this basis the relatively low M_s of this event could be explained. Furthermore, if the depth were such (≈10km) that the LR excitation was considerably diminished for a strike-slip source as shown in Figure 21, then low M_s would certainly be expected. Note also that Figure 21 implies that very shallow dip-slip sources would also have low M_s.

Rayleigh waves from events E, F, and J were well recorded on the network used for this study, with at least five observations each. Therefore, low M_s is probably not due to the stations' all being near a node of the radiation pattern. Examination of LQ/LR radiation patterns reveals that for cases where LR excitation is small, LQ excitation is often large, a fact making the sum of Love-wave and Rayleigh-wave M_s's an improved discriminant. Figure 23 shows the results from this combination for all events. Although now a better separation of the two populations exists, it is not sufficient to insure with high confidence identification of Southwestern United States explosions and earthquakes.

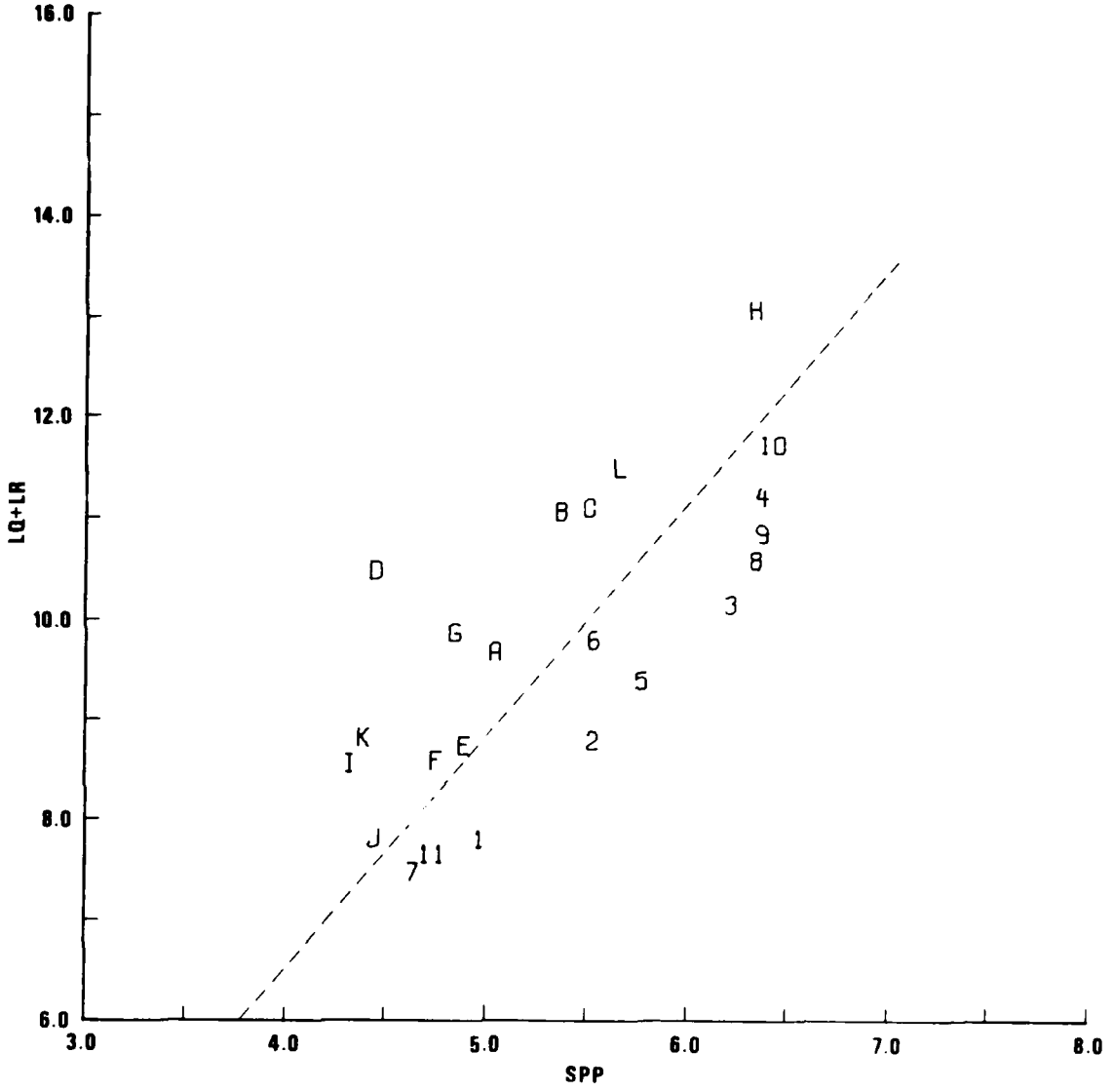

Figure 23 M_S (Rayleigh) + M_S (Love) versus m_b for selected Southwestern United States events.

Complexity

The complexity of the P signal is considered a source discriminant because it stems either from depth of focus, which would entail additional phases from the upgoing wave (the free-surface reflections will be most pronounced) or to prolonged signal generation from complex, spatially extended fault ruptures. The complexity measure has been computed from the vertical short-period tape recordings available for the event set. The complexity computation method was to window the recordings from 30 sec before the P arrival to 35 sec after, square the data samples in these windowed traces, integrate with a 3-sec moving average (moved 1/20 sec for each output point), and take the square root of the integrated trace. The complexity value is formed from this final trace and results from subtracting a noise estimate based on the 10 sec preceding P from the trace comprising 35 sec after it and then ratioing the 5-35 sec portion after P to the 0-5 sec portion after P. Event mean complexities are shown in Figure 24 versus P-wave m_b. The range in complexity values is rather narrow, except for three events, which are the Baja California, Coyote Mountain, and Caliente earthquakes. Each of these three earthquakes clearly shows its complex character in the NP-NT and RK-ON recordings of Figures 17 and 18 respectively. Source depth alone cannot fully explain the large complexity, and a preferable interpretation would be a prolonged rupture duration or extended source time function.

Figure 24 shows that there is some separation between earthquakes and explosions but whether or not it is due to the generally higher explosion m_b's is not clear. The data in Figure 24 must also be questioned because the data points are event means over varying sets of stations. Lambert et al. (1969) and Davies and Julian (1972) showed that complexity is highly dependent on the receiver location and should exhibit scatter among stations equivalent to any proposed source differences. Because of data recovery problems and varying station operation times, the network is different for each event of Figure 24, and significant biases are possible. It may be preferable to consider complexity on a single-station basis as shown for NP-NT and RK-ON in Figure 25. Because of data unavailability or poor quality, several events are missing

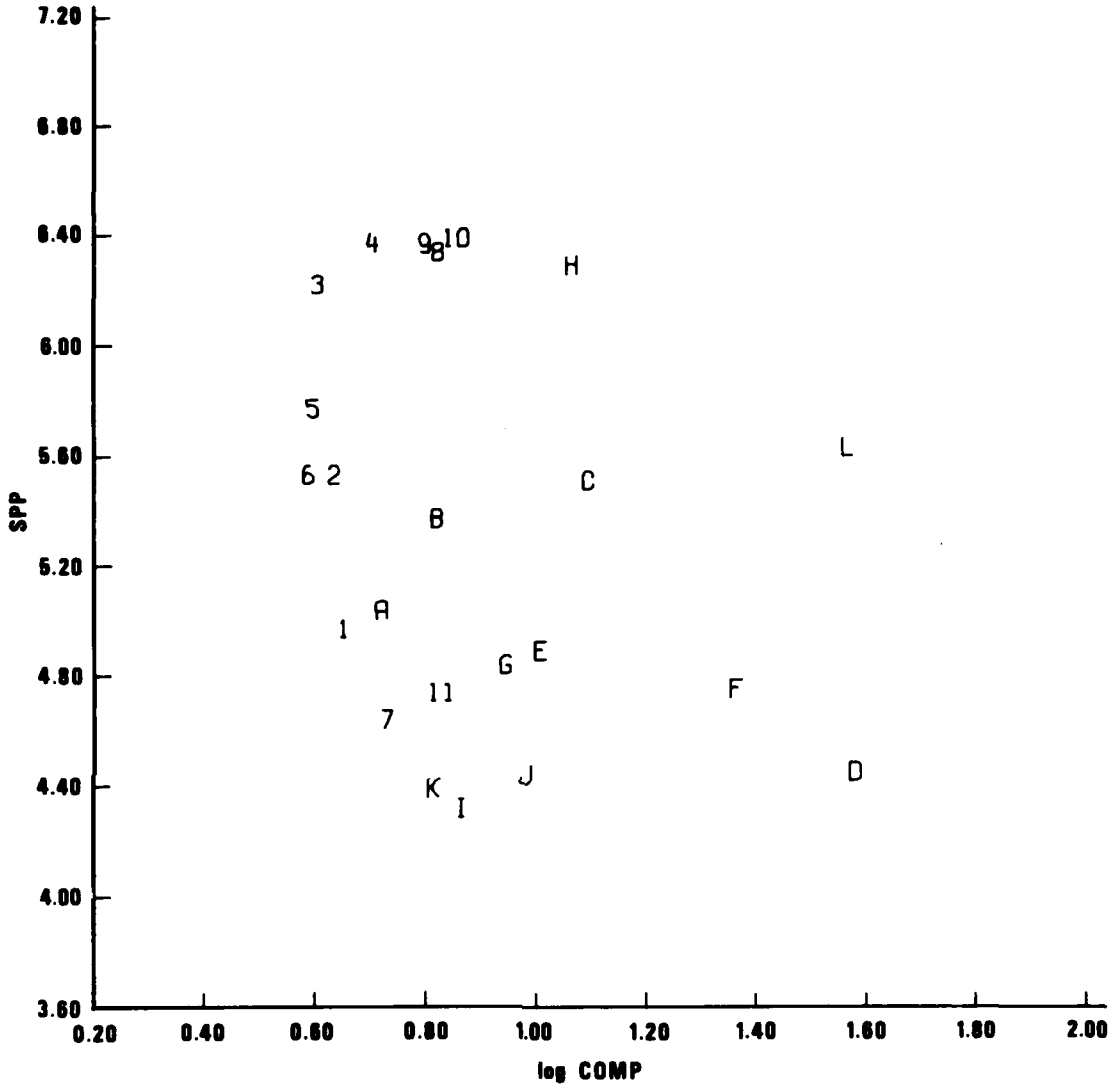

Figure 24 m_b versus complexity for selected Southwestern United States events.

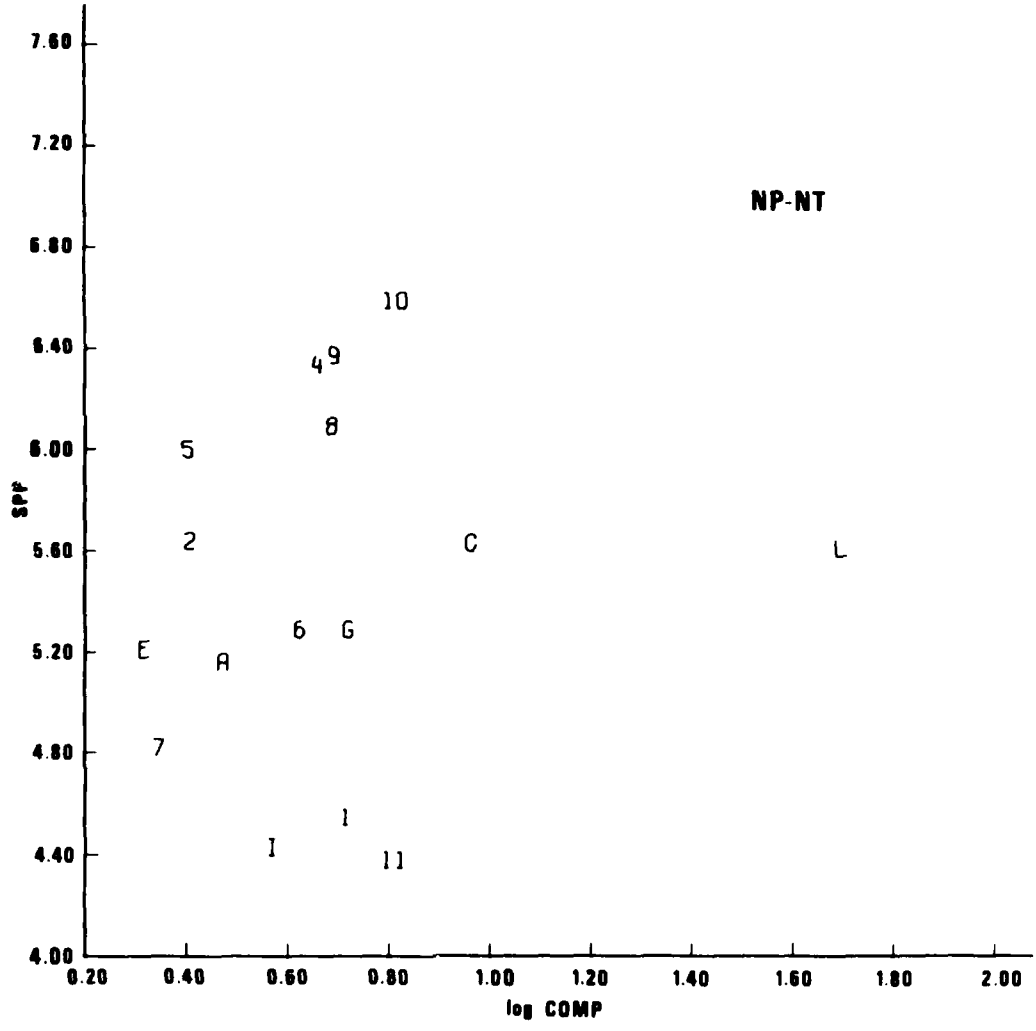

Figure 25 m_b versus complexity of signals recorded at NP-NT and RK-ON from selected Southwestern United States events.

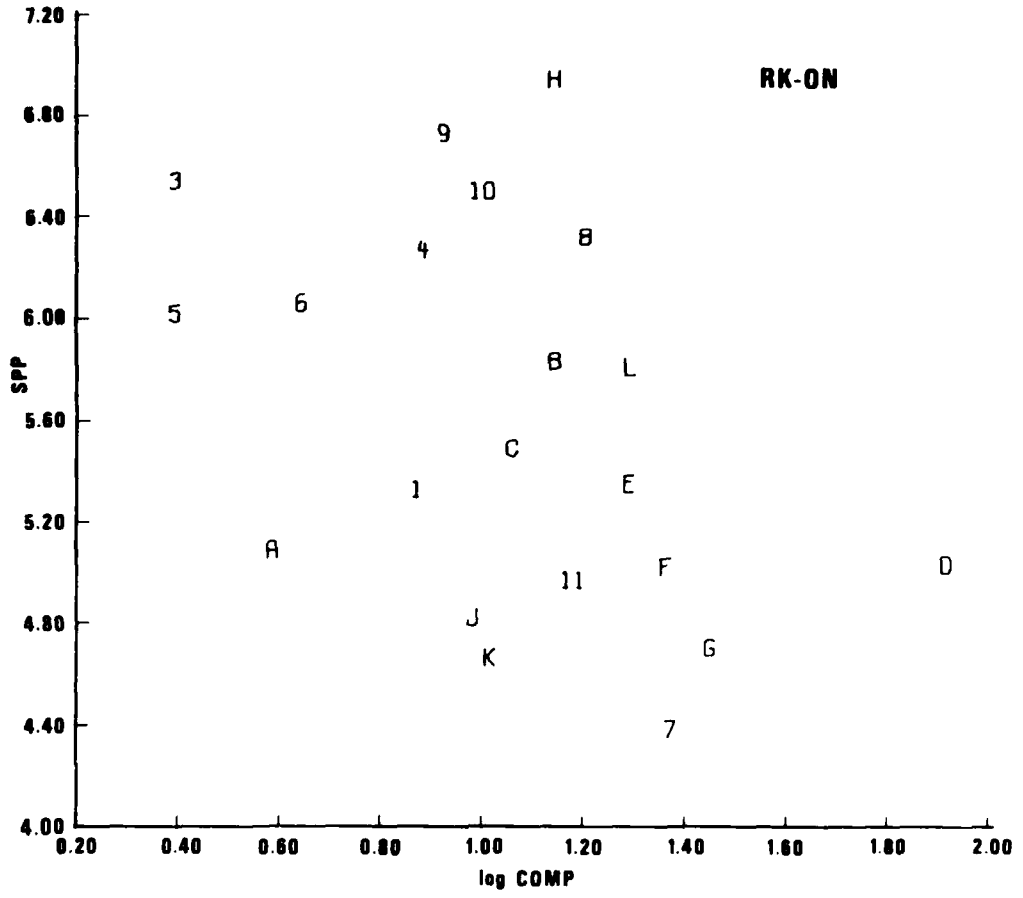

Figure 25 (cont.) m_b versus complexity of signals recorded at NP-NT and RK-ON from selected Southwestern United States events.

from this plot, but there are enough to indicate that complexity fails to separate the two populations. Note, however, that no explosion has a high complexity and that the range of explosion complexities is much less than that of earthquakes. The large complexity values at RK-ON for RULISON and GASBUGGY are not reliable due to the regional recording distance and the low S/N ratios (see Figure 18). Generally, the larger explosions have higher complexity, which may be due to delayed tectonic strain release.

P-Wave Spectral Ratios

A short-period spectral ratio has been computed according to

$$SPSR = \int_{1.56}^{1.87} A(f)df / \int_{0.47}^{0.78} A(f)df$$

where sums over discrete Fourier amplitude coefficients replace the integrals. The spectrum A(f) is computed on the first 6.4 seconds of the P wave. The network average spectral ratios are plotted versus m_b in Figure 26. At a given m_b the explosion spectral ratios are generally higher than earthquake ones. This observation agrees with the ω^{-2} and ω^{-3} high-frequency slope models for explosions and earthquakes, respectively, outlined theoretically in an earlier section of this report and supported by real spectra shown in Figure 17 and 18. The observed decrease of spectral ratio as a function of yield is also in agreement with the theory. Still, no complete separation is made on the basis of spectral ratio for our events. Event H in Figure 26, the Borrego Mountain earthquake, falls farthest into the explosion population, but because of being overdriven on LRSM recordings, its spectral ratio is from one station only (WH2YK) and it could be heavily biased by a station effect. Attenuation corrections were made to A(f) (see P-wave spectrum section above) with the aim of removing variable path effects, thus determining a quantity more representative of the source. The resulting spectral ratios (not shown) separated no more clearly than those shown in Figure 26.

Following Anglin (1971), P-wave spectral ratio vs. complexity was plotted in Figure 27. Anglin obtained a fair separation of his populations, composed of Eurasian events, mostly on the basis of spectral ratio ("third moment of frequency" in his paper) with little classification power stemming from

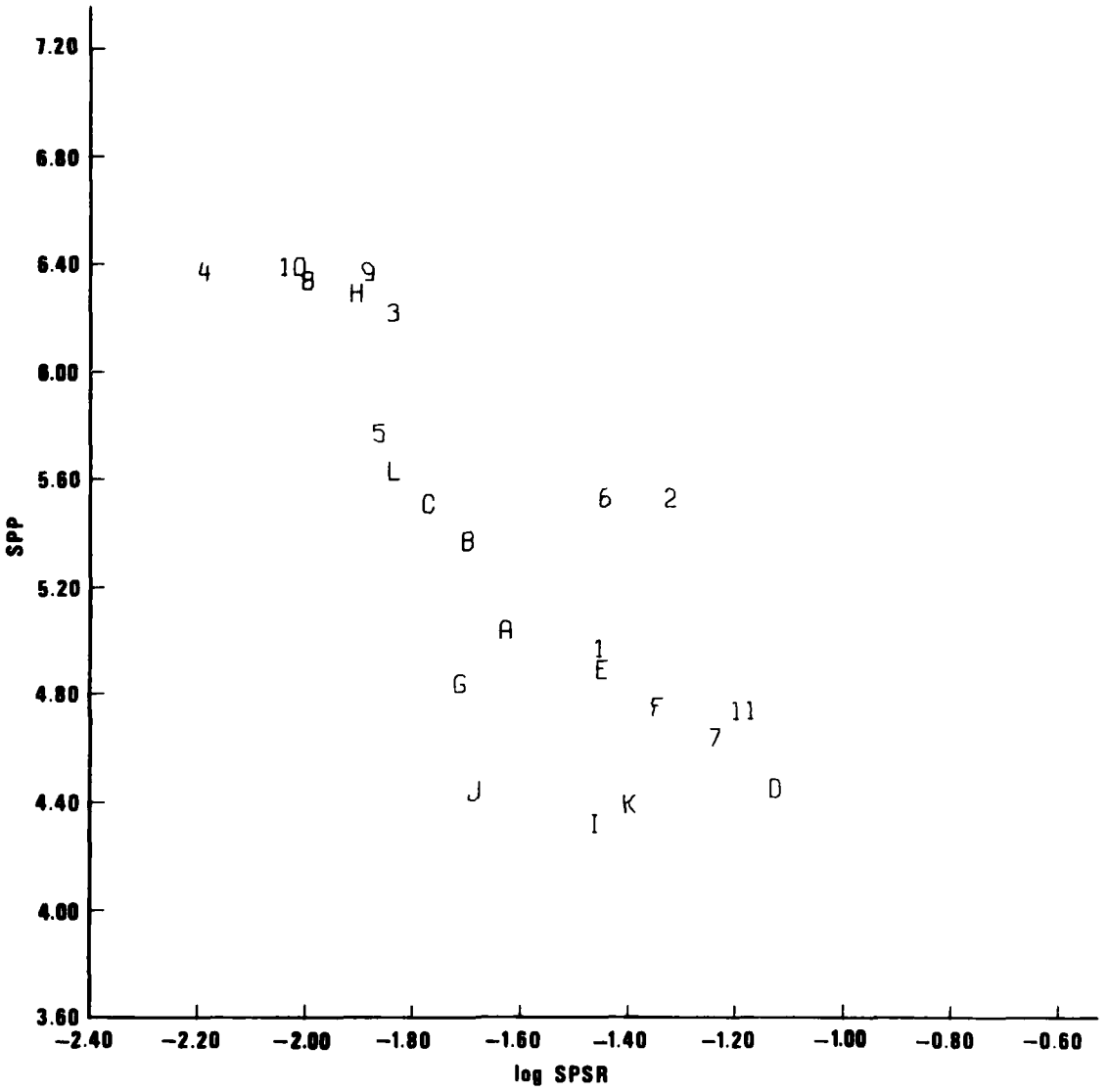

Figure 26 m_b versus P-wave spectral ratio for selected Southwestern United States events.

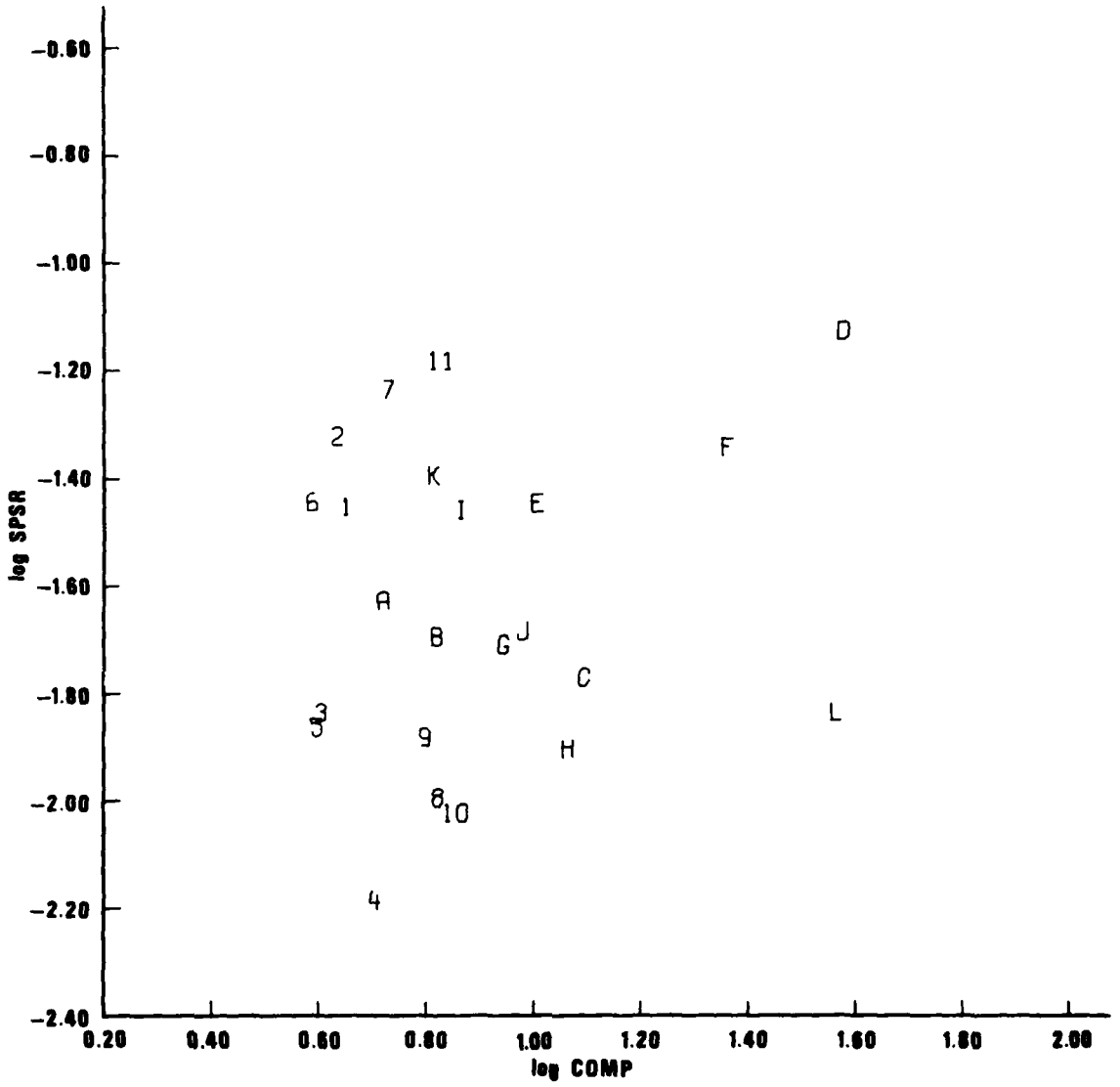

Figure 27 P-wave spectral ratio versus complexity for selected Southwestern United States events.

complexity. No attenuation corrections were made in his work, and the "third moment of frequency" may be measuring a difference in source-path effects either in addition to or rather than an actual difference in source spectra between explosions and earthquakes. For data shown in Figure 27, there appears to be more discrimination power in complexity than in the spectral ratio, which is corrected for attenuation, but there is no satisfactory separation of events in this plot.

Rayleigh-Wave Spectral Ratios

Von Seggern and Lambert (1970) studied the discrimination power of spectral ratio from long-period Rayleigh waves for a sample of global events. Their results show that while explosions generate LR waves with a fairly constant observed spectral ratio, earthquakes can exhibit values in the same range, but also much higher or much lower. The LR spectral ratio is computed for our events according to

$$LPSR = \int_{.046}^{.071} A(f)df / \int_{.028}^{.045} A(f)df$$

where sums of discrete transform points replace the integrals. The time window was dependent on path length, from the expected arrival time of T = 50+ sec to that of T = 10 sec. This definition is close to von Seggern and Lambert's, and the resulting network average values are plotted versus M_s in Figure 28. This plot shows no separation between earthquakes and explosions and, in fact, shows the same general picture as in von Seggern and Lambert, with explosions confined to median values and earthquakes ranging on both sides. These results agree with theoretical predictions of Rayleigh-wave excitation from double-couple sources which generate a variety of Rayleigh-wave spectral shapes, dependent on source depth, fault orientation, and the azimuth of the receiver.

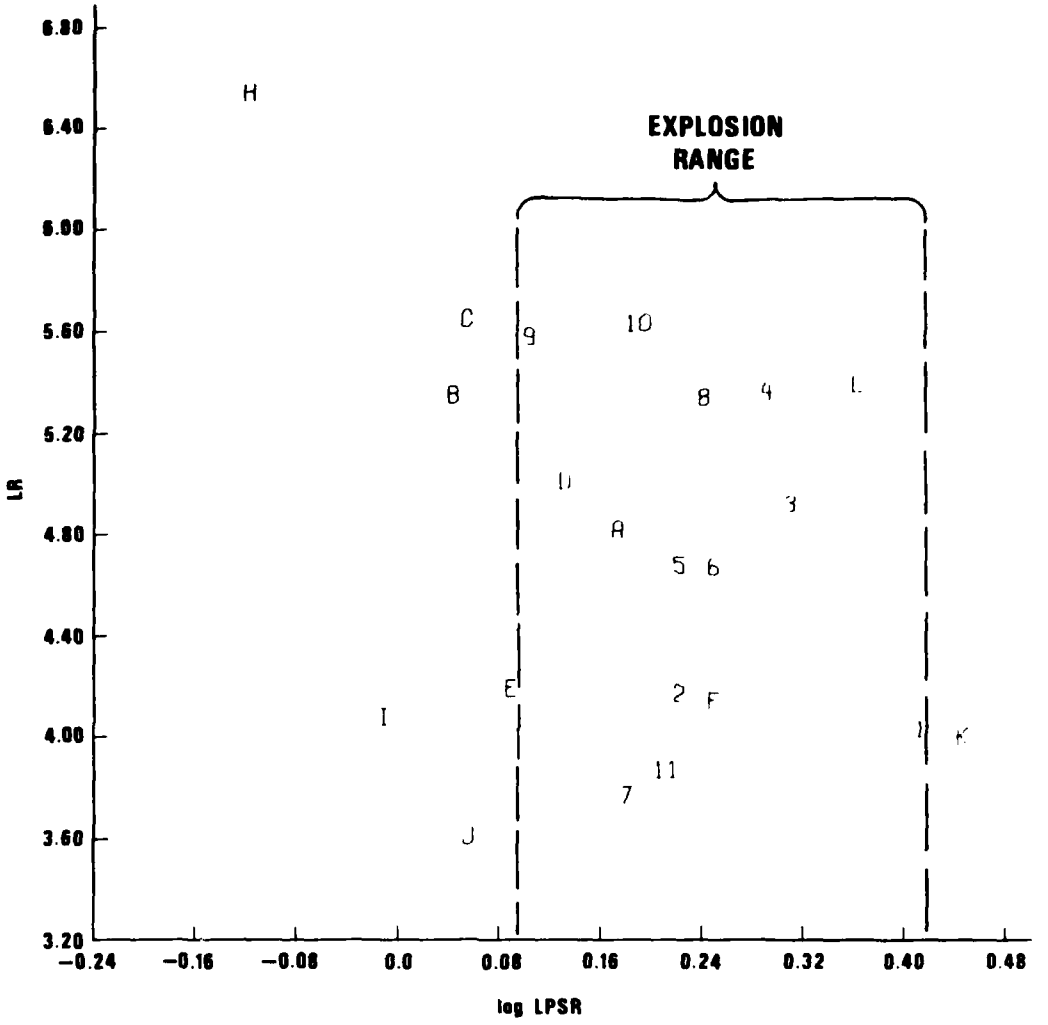

Figure 28 M_S versus Rayleigh-wave spectral ratio for selected Southwestern United States events.

MULTIPLE DISCRIMINATION

In the previous section, the capability of various seismic measurements to classify the explosions and earthquakes in our event set was examined. These discriminants were largely discussed independently and more qualitatively than quantitatively. In this section, by applying statistical techniques, the power of the various discrimination measures will be examined quantitatively in a unified approach. A multiple discrimination technique is used to identify, rank, and fully utilize meaningful discrimination parameters. A list of the parameters used in this experiment is given in Table VI; all of these parameters were displayed in one or more figures in the previous section, and their values for the individual stations can be found in Table IV.

Multiple discrimination is used because significant classification information is contained in almost all parts of the seismogram and in both the frequency and time domains. Although the main effort is directed toward network discrimination, the discriminating capability of single sites--as opposed to the entire network--will be examined. In this experiment our data set is treated as a training set, where correct classification is known a priori. Booker and Mitronovas (1964) did some pioneering work on seismic multiple discrimination based upon finding discriminant functions for known groups, but investigators have performed little subsequent work using more than a few parameters.

Description of Discrimination Experiments to be Performed

The data base shown in Table IV was used in three separate experiments aimed at evaluating the effectiveness of several possible discriminants. In the first experiment, data from all network stations were combined using Ringdal's (1976) method to give estimates of the event magnitudes. These magnitude estimates were used to calculate linear discriminant functions for selected subsets of the ten variables defined as discriminants here. In the second experiment, discriminant functions were calculated as before, but using data from one station in place of the estimates determined by the whole network. In the third experiment single-station discriminant functions were

---

Ringdal, F., (1976). Maximum-likelihood estimation of seismic magnitude, Bull. Seism. Soc. Am., 66, 789-802.

TABLE VI

Network Discrimination Parameters for the Multiple Discrimination Experiment

Event	SPP	SPS	LPP	LPS	LQ	LR	log SPSR	log LPSR	log comp	1st mtn
1	4.97	*4.97	*4.96	*4.10	3.78	4.03	-1.453	0.412	0.652	0.
2	5.53	4.23	3.55	4.06	4.62	4.17	-1.322	0.221	0.635	0.
3	6.22	*5.18	3.68	4.89	5.23	4.92	-1.838	0.308	0.604	0.
4	6.37	5.11	4.07	5.17	5.86	5.36	-2.187	0.290	0.705	0.
5	5.77	4.26	3.39	4.42	4.71	4.68	-1.863	0.221	0.596	0.
6	5.53	*4.73	3.61	4.76	5.13	4.67	-1.444	0.248	0.588	0.
7	4.64	*5.07	*4.28	3.35	3.71	3.77	-1.237	0.180	0.730	0.
8	6.34	5.14	4.37	5.08	5.25	5.34	-1.995	0.240	0.822	0.
9	6.37	5.20	4.26	5.40	5.27	5.58	-1.884	0.103	0.799	0.
10	6.43	4.79	4.72	5.61	6.11	5.63	-2.023	0.189	0.858	0.
11	4.74	4.68	*4.18	4.67	3.79	3.87	-1.183	0.212	0.830	0.
A	5.04	*4.51	4.13	4.75	4.86	4.82	-1.628	0.172	0.720	1.
B	5.37	*4.56	4.26	5.32	5.72	5.35	-1.697	0.043	0.821	1.
C	5.51	5.05	5.02	5.85	5.46	5.65	-1.771	0.053	1.094	1.
D	4.45	4.20	4.03	5.09	5.47	5.01	-1.125	0.131	0.578	1.
E	4.89	*4.89	3.94	4.44	4.55	4.19	-1.447	0.088	1.008	1.
F	4.75	*4.67	*4.31	4.04	4.45	4.14	†-1.344	0.248	1.362	0.
G	4.84	4.28	4.32	5.11	5.09	4.78	-1.711	0.517	0.945	1.
H	6.33	6.14	5.63	6.08	6.54	6.54	-1.095	†-0.118	1.065	1.
I	4.32	*4.32	3.58	4.39	4.48	4.08	-1.460	-0.012	0.866	1.
J	4.44	*4.65	*4.29	4.05	4.20	3.61	-1.686	0.055	0.981	0.
K	4.39	4.18	*4.41	4.08	4.82	4.00	-1.396	0.445	0.815	1.
L	5.63	*4.36	4.52	5.34	6.11	5.39	-1.836	†0.361	1.565	1.

* no detection; magnitude is average of noise levels

† spectral ratio at all detecting stations was affected by noise

SPP: Short-period P m_b

SPS: Short-period S m_b

LPP: Long-period P m_b

LPS: Long-period S m_b

LQ: Love-wave M_s

LR: Rayleigh-wave M_s

log SPSR: log short-period P-wave spectral ratio

log LPSR: log long-period LR-wave spectral ratio

log comp: log complexity

1st mtn: polarity of first motion

averaged to perform discrimination based upon the network. Now, before discussing the experimental results, Ringdal's method is presented.

Estimation of Event Magnitudes

The magnitude m of a seismic event is conventionally estimated by computing the arithmetic mean $\bar{m}_i$ of the magnitudes that each detecting station measured. During this process certain information is lost, namely that the signal was less than the noise level at non-detecting stations. Ignoring those stations where the signal was below the threshold of detection eliminates what would generally be, for a perfectly detecting (noise-free) network, the smaller values of m_i. The arithmetic mean would thus tend to be biased so that $\bar{m}_i > m$. The maximum-likelihood estimator that Ringdal (1976) proposed is a method of incorporating into the computation the constraint that, for non-detecting stations, the station magnitude is less than some specified noise level.

For an event of magnitude m, assume that the set of magnitudes m_i, which would be measured by seismic stations of a noise-free network, comprises a Gaussian distribution having mean μ and standard deviation σ. When the number of stations in the network becomes infinite, the estimated $\hat{\mu} = m$. If all stations detect the signal, then the best estimate of μ is the arithmetical mean $\bar{m}_i$. If, however, the instantaneous noise level α_i at some stations is too high for the signal to be detected (i.e., $\alpha_i > m_i$, assuming S/N = 1 is sufficient for detection), then Ringdal's method permits calculating the most likely Gaussian distribution such that the detecting stations measure magnitudes m_i and such that $m_i < \alpha_i$ at the non-detecting stations. The mean value of this most likely distribution is the maximum-likelihood estimate of m, μ_{lik}. For the purpose of calculating μ_{lik}, the instantaneous noise levels have been measured on the LRSM recordings at the expected arrival times of short-period P and S and long-period P, S, LQ, and LR when these signals could not be detected on the seismograms.

Consider a family of Gaussian distributions where each is characterized by the parameters (μ_j, σ_j). For any given member of this family the probability $P_1(m_i)dm_i$ that a detecting station would measure the magnitude to be in the range dm_i about m_i is

$$P_1(m_i;\mu_j,\sigma_j)dm_i = \frac{1}{\sqrt{2\pi}\,\sigma_j}\exp\left[-\tfrac{1}{2}\left(\frac{m_i - \mu_j}{\sigma_j}\right)^2\right]dm_i \qquad (1)$$

For a station with a sharp detection threshold α_i, the probability $P_2(m_i < \alpha_i)$ that the signal would be less than α_i and therefore undetected is

$$P_2(m_i < \alpha_i;\ \mu_j,\ \sigma_j) = \frac{1}{\sqrt{2\pi}\,\sigma_j} \int_{-\infty}^{\alpha_i} \exp\left[-\tfrac{1}{2}\left(\frac{m_i-\mu_j}{b_j}\right)^2\right] dm_i \qquad (2)$$

Ringdal's maximum-likelihood estimate of m is thus the value of μ_j for which the function

$$L\ (\mu_j,\sigma_j;m_1,m_2,\ldots,\alpha_1,\alpha_2,\ldots)\ dm_1\ dm_2\ldots = \prod P_1(m_i;\mu_j,\sigma_j)\ dm_i \cdot \prod P_2(m_i < \alpha_i;\ \mu_j,\ \sigma_j) \qquad (3)$$

detecting stations non-detecting stations

attains the greatest value. One may calculate μ_{lik} simply by evaluating the likelihood function L for all values of μ_j and σ_j incremented over a suitable range and choosing the pair (μ_j,σ_j) for which L attains a maximum.

In several instances (short-period S for events 1, 3, 6, 7, E, F, I, J, and L; long-period P for events 1, 7, 11, F, J, and K; long-period S for event 1) neither $\bar{m}_i$ nor μ_{lik} could be calculated since all stations in the network measured only noise. For these cases the arithmetic mean of the noise level $\bar{\alpha}_i$ was computed; this value was used as an approximation to m, although in most cases this mean is expected to be higher than the true m. For many events LQ could not be measured at most stations because the long-period horizontal instruments were overdriven. In four instances (events 10, B, C, and H), supplemental information was used to infer the magnitude of LQ from the measured value of LR (Table IV). Arithmetic means were calculated for the logarithms of the short-period and long-period spectral ratios and for the logarithms of the complexities. For calculating the network means of these last three variables, all values judged unreliable because of interfering noise were deleted because in these cases the Ringdal estimate μ_{lik} is meaningless. Finally, each event was assigned a tenth variable, whose value was unity if any network station detected a clear dilational first motion and which was otherwise zero.

Discriminant Fuctions

The data for the first discrimination experiment consist of the twenty-three vectors $\vec{X} = (X_1, X_2, \ldots, X_p)$ (listed in Table VI) where X_i is one of

the ten variables whose network mean values have been calculated using procedures described above. Because it is known a priori which of these data vectors represent explosions and which represent earthquakes, this set of vectors can be used as a "training set" in order to provide discriminant functions for classifying future data vectors. However, because these discriminant functions could not be correctly applied to events outside the Western United States, this study will not focus on the numerical coefficients of these functions but rather on the subset of variables $X_1, X_2, \ldots, X_p$ which gives the "best" discriminant. Thus, for each discriminant tested, the a posteriori probabilities of correctly identifing each event of the training set are examined by applying the calculated discriminant function to it. In this manner one finds which subsets of variables yield the best separation between earthquakes and explosions in the training set.

This report assumes that the eleven explosion and twelve earthquake data vectors are members of two p-dimensional multinormal populations with mean vectors $\vec{\mu}_1$ and $\vec{\mu}_2$ and with a common covariance matrix $\underset{\sim}{\Sigma}$. Assumption of equal covariance for the two populations of seismic data leads only to small errors (Shumway and Blandford, 1970). The probability of classifying a data vector $\vec{X}$ as an explosion, $P_1(\vec{X})$, and the probability of classifying it as an earthquake, $P_2(\vec{X})$, are assumed a priori to be 0.5, although for this data set they are actually 11/23 and 12/23, respectively. Under these assumptions the classification probabilities are given by (Anderson, 1958)

$$P_j(\vec{X}) = \frac{1}{(2\pi)^{p/2}|\underset{\sim}{\Sigma}|^{1/2}} \exp\left[-\tfrac{1}{2}(\vec{X} - \vec{\mu}_j)' \underset{\sim}{\Sigma}^{-1} (\vec{X} - \vec{\mu}_j)\right] \quad j = 1,2 \qquad (4)$$

Here the "-1" exponent implies the inverse matrix, and the prime implies the transpose matrix.

Taking the ratio,

$$\frac{P_1(\vec{X})}{P_2(\vec{X})} = \exp\{\vec{X} \cdot \vec{D} + C\}, \qquad (5)$$

Shumway, R. H., and R. R. Blandford (1970). A simulation of seismic discriminant analysis. SDL Report No. 261, Teledyne Geotech, Alexandria, Virginia.

Anderson, T. W. (1958). An Introduction to Multivariate Statistical Analysis. New York, NY., John Wiley and Sons.

where

$$\vec{D} = \underset{\sim}{\Sigma}^{-1} (\vec{\mu}_1 - \vec{\mu}_2) \tag{6}$$

and

$$C = -\tfrac{1}{2} (\vec{\mu}_1 + \vec{\mu}_2)' \underset{\sim}{\Sigma}^{-1} (\vec{\mu}_1 - \vec{\mu}_2). \tag{7}$$

The criterion upon which discrimination is based is thus

$$P_1(\vec{x}) > P_2(\vec{x}) \text{ iff } \vec{X} \cdot \vec{D} + C > 0. \tag{8}$$

We shall refer to $\vec{X} \cdot \vec{D} + C$, sometimes known as the group separation function, simply as the discriminant function. We may rewrite the equation (5) as

$$\frac{P_1(\vec{X})}{P_2(\vec{X})} = \exp \{\vec{X} \cdot \vec{D}_1 + C_1 - \vec{X} \cdot \vec{D}_2 - C_2\}, \tag{9}$$

where

$$\vec{D}_j = \underset{\sim}{\Sigma}^{-1} \vec{\mu}_j \quad j = 1,2 \tag{10}$$

and

$$C_j = -\tfrac{1}{2} \vec{\mu}_j' \underset{\sim}{\Sigma}^{-1} \vec{\mu}_j \quad j = 1,2 \tag{11}$$

We shall refer to $\vec{X} \cdot \vec{D}_1 + C_1$ and $\vec{X} \cdot \vec{D}_2 + C_2$ as group classification functions, although they also are sometimes called discriminant functions, a name we reserve for $\vec{X} \cdot \vec{D} + C$. Adding unity to both sides of equation (9), we have

$$\frac{P_1(\vec{X})}{P_2(\vec{X})} + \frac{P_2(\vec{X})}{P_2(\vec{X})} = \frac{\exp(\vec{X} \cdot \vec{D}_1 + C_1)}{\exp(\vec{X} \cdot \vec{D}_2 + C_2)} + \frac{\exp(\vec{X} \cdot \vec{D}_2 + C_2)}{\exp(\vec{X} \cdot \vec{D}_2 + C_2)}$$

Taking reciprocals, we find for the <u>a posteriori</u> probability of classifying $\vec{X}$ as an earthquake

$$P_2(\vec{X}) = \frac{\exp(\vec{X} \cdot \vec{D}_2 + C_2)}{\exp(\vec{X} \cdot \vec{D}_1 + C_1) + \exp(\vec{X} \cdot \vec{D}_2 + C_2)} \tag{12}$$

or as an explosion

$$P_1(\vec{X}) = \frac{\exp(\vec{X} \cdot \vec{D}_1 + C_1)}{\exp(\vec{X} \cdot \vec{D}_1 + C_1) + \exp(\vec{X} \cdot \vec{D}_2 + C_2)}. \tag{13}$$

In actual practice the population parameters $\vec{\mu}_1$, $\vec{\mu}_2$, and $\underset{\sim}{\Sigma}$ are unknown and must be estimated by the parameters $\vec{\bar{X}}_1$, $\vec{\bar{X}}_2$ and $\underset{\sim}{S}$, which are calculated from

the sample of twenty-three events. For every set of variables X_i selected as a possible discriminant, we thus find the linear discriminant function and group classification functions (evaluated for arbitrary data vector $\vec{X}$) to be

$$\vec{D} \cdot \vec{X} + C = \vec{X}' \underset{\sim}{S}^{-1} (\vec{\bar{X}}_1 - \vec{\bar{X}}_2) - \tfrac{1}{2}(\vec{\bar{X}}_1 + \vec{\bar{X}}_2)' \underset{\sim}{S}^{-1} (\vec{\bar{X}}_1 - \vec{\bar{X}}_2) \tag{14}$$

and

$$\vec{D}_j \cdot \vec{X} + C_j = \vec{X}' \underset{\sim}{S}^{-1} \vec{\bar{X}}_j - \tfrac{1}{2} \vec{\bar{X}}_j' \underset{\sim}{S}^{-1} \vec{\bar{X}}_j \qquad j = 1,2 \tag{15}$$

respectively. A measure of the effectiveness of the discriminant function is then given by the <u>a posteriori</u> probability for the k-th event

$$P_j(\vec{X}_k) = \frac{\exp(\vec{X}_k \cdot \vec{D}_j + C_j)}{\exp(\vec{X}_k \cdot \vec{D}_1 + C_1) + \exp(\vec{X}_k \cdot \vec{D}_2 + C_2)} \qquad j = 1,2;\ k = 1,23 \tag{16}$$

Another measure of the separation of the two groups is provided by Wilks' Λ-criterion, defined as

$$\Lambda(\vec{X}) = \frac{\det \underset{\sim}{W}}{\det \underset{\sim}{T}} \tag{17}$$

where $\underset{\sim}{W}$ is the within -group cross-product matrix and $\underset{\sim}{T}$ is the total cross-product matrix. Letting X_{jki} denote the i-th component of the k-th vector of the j-th group, these matrices are given by

$$W_{i\ell} = \sum_{j=1}^{2} \sum_{k=1}^{n_j} (X_{jki} - \bar{X}_{j\cdot i})(X_{jk\ell} - \bar{X}_{j\cdot \ell}) \tag{18}$$

and

$$T_{i\ell} = \sum_{j=1}^{2} \sum_{k=1}^{n_j} (X_{jki} - \bar{X}_{\cdot\cdot i})(X_{jk\ell} - \bar{X}_{\cdot\cdot \ell}) \tag{19}$$

where the dot subscript notation indicates averaging over that subscript which has been replaced by a dot. Since Wilks' Λ-statistic is poorly tabulated, we shall instead measure group separation (actually the hypothesis tested is that of equality of group means) by means of a statistic which is derived from Λ

and which has approximately an F-distribution (Jennrich, 1977). The Λ-criterion may also be used to test which variable X_{p+1} gives the best discrimination when added to the set $(X_1, X_2,\ldots,X_p)$. The question of choosing the proper set of variables is discussed in the next section.

Stepwise Discriminant Analysis

From the ten variables listed in Table VI, there exist 1013 different subsets $(X_1, X_2,\ldots, X_p)$ of two or more variables for which the discriminant function could be calculated. Clearly, only a few of these subsets should be examined. Some subsets (e.g., short-period P, LR) were selected for testing because they are well-known, commonly-applied discriminants; others were selected because they contain significant composite information from a single seismic phase, e.g., short-period magnitude, short-period spectral ratio, and complexity from P waves. However, to determine the subset which, in accordance with some suitable criterion, is the "best" subset for discrimination, an analytic procedure described below is employed.

The stepwise discriminant analysis program used here, BM07M (Jennrich), 1977), is a "step-up" procedure. After the discriminant analysis has been performed for a subset of variables $(X_1, X_2,\ldots, X_p)$, analysis is then performed for another subset obtained by adding, and sometimes deleting, a variable in the next step. The method of selecting variables to be added or deleted is based upon the partial Λ-statistic, defined by the multiplicative increment

$$\Lambda'(X,u) = \frac{\Lambda(\overrightarrow{X,u})}{\Lambda(\overrightarrow{X})} \tag{20}$$

in Wilks' Λ-criterion, obtained by adding the variable u to the set $X = (X_1, X_2,\ldots, X_p)$ or by deleting it from the set $X= (X_1, X_2,\ldots,X_p,u)$. For our data set the corresponding F-statistic is (Jennrich, 1977)

$$F = (23-2-p)\,\frac{1-\Lambda'(\overrightarrow{X,u})}{\Lambda'(\overrightarrow{X,u})} \tag{21}$$

This statistic is known as either the "F-to-enter" or the "F-to-remove" statistic depending on whether the variable u is being added to or deleted from the set of variables used for discrimination in the previous step. The

---

Jennrich, R. I. (1977). Stepwise discriminant analysis, in Statistical Methods for Digital Computers, K. Enslien et al. (eds.). New York, NY John Wiley and Sons.

numbers of degrees of freedom are 1 and 21-p for F-to-enter and 1 and 22-p for F-to-remove. To move from one step to the next, the variable with the smallest F-to-remove is deleted, if that statistic is less than some specified threshold. If the F-to-remove values are such that all variables currently entered are retained, then that one of the remaining variables which has the largest F-to-enter is added, provided that the F value is higher than another specified threshold and that the tolerance is greater than some suitable cut-off value. (The tolerance is given by one minus the square of the variable's within-group multiple correlation with the variables already entered.) As a result of this procedure the variables are ranked at each step, according to their ability to enhance the discrimination capability of those variables already found significant. Variables which become superfluous after adding others are lowered in rank and deleted if their informational content is low enough. By specifying satisfactory values of the F-to-enter and F-to-remove thresholds, one may find the "best" subset of variables; that is, the smallest set yielding the greatest group separation measured by Wilks' Λ-criterion. Since the degrees of freedom of the denominator of the F-statistic must lie in the range 21 to 12, satisfactory thresholds of F-to-enter and F-to-remove were somewhat arbitrarily taken to be 3.0 and 4.0 respectively. Note that the procedure for selecting the "best" subset of variables is arbitrary and that other investigators may choose different criteria for selecting the "best" subset.

Results of the Stepwise Discrimination Analysis

For the chosen values of the F-to-enter and F-to-remove thresholds, four of the ten variables were entered into the discrimination algorithm: first motion, complexity, short-period P, and short-period spectral ratio (see Table VII-A). For this subset of variables the lowest *a posteriori* probability of correct classification was 0.916, which was found for one of the two earthquakes without dilatational first motion (Table X). As expected, examination of the F-to-remove values of the retained variables shows that first motion was the key factor in the discrimination. When thresholds were set low enough for all ten variables to be entered and retained (Table VII-B), the *a posteriori* probabilities were even greater than before, with the lowest value becoming 0.973. Note that this situation does not necessarily mean that the addition of six other variables would significantly enhance discrimination capability outside of our

TABLE VII (A)

Summary of Stepwise Discriminant Analysis
Using Network Estimates--Ten Variables

F-to-Enter = 4.00
F-to-Remove = 3.00

Step number	Variable enter	Variable removed	F-to-Enter or remove	Degrees of freedom	Wilk's Λ-statistic	Degrees of freedom	F-approximation to Λ	Degrees of freedom
1	lst mtn		50.2174	1,21	0.2949	1,1,21	50.2174	1,21
2	log comp		7.2762	1,20	0.2162	2,1,21	36.2510	2,20
3	SPP		5.0813	1,19	0.1706	3,1,21	30.7928	3,19
4	log SPSR		7.3529	1,18	0.1211	4,1,21	32.6549	4,18

Variables included and excluded during final step:

Variable included	F-to-remove	Degrees of freedom	Variable excluded	F-to-enter	Degrees of freedom
lst mtn	29.4320	1,18	log LPSR	2.9980	1,17
SPP	13.8064	↓	SPS	1.2545	↓
log comp	10.8158		LQ	0.2958	
log SPSR	7.3529		LPP	0.1683	
			LPS	0.0707	
			LR	0.0241	

TABLE VII (B)

Summary of Stepwise Discriminant Analysis
Using Network Estimates--Ten Variables

F-to-Enter = 0.01
F-to-Remove = 0.005

Step number	Variable enter	Variable removed	F-to-Enter or remove	Degrees of freedom	Wilk's Λ-statistic	Degrees of freedom	F-approximation to Λ	Degrees of freedom
1	1st mtn		50.2174	1,21	0.2949	1,1,21	50.2174	1,21
2	log comp		7.2762	1,20	0.2162	2,1,21	36.2510	2,20
3	SPP		5.0813	1,19	0.1706	3,1,21	30.7928	3,19
4	log SPSR		7.3529	1,18	0.1211	4,1,21	32.6548	4,18
5	log LPSR		2.9980	1,17	0.1030	5,1,21	29.6232	5,17
6	LQ		0.3896	1,16	0.1005	6,1,21	23.8646	6,16
7	LPS		0.6571	1,15	0.0963	7,1,21	20.1108	7,15
8	SPS		0.5248	1,14	0.0928	8,1,21	17.1051	8,14
9	LR		0.2287	1,13	0.0912	9,1,21	14.3922	9,13
10	LPP		0.1225	1,12	0.0903	10,1,21	12.0910	10,12

Variables included during final step:

Variable included	F-to-remove	Degrees of freedom
1st mtn	8.1146	1,12
log SPSR	5.6622	
log comp	4.4187	
SPP	2.2590	
log LPSR	1.6928	
LQ	1.1345	
LR	0.2979	
LPS	0.1471	
SPS	0.1334	
LPP	0.1225	

"training set". This is true because high a posteriori probabilities are, to a certain extent, an artifact of the large number of variables and the fact that each new variable is forced to work for the training set. The F-statistic approximation to Wilks' Λ-criterion actually corresponds to a greater separation of group means in the case of the four variables than in the case of all ten, even though in both cases F greatly exceeds the value of the 99.95 percentage point for the appropriate numbers of degrees of freedom.

Again note that the determination of first motions was frequently rather subjective, so one should exercise caution in accepting the validity of any discriminant function that this potentially unreliable variable influences. Therefore, the stepwise discriminant analysis was repeated using the same data base as before, but this time omitting the tenth (first motion) variable. Using the same F-to-enter and F-to-remove thresholds as before, the program first entered the same two variables previously entered immediately after the first motion --complexity and short-period P-- but then it added Love waves into the discriminant function and deleted complexity (Table VIII-A). Thus, of all possible subsets of the nine variables, the pair of short-period P and LQ is the best discriminant. However, since the F-to-enter value of the short-period spectral ratio, 3.994, was so close to the arbitrarily chosen threshold of 4.00, the discriminant analysis was repeated using a threshold that allowed short-period spectral ratio to be entered as the third variable. The lowest a posteriori probabilities were quite high (Table X), but as in the previous cases this does not necessarily indicate a significant improvement in separating the two groups.

The lowest a posteriori probability found in both the three- and nine-variables cases was that of event E, the Denver earthquake. This event was deleted from the data base and the three-variable discriminant function was recomputed on the basis of the remaining twenty-two events. When this new discriminant was applied to event E, the probability of this event's being an earthquake was calculated to be 0.703. Thus, the SPP-LQ-SPSR discriminant was capable of correctly classifying the most anomalous event, even when that event was not used in the training set to compute the discriminant function.

TABLE VIII (A)

Summary of Stepwise Discriminant Analysis Using Network Estimates--Nine Variables (First Motion Removed)

F-to-Enter = 4.00
F-to-Remove = 3.00

Step number	Variable enter	Variable remove	F-to-Enter or remove	Degrees of freedom	Wilk's Λ-statistic	Degrees of freedom	F-approximation to Λ	Degrees of freedom
1	log comp		15.2109	1,21	0.5799	1,1,21	15.2109	1,21
2	SPP		5.4276	1,20	0.4561	2,1,21	11.9227	2,20
3	LQ		15.3873	1,19	0.2520	3,1,21	18.7954	3,19
4		log comp	1.1098	1,19	0.2668	2,1,21	27,4874	2,20

Variables included and excluded during final step:

Variable included	F-to-remove	Degrees of freedom	Variable excluded	F-to-enter	Degrees of freedom
SPP	52.2808	1,20	log SPSR	3.9941	1,19
		↓	SPS	2.0145	↓
LQ	36.1959		log LPSR	2.1304	
			LPP	1.9791	
			LR	1.9261	
			log comp	1.1098	
			LPS	0.8812	

TABLE VIII (B)

Summary of Stepwise Discriminant Analysis Using Network Estimates--Nine Variables (First Motion Removed)

F-to-Enter = 0.01
F-to-Remove = 0.005

Step number	Variable enter	Variable removed	F-to-Enter or remove	Degrees of freedom	Wilk's Λ-statistic	Degrees of freedom	F-approximation to Λ	Degrees of freedom
1	log comp		15.2109	1,21	0.5799	1,1,21	15.2109	1,21
2	SPP		5.4276	1,20	0.4561	2,1,21	11.9228	2,20
3	LQ		15.3873	1,19	0.2520	3,1,21	18.7954	3,19
4	log SPSR		5.2097	1,18	0.1955	4,1,21	18.5223	4,18
5	log LPSR		3.3666	1,17	0.1632	5,1,21	17,4394	5,17
6	LR		0.7695	1,16	0.1557	6,1,21	14.4640	6,16
7	SPS		0.3503	1,15	0.1521	7,1,21	11.9444	7,15
8	LPS		0.0707	1,14	0.1513	8,1,21	9.8127	8,14
9	LPP		0.0006	1,13	0.1513	9,1,21	8.0998	9,13

Variables included during final step:

Variables included	F-to-remove	Degrees of freedom
SPP	19.7204	1,13
log SPSR	5.2119	
LQ	2.3236	
log comp	1.3181	
log LPSR	0.7874	
LR	0.3046	
SPS	0.1372	
LPP	0.0662	
LPS	0.0006	

Note again that several of the values of the short-period S and long-period P magnitudes were actually upper bounds of true values too small to be detected at any station. To judge how seriously discrimination was affected by the use of these upper bounds, a seven-variable discriminant function was calculated which did not use short-period S, long-period P, or first motion. The discrimination capability of the seven-variable subset was about the same as that of the nine-variable subset. Therefore, the two especially noisy variables did not contribute any significant information --or misinformation-- to the rest of the data base.

The magnitudes of the Love waves could not always be measured directly and sometimes had to be inferred from Rayleigh-wave magnitudes. A discriminant function without the unreliable Love-wave data had to be examined, and, so, the stepwise discriminant analysis was repeated, suppressing the Love-wave and first motion variables. Table IX indicates that the significant variables in this case were short-period P, Rayleigh waves, and short-period spectral ratio. This particular discriminant correctly classified all twenty-three events, although it did yield a rather low a posteriori probability for the Denver earthquake.

In summary, stepwise discriminant analysis was used to calculate three different, potentially useful, discriminant functions. The first of these discriminants amounts to little more than the criterion that events exhibiting dilatational first motions are earthquakes. If this first-motion criterion is judged unreliable, then the most powerful discriminant is one based upon short-period P, Love waves, and short-period spectral ratio. If Love-wave data is unavailable, then the next-best set of variables is short-period P, Rayleigh waves, and short-period spectral ratio. Thus, by adding SPSR the discrimination capability of the classical $M_s - m_b$ relation is somewhat enhanced, and the discriminant is even more effective when M_s is measured by Love waves rather than by Rayleigh waves. Note, however, that several of the twenty-three events studied were included in the training set specifically because of their failure to be clearly classified on the basis of the classical $M_s - m_b$ criterion.

Evaluation of Subsets of Discriminants

Although results from the stepwise analysis revealed which subset of

TABLE IX

Summary of Stepwise Discriminant Analysis Using Network Estimates--Eight Variables (First Motion and Love Waves Removed)

F-to-Enter = 4.00
F-to-Remove = 3.00

Step number	Variable enter	Variable removed	F-to-Enter or remove	Degrees of freedom	Wilk's Λ-statistic	Degrees of freedom	F-approximation to Λ	Degrees of freedom
1	log comp		15.2109	1,21	0.5799	1,1,21	15.2109	1,21
2	SPP		5.4276	1,20	0.4561	2,1,21	11.9227	2,20
3	LR		12.5992	1,19	0.2743	3,1,21	16.7581	3,19
4		log comp	1.6830	1,19	0.2986	2,1,21	23.4933	2,20
5	log SPSR		6.3883	1,19	0.2234	3,1,21	22.0112	3,19

Variables included and excluded during final step:

Variables included	F-to-remove	Degrees of freedom	Variables excluded	F-to-enter	Degrees of freedom
SPP	59.8105	1,19	log comp	2.9698	1,18
LR	30.6677	↓	log LPSR	0.6737	↓
log SPSR	6.3883		LPS	0.0647	
			SPS	0.0142	
			LPP	0.0106	

variables was the "best" subset for discrimination, it is useful to evaluate the ability of certain other discriminants to correctly classify the twenty-three events of the training set. The results are given below of attempts at classification where these other subsets of discriminants were used.

SPP,LR: The classical $M_s - m_b$ discriminant correctly classified all twenty-three events, although the a posteriori probability was rather low for both event E (the Denver earthquake) and event J (BENHAM aftershock). Comparing the results of this discriminant (Table XI) with those of the SPP-LR-SPSR case (Table X) shows that adding the short-period spectral ratio significantly widened the separation of event J from the explosions but that it had only minimal effect on event E (Figure 26 indicates this result was expected). Two explosions, events 7 and 11, also had low a posteriori probabilities. Figure 20 shows that although these events lie close to the hypothetical least-squares regression line passing through the explosion population, they also lie close to outlying earthquakes that are widely scattered about that population for small m_b.

SPP, LPS: This discriminant misclassified the Baja earthquake and strongly misclassified RULISON. Note that the very large magnitude of LPS for RULISON (Figure 14) is suspect, however, because this value was based upon two detections and two noise levels, and the two detections themselves were very noisy, if not spurious. Omitting RULISON from the training set would lead to correct classification by this discriminant of all the other events, including the Baja earthquake.

SPP, LPP: For the twenty-three events as a whole, this was a poor discriminant, misclassifying four events. Six of the events in the training set had no detectable long-period P waves, however, and were characterized by upper bounds for LPP (Figure 16). When these six events were deleted from the analysis, this discriminant became the most effective one tested; even the outliers in each of the two groups were widely separated from the other group. Thus SPP-LPP is a valuable discriminant when long-period P waves can be detected, but note that LPP cannot be measured for explosions with $m_b \lesssim 5.2$.

SPP, SPS: For the full data set, including the nine upper bounds, this pair of variables was useless as a discriminant (Figure 13). However, when considering only the fourteen events actually detecting SPS, this discriminant misclassified only RULISON, which was misclassified strongly. However, like the

TABLE X

A Posteriori Probabilities—Stepwise Discriminant Analysis

event \ test*	1	2	3	4	5	6	7	8
1	1.000	1.000	.998	.999	1.000	1.000	1.000	.951
2	1.000	1.000	.994	1.000	1.000	1.000	1.000	1.000
3	1.000	1.000	.999	1.000	1.000	1.000	1.000	1.000
4	1.000	1.000	.971	.862	.995	.871	.996	.992
5	1.000	1.000	.999	.999	1.000	1.000	1.000	.995
6	1.000	1.000	.678	.972	1.000	.986	1.000	.999
7	1.000	1.000	.963	.993	.986	.998	.992	.928
8	1.000	1.000	1.000	1.000	1.000	1.000	1.000	.999
9	1.000	1.000	1.000	1.000	1.000	1.000	1.000	.999
10	1.000	1.000	.885	.905	.996	.917	.994	.995
11	1.000	1.000	.975	.998	1.000	1.000	1.000	.983
A	1.000	1.000	.899	.975	.993	.978	.996	.998
B	1.000	1.000	.997	.999	1.000	1.000	1.000	.999
C	1.000	1.000	.905	.968	1.000	.975	1.000	1.000
D	1.000	1.000	1.000	1.000	1.000	1.000	1.000	1.000
E	1.000	1.000	.762	.764	.980	.703	.965	.528
F	.916	.973	.859	.789	.996	.723	.994	.684
G	1.000	1.000	.998	1.000	1.000	1.000	1.000	1.000
H	.999	1.000	.934	.880	1.000	.916	1.000	.990
I	1.000	1.000	.999	1.000	1.000	1.000	1.000	1.000
J	.999	1.000	.952	1.000	1.000	1.000	1.000	.996
K	1.000	1.000	1.000	1.000	1.000	1.000	1.000	.999
L	1.000	1.000	.998	1.000	1.000	1.000	1.000	.980
shots classified as quakes	0	0	0	0	0	0	0	0
quakes classified as shots	0	0	0	0	0	0	0	0
fraction of events misclassified	.00	.00	.00	.00	.00	.00	.00	.00
average a posteriori probability	.996	.999	.946	.961	.998	.971	.997	.957
F-approximation to Λ-statistic	32.655	12.091	27.487	22.400	8.100	24.772	11.732	22.011
degrees of freedom	4,18	10,12	2,20	3,19	9,13	3,18	7,15	3,19

TABLE X (Continued)

A Posteriori Probabilities--Stepwise Discriminant Analysis

*Test #	Discriminant Tested
1	F-to-Enter = 4.00, F-to-Remove = 3.00 (SPP, log SPSR, log comp, 1st mtn)
2	F-to-Enter = 0.01, F-to-Remove = 0.005 (all 10 variables)
3	no 1st mtn, F-to-Enter = 4.00, F-to-Remove = 3.00 (SPP, LQ)
4	SPP, LQ, log SPSR
5	no 1st mtn, F-to-Enter = 0.01, F-to-Remove = 0.005 (all other 9 variables)
6	SPP, LQ, log SPSR; 22 events (no event E)
7	7 variables (no SPS, LPP, 1st mtn)
8	no LQ or 1st mtn, F-to-Remove = 3.00 (SPP, LR, log SPSR)

TABLE XI

A Posteriori Probabilities--Selected Discriminants Using Network Estimates

event \ test	1	2	3	4	5	6	7	8	9	10	11	12	13	14	15
1	.882	.779	.080	-----	.301	-----	.659	.387	.758	.836	.894	.996	.987	.997	1.000
2	.999	.994	.864	1.000	.641	.927	.506	.956	.918	.841	1.000	.999	.998	.982	.999
3	1.000	.993	.960	1.000	.804	-----	.591	.915	.983	.903	.999	1.000	1.000	.972	.991
4	.998	.988	.937	1.000	.849	.932	.584	.611	.922	.848	.891	.995	.986	.713	.516
5	.995	.991	.940	1.000	.735	.973	.515	.533	.961	.910	.960	.999	.997	.984	.997
6	.937	.775	.848	1.000	.582	-----	.537	.897	.942	.890	.999	.872	.819	.659	.562
7	.643	.964	.146	-----	.180	-----	.465	.413	.460	.714	.843	.949	.904	.990	.999
8	.997	.991	.879	1.000	.840	.912	.542	.852	.927	.676	.952	1.000	.999	.971	.988
9	.985	.959	.908	1.000	.844	.901	.431	.938	.942	.697	.992	1.000	.997	.964	.980
10	.988	.915	.810	.997	.881	.988	.504	.876	.919	.620	.946	.967	.930	.445	.133
11	.698	.031	.211	-----	.244	.032	.493	.625	.317	.536	.874	.964	.926	.989	.997
A	.983	.872	.627	1.000	.618	-----	.524	.809	.325	.224	.579	.973	.964	.779	.965
B	.993	.950	.508	.998	.471	-----	.622	.612	.359	.366	.502	.999	.997	.988	.996
C	.998	.993	.790	1.000	.466	.790	.609	.591	.795	.804	.952	.993	.990	.930	.988
D	1.000	1.000	.842	1.000	.809	.933	.555	.594	.999	.995	1.000	1.000	1.000	1.000	.999
E	.565	.763	.614	1.000	.722	-----	.604	.685	.871	.729	.908	.683	.667	.378	.593
F	.800	.461	.828	-----	.752	-----	.472	.657	.994	.975	.997	.855	.824	.455	.818
G	.997	.995	.800	1.000	.678	.747	.256	.952	.818	.588	.995	.999	.998	.982	.998
H	.990	.714	.672	1.000	.241	.909	.723	.085	.368	.752	.205	.991	.989	.979	.998
I	.997	.990	.735	1.000	.852	-----	.683	.970	.871	.484	.992	.999	.998	.962	.993
J	.562	.873	.905	-----	.843	-----	.640	.990	.931	.654	1.000	.866	.804	.402	.562
K	.985	.919	.932	-----	.824	.944	.316	.936	.795	.403	.952	1.000	.998	.991	.993
L	.889	.762	.478	.995	.319	-----	.359	.542	.992	.992	1.000	.996	.991	.989	.997
shots classified as quakes	0	1	3	0	3	1	3	2	2	0	0	0	0	1	1
quakes classified as shots	0	1	1	0	4	0	4	1	3	4	1	0	0	3	0
fraction of events misclassified	.00	.09	.17	.00	.30	.08	.30	.13	.22	.17	.04	.00	.00	.17	.04
average a posteriori probability	.908	.855	.709	.999	.628	.832	.530	.714	.792	.715	.888	.961	.946	.848	.872
F-approximation to A-statistic	23.493	15.884	6.147	49.609	3.4417	5.3415	0.664	7.121	11.923	7.345	13.511	19.815	26.802	17.178	14.507
degrees of freedom	2,20	2,20	2,20	2,14	2,20	2,9	2,20	2,20	2,20	2,20	3,19	3,19	2,20	2,20	3,19

TABLE XI (Continued)

A Posteriori Probabilities--Selected Discriminants Using Network Estimates

*Test #	Discriminant Tested
1	SPP, LR
2	SPP, LPS
3	SPP, LPP
4	SPP, LPP (no noise levels)
5	SPP, SPS
6	SPP, SPS (no noise levels)
7	LR, log LPSR
8	SPP, log SPSR
9	SPP, log comp
10	log SPSR, log comp
11	SPP, log SPSR, log comp
12	SPP, LQ,LR
13	SPP, LQ + LR
14	$\frac{LQ}{SPP}, \frac{LR}{SPP}$
15	$\frac{1}{\sqrt{SPP^2 + LQ^2 + LR^2}}$. (SPP, LQ, LR)

case of long-period S, the RULISON SPS magnitude is uncertain because it is based upon three noise levels and a single noisy detection. If this borderline "detection" had been considered a noise measurement, then this variable pair would have correctly classified the remaining thirteen events. This discriminant may be useful for events whose magnitude (m_b) is large enough for detection of SPS. Figure 13 suggests $m_b > 5\ 1/2$ for explosions and $m_b > 5$ for earthquakes for SPS detection.

LR,LPSR: This pair of variables yields no discrimination. Thus long-period surface waves alone are insufficient for discrimination, as expected on theoretical grounds.

SPP,SPSR and SPP, complexity: These two pairs of variables are ineffective as discriminants. The former misclassified three events, and the latter misclassified five events. When combined to form the triad SPP-SPSR-complexity, however, they misclassified only the Borrego Mountain earthquake (although the Caliente earthquake is a marginal case). This three-variable discriminant is noteworthy because it used only short-period P-wave data.

SPP, LQ, LR: This discriminant was tested in two different ways. In the first test the discriminant function for these three variables, calculated in the manner previously described, was found to be

$$13.098 \cdot SPP - 5.985 \cdot LQ - 4.674 \cdot LR - 18.122 = 0.0$$

In the second test the sum of the Rayleigh-wave and Love-wave magnitudes was treated as one variable (Figure 23), and the discriminant function was found to be

$$10.879 \cdot SPP - 4.488(LQ + LR) - 14.626 = 0.0$$

Although controversy may arise over what is physically more meaningful, the individual values of LQ and LR or their sum, there is still value in treating the two surface-wave magnitudes as one variable on account of the facility with which a discriminant line in a plane may be graphically manipulated. A discriminant plane in a three-dimensional space must be treated by analytic methods alone. One would ordinarily expect the transformation from the three-dimensional space to the plane to involve a loss of information, but since LQ versus LR is itself a poor discriminant, the pair SPP, LQ + LR gives

satisfactory results when compared with those of the triad SPP,LQ,LR. Because $M_s - m_b$ was a poorer discriminant for the data set than the SPP,LQ pair (Table X), neither of the two discriminants involving LR gives results quite so good as SPP,LQ alone. Again note that poor separation on $M_s - m_b$ plots was one criterion for the inclusion of several of the events in the training set.

The values of F-to-enter and F-to-remove for short-period P, which were calculated in the stepwise experiments, indicate that various discriminant functions gave significance to the difference in the mean of m_b for the two populations ($\bar{m}_b$ = 5.72 for explosions and 5.00 for earthquakes). Thus, m_b was acting as a weak discriminant by itself. Since, for the purposes of discrimination, what is important is not the magnitude of short-period P itself but rather its relation to the other variables, two discriminants were tested that were in some sense "normalized", to correct for m_b variations. In the first test the magnitudes of LQ and LR, each divided by m_b, were used as a discriminant pair. This test resulted in four misclassifications. The second test was a three-variable discrimination experiment in which the magnitudes of SPP,LQ, and LR were each divided by the square root of the sum of their squares. This test is equivalent to the earlier three-variable discriminant except that now each of the twenty-three data points lies at unit distance from the origin of the three-dimensional space. This test resulted in one misclassification. Thus, discrimination based on magnitude ratios such as $\frac{LQ}{P}$, $\frac{LR}{P}$, etc., is less effective, perhaps justifiably, than discrimination based on the magnitudes themselves.

If the SPP,LQ and SPP,LR discriminant lines have the form LQ = a·SPP + b and LR = c·SPP + d, then the earthquake and explosion populations will lie within different regions on a plot of (LQ - a·SPP) versus (LR - c·SPP). Because the slopes a and c are close to unity, a useful discriminant not affected by m_b differences in the two populations is (LQ-SPP) versus (LR-SPP). For our data set this discriminant (not tabulated) resulted in no misclassifications.

Single-Station Discrimination

Several of the discrimination tests that had been performed using event magnitudes from network data were repeated using data from only one station. Since more data were available from NP-NT and RK-ON than from the other

stations, data from each of these stations were used separately in an attempt to evaluate the effectiveness of single-station discrimination functions. Tables XII and XIII indicate that there were many gaps in the available data, even for those two most complete station records. Some discriminants could not be evaluated for certain events because of missing data (expecially due to over-driven long-period recordings and unavailable digital data); and others were inapplicable because of failure to detect all variables used in the discriminant function, especially long-period P and short-period S.

Results of the single-station tests (Tables XII and XIII) show that even those discriminants that worked well in the previous experiments now misclassified a number of events. The large scatter of single-station measurements of event magnitudes about the "true" values (i.e., the network-based estimates) causes significant overlap of the earthquake and explosion populations for any subset of the ten variables. Thus, discrimination based upon a network is significantly more powerful than discrimination based on a single station because: 1) the training set data base is more nearly complete; and 2) the magnitude estimates are more accurate, hence the population variances are smaller. The question remains of whether a method of handling network data exists which is preferable to the method already outlined. A case could be made that averaging measurements from the entire network, either by the conventional arithmetic mean or by the maximum-likelihood method, blurs out station effects and source-path effects which might affect discrimination. Therefore, an alternate process is examined in which discriminant functions are calculated individually at each station and are then combined to perform classification based upon the entire network.

Multiple-Station Discriminant Functions--Theory

In calculating the discriminant functions detailed thus far, we assumed that the covariance matrices of the earthquake and explosion populations were identical. To calculate multiple-station discriminant functions, we further assume that the covariance matrices are the same for the data measured at each network station. This common covariance $\underset{\sim}{\Sigma}$ is approximated by the sample population covariance $\underset{\sim}{S}$ obtained by considering the pooled data from the entire network. In order to obtain $\underset{\sim}{S}$ it is necessary to reject all incomplete data vectors, i.e., data for a given event and a given station for which one or

TABLE XII

A Posteriori Probabilities—Selected Discriminants Using NP-NT Estimates

event \ test*	1	2	3	4	5	6	7	8	9	10
1	.281	.383	---	---	.911	.787	.287	.769	.746	.300
2	.750	.850	---	.353	.976	.970	.702	.860	.978	.757
3	----	----	----	----	----	----	----	----	----	----
4	----	.858	.818	.985	1.000	----	.736	----	----	----
5	.854	.827	----	.943	.998	.825	.774	.662	.882	.830
6	.330	.387	.533	----	.942	.952	.511	.820	.951	.312
7	----	----	----	----	----	.687	.536	.800	.759	----
8	.762	.641	.755	.978	----	.406	.673	.320	.446	.699
9	----	.732	.867	.984	.389	.764	.730	.427	.788	----
10	.855	.769	.893	.995	1.000	.625	.723	.272	.633	.801
11	----	.355	.130	----	1.000	.161	.217	.463	.128	----
A	.461	.279	----	----	----	.792	.444	.515	.731	.433
B	.718	.758	.825	----	.989	----	----	----	----	.761
C	.385	.609	.803	.558	----	.668	.581	.730	.729	.470
D	----	.961	.885	----	----	----	----	----	----	----
E	.503	----	.301	----	----	.382	.352	.272	.275	----
F	----	----	----	----	----	----	----	----	----	----
G	.509	.337	.599	----	----	.858	.540	.689	.854	.494
H	----	----	----	----	----	----	----	.553	----	----
I	.891	.822	.783	----	.995	.958	.673	.607	.952	.883
J	----	----	----	----	----	----	----	----	----	----
K	.916	----	----	.998	----	----	----	----	----	----
L	----	.563	.455	----	----	.504	.869	.873	.797	----
shots classified as quakes	2	3	1	1	1	2	2	4	2	2
quakes classified as shots	2	2	2	0	0	1	2	1	1	3
total number of events	13	16	13	8	10	15	16	16	15	11
fraction of events misclassified	.31	.31	.23	.13	.10	.20	.25	.31	.20	.45
average a posteriori probability	.632	.633	.611	.849	.920	.689	.584	.602	.710	.613

TABLE XII (Continued)

A Posteriori Probabilities--Selected Discriminants Using NP-NT Estimates

*Test #	Discriminant Tested
1	SPP, LQ
2	SPP, LR
3	SPP, LPS
4	SPP, SPS
5	LR, log LPSR
6	SPP, log SPSR
7	SPP, log comp
8	log SPSR, log comp
9	SPP, log SPSR, log comp
10	SPP, LQ, LR

TABLE XIII

A Posteriori Probabilities—Selected Discriminants Using RK-ON Estimates

event \ test*	1	2	3	4	5	6	7	8	9	10	11
1	.906	----	----	----	----	----	.315	.545	.603	.4.9	----
2	----	----	----	----	----	.646	----	----	----	----	----
3	.950	.984	1.000	.996	----	.581	.845	.907	.856	.950	.956
4	.686	.896	.938	.316	----	.527	.590	.710	.565	.625	.751
5	.971	.983	.999	.949	----	.706	.519	.866	.838	.805	.969
6	.676	.977	.999	.942	----	.824	.754	.785	.760	.874	.853
7	.145	.057	----	----	----	----	.254	.146	.339	.189	.126
8	.893	.755	.998	.878	1.000	.429	.800	.542	.393	.698	.810
9	----	.969	1.000	.977	1.000	.309	.701	.761	.518	.683	----
10	----	.920	.999	.651	----	.505	.608	.689	.466	.560	----
11	.694	.462	----	----	----	.568	.683	.301	.503	.674	.616
A	----	.965	1.000	----	1.000	.490	.498	.339	.190	.224	----
B	.748	.729	.379	----	----	----	.428	.519	.576	.502	752
C	.905	.970	.983	.980	1.000	.809	.459	.536	.493	.456	.936
D	----	.971	1.000	.988	----	.729	.625	.927	.908	.912	----
E	.556	.592	1.000	.907	----	.498	.427	.690	.628	.541	.571
F	.277	.493	----	----	----	----	----	.775	----	----	.352
G	----	.992	1.000	.991	1.000	.287	.854	.845	.758	.922	----
H	----	----	----	.350	1.000	----	.277	.308	.642	.423	----
I	.987	.969	1.000	----	----	----	----	----	----	----	.974
J	.675	.611	.996	----	----	----	.852	.619	.473	.807	.622
K	.906	.821	1.000	----	----	----	.904	.666	.506	.878	.853
L	----	.567	.926	.446	----	----	.572	.608	.695	.722	----
shots classified as quakes	1	2	0	1	0	2	2	2	3	2	1
quakes classified as shots	1	1	1	2	0	3	5	2	3	3	1
total number of events	15	20	17	13	6	14	20	21	20	20	14
fraction of events misclassified	.13	.15	.06	.23	.00	.36	.35	.19	.30	.25	.14
average a posteriori probability	.732	.784	.954	.798	1.000	.565	.598	.623	.586	.643	.724

TABLE XIII (Continued)

A Posteriori Probabilities--Selected Discriminants Using RK-ON Estimates

*Test #	Discriminant Tested
1	SPP, LQ
2	SPP, LR
3	SPP, LPS
4	SPP, LPP
5	SPP, SPS
6	LR, log LPSR
7	SPP, log SPSR
8	SPP, log comp
9	log SPSR, log comp
10	SPP, log SPSR, log comp
11	SPP, LQ, LR

more of the variables used in the discriminant could not be measured, either due to missing data or to noise thresholds. It is to be expected that the value of $\underset{\sim}{S}$ calculated in this manner from the pooled data is less accurate than the value which was calculated from the network-averaged data, because: 1) many measurements of signal amplitudes, spectral ratios, and complexities had to be deleted from the calculation since they were components of incomplete data vectors; and 2) it was impossible to utilize the maximum-likelihood estimator for the magnitudes of weak signals. (An alternative procedure that also was tested would be to use the same $\underset{\sim}{S}$ matrix which previously was calculated for the network discriminant case.) Although the covariance at each station is the same, the population means are not; so for the m-th station of the N_s station network, the means of the earthquake and explosion populations as measured at that station are calculated to be X_{1m} and X_{2m}. Equation (14) and (15) indicate the discriminant function and classification function for the m-th station alone to be

$$\vec{D}_m \cdot \vec{X}_m + C_m = \vec{X}_m' \underset{\sim}{S}^{-1} (\vec{\bar{X}}_{1m} - \vec{\bar{X}}_{2m}) - \tfrac{1}{2} (\vec{\bar{X}}_{1m} + \vec{\bar{X}}_{2m})' \underset{\sim}{S}^{-1} (\vec{\bar{X}}_{1m} - \vec{\bar{X}}_{2m}) \qquad (22)$$

and

$$\vec{D}_{jm} \cdot \vec{X}_m + C_{jm} = \vec{X}_m' \underset{\sim}{S}^{-1} \vec{\bar{X}}_{jm} - \tfrac{1}{2} \vec{\bar{X}}_{jm}' \underset{\sim}{S}^{-1} \vec{\bar{X}}_{jm}. \quad j = 1,2; \; m = 1,\ldots,N_s. \qquad (23)$$

Using these functions, the <u>a posteriori</u> probability $p_{jm}(\vec{X}_{km})$ that the k-th event of the training set belongs to the j-th group, as determined by the m-th station, can be calculated, where $\vec{X}_{km}$ denotes the data vector of the k-th event measured at the m-th station. However, there is more interest in classification probabilities $p_j(\vec{X}_k)$ determined by the entire network, where $\vec{X}_k$ denotes the vector of all observations of the k-th event $(\vec{X}_{k1}, \vec{X}_{k2}, \ldots, \vec{X}_{kN_s})$. In order to determine these probabilities, the discriminant function is employed for the network as a whole, which is simply (Shumway and Blandford, 1972)

$$d(\vec{X}_k) = \sum_{m=1}^{N_s} \vec{D}_m \cdot \vec{X}_{km} + \sum_{m=1}^{N_s} C_m. \qquad (24)$$

To classify a given event, then, take the sum of the values of the individual-station discriminant functions applied to that event and classify it as an explosion or an earthquake based upon whether that sum is positive or negative.

By introducing the classification functions for the network, as given by

$$d_j(\vec{X_k}) = \sum_{m=1}^{N_s} \vec{D_{jm}} \cdot \vec{X_{km}} + \sum_{m=1}^{N_s} C_{jm} \qquad j = 1,2 \tag{25}$$

the a posteriori probabilities that an event is an explosion or an earthquake, as determined by the network, are obtained from equations 13 and 12 as

$$P_1(\vec{X_k}) = \frac{\exp[d_1(\vec{X_k})]}{\exp[d_1(\vec{X_k})] + \exp[d_2(\vec{X_k})]} = \frac{1}{1 + \exp[-d(\vec{X_k})]} \tag{26}$$

$$P_2(\vec{X_k}) = \frac{\exp[d_2(\vec{X_k})]}{\exp[d_1(\vec{X_k})] + \exp[d_2(\vec{X_k})]} = \frac{1}{1 + \exp[d(\vec{X_k})]} \tag{27}$$

It should be known whether the individual station discriminant functions are less reliable for some stations than for others before combining them to form the network discrimination functions. Unreliable stations could then be deleted from the sum over the network (equation 24). To assess station reliability, a criterion for estimating the probability of misclassification by a single discriminant function must be examined.

For the discriminant function with known parameters, given by (6) and (7), the probability of misclassifying an explosion as an earthquake is given by

$$P(2|1) = \Phi(-\frac{\delta}{2}) \tag{28}$$

where Φ (Z) denotes the normal distribution function and δ^2 is the Mahalanobis distance (Morrison, 1976), defined as

$$\delta^2 \equiv (\vec{\mu_1} - \vec{\mu_2})' \underset{\sim}{\Sigma}^{-1} (\vec{\mu_1} - \vec{\mu_2}). \tag{29}$$

Since the parameters are unknown in practice, one must estimate P(2|1) by

$$\hat{P}(2|1) = \Phi(-\frac{D}{2}) \tag{30}$$

where

$$D^2 = (\vec{\bar{x}}_1 - \vec{\bar{x}}_2)' \underset{\sim}{S}^{-1} (\vec{\bar{x}}_1 - \vec{\bar{x}}_2). \tag{31}$$

Morrison, D. F. (1976). Multivariate Statistical Methods. McGraw-Hill Publ. Co., New York.

Dunn (1971) and McLachlan (1974) demonstrated the inadequacy of $\hat{P}(2|1)$ and investigated the conditions under which other functions are preferable as estimators of $P(2|1)$. For the purpose of this study, however, the significant result is not the exact value of the misclassification probability calculated by means of equation (30) or some other estimator, but rather the simple criterion that discriminant functions for which D^2 is small have a higher misclassification probability than do those for which D^2 is large.

The Mahalanobis distance for multiple-station discrimination is given by the sum of D^2 for each of the N_s single-station discriminant functions. Therefore, one should evaluate (30) for each station in the network and identify stations with the smallest D^2 as stations contributing the least to the network discriminant (24) and a posteriori probabilities (26,27). Stations with sufficiently small D^2 may than be deleted from the analysis. Identification of stations that yield poor discrimination for a given subset of variables may also relate valuable information about the source-path effects of these variables.

Evaluation of Selected Multiple-Station Discriminant Functions

Several particular subsets of variables tested as discriminants in the network and single-station experiments were also tested as multiple-station discriminants. The test results showed that the subsets which were most effective as network discriminants were also the most effective as multiple-station discriminants. However, in using multiple-station discriminant functions, some problems did develop because of missing data or because noise levels exceeded weak signal amplitudes; the problems reduced the number of stations detecting the chosen variables. Thus, few single-station discriminants were used to calculate the network discriminant for a given event, and the single-station discriminants themselves were calculated from the data of only a few events.

For the ten selected discriminants, a posteriori probabilities for each event and both D^2 and the number of detections for each station are listed in

---

Dunn, O. J. (1971). Some expected values for probabilities of correct classification in discriminant analysis. Technometrics, 13, 345-353.

McLachlan, G. J. (1974). Estimation of the errors of misclassification on the criterion of asymptotic mean square error. Technometrics, 16, 255-260.

Table XIV. Note the number of detections when evaluating the reliability of a single-station discriminant function. This is necessary because stations detecting only a few events from either or both of the populations would likely measure, by means of D^2, a large separation between the two groups. Thus, while such stations seem to have reliable discriminant functions as far as D^2 is concerned, in reality they are probably less reliable than stations with lower values of D^2 which have more detections. If one such station strongly misclassifies a certain event, then the sum (24) may also classify it incorrectly. Note, for instance, that in the case of the common $M_s - m_b$ discriminant, D^2 is low for NP-NT and WH-YK. If the analysis is repeated omitting data from these two stations, the misclassification of RULISON is eliminated but also the only station detecting both M_s and m_b for the Borrego Mountain earthquake is deleted. The reliability of BE-FL is also questionable because the observed explosion population consisted of only one event. The $M_s - m_b$ discriminant functions for the seven stations are shown in Figure 29.

By eliminating all data vectors incomplete because some variables used in a given discriminant function were undetected, a bias is introduced into the pooled data used to compute the covariance matrix. Therefore, the multiple-station discriminant analysis was repeated using instead the covariance matrices calculated for the network maximum-likelihood magnitude estimates. While this process seemed to improve the results somewhat for discriminants not involving digital data (Table XV), the discriminants involving SPSR, LPSR, and/or complexity behaved erratically, a situation expected because the maximum-likelihood estimator for these three variables also deleted noisy observations. The principle difference between the two estimates of the covariance for the digital data is that, for the maximum-likelihood estimator, means are computed for each event and then the covariance is computed using those means with equal weight, whereas for the pooled data, the covariance is computed directly from the individual observations. While the latter method is probably preferable for complexity and spectral ratios, the maximum-likelihood estimates may yield more accurate covariances for the other variables. For evidence of this accuracy, note that the $M_s - m_b$ discriminant correctly classifies RULISON when the covariance matrix from the network case is used.

TABLE XIV

A Posteriori Probabilities--Selected Discriminants
Using Multiple-Station Discriminant Functions

event \ test*	1	2	3	4	5	6	7	8	9	10	11
1	.999	1.000	----	----	.875	.340	.121	.914	.503	.999	1.000
2	.999	1.000	.997	.647	.688	.997	.708	.897	.998	1.000	1.000
3	1.000	1.000	1.000	1.000	.940	.995	.994	.932	.999	1.000	1.000
4	1.000	1.000	1.000	.984	.999	.991	.999	.908	.997	1.000	1.000
5	1.000	1.000	1.000	.953	.981	.980	.997	.990	.999	1.000	1.000
6	1.000	1.000	.978	.944	.992	.997	.992	.988	1.000	1.000	1.000
7	.999	.993	.850	----	.318	.114	.088	.815	.267	1.000	.998
8	1.000	1.000	1.000	.993	.988	1.000	.996	.992	1.000	1.000	1.000
9	.999	1.000	1.000	1.000	.992	.999	.997	.726	.999	.999	1.000
10	.911	1.000	1.000	1.000	1.000	.993	.991	.608	.990	.871	1.000
11	.934	.304	.011	----	.459	.068	.136	.559	.121	.847	.567
A	.898	.999	.996	----	.469	.954	.576	.308	.876	.980	1.000
B	.928	1.000	1.000	.996	.648	.644	.949	.885	.959	.929	1.000
C	.999	1.000	.999	.999	.920	.741	.782	.742	.884	1.000	1.000
D	1.000	1.000	1.000	1.000	.907	.895	.999	.990	.998	1.000	1.000
E	1.000	1.000	1.000	1.000	.998	.911	.974	.731	.952	1.000	1.000
F	.341	.424	----	----	.845	----	.891	----	----	.452	.418
G	.927	1.000	1.000	1.000	.114	.985	.847	.645	.984	.949	.999
H	.870	.511	.726	.993	----	.373	.261	.980	.783	.773	----
I	1.000	1.000	1.000	.999	.828	1.000	.914	.585	.998	1.000	1.000
J	.919	.820	.994	----	.973	.900	.705	.443	.869	.936	.646
K	1.000	.983	.998	----	.897	.974	.717	.283	.880	.990	.988
L	.722	.973	.531	.682	----	.398	.990	.996	.989	.800	.986
shots classified as quakes	0	1	1	0	1	3	3	0	2	0	0
quakes classified as shots	1	1	0	0	2	2	1	2	0	1	1
total number of events	23	23	21	16	21	22	23	22	22	23	22
fraction of events misclassified	.04	.09	.05	.00	.14	.23	.17	.09	.09	.04	.05
average a posteriori probability	.932	.913	.909	.949	.811	.784	.766	.769	.866	.937	.936
total number of observations	72	99	82	28	75	87	89	86	85	68	82

TABLE XIV (Continued)

A Posteriori Probabilities--Selected Discriminants
Using Multiple-Station Discriminant Functions

D^2 for Single-Station Discriminant Functions

station \ test*	1	2	3	4	5	6	7	8	9	10	11
BE-FL	-----	9.858	8.244	-----	0.764	-----	-----	-----	-----	-----	10.609
HN-ME	11.718	8.586	4.901	3.261	0.371	1.222	0.110	0.859	1.245	13.598	9.236
NP-NT	2.105	1.437	2.051	-----	2.640	2.519	0.736	0.937	2.718	1.674	-----
PG-BC	3.278	4.981	4.640	5.387	0.209	1.246	2.339	1.326	2.380	3.550	5.361
RK-ON	2.436	4.337	6.552	4.014	0.841	1.195	2.052	1.052	2.184	2.838	4.667
SV-QB	15.498	14.886	4.490	1.438	1.377	1.545	0.523	0.089	1.626	19.441	15.950
WH-YK	1.938	0.821	3.479	4.938	5.870	3.258	1.180	2.010	2.523	2.477	-----

Number of (Explosions, Earthquakes) Detected

BE-FL	---	4,1	4,1	---	5,2	---	---	---	---	---	4,1
HN-ME	8,2	10,4	6,4	1,5	9,5	10,2	10,2	10,2	10,2	8,2	10,4
NP-NT	6,7	9,7	6,7	---	8,2	9,6	10,6	9,7	9,6	6,5	---
PG-BC	8,5	10,10	8,9	6,7	7,6	11,10	11,10	11,10	11,10	8,5	10,10
SV-QB	6,3	8,3	6,4	1,1	4,4	8,3	9,3	8,3	8,3	5,3	8,3
WH-YK	6,6	7,6	6,4	1,3	6,3	5,3	6,1	5,1	5,1	6,6	---

*Test #	Discriminant Tested
1	SPP, LQ
2	SPP, LR
3	SPP, LPS
4	SPP, LPP
5	LR, log LPSR
6	SPP, log SPSR
7	SPP, log comp
8	log SPSR, log comp
9	SPP, log SPSR, log comp
10	SPP, LQ, LR
11	SPP, LR (no data from NP-NT or WH-YK)

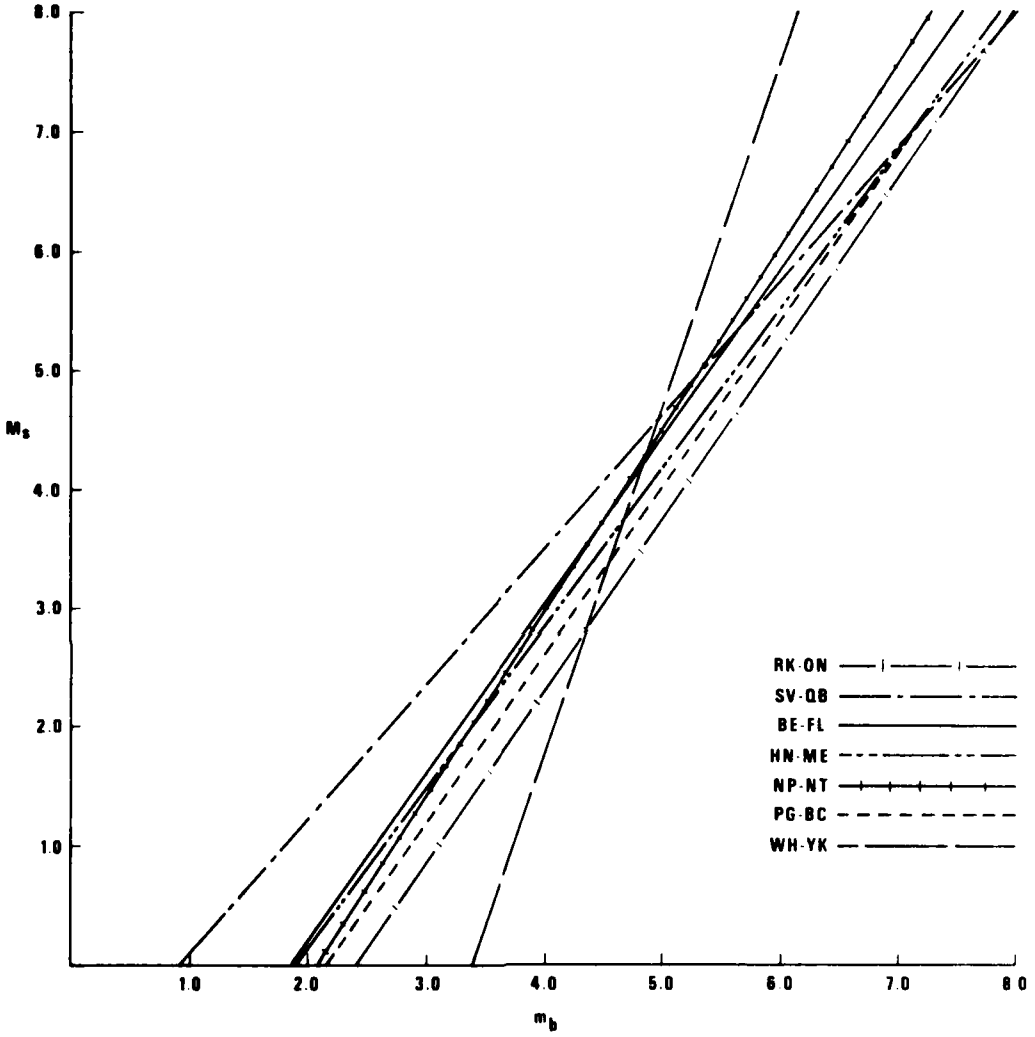

Figure 29 Single-station M_S-m_b discriminant functions.

TABLE XV

A Posteriori Probabilities—Selected Discriminants Using Multiple-Station Discriminant Functions and Network Covariance Estimates

event \ test*	1	2	3	4	5	6	7	8	9	10	11
1	1.000	1.000	-----	-----	.911	.964	.063	.980	1.000	1.000	1.000
2	1.000	1.000	1.000	.971	.639	1.000	.668	.964	1.000	1.000	1.000
3	1.000	1.000	1.000	1.000	.970	1.000	.988	.912	1.000	1.000	1.000
4	1.000	1.000	1.000	1.000	.999	.997	.996	.784	.772	1.000	1.000
5	1.000	1.000	1.000	1.000	.980	1.000	.980	.946	1.000	1.000	1.000
6	1.000	1.000	1.000	1.000	.992	1.000	.941	.994	1.000	1.000	1.000
7	1.000	1.000	.980	-----	.336	.879	.038	.773	1.000	1.000	1.000
8	1.000	1.000	1.000	1.000	.965	1.000	.991	.996	1.000	1.000	1.000
9	1.000	1.000	1.000	1.000	.973	1.000	.996	.532	.169	1.000	1.000
10	.972	1.000	1.000	1.000	.999	.992	.987	.323	.002	.946	1.000
11	1.000	.650	.001	-----	.626	.060	.048	.319	.974	.996	.922
A	.972	1.000	1.000	-----	.462	.996	.778	.551	.134	1.000	1.000
B	.997	1.000	1.000	1.000	.783	.543	.849	.554	.236	.999	1.000
C	1.000	1.000	1.000	1.000	.894	.961	.550	.515	.985	1.000	1.000
D	1.000	1.000	1.000	1.000	.929	.738	.987	.906	1.000	1.000	1.000
E	1.000	1.000	1.000	1.000	.998	.931	.932	.348	.033	1.000	1.000
F	.138	.199	-----	-----	.711	-----	.807	-----	-----	.272	.199
G	.990	1.000	1.000	1.000	.074	1.000	.862	.800	.999	.988	1.000
H	.981	.864	.929	1.000	-----	.997	.148	.991	1.000	.966	-----
I	1.000	1.000	1.000	1.000	.850	1.000	.922	.684	.988	1.000	1.000
J	.932	.609	.993	-----	.934	.989	.771	.504	.528	.907	.426
K	1.000	1.000	.996	-----	.881	.997	.911	.682	.567	1.000	1.000
L	.889	1.000	.966	.592	-----	.755	.656	.866	1.000	.904	1.000
shots classified as quakes	0	0	1	0	1	1	3	2	2	0	0
quakes classified as shots	1	1	0	0	2	0	1	1	3	1	2
total number of events	23	23	21	16	21	22	23	22	22	23	22
fraction of events misclassified	.04	.04	.05	.00	.14	.05	.17	.14	.23	.04	.09
average a posteriori probability	.951	.927	.946	.973	.805	.900	.733	.724	.745	.956	.934
total number of observations	72	99	82	38	75	87	89	86	85	68	82

TABLE XV (Continued)

A Posteriori Probabilities--Selected Discriminants Using Multiple-Station Discriminant Functions and Network Covariance Estimates

D^2 for Single-Station Discriminant Functions

station \ test*	1	2	3	4	5	6	7	8	9	10	11
BE-FL	-----	22.836	15.011	-----	0.992	-----	-----	-----	-----	-----	22.836
HN-ME	19.935	20.073	10.082	8.814	0.283	4.306	0.126	1.703	6.770	29.937	20.073
NP-NT	3.704	3.230	3.455	-----	3.408	7.780	0.472	1.032	6.741	2.839	-----
PG-BC	5.140	11.529	6.478	26.209	0.221	1.515	1.589	0.579	2.250	7.095	11.529
RK-ON	4.279	9.967	10.964	16.145	0.811	2.179	1.398	0.422	2.146	6.324	9.967
SV-QB	28.962	24.609	4.429	29.384	3.787	9.233	0.423	1.852	5.902	3.669	-----

Number of (Explosions, Earthquakes) Detected

BE-FL	---	4,1	4,1	---	5,2	---	---	---	---	---	4,1
HN-ME	8,2	10,4	6,4	1,5	9,5	10,2	10,2	10,2	10,2	8,2	10,2
NP-NT	6,7	9,7	6,7	---	8,2	9,6	10,6	9,7	9,6	6,5	---
PG-BC	8,5	10,10	8,9	6,7	7,6	11,10	11,10	11,10	11,10	8,5	10,10
RK-ON	8,7	9,11	7,10	7,6	9,5	10,10	10,11	10,10	10,10	7,7	9,11
SV-QB	6,3	8,3	6,4	1,1	4,4	8,3	9,3	8,3	8,3	5,3	8,3
WH-YK	6,6	7,6	6,4	1,3	6,3	5,3	6,1	5,1	5,1	6,6	---

*Test #	Discriminant Tested
1	SPP, LQ
2	SPP, LR
3	SPP, LPS
4	SPP, LPP
5	LR, log LBR
6	SPP, log SPSR
7	SPP, log comp
8	log SPSR, log comp
9	SPP, log SPSR, log comp
10	SPP, LQ, LR
11	SPP, LR (no data from NP-NT or WH-YK)

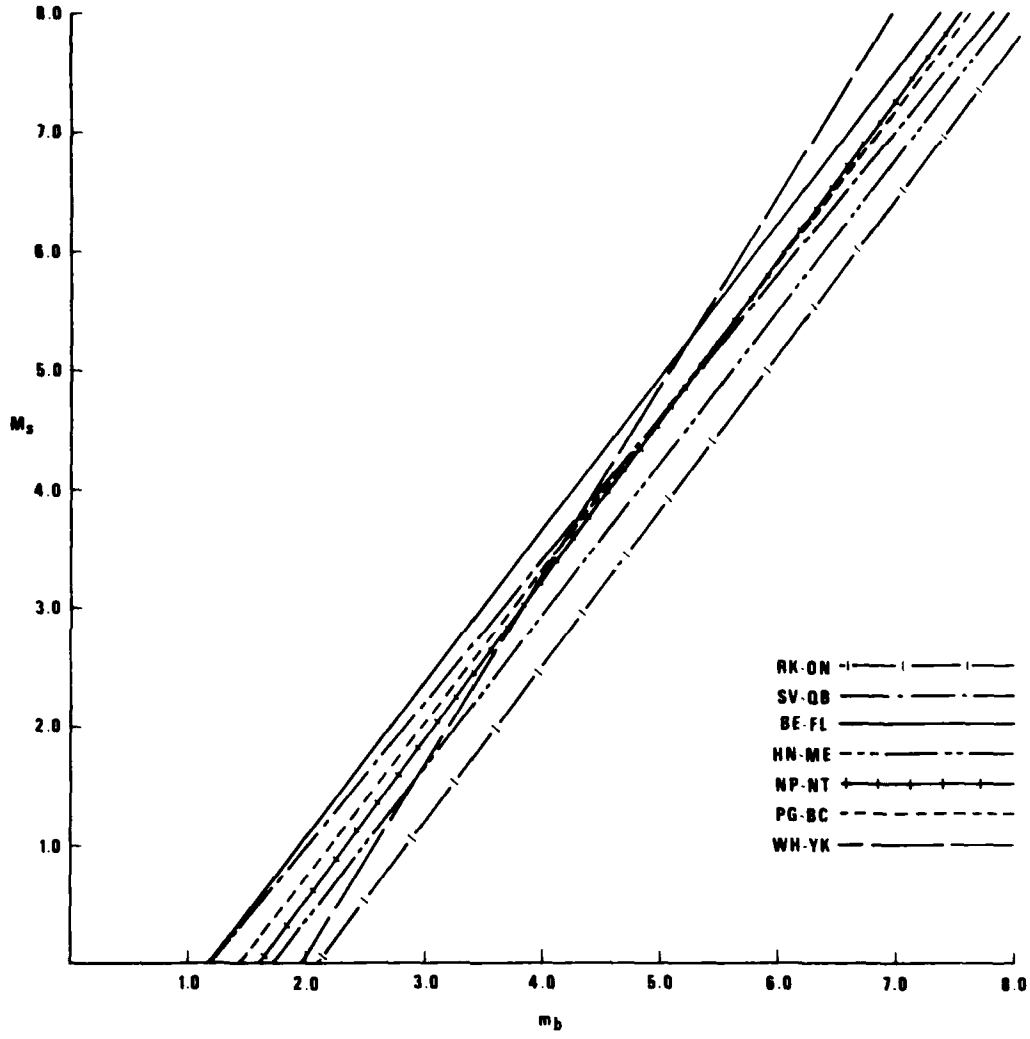

Figure 30 Single-station M_S-m_b discriminant functions with covariance matrices computed from network estimates of event magnitudes.

Also note that the value of D^2 was greater for every station when the network covariance was applied to each of the discriminants not using digital data. The effect of using the network covariance in the $M_s - m_b$ discriminant functions is shown in Figure 30.

Summary of the Three Experiments

In the first experiment, the maximum-likelihood estimator was used to calculate network averages of each variable's magnitude for each event, excluding spectral ratios and complexity. A process of stepwise discriminant analysis selected the most effective subsets of the ten variables. The discrimination capabilities of these and certain other subsets were evaluated according to three criteria: 1) the number of training set events which the discriminant misclassified; 2) the a posteriori probabilities, which measured how strongly a given event was classified into one of the two populations; 3) the F-approximation to Wilks' Λ-statistic, which measured how well the discriminant separated the means of the two groups. The polarity of the first motion was found to be the best discriminant. The results also showed that the effectiveness of the classical $M_s - m_b$ discriminant was enhanced when SPSR was added as a third variable and that it was enhanced still further when M_s was measured from LQ rather than from LR. Other discriminant pairs were found effective, though only when applied to events large enough to permit the magnitudes of all variables to be determined. Among them were SPP-SPS, SPP-LPS, and, particularly, SPP-LPP. The discriminant SPP-SPSR-complexity proved of some value in the absence of long-period data. Results also showed that forming ratios of magnitudes gave poorer discrimination than the magnitudes themselves. Finally, the Λ-statistic indicated a large separation of population means for almost every discriminant, even those which misclassified some events. Thus, the percentage point corresponding to the value found for the F-statistic tends to be misleadingly high in its evaluation of a discriminant's effectiveness.

The network discrimination method has two advantages over single-station discrimination. First, since the magnitude of each variable is calculated as an event mean, incomplete observations may be retained in the data set. For example, if the discriminant in question is $M_s - m_b$, then a station measurement of m_b may be used in the calculation of the mean m_b for that event

despite the absence of data for M_s from that station. Second, because event magnitudes based upon network detections are more accurate than are those based on individual station detections, the scatter of events in the two populations is reduced and there is less overlap. This is particularly true of events for which some stations were unable to measure all the variables on account of noise and for which magnitudes were then calculated by means of the maximun-likelihood estimator.

The principal disadvantage of the network method was that source-path effects and station effects were ignored, so the magnitudes of some events may have been systematically influenced by discordant values from particular stations. Another disadvantage was that a different number and configuration of stations was usually used to estimate the means of different variables for a given event.

The second experiment consisted of evaluating certain previously tested discriminants using data only from NP-NT or RK-ON. Results showed that no discriminant was very effective because for many events no one station detected all necessary variables. Thus, the size of the training set was reduced, and the event magnitudes retained were unreliable, causing the two populations to overlap. The single-station discriminant functions were more poorly determined in this experiment than in the multiple-station experiment because in the latter case the covariance matrices were calculated with pooled data from all stations rather than from each station's data alone.

The third experiment used the covariances of pooled data to calculate single-station discriminant functions which were summed to give a discriminant function for the entire network. Results showed that, for discriminants not involving spectral ratios or complexity, covariances calculated using the method of the first experiment were preferable to those based upon pooled data. For the most part, the effective discriminants were the same as those in the first experiment. However, there were more misclassifications by multi-station discriminants than by those based on network averages. In spite of this situation, average a posteriori probabilities were sometimes higher for the multiple-station case, indicating that this method tends to classify --or misclassify-- events strongly. A bad observation or a bad discriminant function for a

single station can, therefore, strongly affect the classification of an event.

The multiple-station discriminant function has at least two advantages. First, single-station discriminants can be ranked according to their values of D^2, and stations with low D^2 can be deleted from the data base. One might thus accommodate certain source-path effects by using multiple-station discriminants. Second, by not separately computing network averages of each variable and by retaining only those observations which detected all the necessary variables, a uniform data base is used for each of the variables for a given event. Discarding stations with incomplete observations creates a smaller volume of data than was retained in the first experiment; nevertheless, for a given event, the means for each variable are computed on the basis of observations from the same set of stations, and thus one may avoid possible biases in the means of different variables stemming from different station configurations and different variances due to nonuniform sample sizes.

The problem of missing data, already discussed in connection with single-station discrimination functions, causes many events to be deleted from the training set for many stations, resulting in poorly determined discriminant functions. The scatter in the magnitudes is also large for individual stations, and the maximum-likelihood estimator of event magnitudes is inapplicable. In the final analysis, therefore, discrimination based upon network magnitude estimates is preferable to that based on multiple-station discriminant functions unless: 1) there is a large data base of complete observations for events in both populations of the training set for each station; 2) the magnitudes measured at each station are not widely scattered around the true values; 3) the magnitudes are large enough that a bias is not introduced by the rejection of data vectors which, because of noise, did not include certain variable(s).

Recommendations on Classification of Unknown Events

While applying discriminant functions to events whose classification is unknown a priori is a simple process, it requires that an adequately large training set of known explosions and earthquakes be in the same source region as the unknown events. For both known and unknown events, magnitudes of the short-period and long-period P waves and S waves and those of the surface waves,

LQ and LR, should be measured, and the short-period spectral ratio should be calculated. (Discrimination based upon polarity of first motions can be carried out without reference to any discriminant function or training set). Ringdal's method should be used to compute event magnitudes using noise levels at the expected arrival times for all the stations in the network that do not detect the signal. The training set should be used to compute these seven discriminant functions: *SPP-SPS*, *SPP-LPP*, *SPP-LPS*, *SPP-LQ*, SPP-LR, SPP-LQ-SPSR, and SPP-LR-SPSR. Since the relative effectiveness of these discriminants may not be the same for events outside the Western United States as for events in this study, the number of a posteriori event misclassifications for each discriminant in the training set should be noted so that arbitrary weights can be assigned to the "best" discriminant functions. Classification based on the seven weighted discriminants (or as many as are applicable to the given region) is assumed more reliable than classification based on any one discriminant alone.

Each of the seven discriminant functions can be evaluated for the data vector consisting of magnitudes measured for a given unknown event. For the unknown events, however, we introduce the a priori probabilities h and 1-h for an explosion or an earthquake respectively and loss function $\ell(i,j)$ for classifying an event from the j-th population as one from the i-th. The criterion for discrimination, formerly equation (8), becomes (Morrison, 1976)

$$P_1(\vec{X}) > P_2(\vec{X}) \text{ if } \quad \vec{X} \cdot \vec{D} + C > \log_e \left[\frac{(1-h)\,\ell(1;2)}{h\,\ell(2;1)}\right]. \tag{32}$$

In addition, the appropriate changes are made in the computation of the classification probabilities given by (13).

The final step in the classification process is to take the sum, with arbitrary weights assigned to the "best" discriminants, of the classification probabilities calculated for each of the N discriminants ($N \leq 7$) and compute the mean probabilities

$$\overline{P_i(\vec{X})} = \frac{1}{N} \sum_{j=1}^{N} W_j [P_i(\vec{X})]_j \qquad i = 1,2. \tag{33}$$

One may assume for small events that discriminants SPP-SPS, SPP-LPP, and possibly SPP-LPS will be inapplicable. If an event is so small that no surface waves can be measured, then it may be classified, though not confidently, using the discriminant SPP-SPSR-complexity.

CONCLUSION

Results for seismic discrimination of events, selected from the Southwestern United States, were in good agreement with theoretical considerations and with past studies on other event groups in this region. Specifically, agreement existed between expectations and results for:

1) SP-LR. Theory predicts that only a few tenths separate smaller magnitude events on $M_s - m_b$ plots if the earthquakes are shallow. Our data included three that were only marginally separated from explosions. Two of these events were strike-slip (Baja California and Denver earthquakes) and the third was a mixture of strike-slip and dip-slip (BENHAM aftershock).
2) SPS-SPP or LPS-LPP. Shear waves from explosions are predicted to be relatively small. Our data shows that short-period or long-period S-wave amplitude is a good discriminant if it can be measured and that it should definitely be included in multiple-discrimination analysis.
3) SPP-LQ. For LQ as for shear waves, theory and past experience predict relatively less generation for explosions. Our data showed that LQ, if measurable, enhances discrimination because explosions have smaller LQ amplitudes and earthquakes often have large LQ when LR is small.
4) LPP-SPP. Theory predicts cancellation of LPP for shallow explosions. Data in this study supports this theory, showing that LPP, if measurable, is a good discriminant.
5) Corner frequency of P-wave spectrum. Because of more prolonged source time functions, earthquakes will have lower corner frequencies for a given seismic moment. This discriminant was studied at only two stations, but results were still encouraging. However, much higher P-wave S/N ratio is required than for m_b measurement in order to estimate these spectral parameters.
6) P-wave spectral ratio. Theory predicts no clear results for the band used in this study -- roughly 0.5 - 2.0 Hz. Likewise, our data showed little or no separation between earthquakes and explosions, even

after application of presumed attenuation corrections appropriate to each event's source area.

7) Complexity of P-wave signal. Only small enhancement of the coda level is possible because of the deeper crustal focus of earthquakes. For earthquakes with simple, short-duration rupture mechanisms, no increase in the coda level should occur. Although data from our event set showed that complexity was of some discrimination value, it is highly path-receiver dependent, making it unreliable.

8) Rayleigh-wave spectral ratio. This parameter, in the .02 - .05 Hz band used here, is known to vary in theory over a larger range of values for earthquakes than for explosions. Our data supported this prediction, and no separation was found between the two source types.

In addition to these discriminants, first motion was studied. In theory, first motion is an almost infallible method of identifying earthquakes, if clear dilatations are present. Although results from our events favored the first-motion discriminant, accuracy of first-motion data in practice is so debatable and the threshold so high for positive reading that these results are of limited importance. The theory of higher-mode surface waves was also discussed. However, examination of long-period recordings for our earthquakes did not reveal sufficient positive identifications of these arrivals to utilize them as another discrimination parameter.

A stepwise multiple-discrimination program provided a means of ranking the importance of the discriminants in classifying the two groups of the data set (explosions and earthquakes) used in this study. Ignoring first motion, they were ranked in the network experiment in order of value as discriminants thus:

1 - short-period P magnitude
2 - short-period P spectral ratio
3 - LQ magnitude
4 - complexity
5 - long-period LR spectral ratio
6 - LR magnitude
7 - short-period S magnitude

8 - long-period P magnitude

9 - long-period S magnitude

This ranking is tenuous because of the large number of missing data values, forcing reliance on poorly estimated values for several discriminants for many of the events. Changes in the ranking would undoubtedly occur with a new "training set." Note also that this is a single-dimension viewpoint and that the worth of each variable is highly dependent on the sampling procedure. For instance, although long-period S magnitudes were distributed similarly for the earthquakes and explosions of this study (see Figure 14), it was shown that in conjunction with other data, long-period S waves are a valuable discriminant.

Results of numerous experiments with the stepwise discriminant analysis program have been summarized adequately in the test and tables. Reiterated here are these important results:

1) The lowest a posteriori probability of correct classification for the 23 events was .983 when all ten variables were used. Removing first motion decreased this to .955.
2) A particularly good discriminant pair was m_b versus M_s when M_s was estimated from the combined LQ + LR amplitude. The lowest a posteriori probability for this pair was .683, the value for the Denver earthquake.
3) A combination of short-period discriminants, namely m_b, short-period spectral ratio, and complexity, misclassified only the Borrego Mountain earthquake. (Recall that m_b alone gives some separation between the two groups.) Spectral ratio and complexity as a pair misclassified four events, with several others nearly misclassified. Thus, discrimination using short-period P-wave data alone is probably not adequate.
4) Stepwise discrimination analysis using the data from only one station showed significantly smaller average a posteriori probabilities than analysis using network data for an identical parameter set.
5) Discrimination using discriminant functions averaged over separate functions computed for each station alone is inferior to starting with network-averaged parameters and using a network discrimination function.

Corner-frequency and moment parameters were not tested in the multiple-dis-discrimination work because of the small amount of data accumulated and the

rather subjective way of estimating parameters. Still, where digital data is available and when a more objective approach to estimating these parameters is implemented, they should be included because even the limited results here demonstrated their potential classification power.

The data set for this study contained only single explosions and no shot arrays. Traditional discrimination tests involving complexity and possibly those involving first motion would be inapplicable to multiple explosions. Tests based upon ratios of short-period to long-period data, such as $M_s - m_b$, would also be invalid for such events. Perhaps the best teleseismic discriminants applicable to shot arrays are the ratio of short-period S to m_b and of long-period P or S to M_s; at regional distances, the ratio of crustal P phases to L_g could be used as a short-period substitute for $M_s - m_b$.

There are no reasons to think that path or receiver effects peculiar to this study would negate the conclusions regarding the worth of the various discriminants studied. Note that the conclusions are robust because network estimates of parameters were made. Less positive conclusions would have been reached if only data from one station were used. Statistics of the multiple discrimination experiment clearly demonstrated this test. In addition, using a network obviously lowers the threshold for application of the discriminants and allows magnitude estimates to be made according to Ringdal's (1976) method, which is a powerful tool in overcoming magnitude bias due to a combination of detection threshold and path and station effects.

Results of this study show that some earthquakes in the Southwestern United States are only marginally separated from explosions, even with the application of a number of discrimination parameters. The failure of the $M_s - m_b$ pair to separate events clearly is an important finding here. No common thread seems to link those three events (Denver earthquake, Baja earthquake, and BENHAM Aftershock) that were particularly hard to discriminant. They were in distinct, separate areas, had no common source mechanism, and had different depths of focus.

This study indicates that confident seismic discrimination requires both long-period and short-period recordings and that horizontal motion recordings

are quite helpful in both passbands. Though pP analysis has been virtually ignored because of the generally shallow event depths, the authors believe that efforts to extract depth information could lead to some additional aid for classification of Southwestern United States events.

ACKNOWLEDGEMENT

Much of the task of data collection for this study was performed by E. I. Sweetser. Comments on drafts of this report by R. R. Blandford and R. H. Shumway are much appreciated.

REFERENCES

Aboudi, J. (1972). The response of an elastic halfspace to the dynamic expansion of an embedded spherical cavity. Bull. Seism. Soc. Am., 62, 115-128.

Aki, K. (1967). Scaling law of seismic spectrum. J. Geophys. Res., 72, 1217-1231.

Aki, K., P. Reasenberg, T. DeFazio, and Y.-B. Tsai (1969). Near-field and far-field seismic evidences for triggering of an earthquake by the BENHAM explosion. Bull. Seism. Soc. Am., 59, 2197-2207.

Aki, K., and Y.-B. Tsai (1972). Mechanism of Love-wave excitation by explosive sources. J. Geophys. Res., 77, 1452-1475.

Aki, K. (1972). Scaling law of earthquake source-time function. Geophys. J., 31, 3-26.

Aki, K., M. Bouchon, and P. Reasenberg (1974). Seismic source function for an underground nuclear explosion. Bull. Seism. Soc. Am., 64, 131-148.

Alexander, S. S. (1963). Surface wave propagation in the Western United States. Ph.D. Thesis, California Institute of Technology, Pasadena, California.

Allen, C. R., L. T. Silver, and F. G. Stehi (1960). Agua Blanca fault - a major transverse structure of northern Baja California. Bull. Geol. Soc. Am., 71, 457-482.

Allen, C. R., P. St. Amand, C. F. Richter, and J. M. Nordquist (1965). Relationship between seismicity and geologic structure in the southern California region. Bull. Seism. Soc. Am., 55, 753-797.

Anderson, T. W. (1958). An Introduction to Multivariate Statistical Analysis. New York, NY., John Wiley and Sons.

Andrews, D. J. (1973). A numerical study of tectonic strain release by underground explosions. Bull. Seism. Soc. Am., 63, 1375-1391.

Anglin, F. M. (1971). Discrimination of earthquakes and explosions using short-period seismic array data. Nature, 233, 51-52.

Archambeau, C. B., E. A. Flinn, and D. G. Lambert (1969). Fine structure of the upper mantle. J. Geophys. Res., 74, 5825-5865.

Archambeau, C. B., and C. Sammis (1970). Seismic radiation from explosions in prestressed media and the measurement of tectonic stress in the earth. Rev. Geophys., 8, 473-499.

Archambeau, C. B. (1972). The theory of stress wave radiation from explosions in prestressed media. Geophys. J., 29, 329-366.

Archuleta, R. J., and J. N. Brune (1975). Surface strong motion associated with a stick-slip event in a foam rubber model of earthquakes. Bull. Seism. Soc. Am., 65, 1059-1072.

Atwater, T. (1970). Implications of plate tectonics for the Cenozoic tectonic evolution of western North America. Geol. Soc. Amer. Bull., 81, 3513-3536.

Bakun, W. H., and L. R. Johnson (1970). Short-period spectral discriminants for explosions. Geophys. J., 22, 139-152.

Barazangi, M., W. Pennington, and B. Isacks (1975). Global study of seismic wave attentuation in the upper mantle behind island arcs using pP waves. J. Geophys. Res., 80, 1079-1092.

Barker, T. G., T. C. Bache, J. T. Cherry, N. Rimer, and J. M. Savino (1976). Prediction and matching of teleseismic ground motion (body and surface waves) from the NTS MAST explosion. Report No. SSS-R-76-2727, Systems, Science, and Software, La Jolla, California.

Basham, P. W. (1969). Canadian magnitudes of earthquakes and nuclear explosions in south-western North America. Geophys. J., 17, 1-14.

Basham, P. W., D. H. Wiechert, and F. M. Anglin (1970). An analysis of the BENHAM aftershock sequence using Canadian recordings. J. Geophys. Res., 75, 1545-1556.

Ben-Menahem, A., and D. G. Harkrider (1964). Radiation patterns of seismic surface waves from buried dipolar point sources in a flat stratified earth. J. Geophys. Res., 69, 2605-2620.

Biswas, N. N., and L. Knopoff (1974). The structure of the upper mantle under the United States from the dispersion of Rayleigh waves. Geophys. J., 36, 515-539.

Blake, F. C. (1952). Spherical wave propagation in solid media. J. Acoust. Soc. Amer., 24, 211-215.

Blandford, R., and D. Clark (1974). Detection of long-period S from earthquakes and explosions at LASA and LRSM stations with application to positive and negative discrimination of earthquakes and underground explosions. Report No. SDAC-TR-74-15, Teledyne Geotech, Alexandria, Virginia. (AD 401 3672)

Blandford, R. R. (1975). Use of source-region-station-time corrections at NTS for depth estimation. Report No. SDAC-TR-75-4, Teledyne Geotech. (ADA 025349)

Bolt, B. A., C. Lomnitz, and T. V. McEvilly (1968). Seismological evidence on the tectonics of central and northern California and the Mendocino Escarpment. Bull. Seism. Soc. Am., 58, 1725-1767.

Booker, A., and W. Mitronovas (1964). An application of statistical discrimination to classify seismic events. Bull. Seism. Soc. Am., 54, 961-971.

Bouchon, M. (1976). Teleseismic body wave radiation from a seismic source in a layered medium. Geophys. J., 47, 515-530.

Brace, W. F., and J. D. Byerlee (1970). California earthquakes, w. only shallow focus. Science, 156, 1573-1575.

Braile, L. W., R. B. Smith, G. R. Keller, R. M. Welch, and R. P. Meyer (1974). Crustal structure across the Wasatch Front from detailed seismic refraction studies. J. Geophys. Res., 79, 2669-2677.

Briscoe, H. W., and J. Walsh (1967). Ratios of spectral densities. Seismic Discrimination-- Semiannual Technical Summary, 30 June 1967, Lincoln Laboratory, Lexington, Mass.

Brune, J. N., and P. W. Pomeroy (1963). Surface-wave radiation patterns for underground nuclear explosions and small magnitude earthquakes. J. Geophys. Res., 68, 5005-5028.

Brune, J. N. (1970). Tectonic stress and the spectra of seismic shear waves from earthquakes. J. Geophys. Res., 75, 4997-5010

Burridge, R., and L. Knopoff (1964). Body force equivalents for seismic dislocations. Bull. Seism. Soc. Am., 54, 1875-1888.

Canitez, N., and M. N. Toksöz (1971). Focal mechanism and source depth of earthquakes from body- and surface-wave data. Bull. Seism. Soc. Am., 61, 1369-1379.

Carpenter, E. W. (1964). Teleseismic methods for the detection, identification, and location of underground explosions. VESIAC Report 4410-67-X, Acoustics and Seismics Laboratory, University of Michigan, Ann Arbor, Michigan.

Cleary, J., and A. L. Hales (1966). An analysis of the travel times of P waves to North American stations, in the distance range 32° to 100°. Bull. Seism. Soc. Am., 56, 467-489.

Cleary, J. (1967). Analysis of the amplitudes of short-period P waves recorded by Longe Range Seismic Measurements stations in the distance range 30° to 102°. J. Geophys. Res., 72, 4705-4712.

Cohen, T. (1970). Source-depth determination using spectral, pseudo-autocorrelation, and cepstral analysis. Geophys. J., 20, 223-231.

Cohen, T. J., R. L. Sax, and H. L. Husted (1972). Spectral whitening with application to explosion pP. Seismic Data Laboratory Report No. 282, Teledyne Geotech, Alexandria, Virginia. (AD 750 781)

Cook, K. L., and R. B. Smith (1967). Seismicity in Utah, 1850 through June 1965. Bull. Seism. Soc. Am., 57, 689-718.

Cook, K. L. (1969). Active rift system in the Basin and Range province. Tectonophysics, 8, 469-511.

Dahlen, F. A. (1974). On the ratio of P-wave to S-wave corner frequencies for shallow earthquake sources. Bull. Seism. Soc. Am., 67, 1159-1180.

Dahlman, O., H. Israelson, A. Austegard, and G. Hornstrom (1974). Definition and identification of seismic events in the USSR in 1971. Bull. Seism. Soc. Am., 64, 607-636.

Davies, D., and D. P. McKenzie (1969). Seismic travel-time residuals and plates. Geophys. J., 18, 51-63.

Davies, J. B., and S. W. Smith (1968). Source parameters of earthquakes and discrimination between earthquakes and nuclear explosions. Bull. Seism. Soc. Am., 58, 1503-1517.

Davies, D., and B. R. Julian (1972). A study of short period P-wave signals from LONGSHOT. Geophys. J., 29, 185-202.

Derr, J. S. (1970). Discrimination of earthquakes and explosions by the Rayleigh-wave spectral ratio. Bull. Seism. Soc. Am., 60, 1653-1668.

Der, Z. A. (1973). $M_s - m_b$ characteristics of earthquakes in the eastern Himalayan regions. SDL Report No. 296, Teledyne Geotech, Alexandria, Virginia.

Der, Z. A., R. P. Massé, and J. P. Gurski (1975). Regional attenuation of short-period P and S waves in the United States. J. Geophys. Res., 40, 85-106.

Der, Z. A. (1976). On the existence, magnitude, and causes of broad regional variations in body-wave amplitudes. SDAC Report No. TR-76-8. Teledyne Geotech, Alexandria, Virginia.

Der, Z. A. and T. W. McElfresh, (1977). The relationship between anelastic attenuation and regional amplitude anomalies of short-period P waves in North America, Bull. Seism. Soc. Am., 67, 1303-1317.

Douglas, A., J. A. Hudson, and V. K. Kembhavi (1971). The relative excitation of seismic surface and body waves by point sources. Geophys. J., 23, 451-460.

Douglas, A. D., J. Corbishley, C. Blamey, and P. D. Marshall (1972a). Estimating the firing depth of underground explosions. Nature, 237, 26-28.

Douglas, A., J. A. Hudson, and C. Blamey (1972b). A quantitative evaluation of seismic signals at teleseismic distances -- III: Computed P and Rayleigh wave seismograms. Geophys. J., 28, 385-410.

Douglas, A., P. D. Marshall, P. G. Gibbs, J. B. Young, and C. Blamey (1973) P signal complexity re-examined. Geophys. J., 33, 195-233.

Douglas, A., J. B. Young, and J. A. Hudson (1974a). Complex P-wave seismograms from simple earthquake sources. Geophys. J., 37, 141-150.

Douglas, A., J. A. Hudson, P. D. Marshall, and J. B. Young (1974b). Earthquakes that look like explosions. Geophys. J., 36, 227-233.

Dunn, O. J. (1971). Some expected values for probabilities of correct classification in discriminant analysis. Technometrics, 13, 345-353.

Eaton, J. (1963). Crustal structure from San Francisco, California, to Eureka, Nevada, from seismic refraction measurements. J. Geophys. Res., 68, 5789-5806.

Eisler, J. D., F. Chilton, and F. M. Sauer (1966). Multiple subsurface spalling by underground nuclear explosions. J. Geophys. Res., 71, 3023-3027.

Enescu, D., A. Georgesu, D. Jianu, and I. Zamarca (1973). Theoretical model for the process of underground explosions. Contributions to the problem of the separation of large explosions from earthquakes. Bull. Seism. Soc. Am., 73, 765-786.

Ericsson, U. A. (1970). Event identification for test ban control. Bull. Seism. Soc. Am., 60, 1521-1546.

Evernden, J. F. (1969). Identification of earthquakes and explosions by use of teleseismic data. J. Geophys. Res., 74, 3828-3856.

Evernden, J. (1970). Magnitude versus yield of explosions. J. Geophys. Res., 75, 1028-1032.

Evernden, J., and D. Clark (1970). Study of teleseismic P, Part II: Amplitude data. Phys. Earth Planet. Interiors, 4, 24-31.

Evernden, J. F. (1971). Location capability of various seismic networks. Bull. Seism. Soc. Am., 61, 241-273.

Evernden, J. F., and J. Filson (1971). Regional dependence of surface-wave versus body-wave magnitudes. J. Geophys. Res., 76, 3303-3308.

Evernden, J. F., W. J. Best, P. W. Pomeroy, T. V. McEvilly, J. M. Savino, and L. R. Sykes (1971). Discrimination between small-magnitude earthquakes and explosions. J. Geophys. Res., 76, 8042-8055.

Evernden, J. (1975). Further studies on seismic discrimination. Bull. Seism. Soc. Am., 65, 359-392.

Evernden, J. (1976). Study of seismological evasion, Part III. Evaluation of evasion possibilities using codas of large earthquakes. Bull. Seism. Soc. Am., 66, 549-592.

Frantti, G. E. (1963). Energy spectra for underground explosions and earthquakes. Bull. Seism. Soc. Am., 53, 995-1005.

Frasier, C. W. (1972). Observations of pP in the short-period phases of NTS explosions recorded at Norway. Geophys. J., 31, 99-109.

Forsyth, D. W. (1976). Higher-mode Rayleigh waves as an aid to seismic discrimination. Bull. Seism. Soc. Am., 66, 827-842.

Geyer, R. L., and S. T. Martner (1969). SH waves from explosive sources. Geophysics, 34, 893-905.

Gilbert, F. (1973). The relative efficiency of earthquakes and explosions in exciting surface waves and body waves. Geophys. J., 33, 487-488.

Glover, P., and S. S. Alexander (1970). A comparison of the Lake Superior and Nevada Test Site regions. SDL Report No. 243, Teledyne Geotech, Alexandria, Virginia. (AD 865 512)

Gough, D. I. (1973). The geophysical significance of geomagnetic variation anomalies. Phys. Earth. Planet. Int., 7, 379-388.

Greenfield, R. J. (1971). Short-period P-wave generation by Rayleigh-wave scattering at Novaya Zemlya. J. Geophys. Res., 76, 7988-8002.

Grover, A. (1973). Radiation from an explosion in a non-uniformly prestressed medium. Geophys. J., 32, 351-371.

Guha, S. K., and W. Stauder (1970). The effect of focal depth on the spectra of P waves. II. Observational studies. Bull. Seism. Soc. Am., 60, 1457-1477.

Gumper, F. J., and C. Scholz (1971). Microseismicity and tectonics of the Nevada seismic zone. Bull. Seism. Soc. Am., 61, 1413-1432.

Hales, A. L., and J. L. Roberts (1970). The travel times of S and SKS. Bull. Seism. Soc. Am., 60, 461-489.

Hamilton, W., and W. B. Meyers (1966). Cenozoic tectonics of the Western United States. Rev. of Geophys., 4, 509-549.

Hamilton, R. M., and J. H. Healy (1969). Aftershocks of the BENHAM nuclear explosion. Bull. Seism. Soc. Am., 59, 2271-2281.

Hamilton, R. M., B. E. Smith, F. G. Fisher, and P. J. Paponek (1972). Earthquakes caused by underground nuclear explosions on Pahute Mesa, Nevada Test Site. Bull. Seism. Soc. Am., 62, 1319-1341.

Hanks, T. C., and W. Thatcher (1972). A graphical representation of seismic source parameters. J. Geophys. Res., 77, 4393-4405.

Hanks, T. C., and M. Wyss (1972). The use of body-wave spectra in the determination of seismic source parameters. Bull. Seism. Soc. Am., 62, 561-590.

Harkrider, D. G. (1964). Surface waves in multilayered elastic media, I, Rayleigh and Love waves from buried sources in a multilayered elastic halfspace. Bull. Seism. Soc. Am., 54, 627-679.

Harkrider, D. G. (1970). Surface waves in multilayered elastic media. II. Higher mode spectra and spectral ratios from point sources in plane layered earth models. Bull. Seism. Soc. Am., 60, 1937-1988.

Hasegawa, H. S. (1971). Analysis of teleseimic signals from underground nuclear explosions originating in four geological environments. Geophys. J., 24, 365-381.

Haskell, N. A. (1964). Total energy and energy spectral density of elastic wave radiation from propagating faults. Bull. Seism. Soc. Am., 54, 1811-1841.

Haskell, N. A. (1966). Total energy and energy spectral density of elastic wave radiation propagating faults. Part II. A statistical source model. Bull. Seism. Soc. Am., 56, 125-140.

Hattori, S. (1972). Investigation of seismic waves generated by small explosions. Bull. Int. Inst. Seismol. Earthquake Eng., 9, 27-105.

Healy, J. H. (1963). Crustal structure along the coast of California from seismic-refraction measurements. J. Geophys. Res., 68, 5777-5787.

Healy, J. H., C. Y. King, and M. E. O'Neill (1971). Source parameters of the SALMON and STERLING nuclear explosions from seismic measurements. J. Geophys. Res., 76, 344-355.

Healy, J. H., W. W. Rubey, D. T. Griggs, and C. B. Rayleigh (1968). The Denver earthquakes. Science, 161, 1301-1310.

Helmberger, D. V., and D. G. Harkrider (1972). Seismic source descriptions of underground explosions and a depth discriminant. Geophys. J., 31, 45-66.

Helmberger, D. V. (1973). On the structure of the low velocity zone. Geophys. J., 34, 251-263.

Herrin, E., and J. Taggart (1962). Regional variations in P_n velocities and their effect on the location of epicenters. Bull. Seism. Soc. Am., 52, 1037-1046.

Herrin, E., and J. Taggart (1968). Regional variations in P travel times. Bull. Seism. Soc. Am., 58, 1325-1337.

Hirasawa, T. (1971). Radiation patterns of S waves from underground nuclear explosions. J. Geophys. Res., 76, 6440-6454.

Holzer, F. (1965). Measurement and calculations of peak shock-wave parameters from underground nuclear detonations. J. Geophys. Res., 70, 893-905.

Hudson, J. A., and A. Douglas (1975). On the amplitudes of seismic waves. Geophys. J., 42, 1030-1044.

Isacks, B., J. Oliver, and L. R. Sykes (1968). Seismology and the new global tectonics. J. Geophys. Res., 73, 5855-5900.

Jeffreys, H. (1931). On the cause of oscillatory movements in seismograms. Monthly Notices of the Royal Astonomical Society, 8, 408-416.

Jennrich, R. I, (1977). Stepwise discriminant analysis, in Statistical Methods for Digital Computers, K. Enslien et al. (eds.) New York, John Wiley and Sons.

Johnson, L. (1967). Array measurements of P velocities in the upper mantle. J. Geophys. Res., 72, 6309-6325.

Julian, B. R., and D. L. Anderson (1968). Travel times, apparent velocities and amplitudes of body waves. Bull. Seism. Soc. Am., 58, 339-366.

Keilis-Borok, V. I., and T. B. Yanovskaya (1962). Dependence of the spectrum of surface waves on the depth of the focus with the earth's crust. Izv. Akad. Nauk. USSR, Geophys. Ser., 11, p. 1532-1539. (English translation).

Keller, G. R., R. B. Smith, and L. W. Braile (1975). Crustal structure along the Great Basin - Colorado Plateau transition from seismic refraction studies. J. Geophys. Res., 80, 1093-1098.

Kim, W. H., and C. Kisslinger (1967). Model investigations of explosions in prestressed media. Geophysics, 32, 633-651.

King, P. B. (1969). The tectonics of North America--A discussion to accompany the tectonic map of North America. United States Geological Survey, Department of the Interior, Washington, D. C.

Kisslinger, C., E. J. Mateker, and T. V. McEvilly (1961). SH waves from explosions in soil. J. Geophys. Res., 66, 3487-3497.

Kogeus, K. (1968). A synthesis of short-period P-wave records from distant explosion sources. Bull. Seism. Soc. Am., 58, 663-680.

Kolar, O. C., and N. L. Pruvost (1975). Earthquake simulation by nuclear explosions. Nature, 253, 242-245.

Kovach, R. L., and R. Robinson (1969). Upper-mantle structure in the Basin and Range Province, Western North America, from the apparent velocities of S waves. Bull. Seism. Soc. Am., 59, 1653-1665.

Kulhanek, O. (1971). P-wave amplitude spectra of Nevada underground nuclear explosions. Pure Appl. Geophys., 88, 121-136.

Lacoss, R. T. (1969). A large-population LASA discrimination experiment. Technical Note 1969-24, Lincoln Laboratory, Lexington, Mass.

Lambert, D. G., D. H. von Seggern, S. S. Alexander, and G. A. Galat (1969). The LONG SHOT experiment. Volume II. Comprehensive analysis. SDL Report No. 234, Teledyne Geotech, Alexandria, Virginia. (AD 698 319)

Lambert, D. G., E. A. Flinn, and C. B. Archambeau (1972). A comparative study of the elastic wave radiation from earthquakes and underground explosions. Geophys. J., 29, 403-432.

Landers, T. (1972). Some interesting central Asian events on the M_s:m_b diagrams. Geophys. J., 31, 329-339.

Langston, C. A. (1976). A body wave inversion of the Koyna, India, Earthquake of December 10, 1967, and some implications for body wave focal mechanisms. J. Geophys. Res., 81, 2517-2529.

Leet, L. D. (1962). The detection of underground explosions. Scientific American, 206, 55-59.

Liebermann, R. C., and P. W. Pomeroy (1969). Relative excitation of surface waves by earthquakes and underground explosions. J. Geophys. Res., 74, 1575-1590.

Liebermann, R. C., and P. W. Pomeroy (1970). Source dimensions of small earthquakes as determined from the size of the aftershock zone. Bull. Seism. Soc. Am., 60, 879-890.

Love, A. E. H. (1944). A Treatise on the Mathematical Theory of Elasticity. New York, New York, Dover Publications.

Major, M. W., and R. B. Simon (1968). A seismic study of the Denver (Derby) Earthquakes. Quarterly of the Colorado School of Mines, 63, 9-56.

Manchee, E. B. (1972). Short-period seismic discrimination. Nature, 239, 152-153.

Manchee, E. B., and H. S. Hasegawa (1973). Seismic spectra of Yucca Flat underground explosions observed at Yellowknife, Northwest Territories. Can. J. Earth Sci., 10, 421-427.

Marshall, P. D. (1970). Aspects of the spectral differences between earthquakes and underground explosions. Geophys. J., 20, 397-416.

Marshall, P. D., and P. W. Basham (1972). Discrimination between earthquakes and underground explosions employing an improved M_S scale. Geophys. J., 28, 431-458.

Maruyama, T. (1963). On the force equivalents of dynamic elastic dislocations with reference to the earthquake mechanism. Bull. Earthquake Res. Inst., 41, 467-486.

Massé, R. P., M. Landisman, and J. B. Jenkins (1972). An investigation of the upper-mantle compressional velocity distribution beneath the Basin and Range Province. J. Geophys. Res., 30, 19-36.

Massé, R. P., D. G. Lambert, and D. G. Harkrider (1973). Precision of the determination of focal depth from the spectral ratio of Love/Rayleigh surface waves. Bull. Seism. Soc. Am., 63, 59-100.

McEvilly, T. V., and W. A. Peppin (1972). Source characteristics of earthquakes, explosions, and afterevents. Geophys. J., 31, 67-82.

McKeown, F. A., and D. D. Dickey (1969). Fault displacements and motion related to nuclear explosions. Bull. Seism. Soc. Am., 59, 2253-2270.

McLachlan, G. J. (1974). Estimation of the errors of misclassification on the criterion of asymptotic mean square error. Technometrics, 16, 255-260.

Meister, L. J., R. O. Burford, G. A. Thompson, and R. L. Kovach (1968). Surface strain changes and strain energy release in the Dixie Valley - Fairview Peak Area, Nevada. J. Geophys. Res., 73, 5981-5994.

Menard, H. W. (1960). The East Pacific Rise. Science, 132, 1737-1746.

Mikumo, T. (1965). Crustal structure in central California in relation to the Sierra Nevada. Bull. Seism. Soc. Am., 55, 65-83.

Mitchell, B. J. (1975). Regional Rayleigh-wave attenuation in North America. J. Geophys. Res., 80, 4904-4916.

Molnar, P., and J. Oliver (1969). Lateral variations of attenuation in the upper mantle and discontinuities in the lithosphere. J. Geophys Res., 74, 2648-2682.

Molnar, P., K. Jacob, and L. R. Sykes (1969). Microearthquake activity in eastern Nevada and Death Valley, California, before and after the nuclear explosion BENHAM. Bull. Seism. Soc. Am., 59, 2177-2184.

Molnar, P. (1971). P-wave spectra from underground nuclear explosions. Geophys. J., 23, 273-287.

Molnar, P., B. E. Tucker, and J. N. Brune (1973). Corner frequencies of P and S waves and models of earthquake sources. Bull. Seism. Soc. Am., 63, 2091-2104.

Morrison, D. F. (1976). Multivariate Statistical Methods. New York, McGraw-Hill Publishing Company.

Mueller, R. A., and J. R. Murphy (1971). Seismic characteristics of underground nuclear detonations, Part I. Seismic spectrum scaling. Bull. Seism. Soc. Am., 61, 1675-1692.

Mueller, S., and M. Landisman (1971). An example of the unified method of interpretation for crustal seismic data. Geophys. J., 23, 365-371.

Muller, G. (1973). Seismic moment and long-period radiation of underground nuclear explosions. Bull. Seism. Soc. Am., 73, 847-857.

Niazi, M., and D. L. Anderson (1965). Upper-mantle structure of Western North America from apparent velocities of P waves. J. Geophys. Res., 70, 4633-4640.

Nuttli, O. W. (1969). Travel times and amplitudes of S waves from nuclear explosions in Nevada. Bull. Seism. Soc. Am., 59, 385-389.

Oliver, J., P. Pomeroy, and M. Ewing (1960). Long-period surface waves from nuclear explosions in various environments. Science, 131, 1804-1805.

Oliver, H. W., L. C. Pakiser, and M. F. Kane (1961). Gravity anomalies in the Central Sierra Nevada, California. J. Geophys. Res., 66, 4265-4271.

Olsen, C. W. (1967). Time history of the cavity pressure and temperature following a nuclear detonation in alluvium. J. Geophys. Res., 72, 5037-5041.

Olsen, C. W. (1970). Soil strain near a nuclear detonation. Bull. Seism. Soc. Am., 60, 1999-2014.

Pakiser, L. C. (1963). Structure of the crust and upper mantle in the Western United States. J. Geophys. Res., 68, 5747-5756.

Pasechnik, I. P., G. G. Dashkov, L. A. Polikarpova, and N. G. Gamburtseva (1970). The magnitude method for identification of underground nuclear explosions. Izv. Phys. Solid Earth, No. 1, January 1970, (English translation).

Peppin, W. A., and T. V. McEvilly (1974). Discrimination among small magnitude events on Nevada Test Site. Geophys. J., 37, 227-243.

Peppin, W. A. (1976). P-wave spectra of Nevada Test Site events at near and very-near distances: Implications for a near-regional body wave-surface wave discriminant. Bull. Seism. Soc. Am., 66, 803-826.

Perret, W. R. (1972). GASBUGGY seismic source measurements. Geophysics, 37, 301-312.

Porath, H., and D. I. Gough (1971). Mantle conductive structures in the Western United States from magnetometer array studies. Geophys. J., 22, 261-275.

Press, F. (1960). Crustal structure in California-Nevada region. J. Geophys. Res., 65, 1039-1051.

Press, F., and C. Archambeau (1962). Release of tectonic strain by underground nuclear explosions. J. Geophys. Res., 67, 337-343.

Press, F., G. Dewart, and R. Gilman (1963). A study of diagnostic techniques for identifying earthquakes. J. Geophys. Res., 68, 2909-2928.

Priestley, K. (1974). Crustal strain measurements in Nevada. Bull. Seism. Soc. Am., 64, 1319-1328.

Prodehl, C. (1970). Seismic refraction study of crustal structure in the Western United States. Geol. Soc. Am. Bull., 81, 2629-2646.

Randall, M. J. (1973). The spectral theory of seismic sources. Bull. Seism. Soc. Am., 63, 1133-1144.

Rasmussen, D., and L. Lande (1968). Seismic analysis of the GASBUGGY explosion and an earthquake of similar magnitude and epicenter. Report No. 68-15, Teledyne Geotech, Garland, Texas.

Reitzel, J. S., D. I. Gough, H. Porath, and C. W. Anderson III (1970). Geomagnetic deep sounding and upper mantle structure in the Western United States. Geophys. J., 19, 213-236.

Ringdal, F. (1976). Maximum-likelihood estimation of seismic magnitude. Bull. Seism. Soc. Am., 66, 789-802.

Rodean, H. C. (1971). Nuclear-Explosion Seismology. USAEC Division of Technical Information, Oak Ridge, Tennessee.

Roy, R. F., E. R. Decker, D. D. Blackwell, and F. Birch (1968). Heat flow in the United States. J. Geophys. Res., 73, 5207-5221.

Ryall, A., and S. D. Malone (1971). Earthquake distribution and mechanism of faulting in the Rainbow Mountain - Dixie Valley - Fairview Peak Area, central Nevada. J. Geophys. Res., 76, 7241-7248.

Sass, J. H., A. H. Lachenbruch, R. J. Munroe, G. W. Green, and T. H. Moses (1971). Heat flow in the Western United States. J. Geophys. Res., 76, 6376-6413.

Savage, J. C. (1966). Radiation from a realistic model of faulting. Bull Seism. Soc. Am., 56, .577-592.

Savage, J. C. (1972). Relation of corner frequency to fault dimensions. J. Geophys. Res. 77, 3788-2795.

Savage, J. C., and R. O. Burford (1973). Geodetic determination of relative plate motion in central California. J. Geophys. Res., 78, 832-845.

Savage, J. C. (1974). Relation between P- and S-wave corner frequencies in the seismic spectrum. Bull. Seism. Soc. Am., 64, 1621-1628.

Savino, J., L. R. Sykes, R. C. Liebermann, and P. Molnar (1971). Excitation of seismic surface waves with periods of 15 to 70 seconds for earthquakes and underground explosions. J. Geophys. Res., 76, 8003-8020.

Sbar, M. L., M. Barazangi, J. Dorman, C. H. Scholz, and R. B. Smith (1972). Tectonics of the intermountain seismic belt, Western United States, microearthquakes, seismicity, and composite fault plane solutions. Geol. Soc. Amer. Bull., 83, 13-28.

Scholz, C. H., M. Barazangi, and M. L. Sbar (1971). Late Cenozoic evolution of the Great Basin, Western United States, as an ensialic interarc basin. Geol. Soc. Amer. Bull., 82, 2979-2990.

Sharpe, J. A. (1942). The production of elastic waves by explosion pressures, Part I. Geophys., 7, 144-154.

Shaw, H. R., R. W. Kistler, and J. F. Evernden (1971). Sierra Nevada plutonic cycle: Part II, tidal energy and a hypothesis for orogenic-epeirogenic periodicties. Geol. Soc. Am. Bull., 82, 869-896.

Shumway, R. H., and R. R. Blandford (1970). A simulation of seismic discriminant analysis. SDL Report No. 261, Teledyne Geotech, Alexandria, Virginia. (AD 881 720)

Shurbet, D. H. (1969). Excitation of Rayleigh waves. J. Geophys. Res., 74, 5339-5341.

Shurbet, D. H., and S. E. Cebull (1971). Crustal low-velocity layer and regional extension in the Basin and Range province. Geol. Soc. Amer. Bull., 82, 3241-2344.

Slemmons, D. B., A. E. Jones, and J. I. Gimlett (1965). Catalog of Nevada earthquakes, 1850-1960. Bull. Seism. Soc. Am., 55, 537-583.

Smith, S. W. (1963). Generation of seismic waves by underground explosions and the collapse of cavities. J. Geophys. Res., 68, 1477-1483.

Smith, R. B., and M. Sbar (1974). Contemporary tectonics and seismicity of the Western United States, with emphasis on the intermountain seismic belt. Geol. Soc. Amer. Bull., 85, 1205-1218.

Snoke, J. A. (1976). Archambeau's elastodynamic source model solution and low-frequency peaks in the far-field displacement amplitude from earthquakes and explosions. Geophys. J., 44, 27-44.

Solomon, S. C., and M. N. Toksöz (1970). Lateral variation of attenuation of P and S waves beneath the United States. Bull. Seism. Soc. Am., 60, 819-838.

Solomon, S. C. (1972a). Seismic wave attenuation and partial melting in the upper mantle of North America. J. Geophys. Res., 77, 1483-1502.

Solomon, S. C. (1972b). On Q and seismic discrimination. Geophys. J., 31, 163-177.

Springer, D. L., and R. L. Kinnaman (1971). Seismic source summary for U. S. underground nuclear explosions, 1961-1970. Bull. Seism. Soc. Am., 61, 1073-1098.

Springer, D. L., and W. J. Hannon (1973). Amplitude-yield scaling for underground nuclear explosions. Bull. Seism. Soc. Am., 63, 477-500.

Stauder, W., and A. Ryall (1967). Spatial distribution and source mechanism of microearthquakes in central Nevada. Bull. Seism. Soc. Am., 57, 1317-1345.

Taylor, G. I. (1950). The instabilities of liquid surfaces when accelerated in a direction perpendicular to their planes. Proc. Roy. Soc. London, Series A, 201, 192-196.

Thatcher, W. (1972). Regional variation of seismic source parameters in the northern Baja California area. J. Geophys. Res., 77, 1549-1565.

Thatcher, W., and J. N. Brune (1973). Surface waves and crustal structure in the Gulf of California region. Bull. Seism. Soc. Am., 63, 1689-1698.

Thatcher, W., T. C. Hanks (1973). Source parameters of southern California earthquakes. J. Geophys. Res., 78, 8547-8576.

Thatcher, W., and R. M. Hamilton (1973). Aftershocks and source characteristics of the 1969 Coyote Mountain earthquake, San Jacinto fault zone, California. Bull. Seism. Soc. Am., 63, 647-661.

Tocher, D. (1958). Earthquake energy and ground breakage. Bull. Seism. Soc. Am., 48, 147-153.

Toksöz, M. N., A. Ben-Menahem, and D. G. Harkrider (1964). Determination of source parameters of explosions and earthquakes by amplitude equalization of seismic surface waves. 1. Underground nuclear explosions. J. Geophys. Res., 69, 4355-4366.

Toksöz, M. N., D. G. Harkrider, and A. Ben-Menahem (1965). Determination of source parameters by amplitude equalization of seismic surface waves. 2. Release of tectonic strain by underground nuclear explosions and mechanisms of earthquakes. J. Geophys. Res., 70, 907-922.

Toksöz, M. N., K. C. Thomson, and T. J. Ahrens (1971). Generation of seismic waves by explosions in prestressed media. Bull. Seism. Soc. Am., 61, 1589-1623.

Toksöz, M. N., and H. H. Kehrer (1972a). Tectonic strain release by underground nuclear explosions and its effect on seismic discrimination. Geophys. J., 31, 141-161.

Toksöz, M. N., and H. H. Kehrer (1972b). Tectonic strain-release characteristics of CANNIKIN. Bull. Seism. Soc. Am., 62, 1425-1438.

Tsai, Y.-B., and K. Aki (1970). Precise focal depth determination from amplitude spectra of surface waves. J. Geophys. Res., 75, 5729-5743.

Tsai, Y.-B., and K. Aki (1971). Amplitude spectra of surface waves from small earthquakes and underground nuclear explosions. J. Geophys. Res., 76, 3940-3952.

U.S. Joint Committee on Atomic Energy (1960). Technical aspects of detection and inspection controls of a nuclear weapons test ban (Summary analysis of hearings before the Special Subcommittee on Radiation and the Subcommittee on Research and Development, April 19-22, (1960). Superintendent of Documents, U.S. Government Printing Office, Washington, D. C.

Veith, K. F., and G. E. Clawson (1972). Magnitude from short-period P-wave data. Bull. Seism. Soc. Am., 62, 435-452.

VESIAC (1962). Proceedings of the colloquium on detection of underground nuclear explosions. VESIAC Special Report No. 4410-36-X, Acoustics and Seismics Laboratory, University of Michigan, Ann Arbor, Michigan.

von Seggern, D., and D. G. Lambert (1970). Theoretical and observed Rayleigh-wave spectra for explosions and earthquakes. J. Geophys. Res. 75, 7382-7402.

von Seggern, D. H. (1972). Seismic shear waves as a discriminant between earthquakes and underground nuclear explosions. Seismic Data Laboratory Report No. 295, Teledyne Geotech, Alexandria, Virginia (AD 747 763).

von Seggern, D., and R. Blandford (1972). Source time functions and spectra for underground nuclear explosions. Geophys. J., 31, 83-97.

von Seggern, D. (1973). Seismic surface waves from Amchitka Island Test Site events and their relation to source mechanism. J. Geophys. Res., 78, 2467-2474.

von Seggern, D. H., and R. R. Blandford (1976). Observed variation in the spectral ratio discriminant from short-period P waves. Report No. SDAC-TR-76-12, Teledyne Geotech, Alexandria, Virginia.

Ward, R. W., and M. N. Toksöz (1971). Causes of regional variation of magnitudes. Bull. Seism. Soc. Am., 61, 649-670.

Warren, R. E., J. G. Sclater, V. Vacquier, and R. F. Roy (1969). A comparison of terrestrial heat flow and transient geomagnetic fluctuations in the Southwestern United States. Geophysics, 34, 463-478.

Weichert, D. H. (1971). Short-period spectral discriminant for earthquake-explosion differentiation. Z. Geophys., 37, 147-152.

Weichert, D. H., and P. W. Basham (1973). Deterrence and false alarms in seismic discrimination. Bull. Seism. Soc. Am., 63, 1119-1132.

Weidner, D., and K. Aki (1973). Focal depth and mechanism of mid-ocean ridge earthquakes. J. Geophys. Res., 78, 1818-1831

Werth, G. C., R. F. Herbst, and D. L. Springer (1962). Amplitudes of seismic arrivals from the M discontinuity. J. Geophys. Res., 67, 1587-1610.

Wiggins, R. A., and D. V. Helmberger (1973). Upper-mantle structure of the Western United States. J. Geophys. Res., 78, 1870-1880.

Willis, D. E., J. DeNoyer, and J. T. Wilson (1963). Differentiation of earthquakes and underground nuclear explosions on the basis of amplitude characteristics. Bull. Seism. Soc. Am., 53, 979-987.

Wilson, J. T., (1965). A new class of faults and their bearing on continental drift. Nature, 207, 343-347.

Wright, J. K., and E. W. Carpenter (1962). The generation of horizontally polarized shear waves by underground explosions. J. Geophys. Res., 67, 1957-1962.

Wyss, M., and J. N. Brune (1971). Regional variations of source properties in southern California estimated from the ratio of short- to long-period amplitudes. Bull. Seism. Soc. Am., 61, 1153-1167.

Wyss, M., T. C. Hanks, and R. C. Liebermann (1971). Comparison of P-wave spectra of underground explosions and earthquakes. J. Geophys. Res., 76, 2716-2729.

Wyss, M., and P. Molnar (1972). Efficiency, stress drop, apparent stress, effective stress, and frictional stress of Denver, Colorado, earthquakes. J. Geophys. Res., 77, 1433-1438.

Yasar, T., and O. W. Nuttli (1974). Structure of the shear-wave low-velocity channel in the Western United States. Geophys. J., 37, 353-364.

York, J. E., and D. V. Helmberger (1973). Low-velocity zone variation in the Southwestern United States. J. Geophys. Res., 78, 1883-1886.

APPENDIX I

Mean Value of Seismic Source Radiation Patterns

APPENDIX I

Mean Values of Seismic Source Radiation Patterns

In order to evaluate the root mean square average of the P-wave radiation pattern $R_{\theta\phi}$, the square of this function is integrated in a spherical coordinate system over all values of the polar angle θ and the meridian angle ϕ, the result is divided by the area of a unit radius spherical surface, and the square root is taken. The expression for the P-wave pattern from a double couple with no resultant moment is:

$$R_{\theta\phi} = \sin 2\theta \cdot \cos\phi$$

Thus the rms value is given by:

$$\overline{R_{\theta\phi}} = \left[\int_0^{2\pi} \int_0^{\pi} R_{\theta\phi}^2 \cdot \sin\theta d\theta d\phi \Big/ \int_0^{2\pi} \int_0^{\pi} \sin\theta d\theta d\phi\right]^{1/2}$$

The integrals are completed with the result that

$$\overline{R_{\theta\phi}} = 2/\sqrt{15}$$

The Rayleigh-wave radiation pattern is a function of: 1) θ, the azimuth (measured counterclockwise) of the observer with respect to the strike of the fault; 2) λ, the angle between the slip vector and the horizontal, measured counterclockwise in the fault plane; 3) δ, the dip of the fault plane from the horizontal; 4) h, the depth of the focus. The expression for the modulus of the complex radiation pattern is taken from Harkrider (1970) as:

$$X_R(\theta,\lambda,\delta,h) = \left[(D_0 + D_3 T_3 + D_4 T_4)^2 + (D_1 T_1 + D_2 T_2)^2\right]^{1/2}$$

where

$T_1 = \sin\theta$
$T_2 = \cos\theta$
$T_3 = \sin 2\theta$
$T_4 = \cos 2\theta$
$D_0 = 1/2 \sin\lambda \sin 2\delta\, B(h)$
$D_1 = -\sin\lambda \cos 2\delta\, C(h)$
$D_2 = \cos\lambda \sin\delta\, A(h)$
$D_3 = \cos\lambda \sin\delta\, A(h)$
$D_4 = -1/2 \sin\lambda \sin 2\delta\, A(h)$
$A_h = -\dot{U}(h)$

$$B(h) = -\left[\left(3 - \frac{4\beta^2}{\alpha^2}\right)_h \dot{U}(h) + \left(\frac{2\beta^2}{\mu\alpha^2}\right)_h Z(h)\right]$$

$$C(h) = -\frac{X(h)}{\mu_h}$$

$\dot{U}(h)$ = radial velocity at depth h normalized by $\dot{W}_o$

$\dot{W}(h)$ = vertical velocity at depth h normalized by $\dot{W}_o$

$Z(h)$ = vertical stress at depth h normalized by $(\dot{W}_o/C_R)$

$X(h)$ = horizontal stress at depth h normalized by $(\dot{W}_o/C_R)$

$\dot{W}_o = \dot{W}(0)$ = vertical velocity at surface

C_R = Rayleigh-wave phase velocity

The root mean square value of $\chi_{LR}(\theta,\lambda,\delta,h)$ is found, for a given focal depth h, by evaluating χ^2_R for all possible orientations in space of the slip and dip vectors and averaging the resulting quantity over all azimuths θ. A spherical coordinate system is determined by allowing δ to take on values from 0 to 2π and λ from 0 to π (see Figure A1). Thus we have

$$\overline{\chi_{R(\lambda,\delta,\theta)}}_h = \left\{ \int_o^{2\pi}\int_o^{2\pi}\int_o^{\pi} \chi^2_R(\theta,\lambda,\delta,h)\,\sin\lambda\, d\lambda\, d\delta\, d\theta \Big/ \int_o^{2\pi}\int_o^{2\pi}\int_o^{\pi} \sin\lambda\, d\lambda\, d\delta\, d\theta \right\}^{1/2}$$

From (A2), we have

$$\chi^2_R(\theta,\lambda,\delta,h) = [D_o^2 + D_3^2T_3^2 + D_4^2T_4^2 + 2D_oD_3T_3 + 2D_oD_4T_4 + 2D_3D_4T_3T_4 + D_1^2T_1^2 + 2D_1D_2T_1T_2 + D_2^2T_2^2]$$

Performing first the integral over θ, we find that terms of the form $\int T_n^2$ equal π while terms of form $\int T_nT_m$ or $\int T_n$ equal zero, so that

$$\int_o^{2\pi} \chi^2_R(\theta,\lambda,\delta,h)d\theta = \pi[2D_o^2 + D_1^2 + D_2^2 + D_3^2 + D_4^2]$$

Integrating (A3) next over δ, we find that all the terms of (A4) are non-zero, with the result that

$$\int_o^{2\pi}\int_o^{2\pi} \chi^2_R(\theta,\lambda,\delta,h)d\delta\, d\theta = \pi^2\left[\left(\frac{A^2(h)}{4} + \frac{B^2(h)}{2}\right)\sin^2\lambda + A^2(h)\cos^2\lambda + C^2(h)\right] \quad (A5)$$

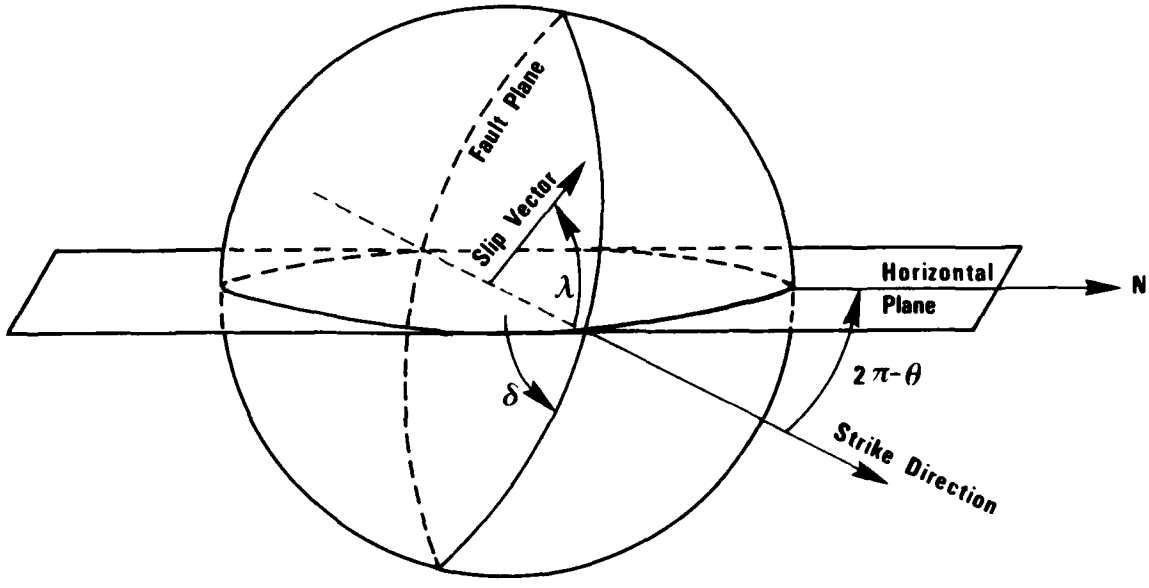

Figure A1 Geometry of spherical coordinate system used for evaluation of integrals.

Integrating (A3) finally over λ, we obtain from (A5)

$$\int_0^{2\pi}\int_0^{2\pi}\int_0^{\pi}\chi_R^2(\theta,\lambda,\delta,h)\sin\lambda\ d\lambda\ d\delta\ d\theta = \pi^2\ [A^2(h) + \frac{2B^2(h)}{3} + 2C^2(h)]$$

Using the fact that

$$\int_0^{2\pi}\ \int_0^{2\pi}\ \int_0^{\pi}\ \sin\lambda\ d\lambda\ d\delta\ d\theta = 8\pi^2$$

with the result (A6), equation (A3) reduces to:

$$\overline{\chi_R(\theta,\lambda,\delta)}_h = \frac{1}{2}\ \sqrt{\frac{A^2(h)}{2} + \frac{B^2(h)}{3} + C^2(h)}$$

The corresponding radiation pattern for Love waves is given in Harkrider (1970) as

$$|\chi_L(\theta,\lambda,\delta,h)| = [(E_o + E_3T_3 + E_4T_4)^2 + (E_1T_1 + E_2T_2)^2]^{1/2}$$

where $E_0 = 0$

$E_1 = \cos\lambda\ \cos\delta\ G(h)$

$E_2 = -\sin\lambda\ \cos2\delta\ G(h)$

$E_3 = 1/2\ \sin\lambda\ \sin2\delta\ \dot{V}(h)$

$E_4 = \cos\lambda\ \sin\delta\ \dot{V}(h)$

$G(h) = \frac{Y(h)}{\mu_h}$

$\dot{V}(h)$ = tangential velocity at depth h, normalized by $\dot{V}_o$

$Y(h)$ = tangential stress at depth h normalized by $(\dot{V}_o/C_L)$

$\dot{V}_o = \dot{V}(0)$ = tangential velocity at surface

C_L = Love-wave phase velocity

Performing the integrals as for the Rayleigh-wave pattern, we obtain for the Love-wave pattern

$$\int_0^{2\pi}\chi_L^2\ (\theta,\lambda,\delta,h)d\theta = \pi[E_1^2 + E_2^2 + E_3^2 + E_4^2]$$

Following through with the integration as for the Rayleigh-wave pattern, we obtain

$$\overline{\chi_L(\theta,\lambda,\delta)}_h = \frac{1}{2}\ \sqrt{G^2(h) + \frac{V^2(h)}{2}}$$

Some special cases are of practical interest. For instance, an earthquake at the surface would have

$$A(0) = \varepsilon_o \qquad G(0) = 0$$

$$B(0) = \left(3 - \frac{4\beta_o^2}{\alpha_o^2}\right)\varepsilon_o \qquad V(0) = 1.0$$

$$C(0) = 0$$

where ε_o is the ellipticity of the particle motion at the surface. Using these values in (A7) and (A9) we obtain

$$\overline{\chi_R(\theta,\lambda,\delta)}_{h=o} = \frac{1}{2}\,|\varepsilon_o|\,\sqrt{\frac{7}{2} - \frac{8\beta_o^2}{\alpha_o^2} + \frac{16\beta_o^4}{3\alpha_o^4}}$$

$$\overline{\chi_L(\theta,\lambda,\delta)}_{h=o} = \frac{1}{2\sqrt{2}}$$

For a Poisson medium, $\alpha^2 = 3\beta^2$, and

$$\overline{\chi_R(\theta,\lambda,\delta)}_{h=o} = \frac{1}{6}\sqrt{\frac{77}{6}}\,|\varepsilon_o|$$

Also of interest are special cases such as pure dip-slip, pure strike-slip, and thrust faults, for which the expressions simplify for all depths. The rms radiation pattern for these cases is derived by changing (A3) to integrals over θ only

$$\overline{\chi_R(\theta)}_{h,\lambda,\delta} = \left\{\int_o^{2\pi} \chi_R^2\,(\theta,\lambda,\delta,h)\,d\theta \Big/ \int_o^{2\pi} d\theta\right\}^{1/2}$$

The integral in the numerator is (A4) while the denominator is simply 2π, so that

$$\overline{\chi_R(\theta)}_{h,\lambda,\delta} = \left[\frac{2D_o^2 + D_1^2 + D_2^2 + D_3^2 + D_4^2}{2}\right]^{1/2}$$

Similarly, using (A8) we obtain for the LQ radiation pattern

$$\overline{\chi_L(\theta)}_{h,\lambda,\delta} = \left[\frac{E_1^2 + E_2^2 + E_3^2 + E_4^2}{2}\right]^{1/2}$$

Using the expressions for D_n and E_n terms given above with the appropriate λ and δ values, we obtain:

I. Strike-slip fault ($\lambda = 0°$, $\delta = 90°$)

$$\overline{\chi_R(\theta)}_{h,\lambda,\delta} = \frac{|\dot{U}(h)|}{\sqrt{2}}$$

$$\overline{\chi_L(\theta)}_{h,\lambda,\delta} = \frac{|\dot{V}(h)|}{\sqrt{2}}$$

II. Dip-slip faults ($\lambda = 270°$, $\delta = 90°$)

$$\overline{\chi_R(\theta)}_{h,\lambda,\delta} = \frac{|X(h)/\mu h|}{\sqrt{2}}$$

$$\overline{\chi_L(\theta)}_{h,\lambda,\delta} = \frac{|Y(h)/\mu h|}{\sqrt{2}}$$

III. Thrust faults ($\lambda = 90°$, $\delta = 45°$)

$$\overline{\chi_R(\theta)}_{h,\lambda,\delta} = \frac{1}{2} \sqrt{B(h)^2 + \frac{1}{2} A(h)^2}$$

$$\overline{\chi_L(\theta)}_{h,\lambda,\delta} = \frac{|\dot{V}(h)|}{2\sqrt{2}}$$

In order to calculate the complete theoretical excitation versus frequency, these results must be multiplied by the other frequency-dependent and medium-dependent factors given in Harkrider (1970) for double-couple sources, thus

$$R(\omega) = k_R^{1/2} \cdot A_R(\omega)\bar{\chi}_R(\omega,\theta).$$

$$L(\omega) = k_L^{1/2} \cdot A_L(\omega)\bar{\chi}_L(\omega,\theta).$$

where

k_R, k_L - wavenumber

A_R, A_L - medium amplitude response.

APPENDIX II

Derivation of the Explosion Spectrum

APPENDIX II

Derivation of the Explosion Spectrum

From Rodean (1971), the relation between the spectrum of the reduced displacement potential $\hat{\psi}(\omega)$ and spectrum of the pressure $\hat{P}(\omega)$ at the cavity radius (or equivalent elastic radius $\underline{a}$) is

$$\hat{\psi}(\omega) = \frac{a/\rho}{\omega_o^2 + 2i\xi\omega_o\omega - \omega^2} \hat{P}(\omega)$$

where

ρ = density

$\omega_o = 2\beta/a$

β = shear velocity

α = compressional velocity

$\xi = \beta/\alpha$

Also, from Rodean (1971) the well-known relation between the displacement spectrum $\hat{u}(r,\omega)$ and $\hat{\Psi}(\omega)$ is

$$\hat{u}(r,\omega) = -\left(\frac{i\omega}{\alpha r} + \frac{1}{r^2}\right) \hat{\Psi}(\omega)$$

where r is the distance from the center of the cavity. Combining (A-10) and (A-11), we have

$$\hat{u}(r,\omega) = -\left(\frac{i\omega}{\alpha r} + \frac{1}{r^2}\right) \frac{a/\rho}{\omega_o^2 + 2i\xi\omega_o\omega - \omega^2} \hat{P}(\omega)$$

Equation (A-12) can be evaluated at r = a in the near field and at r in the far field where we neglect the $1/r^2$ term, so that

$$\hat{u}(a,\omega) = -\left(\frac{i\omega}{\alpha a} + \frac{1}{a^2}\right) \frac{a/\rho}{\omega_o^2 + 2i\xi\omega_o\omega - \omega^2} \hat{P}(\omega)$$

and

$$\hat{u}(r,\omega) \simeq -\left(\frac{i\omega}{\alpha r}\right) \frac{a/\rho}{\omega_o^2 + 2i\xi\omega_o\omega - \omega^2} \hat{P}(\omega).$$

The ratio of the near-field and far-field displacement spectra is then simply

$$\frac{\hat{u}(r,\omega)}{\hat{u}(a,\omega)} \simeq \frac{i\omega}{\alpha r} \Big/ \left(\frac{i\omega}{\alpha a} + \frac{1}{a^2}\right).$$

For a step function at the cavity radius with final displacement D_o, $\hat{u}(a,\omega) = D_o/i\omega$ so that

$$u(r,\omega) \simeq \frac{D_o}{\alpha r} \Big/ \left(\frac{i\omega}{\alpha a} + \frac{1}{a^2}\right)$$

The modulus of this expression is

$$|\hat{u}(r,\omega)| \simeq \frac{aD_o}{r} \left(\omega^2 + \frac{\alpha^2}{a^2}\right)^{-1/2}$$

The same result is also obtained by initially solving the equation of motion with a boundary condition of a step displacement at the cavity radius.